Dissertation

submitted to the

Combined Faculties for the Natural Sciences and for Mathematics

of the Ruperto-Carola University of Heidelberg, Germany

for the degree of

Doctor of Natural Sciences

presented by

Diplom-Biologist Martina Remus

born in Seeheim-Jugenheim

Oral-examination: 10.07.2014

Nbn is essential for hair follicle maintenance and prevention of psoriasis

Referees: Prof. Dr. Christof von Kalle

Prof. Dr. Walter Nickel

Contents

List of figures

List of abbreviations

53BP1	p53 binding protein 1
Akt	Protein kinase-B
AT	Ataxia telangiectasia
ATM	Ataxia telangiectasia mutated
ATP	Adenosine triphosphate
ATR	Ataxia telangiectasia and Rad3-related
BER	Base excision repair
BRCA	Breast cancer
BRCT	Breast cancer carboxy-terminal domain
CD3	Cluster of differentiation 3
cDNA	complementary DNA
c-Myc	Myelocytomatosis oncogene
CNS	Central nervous system
DAPI	4',6-diamidino-2-phenylindole
DDR	DNA damage response
DNA	Deoxyribonucleic acid
DNA-PK	DNA-dependent protein kinase
DNA-PKcs	DNA-dependent protein kinase catalytic subunit
DP	Dermal papilla
DSB	DNA double strand break
Erk	Extracellular signal-regulated kinase
FHA	Fork-head-associated domain

GG-NER	Global genome NER
H3P	Histone 3 phosphorylated on Serine 10
HPRT	Hypoxanthin-phosphoribosyl-transferase
HRR	Homologous recombination repair
IR	Ionizing radiation
IRS	Inner root sheath
Krox20	Early growth response 2 (EGR-2)
MMR	Mismatch repair
Mre11	Meiotic recombination 11
MRN	Mre11-Rad50-Nbn
mRNA	Messenger RNA
mTOR	Mechanistic target of rapamycin
Nbn	Nibrin (Nbs1: Nijmegen breakage syndrome1)
NBS	Nijmegen breakage syndrome
NER	Nucleotide excision repair
NES	Nuclear export signal
NHEJ	Non-homologous end joining
NLS	Nuclear localization domain
OMIM	Online mendelian inheritance in man
PCNA	Proliferating cell nuclear antigen
PI3K	Phosphoinositide 3-kinase
PIKK	Phosphoinositide 3-kinase-related kinase
PUVA	8-methoxypsoralen-ultraviolet-A

RNA	Ribonucleic acid
ROS	Reactive oxygen species
S6	Ribosomal protein S6
SSB	Single strand break
ssDNA	single strand DNA
Stat3	Signal transducers and activators of transcription 3
TC-NER	Transcription-coupled NER
TUNEL	TdT-mediated dUTP-biotin nick end labeling
UV	Ultraviolet
γH2A.X	Histone H2A.X phosphorylated on Serine 139

Zusammenfassung

Die Stabilität unseres Genoms wird kontinuierlich durch endogene und exogene Faktoren gefährdet. Es entstehen Fehler in der DNA Sequenz, die durch DNA Reparaturmechanismen ausgebessert werden. Kommt es nicht dazu kann dies dauerhafte Mutationen zur Folge haben. Diese können zur Entstehung von Krankheiten und zur Entwicklung von Tumoren führen. Für die Reparatur der verschiedenen DNA Schäden gibt es entsprechend unterschiedliche Mechanismen. Eines der Hauptproteine in der Erkennung und Reparatur von DNA Doppelstrangbrüchen ist Nibrin (NBN). Mutationen von NBN führen im Menschen zur erblichen Krankheit Nijmegen-Breakage-Syndrom (NBS) (Varon et al.,1998). Zu dem typischen Erscheinungsbild von NBS Patienten gehört das Auftreten von Mikrozephalie, Immunschwäche, erhöhte Empfindlichkeit gegenüber Strahlungen und eine Veranlagung zur Entwicklung von Tumoren (Varon et al.,1998; Cybulski et al.,2004; Assaf et al.,2008; Bogdanova et al.,2008; Huang et al.,2008; Watanabe et al.,2009). Des Weiteren zeigen diese Patienten unterschiedliche Veränderungen der Haut und deren Bestandteile. So kommt es zu einer Veränderung der Pigmentierung und Porokeratose sowie vereinzelten und dünnen Haaren (van der Burgt et al.,1996; Group,2000; Wolf and Shwayder,2009; Chrzanowska et al.,2012). Auch wurden Mutationen von NBN in malignen Melanomen festgestellt (Debniak et al.,2003; Thirumaran et al.,2006; Meyer et al.,2007). Da unsere Haut die Barriere unseres Köpers ist und ihn vor äußeren Einflüssen schützt, ist eine funktionierende Reparatur von Schäden im Erbgut besonders wichtig, besonders angesichts der hohen Rate von Zellteilungen und Erneuerungen in der Haut. Durch die in NBS Patienten auftretenden Hautveränderungen scheint eine Involvierung von NBN in den Reparaturmechanismen der Haut denkbar zu sein. Um dies zu untersuchen, wurde ein Mausmodell erstellt, in dem *Nbn* nach der Geburt in der Haut ausgeschaltet wird.

Die $Nbn^{Krox20\text{-}Cre}$ Mäuse zeigten einen Verlust des Fellkleides zu einem Zeitpunkt, der mit der ersten Anagenphase nach der Embryonalentwicklung einhergeht. Zu diesem Zeitpunkt kommt es eigentlich zu der Entstehung neuer Haare. Durch den Verlust von Nbn in den Mäusen kam es zu einer Anhäufung von DNA Schäden. Diese konnten nicht repariert werden. Des Weiteren kam es zum Verlust der Stammzelleigenschaften der

Zellen des Haarfollikels. Beides zusammen führte zu Haarverlust und verhinderte die Entstehung neuer Haare. Ältere Mäuse (3 Monate) ohne Nbn zeigten außerdem eine Verdickung der Epidermis. Versuche zeigten, dass es sich dabei um ein der menschlichen Schuppenflechte (Psoriasis) ähnliches Erscheinungsbild handelte. So zeigten die Mäuse eine Vergrößerung der Epidermis, Einwanderung von Immunzellen, Aktivierungen und Veränderungen in der Expression von psoriasis-typischen Markern. Das zusätzliche Ausschalten von *p53* in der Haut der Mäuse führte zu einer Verschlechterung des Erscheinungsbildes. Die Mäuse entwickelten neben der Schuppenflechte Vorstufen von Tumoren in der Haut. Diese Beobachtungen belegen eine wichtige Rolle von Nbn in der Aufrechterhaltung der Homöostase der Haut und des Haarzyklus. Auch wird dadurch ein Mitwirken von Nbn in der Verhinderung von Hautkrebsentstehung und Schuppenflechte deutlich.

Die Rolle von Atm (Ataxia telangiectasia mutated) im Zusammenhang mit Nbn in der Haut wurde ebenfalls anhand eines Mausmodells untersucht. Dabei stellte sich heraus, dass die Rolle von Atm vom Zelltyp abhängt. *Atm* Ausschaltung in den Keratinozyten der Epidermis hatte keinen Einfluss auf das Erscheinungsbild der *Nbn* deletierten Mäuse. Es scheint daher keine essentielle Funktion von Atm im Verbindung mit Nbn in diesen Zellen zu existieren. In den Stammzellen des Haarfollikels hingegen war Atm für die Phosphorylierung von Histon H2A.X nötig. Die vorliegenden Untersuchungen konnten die Funktion von Atm in Verbindung mit Nbn in proliferierenden Zellen zeigen.

Der Verlust von Nbn Aktivität in der Maus führt über einen Verlust der Haarfollikelstammzellen zu einem Haarverlust und über eine gesteigerte Proliferation der basalen Keratinozyten zu einem der menschlichen Schuppenflechte sehr ähnlichem Krankheitsbild.

Abstract

The stability of our genome is constantly threatened by endogenous and exogenous processes causing errors in the DNA. Those have to be repaired as otherwise mutations can give rise to disease or tumor development. This is accomplished by various ways of DNA damage signaling and repair. One of the main proteins involved in the signaling and repair of DNA double strand breaks is Nbrin (NBN). A mutation of this protein is known to cause Nijmegen breakage syndrome (NBS) (Varon et al.,1998). Patients with NBS present with various clinical conditions e.g. microcephaly, immunodeficiency, radio sensitivity and a predisposition for tumor development (Varon et al.,1998; Cybulski et al.,2004; Assaf et al.,2008; Bogdanova et al.,2008; Huang et al.,2008; Watanabe et al.,2009). NBS patients show different skin malignancies as abnormal pigmentation, Porokeratosis and thin and sparse hair (van der Burgt et al.,1996; Group,2000; Wolf and Shwayder,2009; Chrzanowska et al.,2012). Mutations of *NBN* were discovered in malignant melanoma (Debniak et al.,2003; Thirumaran et al.,2006; Meyer et al.,2007). As the skin is our protection against environmental threats and undergoes a continuous self-renewal, the repair of DNA damages is crucial. The skin malignancies of NBS patients point toward an involvement of NBN in the DNA damage signaling and repair in the skin. A mouse model of *Nbn* deletion after birth in the epidermis and hair follicles was created to investigate Nbn function in the skin.

The $Nbn^{Krox20\text{-}Cre}$ mice exhibited a hair loss starting with the first wave of hair follicle growth (anagen phase) after birth. The hair loss was due to an increase of DNA damages and a failure in repair of those. Apoptosis rate was elevated and epidermal stem cell properties were disrupted. The hair follicles were not able to regenerate. Additionally, a thickening of the epidermis was detected in *Nbn* deleted mice with 3 months of age. Analyses revealed that the mice exhibited a psoriasis-like phenotype. An enlargement of the epidermis, invasion of immune cells, activation and expression changes of psoriasis typical markers were observed. Combined inactivation with *p53* led to a worsening of the phenotype of the mice. Precancerous lesions were present. These findings show the importance of Nbn in skin and hair follicle homeostasis and in the prevention of skin cancer and psoriasis.

The role of Atm (Ataxia telangiectasia mutated) in combination with Nbn in the skin was also investigated using a deletion mouse model. The influence of Atm on Nbn was found to depend on the cell type. In keratinocytes only a minor role of Atm was detected. However, Atm played an important role in hair follicle cells, where it was needed for the phosphorylation of Histone H2A.X. The role of Atm in combination with Nbn in proliferating tissue was shown by this.

Loss of Nbn activity in mice leads to the loss of hair follicle stem cells which causes hair loss and an increased proliferation of the basal keratinocytes gives rise to a psoriasis-like phenotype.

1. Introduction

1.1 DNA damage and repair

Throughout a whole lifespan the stability of the genome is constantly threatened by endogenous and exogenous processes which interfere with the DNA (Deoxyribonucleic acid) and induce lesions (Friedberg et al.,2004). This might have serious consequences because the DNA is not renewed during cell cycle but replicated, meaning that every change within the DNA that was not repaired on time, is going to be stabilized as a mutation and passed on to the daughter cells. This may lead to genomic instability. An accumulation of mutations can induce serious defects in the cells, which can cause death, early aging of the effected cells and cancer can also be a consequence. DNA damages within the germline can lead to infertility or cause genetic disorders and illnesses in the offspring. Taken together this demonstrates the importance of proper DNA repair machinery in prevention of genomic instabilities, diseases and cancer.

The exogenous factors most known to induce DNA damage are ultraviolet (UV)-light, radiation and chemicals but food and drugs have to be considered too (Hollaender and Duggar,1938; Friedberg,2003; Friedberg,2008). These last two can influence the endogenous level of damage inducing reactions by increasing the number of metabolism products able to cause DNA lesions. Reactive oxygen, carbonyl species, lipid peroxidation products, nitrogen species and endogenous alkylating agents as well as metabolites of estrogen and cholesterol are known to be endogenous DNA damaging agents (De Bont and van Larebeke,2004). While endogenous damage occurs on its own most exogenous factors can be avoided (Hoeijmakers,2009). For example damages due to UV light can be kept at a minimum by avoiding unprotected exposure of the skin to sun light.

The amount and character of the damage can vary depending on the factor and the affected areas. DNA lesions might consist of changes or deletion of bases and nucleotides leading to a disturbed conformation within the DNA and the inability to perform proper replication. Also breaks of a single or both DNA strands can occur making replication impossible or worse leading to abnormal separation of the chromosomes during cell division (Warmerdam and Kanaar,2010). For all these different types of lesions specialized DNA damage repair mechanisms exist. The DNA

damage response (DDR) can be divided into responses to lesions and breaks on DNA single strands (ssDNA) and to DNA double strand breaks (DSBs) (Figure 1). DDR is initiated by sensor proteins leading to fast and reversible changes in cell-behavior, e.g. cell cycle arrest, senescence or apoptosis of affected cells to reduce spreading of mutations (Stracker and Petrini,2011). The activation of DDR can be observed in preneoplastic lesions representing an inducible obstacle for tumorigenesis (Bartkova et al.,2005; Gorgoulis et al.,2005).

In the following the focus is on DSBs, their repair and signaling while the other DNA damage responses are explained briefly.

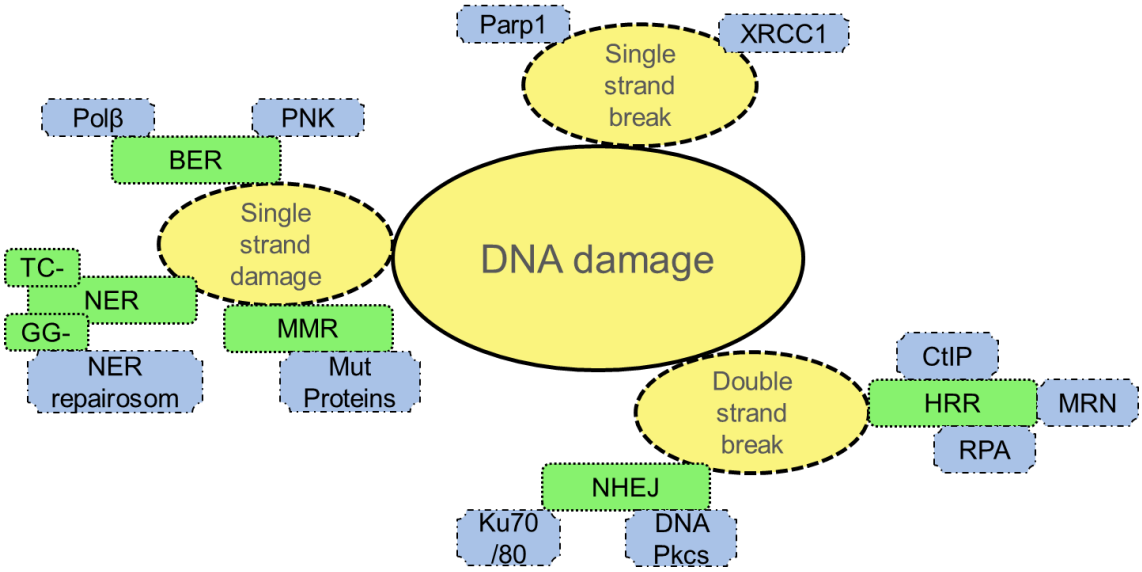

Figure 1: DNA damage repair pathways

In Figure 1 a schema of DNA damage repair pathways is shown. In yellow the different types of DNA damages are indicated. Green symbols show the possible repair pathways belonging to the different damages. The most prominent proteins involved in those repair mechanism are visualized in blue. BER: Base excision repair; NER: Nucleotide excision repair; TC-NER: transcription-coupled NER; GG-NER: global genome NER; MMR: Mismatch repair; NHEJ: Non-homologous end joining; HRR: Homologous recombination repair

1.1.1 Single strand damage repair

Damage of DNA single strands mostly consists of defects on a small number of bases or nucleotides. In some cases a break of a single DNA strand can occur. For each type of ssDNA damage there are specialized repair mechanisms e.g. base or nucleotide excision repair.

1.1.1.1 Base excision repair

The base excision repair (BER) removes small DNA lesions concerning one base. Damages BER repairs are oxidation and alkylation on bases and accidently added Uracil. BER is initiated by DNA glycosylases. Which one is active depends on the existing damage as DNA glycosylases are damage specific. The appropriate glycosylase removes damaged bases through hydrolytation leaving an abasic apurine site. Apurine endonuclease cuts the DNA backbone leaving a 5'desoxyribosephosphate. This is removed by the DNA polymerase Polβ leaving a gap of one nucleotide. Polβ fills this gap by its polymerase activity and the DNA strand is ligated by DNA ligase III. Through the long-patch BER 2-10 bases can be removed and repaired. For this long-patch BER other factors are needed in addition to Polβ, glycosylase, endonuclases (in long-patch BER: flap structure-specific endonuclease 1 (FEN1)) and Poly(ADP-Ribose) polymerase (PARP). Those are Polynucleotidkinase (PNK), proliferating cell nuclear antigen (PCNA) and the polymerase Polδ which act together to cleave the damaged bases, modify the DNA ends and fill the gap. Ligation occurs through DNA ligase I. Long-patch BER can also repair single strand DNA breaks (Hoeijmakers,2001; Bohr,2002; Hoeijmakers,2009).

1.1.1.2 Nucleotide excision repair

Nucleotide excision repair (NER) removes helix distorting DNA lesions concerning one DNA strand. These lesions are often caused by UV light damaging the DNA. During replication those lesions hinder the DNA polymerase to process the DNA strand. The characterization of NER was mostly possible due to a genetic skin disease called Xeroderma pigmentosum (XP). The patients show a hypersensibility to UV exposure leading to hyper- or depigmentation of the exposed skin area. The risk for skin carcinoma development in these patients is increased over a thousand fold compared to non-patient population.

NER involves the nucleotide excision repairosom, a complex of over 25 proteins. This complex can separate and replace a fragment of up to 30 nucleotides. Depending on the cell being actively proliferating or non-dividing different types of NER take place. In non-dividing cells global genome NER (GG-NER) is conducted while in dividing cells transcription-coupled NER (TC-NER) repairs the damage. From these subspecies of NER TC-NER is faster which is needed due to a limited time span for

repair during replication. During both GG-NER and TC-NER the complimentary DNA strand can be used as synthesis foundation which abolishes the risk of wrong repair (Hoeijmakers,2001; Friedberg,2003; Hoeijmakers,2009).

1.1.1.3 Mismatch repair

The most common way within the cell to induce DNA damage is through mistakes during replication. As a consequence one base is inserted at a wrong position and the two DNA strands are not able to pair properly at this position, a mismatch of bases appears. Another reason for this can also be the desamiation of a base or another change on a single base caused by chemicals or other reactive species. Those single base damages can be easily established as mutations if not recognized by damage response machinery. Mismatch repair (MMR) is the pathway reacting to those single base lesions and to insertion and deletion mismatches with a small number of nucleotides involved. First the mismatch is recognized and bound. Then an excision of the wrong base or fragment occurs. The first step is accomplished by various complexes of the Mut protein family which are also involved in the second step. In addition proteins that are part of the BER damage response are engaged and the new synthesis of the DNA fragment and the ligation appear to be mastered mainly by those proteins (Hoeijmakers,2001; Friedberg,2003).

1.1.1.4 Single strand break repair

Breaks of ssDNA are not so common. They are caused by free radicals from cell metabolism attacking desoxyribose or by exogenous substances and processes. ssDNA breaks (SSBs) can arise during BER and be a consequence of Topoisomerase I inhibition. DNA replication and transcription are hindered by SSBs. SSBs are associated with inheritable neurodegenerative diseases.

DNA single strand breaks are detected and bound by Parp1. Parp1 and other proteins are poly(ADP-ribosyl)ated initiating the binding of XRCC1 (X-ray cross-complementing Protein 1). This activates APE1 (Apurinic/apyrimidinic endonuclease 1), PNK and APTX (Aparataxin) to start the end processing. DNA polymerase β fills the gap using the other DNA strand as a template and the DNA pieces are connected via

Ligase III to form a repaired, intact and complementary DNA strand (Polo and Jackson,2011).

1.1.2 Double strand break repair

Breaks in DNA double strands can be caused by ionizing radiation (IR), x rays, UV light, chemicals, reactive oxygen species (ROS) and other free radicals from cell metabolism. Retroviral integration, treatment with Topoisomerase II inhibitors, like etoposide and camptothecin used in cancer treatment, and shortened telomeres due to aging can initiate DSBs. During replication an existing SSB or other lesions on one DNA strand are often transformed into a DSB. DSBs can even be wanted in cells e.g. during development and adaptations in the immune system and enable genetic diversity during meiosis. In mitotic cells DSBs lead to non-intact chromosomes making proper chromosome segregation unlikely. Consequences might be loss of heterozygosity, aneuploidy and chromosomal translocation leading to abnormal cells with a higher risk for cancer. Therefore functional DSB signaling and repair is essential for cancer treatment to limit cell proliferation of abnormal cells and thereby reduce additional accumulation of further mutations. DNA repair for DSBs can be divided into two processes: non-homologous end joining (NHEJ) and homologous recombination repair (HRR). The step deciding what process is chosen is DSB resection which is needed for HRR but not for NHEJ (Hoeijmakers,2001; Friedberg,2003; Wyman and Kanaar,2006; Stracker and Petrini,2011).

1.1.2.1 Non-homologous end joining

Non-homologous end joining is the most common way for DSB repair in cells as it can take place at every point in time during cell cycle. NHEJ is fast and therefore can reduce potential oncogenic translocations (Warmerdam and Kanaar,2010). DSB repair through NHEJ often leads to deletion or insertion on the repair side because NHEJ does not use a template like the homologous chromatin to synthesize over the DSB (Takata et al.,1998). NHEJ therefore is considered to be error prone.

Non-homologous end joining starts with binding of Ku70/Ku80 heterodimer to the broken DNA ends (Figure 2). The Ku heterodimer recruits and activates DNA-PKcs (DNA-dependent protein kinase catalytic subunit) to form a holoenzyme (Gottlieb and

Jackson,1993). DNA-PK (DNA-dependent protein kinase) holoenzyme brings the DNA ends into close proximity to each other making it possible for the nuclease Artemis, PNK, Aprataxin and PNK like factor to process the DNA. DNA polymerase TdT (terminal deoxynucleotidyl transferase) or translesion DNA polymerase polμ or polλ are involved depending on damage characteristics. While TdT is able to add untemplated nucleotides to DNA ends, polμ and polλ are able to incorporate nucleotides from the other DNA end before filling the gap between both ends (Wyman and Kanaar,2006). XLF (XRCC4 like factor) - XRCC4 - Ligase IV complex aggregates the processed DNA to make a complete DNA double strand (Figure 2) (Lieber and Wilson,2010).

For NHEJ alternative pathways exist in case one of its components is mutated or completely absent. Those pathways need small homologies on the DSB ends to function. Components are mostly proteins from HRR like MRN (Mre11 (Meiotic recombination 11)-Rad50-Nbn (Nibrin)) complex, Parp1, XRCC1 and DNA Ligases I and III (McVey and Lee,2008; Lieber and Wilson,2010).

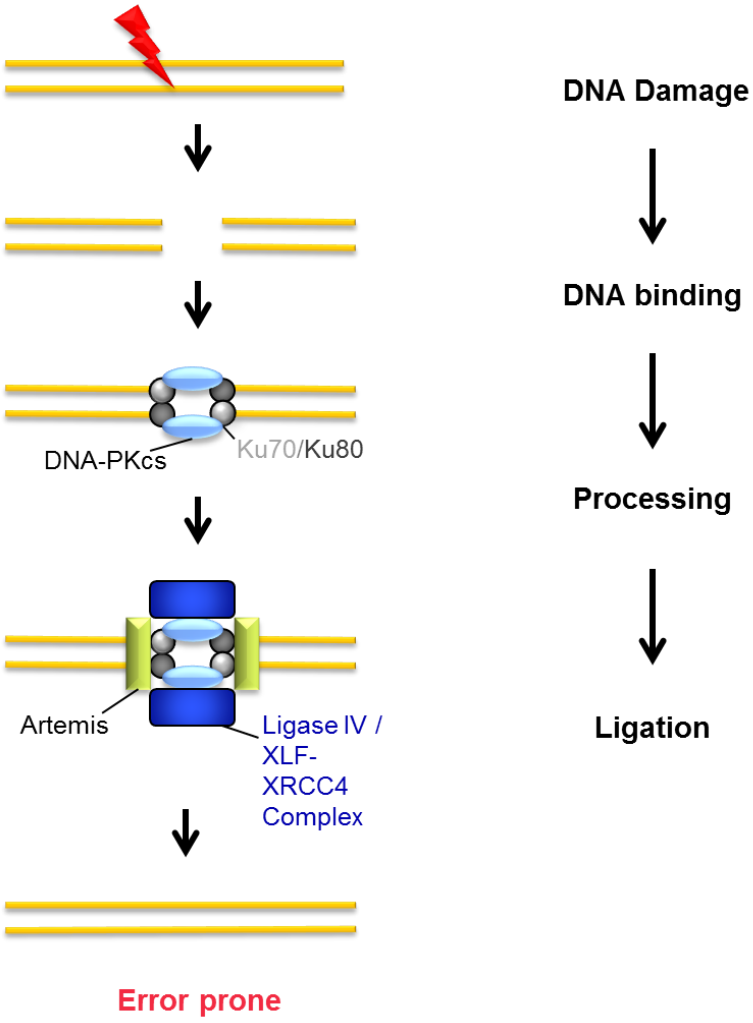

Figure 2: Non homologous end joining

Figure 2 shows a schematic outline of NHEJ. A DSB is induced and the breakage site is recognized and bound. The gap in the DNA strands is bridged and filled. Afterwards the DNA ends are ligated. This pathway is considered error prone because wrong bases might be added as no template is available to synthesis the DNA strand accordingly. Adapted from Lieber and Wilson 2010 (Lieber and Wilson,2010)

1.1.2.2 Homologous recombination repair

During S and G2 phase of the cell cycle DSB repair is accomplished by homologous recombination repair. HRR needs the homologous chromatin to rejoin the broken DNA ends (Takata et al.,1998) and therefore is error free. Insertion of lost bases is possible while homologous recombination takes place.

HRR is initiated by DSB resection starting with binding of Mre11-Rad50-Nbn complex to the ends of broken DNA (Figure 3). Together with auxiliary factors like CtIP (C-terminal binding protein interacting protein), Exo1 (Exonuclease 1), DNA replication ATP-dependent (Adenosine triphosphate) helicase/nuclease DNA2 and

ATP-dependent helicases from RECQ family, the DNA ends are kept in close proximity and 5'- to 3' nucleolytic processing can be accomplished (Longhese et al.,2010). Together with CtIP MRN resects DNA ends producing 3'- single strand (ss) overhangs (Paull and Gellert,1998; Sartori et al.,2007) which ssDNA-binding complex RPA (replication protein A) envelops (Figure 3). RPA is replaced by Rad51, with Rad52 and proteins of the Fanconi anemia (FA) pathway assisting. Proteins of FA pathway e.g. BRCA2 (breast cancer 2) and PALB2 (partner and localizer of BRCA2) are usually acting in detection and repair of interstrand cross-links (Moldovan and D'Andrea,2009). Rad51 and other associated proteins initiate a search for homologous regions on the sister chromatid and strand invasion in the homologous template (Figure 3). After DNA synthesis through PCNA and DNA polymerase β DNA Ligase I is activated. Intermediates of homologous recombination are cleaved and resolved by Resolvase and DNA helicases leaving repaired and intact DNA double strands (Figure 3) (Mazon et al.,2010).

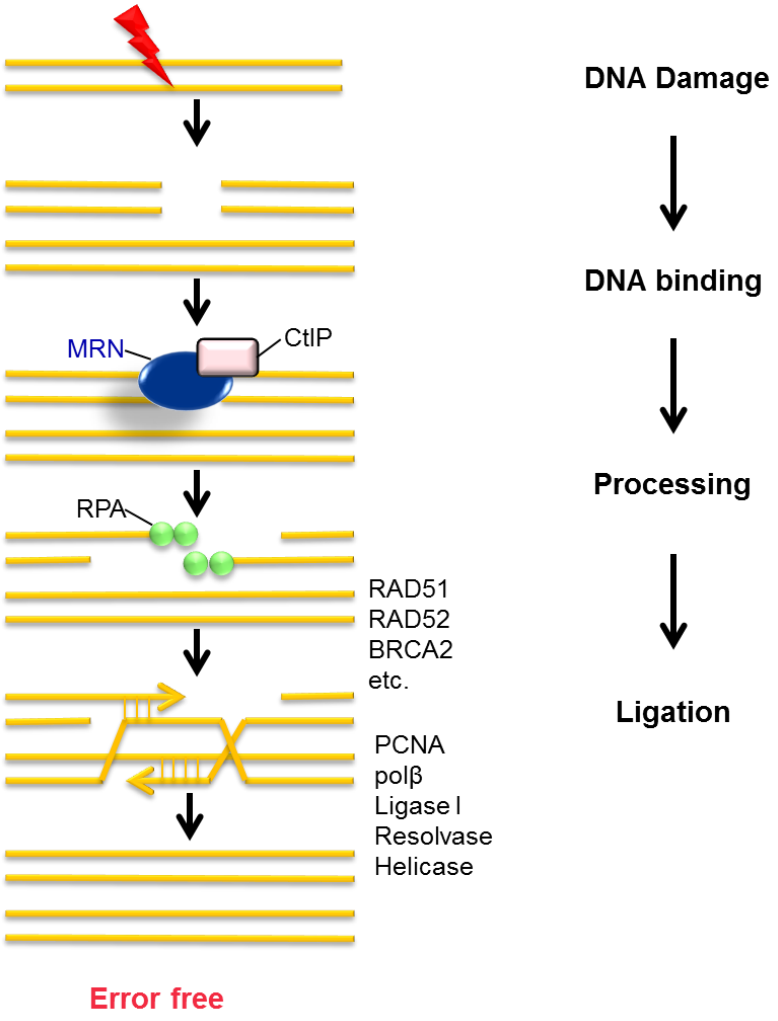

Figure 3: Homologous recombination repair

HRR is visualized in an abbreviated version in Figure 3. The DSB occurs on one of the chromatins. MRN recognizes the free DNA, binds and produces single strand overhangs. Those are necessary to accomplish strand invasion into the sister chromatin. DNA is synthesized according to the matching DNA strand of the sister chromatin. Afterwards the junction is resolved and DNA strands are ligated. HRR is error free due to the homologous chromatin that is used for DNA synthesis. Adapted from Wyman and Kanaar, 2006 and Mazon et al., 2010 (Wyman and Kanaar,2006; Mazon et al.,2010)

1.1.3 Signaling pathways for DNA damages

DNA breaks play a role during cell cycle progression. An unrepaired break can cause abnormal cells, cancer and cell death. Therefore at important steps during the cell cycle DNA integrity is checked and damages lead to an arrest or stop of cell cycle progression. DNA damage checkpoints are before (G1/S) and during replication (intra S) and before cell division (G2/M) (Figure 4). Those checkpoints inhibit segregation and duplication of aggrieved DNA. They do not recognize DNA damages directly but react to complexes formed and accumulated at damage sides. Accumulation of DDR

proteins guarantees a higher interaction rate between proteins and damaged DNA making a fast reaction to DSB possible and reducing the risk for improper activation of DDR. The proteins involved in DNA damage checkpoints can be divided into subgroups by their responsibilities: damage sensors, transducers, mediators and effectors (Warmerdam and Kanaar,2010; Polo and Jackson,2011).

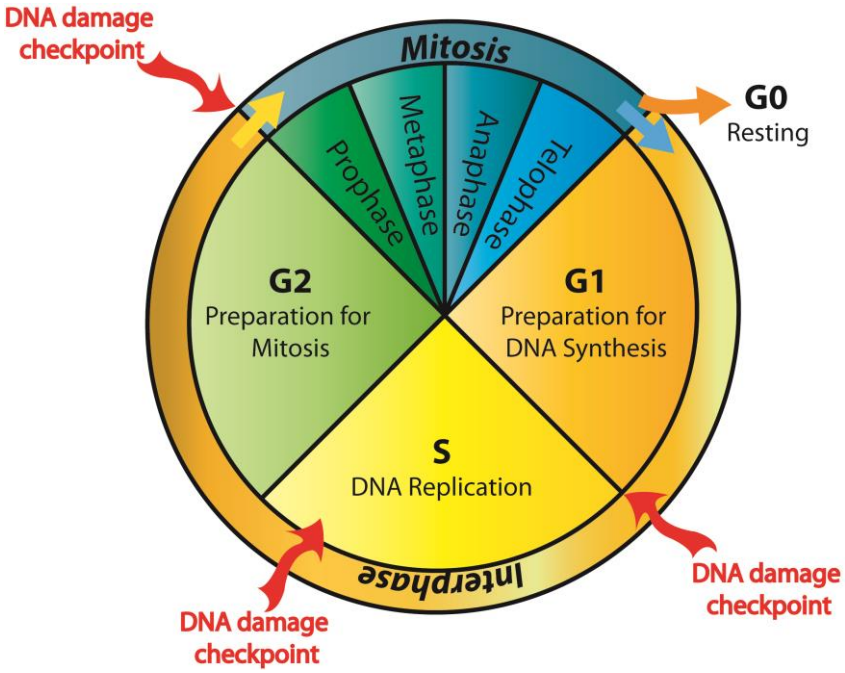

Figure 4: Cell cycle

The cell cycle (Figure 4) is divided into Interphase and Mitosis. Interphase is composed of G1 (growth 1), S and G2 phases. During G1 phase the cell is preparing for DNA synthesis (S). In S phase the DNA is replicated and in G2 phase the cell prepares for Mitosis. During Mitosis the cell divides into two identical cells. Mitosis is subdivided in Pro-, Meta-, Ana- and Telophase. Each phase represents different steps in the process of the separation into two cells. Afterwards the cells can continue cycling or go into resting in G0 phase. During the cell cycle the DNA is checked for damages at G1/S, IntraS and G2/M checkpoints.

The DNA damage checkpoints are controlled by ATM (ataxia telangiectasia mutated) and ATR (Ataxia telangiectasia and Rad3-related) signaling. Both proteins are, like DNA-PKcs, members of the PIKK (phosphoinositide three-kinase-related kinase) family. Proteins targeted by these two pathways are transcription factors, cell cycle regulators, apoptotic machinery and DNA repair factors. Through ATM, ATR and other members of the PIKK family they are phosphorylated on serine and threonine, activating the damage checkpoints and thereby ensuring DNA integrity. Members of the

PIKK family are able to phosphorylate Histone H2A.X on Serine 139 making it γH2A.X (Burma et al.,2001; Stiff et al.,2004; Friesner et al.,2005). This causes a change in chromatin structure making DNA more accessible for e.g. damage repair proteins (Kinner et al.,2008; Lovejoy and Cortez,2009; Warmerdam and Kanaar,2010).

1.1.3.1 ATM signaling

Breaks in double strand DNA induce the ATM pathway leading to cell cycle checkpoint activation. The sensor for DSB is MRN complex (Lavin and Kozlov,2007). DNA ends are bound by the DNA binding domain at the globular head region of Mre11 (Meiotic recombination 11) and the ATPase domain of Rad50 (de Jager et al.,2001). Stability of DNA binding increases with Mre11 heterodimerisation while Rad50 links the DNA ends (de Jager et al.,2001; Williams et al.,2008). Endonuclease activity of Mre11 is also involved in further progressing of the broken DNA (Williams et al.,2008). Lack of Mre11 inhibits binding of DNA breaks and therefore the ATM pathway (Kitagawa et al.,2004). MRN recruits and activates the serine-threonine protein kinase (Savitsky et al.,1995; Kastan and Lim,2000) ATM which itself is a transducer. It has to be noted that MRN is involved in HRR independently of its interaction with ATM. However without ATM involvement activation of cell cycle checkpoint after DSB would not be possible (Shiloh,2003; Lee and Paull,2005; Shiloh,2006). In addition ATM has been shown to be involved in stopping and removing of RNA (Ribonucleic acid) polymerase I and II at DNA breaks (Kruhlak et al.,2007; Shanbhag et al.,2010). Activation of ATM is dependent on its autophosphorylation at Serine 1981 (Bakkenist and Kastan,2003) and binding to MRN complex via NBN's C-terminal binding domain for ATM. Even in absence of NBN ATM is able to phosphorylate p53 on Serine 15 increasing stability of p53 and inducing p53 dependent apoptosis. After autophosphorylation on Serine 1981 the inactive oligomer of ATM is disassociated into active monomers (Bakkenist and Kastan,2003). For complete activation additional autophosphorylation occurs on Serine 367 and 1893 (Kozlov et al.,2006). ATM autophosphorylation is dependent on its previous acetylation which itself is not sufficient to establish DNA binding. Besides acetylation a change in chromatin structure e.g. through DSBs or chemical reagents induces autophosphorylation of ATM (Bakkenist and Kastan,2003). For autophosphorylated and MRN-bound ATM kinase activity is enabled. MRN complex links to both DNA ends and ATM bringing them into

close proximity. The mediator proteins MDC1 (mediator of DNA damage checkpoint 1) interacts with NBN and 53BP1 (p53 binding protein 1) and binds to Rad50. This increases the accumulation of MRN complex at DSB sides. In addition BRCA1, ATM, the effector kinases Chk1 (Checkpoint kinase 1) and Chk2 are activated which spreads the checkpoint signal throughout the nucleus. Phosphorylation of Chk1 by ATM induces disassociation of Chk1 from chromatin. Activation of Chk2 by ATM-dependent phosphorylation enables the protein to phosphorylate Cdc25A (Cell division cycle 25 homolog A). Cdc25A normally dephosphorylates Cdk2 (Cyclin-dependent kinase 2) but its phosphorylation leads to proteasomal degradation. As a consequence Cdk2 is not dephosphorylated detaining DNA synthesis. This reduces the risk of damaged DNA being spread. To ensure the proper activation of the ATM dependent checkpoint proteins like Nbn, Artemis and Histone H2A.X have to be phosphorylated during the pathway. For each checkpoint different proteins are involved in the ATM cascade. All those proteins are phosphorylated and therefore activated through ATM arresting cell cycle at the respective checkpoint. Activation of G1 checkpoint is induced with p53, Mdm2 (mouse double minute 2) and Chk2. S phase checkpoint is activated through Brca1, FANCD2 (FA complementation group D2) and SMC1 (structural maintenance of chromosomes protein 1) while a combination of Brca1 and Rad17 is responsible for cell cycle checkpoint activation at G2/M (Bakkenist and Kastan,2003).

1.1.3.2 ATR signaling

For activation of DNA damage checkpoints via ATR pathway ssDNA is essential. Those can be due to cross-links, DSB with single strand overhangs, base adducts and replicational stress. Heterotrimeric RPA binds directly to ssDNA and signals the accumulation of ssDNA during the damage processing. Increased activation of ATR signaling is due to long ssDNA at DNA break sides. ATR is recruited to the DNA ends by RPA with ATRIP (ATR interacting partner) as bridge protein. Binding of ATR to DNA can also be accomplished through MRN complex. Mre11 can bind to ssDNA producing a conformation of the complex in which Nbn can bind ATR instead of ATM (Williams et al.,2010). Activation of ATR involves ATRIP and 9-1-1 (Rad9-Rad1-Hus1) complex. 9-1-1 is bound from RPA to the DNA on 5'primer ends putting all factors into close proximity. With the help of TopBP1 (topoisomerase-binding protein1) and Calspin Chk1, which is phosphorylated and disassociates from chromatin, and Chk2

are activated. This spreads the signal throughout the nucleus and activates the ATR dependent cell cycle checkpoint. Besides this signaling pathway ATR is active in every cell cycle, controlling replication and repairing damaged replication forks.

1.1.4 The MRN complex

MRN can be considered the sensor for DSB (Lavin and Kozlov,2007) as it directly binds free DNA ends and besides being active in HRR, acts in ATM and ATR cell cycle checkpoint signaling and in an alternative pathways for NHEJ (Lavin and Kozlov,2007; McVey and Lee,2008; Lieber and Wilson,2010; Williams et al.,2010). Its importance is underlined by high genomic conservation of Mre11 and Rad50 through all three life domains: bacteria, archaea and eucaryota (Hopfner et al.,2000; de Jager et al.,2004; Stracker and Petrini,2011). Orthologies of Nbn appear only in eukaryotes and here with a smaller homology than Mre11 and Rad50 but functional conservation is seen in all domains (Dolganov et al.,1996; Carney et al.,1998). The main function of MRN complex in mitotic cells is to promote HRR between sister chromatids after damages during DNA replication (Bressan et al.,1999). In response to DSBs the MRN complex binds to the free DNA ends. It is also able to bind to chromosome ends with extremely short or no telomeres left (Sabourin and Zakian,2008). MRN function at longer telomeres and at replications forks is to avoid DSBs even in the absence of shelterin or ATM (Zhu et al.,2000; Verdun and Karlseder,2007). Main functions of MRN complex are binding and processing of DNA, establishing connections of broken DNA over short and long distances and initiation of DSB repair and checkpoint signaling. Due to all these functions MRN can be assumed to be a sensor, signaling and effector complex. Whenever DSBs arise and are repaired MRN is involved meaning MRN focis are formed in NHEJ, HRR, adaption mechanisms in the immune system (V(D)J rearrangement during B- and T-cell development), at telomeres and replication forks. For example the endonuclease activity of it is involved in HRR induction (Buis et al.,2008; Williams et al.,2008) while false nuclease activity at telomeres can cause fusion of chromosomes (Deng et al.,2009). Which repair or signaling pathway is activated by the MRN complex is dependent on its macromolecular shape and conformation. Availability of interaction sides, post-translational modifications and allosteric regulations due to existing interactions influence the outcome of MRN activity. For example when Mre11 dimer binds two DNA ends it is symmetric, making

it possible for ATM to bind inducing the ATM signaling or to start DSB repair. If Mre11 dimer binds to one DNA end its structure is asymmetric blocking ATM but binding ATR. As a consequence replication forks can be rescued or the ATR pathway starts.

Mre11 and Rad50 form the head region of the MRN complex. This is the main area for binding and processing within the MRN (Stewart et al.,1999). It is composed of two Mre11 nucleases and two Rad50 ABC-ATPase domains with Mre11 bound to Rad50 via its coiled-coil structures (Stewart et al.,1999). Rad50 has ATPase and adenylate kinase activity and is able to bind DNA (Paull and Gellert,1999; Bhaskara et al.,2007). The ATPase domain is spread on two places at the opposite ends of the primary sequence. Those two parts are arranged next to each other when the middle sequence folds and forms a coiled-coil zinc finger domain (Hopfner et al.,2000; Hopfner et al.,2002). This coiled-coil domain allows two MRN complexes to link together enabling larger distances for DNA bridging (Moreno-Herrero et al.,2005). MRE11 comprises a C-terminal DNA binding domain and an N-terminal phosphoesterase. Both 3'-5' dsDNA (double strand DNA) exonuclease and ssDNA endonuclease activities of the MRN complex are due to Mre11 (Hopfner et al.,2001). The ssDNA endonuclase and 3'-5' exonuclease activity of Mre11 are independent of Rad50 and Nbn but an activity increase can be seen when MRN complex is formed (Paull and Gellert,1998; Williams et al.,2007). In addition Nbn binds to Mre11-Rad50. Nbn acts as a regulator and an anchor for other proteins. It is linked to Mre11 via an N-terminal phosphoprotein binding side. Combined with Rad50 it controls nuclease activity from Mre11. Nbn interacts with and activates ATM or ATR. Sterical hindering created through Mre11 binding to one DNA end prevents linking of ATM to Nbn but leaves enough space for ATR to bind. Association of Nbn with ATM is dynamic and DSB dependent while binding to Mre11-Rad50 is constant. Due to two dual phosphopeptide binding domains opposite one another Nbn is a mulitmodular adaptor for phosphorylated proteins during DDR. Some of the known interacting proteins are CtIP, ATR, ATM and MDC1.

1.1.5 Diseases involving DNA signaling and repair proteins

The functional link between genomic deficiencies due to insufficient DDR and cancer is strengthened by several genomic instability disorders showing a moderate to serve increase in cancer formation. These disorders include Bloom's syndrome,

Werner's syndrome, Fanconi anemia (FA), Ataxia telangiectasia (AT), AT like disorder and Nijmegen breakage syndrome (NBS) (Digweed,1993; Hoeijmakers,2001; Bohr,2002; McKinnon,2004).

The listed diseases are rare and inherited in recessive manner. Mutated human genes involved in these genomic instability disorders have been described to be essential for several biological functions such as DNA replication, DNA damage response, DNA repair, cell cycle checkpoint control and apoptosis (Kang et al.,2002; Friedberg et al.,2004; McKinnon,2004; Warmerdam and Kanaar,2010). Mutations among the proteins of the DNA damage response and the signaling of DNA damages or lack of proteins cause serious defects including neurodegenerative diseases, hypersensitivity to sunlight, cancer, early aging and developmental disorders. In mouse model knockout of involved proteins can lead to embryonic lethality (Zhu et al.,2001; Frappart et al.,2005).

Xeroderma pigmentosum, Cockayne syndrome and Trichothiodystrophy are illnesses aroused by defects in NER causing point mutations among the genome. Those diseases are characterized with hypersensitivity against sunlight most obvious in XP patients having an over 1000 fold increased risk for skin cancer induced by UV light. They also show a higher risk for inner tumor formation and neurodegeneration. Cockayne syndrome and Trichothiodystrophy patients on the other hand do not show an increased risk for cancer development. This is due to defects in TC-NER where cells are more sensitive for lesions causing apoptosis induction thereby providing a protection against tumor formation. Increased levels of apoptosis might be responsible for premature aging observed in those patients. In Cockayne syndrome patients reduced growth and neurological defects like mental retardation and dysmyelation are found. For Trichothiodystrophy patients the most obvious appearances are brittle hair and nails and scaly skin. Other symptoms are similar to those observed in Cockayne syndrome (Hoeijmakers,2001; Bohr,2002).

Werner's syndrome and Bloom's syndrome are both associated with defects in HRR in particular defects involving the RECQ helicase. Patients of both illnesses have elevated risk for developing cancer (Hoeijmakers,2001; Bohr,2002). Hereditary non-polyposis colorectal cancer is caused by defects in MMR inducing genome and chromosome instability with an increased mutation rate (Hoeijmakers,2001; Bohr,2002). Genome instability is also involved in Fanconi anemia. FA is a heterogeneous disease with cells highly sensible against DNA damaging agents and

with an elevated cancer risk. Patients with mutations in BRCA1 or BRCA2 show a higher risk for developing breast or ovarian cancer.

Ataxia telangiectasia, AT-like disorder and Nijmegen breakage syndrome are diseases caused by defects within ATM signaling and therefore a non-functional response and repair after DSBs. Etiological for AT is a mutation of ATM. This results in a neurodegenerative disease that has its onset in early childhood. Cerebellar degradation in these patients leads to ataxic movements, progressive dysarthria and ocular telangiectasia and therefore often leads to a life in a wheelchair (McKinnon,2004). Additional symptoms of AT are hypersensitivity to x-rays, chromosome instability, sterility, defects in immune system development and a high risk for lymphomas (Hoeijmakers,2001; McKinnon,2004). AT like disorder is characterized by similar effects as AT but caused by a mutation of Mre11 (Hoeijmakers,2001).

1.1.5.1 Nijmegen breakage syndrome (NBS) [OMIM 251260]

NBS is a hereditary autosomal recessive chromosome instability disorder (Varon et al.,1998). It is caused by a genomic defect of *NBN* (Nibrin, previously known as *NBS1*= Nijmegen breakage syndrome 1) (Varon et al.,1998). The NBN protein is involved in the MRN complex for signaling and initiation of DSB repair. NBS manly occurs in central and eastern European countries with 90 % of patients having the so called "Slavic" 657del5 (c.657-661delACAAA) mutation (Varon et al.,1998). The most frequently observed cytogenetic anomalies are rearrangements on chromosomes 7 and 14. Those chromosomes contain immunoglobulin and T cell receptor genes which undergo recombination involving DSBs during lymphoid development (Varon et al.,1998). Clinical symptoms for NBS are microcephaly, bird shaped face, immunodeficiency, growth and mental retardation, predisposition for lymphoreticular malignancies and in women primary ovarian failure (Varon et al.,1998; Assaf et al.,2008). In addition NBS patients are highly sensitive to radiation and therefore should not be treated with x-rays or CT (x-ray computed tomography) (Varon et al.,1998; Assaf et al.,2008). Those treatments with IR raise the risk to develop cancer in the patients (Varon et al.,1998; Assaf et al.,2008). In female patients heterozygote for *NBN* mutation a 3-fold increase in breast cancer risk was detected (Bogdanova et al.,2008) and the tumor latency und metastasis rate of mammary tumors is increased (Wan and

Crowe,2012). Male patients with haploinsufficiency of *NBN* have a predisposition for prostate cancer (Cybulski et al.,2004). Mutations of *NBN* are additionally found in malignant melanoma (Debniak et al.,2003; Meyer et al.,2007), basal cell carcinoma (Thirumaran et al.,2006), meduloblastoma (Huang et al.,2008) and glioblastoma (Watanabe et al.,2009). Heterozygote mutations of NBN are associated with nasopharyngeal carcinoma (Zheng et al.,2011), lung cancer (Yang et al.,2012), colorectal carcinoma and non-Hodgkin lymphoma (Steffen et al.,2004). In skin besides melanoma development, other malignancies can be observed. An abnormal pigmentation of the skin can be seen in the majority of the patients (van der Burgt et al.,1996; Group,2000; Chrzanowska et al.,2012) and cutaneous noncaseating granulomas were described (Yoo et al.,2008; Vogel et al.,2010). Porokeratosis, a malfunction in epidermis development, was also observed (Wolf and Shwayder,2009). Hair of NBS patients are sparse and thin (Chrzanowska et al.,2012).

1.1.6 Nibrin

Nibrin (NBN) has been identified to be the protein causing Nijmegen breakage syndrome if genetically mutated (Varon et al.,1998). Therefore it was formerly known as NBS1 (Nijmegen breakage syndrome 1). *NBN* is located on human chromosome segment 8q21.3 (Saar et al.,1997). *Nbn* is the mammalian equivalent to *Xrs2* in *Saccharomyces cerevisiae* although only 28 % genetically homologous (Dolganov et al.,1996; Carney et al.,1998). Homologies to human NBN have been found in rat, mouse, dog, cow and monkey but not in chicken (Carney et al.,1998). *NBN* consists of 16 exons interspersed with introns to a complete cDNA (complementary DNA) size of over 50kb. Due to two polyadenylation signals in the 3' untranslated region of the cDNA (positions c.2440G and c.4386T) a 2.4 kb and 4.4 kb transcript exist (Carney et al.,1998; Varon et al.,1998). After splicing an mRNA (messenger RNA) of 754 aa (amino acids) remains and forms the protein with a size of 95 kDa. This protein is absent in NBS patients (Carney et al.,1998). No global similarities to other proteins have been found but two functional domains were identified. These domains are a fork-head-associated domain (FHA) (Hofmann and Bucher,1995) and a breast cancer carboxy-terminal domain (BRCT) (Bork et al.,1997), both located within the amino-terminal region of NBN (Figure 6) (Varon et al.,1998). FHA and BRCT together seem to be important for the formation of nuclear foci involving NBN at DNA damage sides

(Tauchi et al.,2002; Cerosaletti and Concannon,2003). A second BRCT domain was identified in *Xenopus laevis* that seems to be partially conserved in humans (Xu et al.,2008). Mutation screening of NBS patients revealed six different mutations within the *NBN* gene between nucleotides 657 and 1142 (Varon et al.,1998). The most common mutation of the gene 657del5 (c.657-661delACAAA), is placed within Exon 6. This mutation leads to a frame shift creating an alternative start codon and a 70 kDa protein of 555 aa (Figure 5), truncated on its N-terminal part, is expressed (Maser et al.,2001). In addition a small 26 kDa protein can be found containing the N-terminal FHA and BRCT domains of NBN (Figure 5). In the rare mutation 835del4 (c.835-838delCAGA) a similar mechanism can be observed (Tupler et al.,1997; Varon et al.,1998) (Figure 5). All mutations described so far result in a frame shift and an N-terminal truncation removing the FHA and BRCT domains of Nibrin (Varon et al.,1998). In tissue of patients this leads to an expression of a small protein containing FHA and BRCT domains and a bigger protein presenting the C-terminal rest of NBN (Figure 5). These hypomorphic mutations thereby create protein-pieces that are able to partially rescue NBN activity. This is indicated by the reduced lymphoma risk in patients with a high expression of N-terminally truncated 70 kDa NBN protein (Kruger et al.,2007).

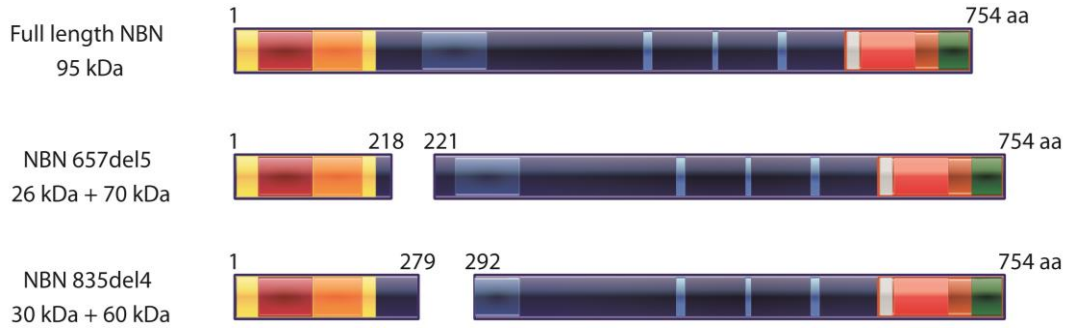

Figure 5: NBN mutations

The full length protein of NBN is shown here. In addition the proteins resulting from the two most common mutations are depicted. Those mutations are 657del5 and 835del4.

NBN is the p95 component of the MRE11-RAD50 complex (Carney et al.,1998) leading to the name of MRE11-RAD50-NBN complex. Both MRE11 and RAD50 are cytoplasmic proteins and in absence of NBN cannot locate in the nucleus (Carney et al.,1998). If NBN is N-terminal truncated NBN, MRE11 and RAD50 can be detected in the nucleus but the characteristic foci formation is inhibited (Desai-Mehta et al.,2001).

Deletion of the last C-terminal 101 aa of *NBN* leaves a protein not able to interact with MRE11 but able to localize in the nucleus and induce foci formation (Desai-Mehta et al.,2001). These findings indicate the essential role of NBN in foci formation after DSBs (Desai-Mehta et al.,2001). The nuclear localization domains (NLS) of Nbn are at amino acids 468-472, 550-554 and 592-596 (Vissinga et al.,2009) (Figure 6). Moreover a nuclear export signal (NES) is part of Nbn (from aa 653 to 662) (Vissinga et al.,2009) (Figure 6). Both NLS and NES are important for the distribution of Nbn in cytoplasm or nucleus. Localization of Mre11 together with Nbn is dependent on both types of signals (Vissinga et al.,2009). Lack of one NLS does not inhibit the nuclear import of NBN but leads to a lower protein level in the nucleus (Desai-Mehta et al.,2001; Vissinga et al.,2009). Additionally DNA binding ability of the MRN complex and MRE11 nuclease activity are regulated by NBN (Paull and Gellert,1999; Lee et al.,2003). This interaction with MRE11 is accomplished at amino acids 653-754 (Figure 6) (Desai-Mehta et al.,2001). At the amino-terminal end *NBN* has an additional motif of 20 aa (aa 734 to 754) (Figure 6) that interacts with ATM (Falck et al.,2005; You et al.,2005). ATM phosphorylates NBN at serine 278, 343, 397 and 615 (Figure 6) (Gatei et al.,2000; Lim et al.,2000; Wu et al.,2000; Zhao et al.,2000). Additional phosphorylation sites of NBN were found via mass spectrometry on serines and threonins at 337, 341, 432 and 602 (Figure 6) (Dephoure et al.,2008; Gauci et al.,2009). The ATM dependent phosphorylation occurs after DNA damage by γ-radiation and UV-light (Gatei et al.,2000; Wu et al.,2000). The timing and accumulation of ATM and NBN and therefore the MRN complex at the damage sites are dependent on these phosphorylations (Wen et al.,2012). The phosphorylation of NBN through ATM also is essential for functional S phase checkpoint pathway (Lim et al.,2000). CHK1, CHK2 and G2/M checkpoint activation require both NBN and ATM activation (Dasika et al.,1999; Gatei et al.,2000; Buscemi et al.,2001). Additional activation of NBN is seen in unwinding of DNA complexes and cleavage of paired hairpin structures (Paull and Gellert,1999). Recently an involvement of NBN in the phosphorylation and thereby activation of Akt (protein kinase-B) kinase was discovered (Wang et al.,2013). Nbn interacts with the mTOR (mechanistic target of rapamycin)/Rictor (rapamycin-insensitive companion of mTOR)/SIN1 (stress-activated protein kinase interacting protein 1) complex (mTORC2) leading to Akt activation (Wang et al.,2013).

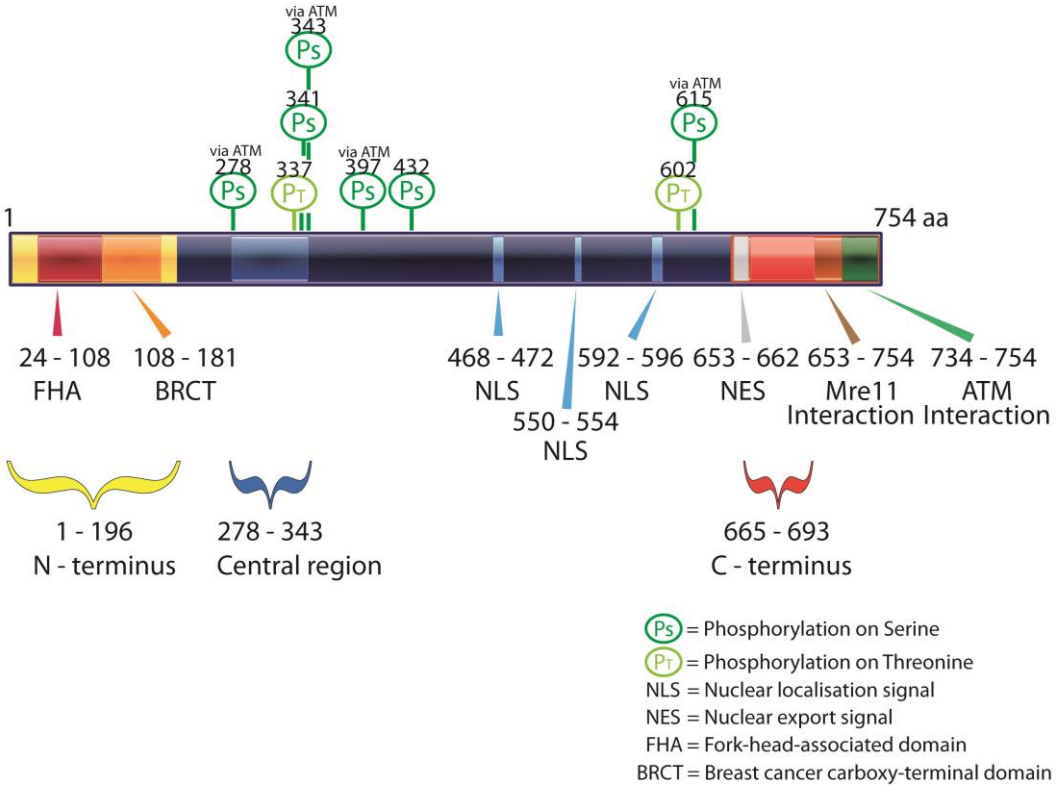

Figure 6: Protein structure of NBN

Figure 6 displays the protein structure of NBN. The phosphorylation sites and types are indicated. The different domains that have been found are visualized in different colors and their location is labeled.

Several mouse models of NBS have been created. Studies on these models were able to point out the essential role of *Nbn* in the development of the central nervous system (CNS) (Frappart et al.,2005; Assaf et al.,2008; Dar et al.,2011; Rodrigues et al.,2013; Liu et al.,2014) and the eye (Yang et al.,2006; Rodrigues et al.,2013). Additionally Nbn was found to be involved in the class switch recombination (Kracker et al.,2005) and V(D)J recombination (Saidi et al.,2010) within the immune systems development, maturation and adjustment. At chromosome ends Nbn is important to maintain telomeres (Ranganathan et al.,2001). The function of *Nbn* in mice so far has been intensively investigated in the CNS, B- and T-cell development.

1.2 Skin and hair

The skin is the organ of the body forming the protective barrier against environmental threats. Together with its appendixes it protects the organism against infections, damaging agents, liquid loss and extreme temperatures. Due to its protective function skin itself is continuously injured on various levels and to various extends. Therefore skin needs a high ability for self-renewal which is accomplished by stem cells within. Proliferation defects can lead to diseases concerning reduced protectoral function of the skin, non-effective wound healing or cancer, depending on hypo- or hyper-proliferation.

1.2.1 Structure of the skin

The skin of mammals is composed of three layers: epidermis, dermis and subcutis. The inner layer is the subcutis. Blood vessels and nerve fibers connecting the skin with underlying tissues are located in the subcutis along with fat cells. The subcutis borders against the collagen rich dermis, while the keratinized epidermis forms the outer layer. The mesenchymally derived dermis provides support and nourishment for the epidermis (Wang et al.,2012). Epidermis and dermis are being separated by a basement membrane formed of extracellular matrix proteins. Ectoderm derived epidermis consists of keratinocytes in different stages of maturation which are arranged in distinguishable layers. Looking from the skin surface these are the Stratum corneum, Stratum lucidum, Stratum granulosum, Stratum spinosum and the Stratum basale, which borders against the basement membrane (BM) (Figure 7). Stratum corneum, Stratum granulosum and Stratum spinosum are also referred to as suprabasal layers while Stratum basale is also named basal layer. High numbers of intermediate filaments assembled of keratin proteins ensure a tight connection between epidermal cells. Within the basal layer cells are highly proliferating. They divide a limited number of cell cycles, differentiate and then detach from the BM to turn into cells of the suprabasal layers thereby traveling towards the skin surface (Barrandon and Green,1987). This process is called cornification and comprises many changes in gene expression. One example is the change in Keratin expression between the layers. Keratin 15 is expressed in stem cells of the hair follicle and the basal keratinocytes (Liu et al.,2003; Morris et al.,2004). Basal keratinocytes, the cells of the Stratum basale, express Keratin 14 while cells of all layers more differentiated (suprabasal layers) express Keratin 10 (Fuchs and Green,1980). The

cornification is not a normal cell death as cells have to be kept in their positions (Eckhart et al.,2013). Cells that finally reach the outmost layer are anucleated, elongated and dead. These cells are being shed and replaced by outward moving cells approximately every two weeks in human. Cells of the basal layer, considered progeny stem cells, on their part can arise from epithelial stem cells that reside in the hair follicle bulge area (Cotsarelis et al.,1990; Jones and Watt,1993; Jones et al.,1995; Taylor et al.,2000; Oshima et al.,2001; Ito et al.,2005; Levy et al.,2007).

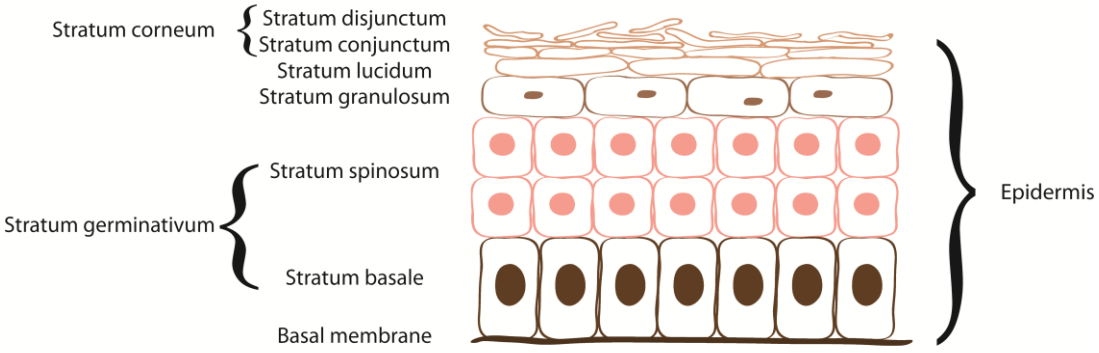

Figure 7: Layers of the epidermis

The different layers of the epidermis are displayed in Figure 7. The basal membrane forms the border towards the dermis. On it the cells of the Stratum basale are localized. Those proliferating cells differentiate, moving towards the skin surface. During this movement they turn into cells of the Stratum spinosum, Stratum granulosum, Stratum lucidum, Stratum conjunctum and Stratum disjunctum. Those last two layers together form the Stratum corneum.

Epidermis consists mainly of keratinocytes and hair follicles but also contains melanocytes for pigmentation, sensory Merkel cells for pressure detection, dentritic Langerhans cells for the immune defense system of the skin and a small amount of extracellular matrix proteins. Dermis on the other hand consists mostly of extracellular matrix proteins. Cells localized in the dermis are fibroblasts, smooth muscle cells, neurons for pain and temperature determination, Mast cells for the immune response and arrector pili muscles that are able to raise the hair. The blood vessels of the skin lie within the dermis. Hair follicles, sebaceous glands and perspiratory glands reach into the dermis but are parts of the epidermis. The opening of the hair channel in the surface of the skin is named Infundibulum. Its lower end is aligned with the sebaceous gland duct insertion into the hair channel (Schneider et al.,2009).

1.2.2 The hair follicle

The first signs of a developing hair follicle can be found around mouse embryonic day 14.5. At this time point a thickening of the epidermis at the side of a later hair follicle can be observed. The placode protrudes slightly into the dermis which gives the induction signal (first dermal signal) and starts the down growth of the placode into the dermis. Thereby a cluster of dermal mesenchymal cells is enveloped by the matrix cells of the down growing developing hair follicle, forming the dermal papilla (DP) (Figure 8) (Hardy,1992; Kishimoto et al.,2000; Wang et al.,2012). The specialized fibroblasts of the DP are thought to control the number of matrix cells and through this influencing the hair size (Paus and Cotsarelis,1999). The cells of the DP release the second dermal signal causing the placode derived cells (matrix cells) to proliferate rapidly thereby producing the hair shaft and inducing maturing of the hair follicles (Hardy,1992; Paus and Cotsarelis,1999; Kishimoto et al.,2000; Wang et al.,2012). The lower part of the hair follicle, where this takes place, is the hair bulb. Reaching the downward boarder of the dermis the hair follicle is mature (Alonso and Fuchs,2006). The bulb contains, besides the dermal papilla and transient amplifying matrix cells, the hair follicle pigmentary unit (Schneider et al.,2009). The pigmentary unit is formed by melanocytes distributed in the hair matrix (Paus and Cotsarelis,1999). Melanocytes of pigmentary unit of the hair produce the hair pigment and thereby color. They originate in the neural crest (Sieber-Blum and Grim,2004; Sieber-Blum et al.,2004). The pattern of hair follicles is controlled by activators and inhibitors like proteins of the Wnt (wingless-type MMTV integration site family) pathway, Dkk-1 (Dickkopf-1), ectodysplasin A receptor (Edar) and BMPs (bone morphogenetic proteins) (Fuchs,2007; Wang et al.,2012).

The hair follicle is constantly separated from the dermis by the basement membrane and therefore is a structure of the epidermis (Alonso and Fuchs,2006). During down growth and rod formation the matrix cells undergo a limited number of cell divisions before differentiation. Those transient amplifying cells cause the hair follicles enlargement to a diameter of several cells. The inner matrix daughter cells travel upward and differentiate into concentric cylinders, building the central hair shaft and engulfing the hair channel. This structure is named inner root sheath (IRS) (Figure 8) (Alonso and Fuchs,2006). Both the IRS and the hair shaft differentiate into three distinguished cell layers (Fuchs,2007). The IRS cells are dead keratinized cells that support the hair shaft. The hair shaft is a fibrous structure that consists of compacted

terminally differentiated dead keratinocytes (Trichocytes) (Schneider et al.,2009). IRS cells accompany the hair shaft during outgrowth and degenerate till they reach the upper part of the hair follicle and apoptosis is induced (Lindner et al.,1997). The hair shaft growing out of the skin surface is not surrounded by IRS cells anymore (Alonso and Fuchs,2006). Besides IRS the hair follicle contains an outer root sheath (ORS). IRS and ORS are separated by the companion layer (Fuchs,2007). The ORS also contains melanocytes (Staricco,1963), Langerhans'cells (Gilliam et al.,1998) and Merkel cells (Kim and Holbrook,1995). It remains in contact to the basement membrane while the inner layer that differentiates to form the IRS has no connection to the basement membrane (Fuchs,2007).

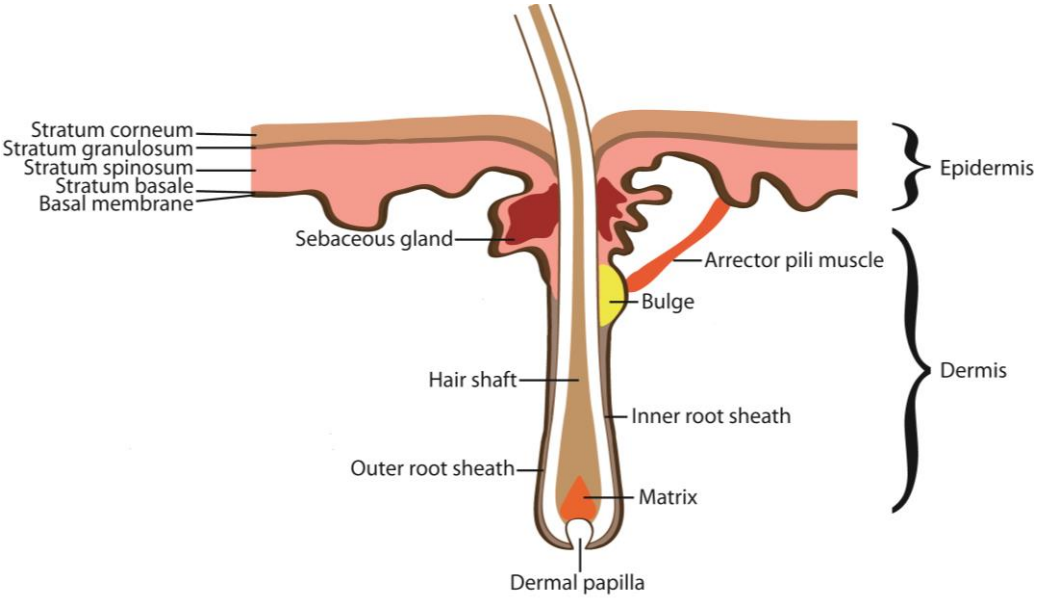

Figure 8: Skin and hair follicle structure

Figure 8 shows the layout of the epidermis. The hair follicle and the sebaceous gland are a part of the epidermis and are surrounded by the basal membrane. This separates all epidermal structures from the dermis. The structural design of the hair follicle with its different compartments is illustrated.

A part of the ORS is the hair bulge. It is located at the insertion of the arrector pili muscle below the opening of the sebaceous gland and marks the end of the permanent portion of the hair follicle (Figure 8) (Cotsarelis et al.,1990). It contains hair follicle stem cells taking part in regeneration of hair during anagen phase (Paus and Cotsarelis,1999). During every down growth of the hair follicle a cell layer is added giving the typical bulge structure. The bulge stem cells are able to form every cell line

of a mature hair follicle (Taylor et al.,2000; Oshima et al.,2001). The bulge remains within the skin even if the rest of the hair is ripped out (Cotsarelis et al.,1990).

1.2.3 Hair cycling

The hair in mammals undergoes a continuous cycle of growth (anagen), regression (catagen) and resting (telogen) (Figure 9) (Alonso and Fuchs,2006). In mice the first mature hair follicles can be found six days after birth (P6) on their backs (Alonso and Fuchs,2006). The hair growth directly after birth still belongs to the hair follicle morphogenesis and does not represent the first anagen phase. Only after first catagen and telogen phases took place the first real anagen phase follows (Muller-Rover et al.,2001). The hair cycle progresses in a wave like form, e.g. first catagen starts at P14 at the head and reaches the tail around P18 (Alonso and Fuchs,2006). First telogen follows at P19 and lasts around two days while later telogen phases can last over two weeks (Alonso and Fuchs,2006). The first anagen phase follows around four weeks after birth (Muller-Rover et al.,2001). While the mouse ages synchronization between hair cycles all over the body decreases (Plikus and Chuong,2008). The correct and continuing cycling of the hair needs many different factors and their interactions. For example anagen phases are terminated with, among other factors, fibroblast growth factor 5 (FGF5) (Hebert et al.,1994; Rosenquist and Martin,1996). Hair follicles during this cycle stages are characterized as long and straight, but they are bend to a degree that the hair lies flat on the body surface (Alonso and Fuchs,2006). After differentiation of all available matrix cells in the hair follicle during anagen phase catagen onset starts (Alonso and Fuchs,2006).

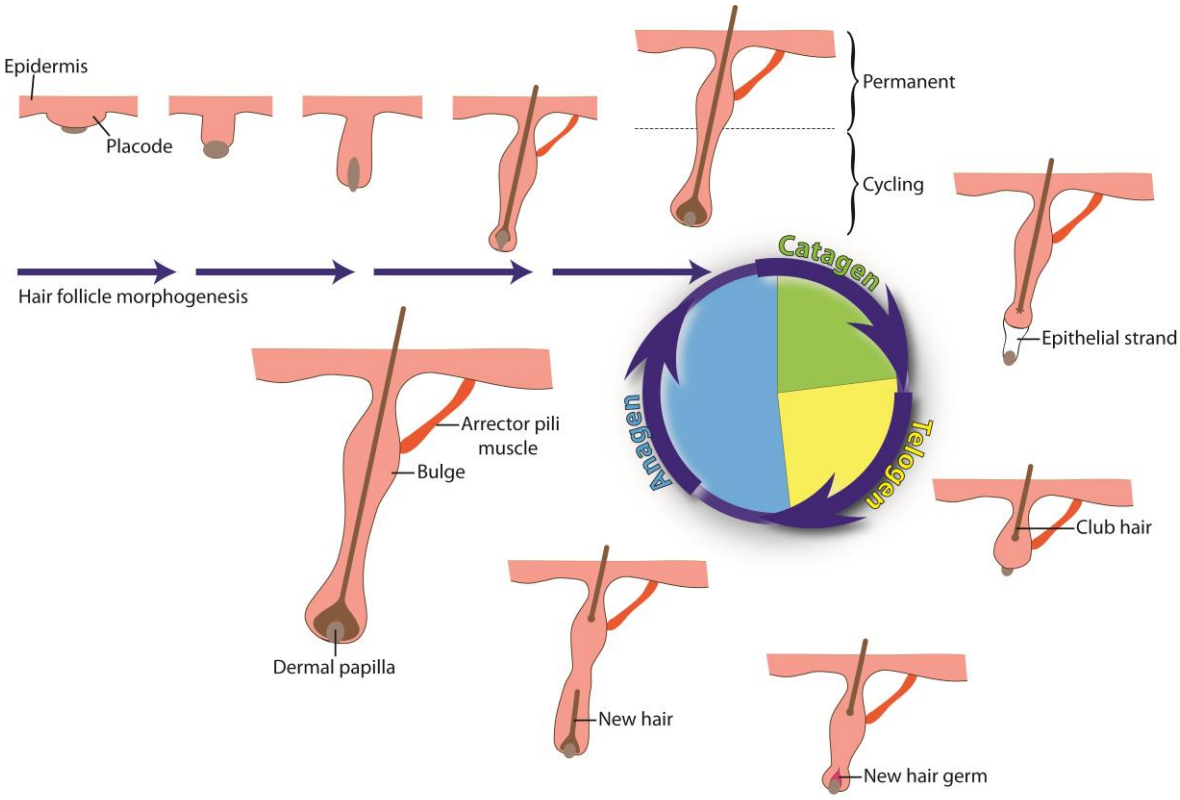

Figure 9: The hair cycle

During embryo development the hair follicle morphogenesis starts and continues after birth. The follicle elongates, the hair is produced and the hair cycle starts. It is divided into anagen, catagen and telogen phase. During catagen phase the hair stops growing and retreats to the skin surface. Through the epithelial strand the dermal papilla stays connected and follows towards the surface. Once the regression continued till the bulge and arrector pili muscle are reached it stops and the club hair is formed. The follicle can rest in telogen phase. Due to a new signal down growth of the follicle is initiated and a new hair germ is formed. This and the growth of the hair are included in anagen phase. The new hair produdes through the same opening in the skin and continues to grow till the next catagen phase follows. Adapted from Fuchs, 2007 (Fuchs,2007)

The catagen phase during hair growth is the phase in which regression takes place. This is established through apoptosis of most follicular keratinocytes and additional melanocytes (Slominski et al.,1994; Lindner et al.,1997). The end of catagen is characterized with condensing of the dermal papilla and its upward movement till it is below the hair follicle bulge (Figure 9) (Paus and Cotsarelis,1999). If the DP is not able to reach the bulge, the hair is not processed any further and quits the cycling, meaning this hair is not regenerated but lost. This process can be induced by hairless protein (Ahmad et al.,1998; Panteleyev et al.,1998; Potter et al.,2001). The only known hair type where this doesn't apply are the whiskers of rodents. For those the dermal papilla never reaches the bulge during cycling (Fuchs,2007). During catagen apoptosis of epithelial cells is observed in ORS and bulge cells but not within cells of the IRS

(Lindner et al.,1997). The hair shaft ceases growth, closes and rounds its end thereby forming the club hair. It rises up to the non-cycling upper follicle and stays anchored there during telogen (Figure 9). An epithelial strand connects the DP with the upper follicle and retracts as the DP nears the upper part (Alonso and Fuchs,2006). This strand is completely disintegrated when the dermal papilla resides directly underneath the permanent and non-cycling upper follicle (Fuchs,2007).

Resting or quiescence phase of hair follicle cycling is the telogen phase. While telogen is named resting phase it does still involve a high number of changes in gen activities (Lin et al.,2004). During this phase the hair shaft turns into a dead club hair that can be shed later e.g. during washing (Paus and Cotsarelis,1999). During telogen the hair follicle stem cells reside on the base of the follicle close to the dermal papilla. A new induction signal can stimulate the stem cells causing them to proliferate and form a new hair (Alonso and Fuchs,2006). The stem cells that are able to form a new hair originate within the bulge (Cotsarelis et al.,1990).

During anagen phase the new hair is synthesized (Figure 9). The synthesis is similar to the morphogenesis of hair during embryonic development (Hardy,1992; Alonso and Fuchs,2006). The new hair protrudes through the skin surface using the same opening the former hair occupied (Alonso and Fuchs,2006). With aging of the individual the telogen phase elongates leading to a decelerated hair growth (Schneider et al.,2009).

1.2.4 Differences in epidermal structures between human and mice

Although the general layout of the epidermal structures and the hair cycling in human and mouse is congruently there are differences in the details.

For mice the maintenance of the fur is more crucial compared to humans (Fuchs,2007). In mice 8 types of hair are discriminated. Those are pelage (coat hair), vibrissae (Whiskers), cilia (eyelashes), tail hair, ear hair, hair around feet, nipples, genital and perianal area (Nakamura et al.,2001; Schmidt-Ullrich and Paus,2005; Schneider et al.,2009). While in humans two major types of hair are discriminated: heavily pigmented terminal hair (e.g. on the head) and vellus hair (e.g. on the face) (Schneider et al.,2009). In both species the number of hair follicles per cm^2 is strongly dependent on the body region. In mice club hair stay within the hair channel even when a new hair starts to grow out the same skin opening. This can happen for more than one

cycle, accumulating club hair which contributes to the tightness of the animals fur (Schneider et al.,2009). Human club hair are pushed out during the outgrowth of a new hair and are lost. At birth humans have around 5 million of hair follicles. While the body growth no new hair follicles are added, only existing follicle change their appearance and size and thereby the growing hair (Paus and Cotsarelis,1999). While human fetal hair follicle cycling is synchronized it starts getting non-synchronized after birth. In adult humans every hair has its own cycle rhythm (Paus and Foitzik,2004; Schneider et al.,2009). The hair cycle in mice starts in a wavelike form from back to tail with a very high synchronization. While aging the synchronicity decreases but is not completely lost. The length of the hair cycle phases increases with age in both human and mice. In mice this gain is the same for all over the body, while in human the cycling of hair varies extremely depending on the body region. The anagen phase of hair follicles on the human scalp can last two to 8 years. Within the area of the eyebrow on the other hand it only lasts two to three months. Duration of the anagen phase in this way also determines the maximal hair length for every tissue area (Paus and Cotsarelis,1999). The human scalp hair can rest in telogen phase up to two or three months. Each day a number of 50 to 150 scalp hair are shed due to telogen (Paus and Cotsarelis,1999). In human testosterone has a strong effect on hair growth. It influences the hair via the androgen receptor of the DP (Sawaya,1994; Kaufman,1996). It can cause increases in hair follicle sizes as in growth of a beard during male adolescences or cause miniaturization of hair follicles on the scalp leading to a bald head. The consequence of testosterone depends on the number of androgen receptors, androgen metabolism and the secretory response of the dermal papilla cells (Hembree et al.,1996; Hibberts et al.,1998)

For humans the maintenance of a dense layer of epidermis is an important way for self-protection of the human body (Fuchs,2007). The epidermis of mice is thick at first but thins out two weeks after birth during the first telogen phase and remains thin. It has a size of 10-15 µm on the body and in areas with thick epidermis e.g. footpad 150-400 µm. In both human and mice the epidermis is thicker in areas lacking hair follicles. Human thick epidermis reaches up to 300-400 µm but thin epidermis still has a size of 50-100 µm. These differences depend on the number of cell layers within the epidermal layers. For example the spinous layer is built by multiple keratinocyte layers in humans while in mice it is always one keratinocyte layer. Stratum lucidum does not exist in mice and in human it can be found only in hair free areas like the palm. There

are different types of glands in human and mice. Mice have vibrissae. Those are not the same as whiskers in human males. Human whiskers are terminal hair without further use while vibrissae are important e.g. for the orientation in dark. The vibrissae hair bulb is surrounded by a blood sinus and free ending nerve fibers. Together those structures form a sensory organ.

Another major difference is the pigmentation of the epidermis. The cells responsible for this are melanocytes. In humans they are distributed throughout the epidermis while in mice they are only found in the pigmentary unit of the hair and in the hair itself. In human melanocyte contribute in a high level to the protection against UV light. The number of melanocytes remains the same even if the skin is pigmented stronger. This pigmentation only depends on the activation level of the melanocytes. In mice the skin color can also change. This is dependent in the hair cycle phase. During anagen phase skin is grey to black and converts to a pale pink in telogen phase.

1.2.5 Psoriasis

In humans various skin diseases are known. Those range from infections, reactions to substances, chronic conditions up to cancer. One of the most wildly spread diseases with a high impact on the patient's life quality is psoriasis.

Psoriasis was described for the first time as a distinguished disease by Robert Willan in 1808 (Willan,1808). Psoriasis is a chronic skin disease, with a high variation in distribution from 0 % up to 8,5 % in the population dependent on age, race and geography (Christophers,2001; Parisi et al.,2013). There are different clinical manifestations of psoriasis. Those forms are guttate psoriasis, pustular psoriasis, erythrodermic psoriasis and plaque psoriasis (Griffiths and Barker,2007). Plaque psoriasis is also known as psoriasis vulgaris and is the most common type of the disease (Griffiths and Barker,2007). As most studies were performed on psoriasis vulgaris I will furthermore refer to it as psoriasis.

Except very limited exceptions humans are the only species in which psoriasis occurs in nature. Only two cases in monkeys are known so fare. One case describes it in a rhesus monkey (Lowe et al.,1981) and another one in a cynomolgus monkey (Zanolli et al.,1989).

Compared to the rest of the population patients with psoriasis exhibit a decreased risk to develop other skin diseases like allergic contact dermatitis (Henseler and Christophers,1995). On the other hand the rate of obesity, heart diseases and diabetes seems to be elevated but it is not known if those are negatively influenced by psoriasis or provide a background for psoriasis outbreak (Henseler and Christophers,1995; Basko-Plluska and Petronic-Rosic,2012). The risk for non-melanoma skin cancer, such as squamous cell carcinoma and basal cell carcinoma, is raised while melanoma development is comparable to non-patient population (Pouplard et al.,2013). The increase in non-melanoma skin cancer is dependent on the prior treatment of psoriasis with immunosuppressors and PUVA (8-methoxypsoralen-ultraviolet-A) (Pouplard et al.,2013). Development of solid tumors that are commonly linked to smoking and alcohol consumption are seen more often in psoriasis patients but like diabetes this might not be a consequence but a cause of psoriasis (Pouplard et al.,2013).

The psoriatic areas in patients are sharply distinguishable from non-affected areas. Psoriasis plaques are reddish, itchy, scaly and dander are silvery. The disease mostly appears on body parts were skin is stretched repeatedly like joints. Additionally nails are often affected and an inflammatory arthritis associated with psoriasis (psoriatic arthritis) can appear (Moll and Wright,1973; Hertl,2011). In psoriasis uniform elongation of rete ridges and acanthosis (thickening of the epidermis) can be seen. Simultaneously thinning of suprapapillary epidermis, parakeratosis (nucleus is not degraded), increase in amount of capillarys, a thinning or absence of the granula layer takes place and leucocytes (e.g. Neutrophils and Mast cells) infiltrate the dermis (Griffiths and Barker,2007; Gudjonsson et al.,2007; Hertl,2011).

According to the point of outbreak of disease psoriasis is subdivided in two types (Henseler and Christophers,1985; Stuart et al.,2002). For type 1 psoriasis the first outbreak of the disease occurs under the age of 40 (Henseler and Christophers,1985).) Type 1 is associated with human lymphocyte antigen (HLA) Cw6 and heredity transmission while type 2 is not inherited. Type 2 psoriasis has its onset at an age around 60 years (Henseler and Christophers,1985). The gender of the parent transmitting psoriasis seems to be of relevance. Children from fathers with psoriasis develop the disease more often than those of a mother with psoriasis (Burden et al.,1998; Rahman et al.,1999). The same applies for psoriatic arthritis (Rahman et al.,1999). The role of a genetic component, which is indicated by psoriasis occurring

more often within families, is strengthened by bone marrow transplantations. Patients with psoriasis receiving a bone marrow transplant were free of psoriasis afterwards (Eedy et al.,1990; Jowitt and Yin,1990; Mori et al.,2012). Another patients receiving transplant from a donor with psoriasis was reported to develop psoriasis even while he was psoriasis free before (Snowden and Heaton,1997). In addition several possible gene loci for psoriasis were found (reviewed in (Basko-Plluska and Petronic-Rosic,2012)). As in bone marrow transplant patients the immune cells from the patient are destroyed and replaced with immune cells arising from the transplant, those observations implicate an involvement of the immune system in psoriasis development (Snowden and Heaton,1997).

Psoriasis is considered an autoimmune disease caused by B- and/or T-cell activation without a detectable inflammation or other source (Davidson and Diamond,2001). The T-cell population accumulating in psoriasis produces type 1 cytokines and expresses Interleukin-17 (Uyemura et al.,1993; Teunissen et al.,1998). In non-affected skin areas of psoriasis patients levels of some cytokines, e.g. TNF-α, IL-1α and IL-1β, are raised compared to non-patient population (Uyemura et al.,1993). Additionally T helper cells type 1 and type 17 were identified in psoriasis lesions (Lowes et al.,2008). Both Interleukine-17 level and Interleukine-22 expression is elevated in psoriasis (Wolk et al.,2006; Lowes et al.,2008). The expression patterns of many proliferation modulating factors were researched in the skin of psoriasis patients. For example Signal transducers and activators of transcription 3 (Stat3) is activated in psoriasis (Sano et al.,2005) and blockage of Stat3 activation with STA-21 (deoxytetrangomycin, antibiotic) leads to a recovery of psoriasis (Song et al.,2005; Miyoshi et al.,2011). In cell culture STA-21 reduces the expression of the Stat3 transcriptional target and cell cycle progression promoter c-Myc (myelocytomatosis oncogene) (Miyoshi et al.,2011). An up regulation of c-Myc can be seen in culture of cells from psoriasis lesions but the level of c-Myc and p53 expression was found to be unchanged in psoriasis patients (Elder et al.,1990; Schmid et al.,1993). This indicates differences between cells within the actual lesion and cells of psoriasis patients in culture. Therefore the underlying processes of psoriasis cannot be mimicked in cell culture. For research on psoriasis various mouse models were created. They include spontaneous, transgene, reconstituted and xenograft models but none were able to mimic human psoriasis in all known factors (Gudjonsson et al.,2007; Wagner et al.,2010; Johnson-Huang et al.,2012; Augustin et al.,2013; Perera et al.,2014). This is due to differences in the skin of human and mice described before.

1.2.6 DNA damage in the skin

The skin forms the outer barrier of the body against the environment. Due to this barrier function and the exposure to UV from sunlight, the skin cells have a high risk to DNA damages caused by exogenous factors. Epidermal cells also have an elevated risk to obtain DNA damages due to mistakes during replication because skin cells undergo a constant proliferation and division to replace the shed cells. In addition the IR from radiotherapeutic treatment has a high effect on skin. This is indicated by occurrence of acute and chronic dermatitis and a higher rate of skin cancers in patients with IR treatment (Goldschmidt and Sherwin,1980). In all cases proper DNA damage signaling and repair is essential to maintain a functional and healthy skin. As the example of NBN deficient patients shows, a defective DNA damage signaling and repair causes a vast number of different defects in the skin up to development of skin cancer.

About the concrete functions and pathways of DNA damage signaling and repair in skin little is known. So fare it was shown that continuous application of UV radiation results in a reduced speed in degradation of the UV products in epidermal stem cells and progenitor cells compared to more differentiated skin cells (Nijhof et al.,2007). This can raise the amount of DNA damages after a certain dose of UV. It was observed that the apoptosis rate after UV B depends strongly on the epidermal layer. It decreases from the inner layer to the outer layer (Schafer et al.,2010). Basal cells show a high rate of apoptosis while suprabasal cells show much lower apoptosis levels (Schafer et al.,2010). After UV B irradiation NFE2L2 (Nuclear factor (Erythroid-derived 2)-like 2) expression selectively protects suprabasal keratinocytes against apoptosis by activation of cytoprotective genes and resulting amplified ROS detoxification (Schafer et al.,2010). This finding explains the apoptosis gradient after UV B application and the mechanism might contribute to skin cancer prevention by eliminating damaged stem cells that are located in the basal epidermal layer (Schafer et al.,2010). On the other hand it was also demonstrated the epidermal stem cells are resistant to radiation while progenitors are irradiation sensitive (Rachidi et al.,2007). The irradiated epidermal stem cells show a down regulation in genes involved in apoptosis while genes enhancing the proliferation are up regulated compared to progenitor cells (Rachidi et al.,2007). For example p53 is normally expressed throughout the complete epidermis but after a phosphorylation due to UV light phosphorylated p53 can only be observed in basal epidermal layers, where the epidermal stem cells are located (Finlan et al.,2006). In addition activation of EGFR (epidermal growth factor receptor) can be observed in

epidermal cells after UV treatment (El-Abaseri et al.,2006). EGFR activation leads to an elevated rate of proliferation of epidermal cells and a suppression of apoptosis. Both functions of EGFR can contribute to formation of epidermal hyperplasia (El-Abaseri et al.,2006).

In keratinocyte stem cells DNA breaks, both single and double strand breaks, are repaired faster and more efficient then in keratinocyte progenitors (Harfouche et al.,2010). The fast repair is dependent on the level of Fgf2 (fibroblast growth factor 2), which is lower in progenitors (Harfouche et al.,2010). Artificial elevation of Fgf2 in progenitors leads to an increase in repair activity comparable to that seen in epidermal stem cells (Harfouche et al.,2010). This fast repair in epidermal stem cells contributes to the resistant of stem cells against apoptosis as damages are repaired before cell cycle checkpoints can be activated. Along with the findings in keratinocyte stem cells, multipotent hair follicle bulge stem cells have develop two mechanisms to raise their resistance against cell death due to DNA damages (Sotiropoulou et al.,2010). They show stabilization of p53 and a higher expression of Bcl-2 (B-cell lymphoma 2) (Sotiropoulou et al.,2010). In addition they also have an elevated rate of NHEJ DNA repair that is controlled by DNA-PK (Sotiropoulou et al.,2010). NHEJ is known to be error prone and a consequence of these mechanisms in hair follicle stem cells is the accumulation of DNA damages without undergoing a necessary apoptosis. This raises the risk to develop skin cancers.

These findings illustrate the importance of proper DNA damage signaling and repair in the epidermis. Two mouse models with a deletion of a DNA damage signaling protein underline this. The deletion of *ATR* and *ATR* and *p53* in adult mice leads to a defect in hair follicle regeneration and a high inflammation of the inner epithelium (Ruzankina et al.,2007; Ruzankina et al.,2009). This effect is more prominent in double deleted animals than in those with Atr deletion alone. Albeit slow both double and single defective animals regenerate hair follicles (Ruzankina et al.,2009(Ruzankina et al.,2007)). After continuous depilation in ATR deleted mice the hair is not regenerated due to a loss of hair follicle stem cells (Ruzankina et al.,2007). The animals show an accumulation of defective cells in the epidermis that inhibit the regeneration of new cells from the healthy epidermal stem cells. The inflammation of the intestine finally results in the death of the animals (Ruzankina et al.,2009). Brca1 deficiency after embryonic day E12 in mice results in a reduced number of hair follicles and a

continuous degeneration of the existing hair follicles (Sotiropoulou et al.,2013). No hair is formed and the hair follicle stem cells are lost during aging of the animal. A combined deletion of p53 completely rescues the Brca1 phenotype (Sotiropoulou et al.,2013). In adult mice deletion of Brac1 leads to an impairment in regeneration of hair (Sotiropoulou et al.,2013).

1.3 Krox20

A long term study on the effect of deletion of the DNA damage signaling and repair protein Nbn in the skin and its influence on hair follicle regeneration and cycling was conducted. Therefore a mouse model with a knockout that would not affect the inner epithelium to such an extent as in the Atr and p53 deficient mice was needed (Ruzankina et al.,2009). Additionally the risk for premature lethality had to be limited and the possibility for the mice to properly start the development of normal skin and hair follicles before the onset of the knockout was wanted. Therefore an *Nbn* deletion under Krox20-Cre recombinase was done in this study.

Krox20 is also known as EGR2 (early growth response 2) (Joseph et al.,1988). In the following I will always refer to it as Krox20 as the Cre recombinase is named Krox20-Cre recombinase. The *Krox20* gene encodes a transcription factor containing three zinc-finger domains which is active during G0/G1 phase (Chavrier et al.,1988; Chavrier et al.,1990). Expression of the 3,2 kb transcript is observed in testis, thymus, spleen, epidermis, hair follicle, neural crest cells and in the developing CNS (Chavrier et al.,1988; Wilkinson et al.,1989; Gambardella et al.,2000; Young et al.,2003). Krox20 controls myelination of the Schwann cells and therefore the myelination within the peripheral nervous system (Topilko et al.,1994). Deletion of *Krox20* leads to uncompleted myelin sheaths, continuous proliferation and apoptosis of Schwann cells (Topilko et al.,1994; Zorick and Lemke,1996). In Schwann cells the expression of *Krox20* inhibits apoptosis via TGFβ (Transforming growth factor β) and inactivates JNK(c-Jun N-terminal kinase)-c-Jun pathway thereby causing cell cycle exit and subsequently proliferation arrest (Parkinson et al.,2004). These functions of Krox20 serve to protect Schwann cells and ensure an elongated lifetime of these cells. In addition a role in endochondral formation of bones was described (Levi et al.,1996) and

its deletion results in alteration of hindbrain development (Schneider-Maunoury et al.,1993).

Krox20 expression was described within the epidermis and the hair follicle starting during the hair follicle development and continuing after birth (Gambardella et al.,2000; Young et al.,2003). It was demonstrated that the expression of *Krox20* has its onset at E16 as small patterns in epithelial cells on the upper part of the hair germ (Gambardella et al.,2000). At E19 it can be found in the sebaceous gland, the bulge area and the developing hair canal (Gambardella et al.,2000). Shortly before (E21) and after birth *Krox20* is expressed in the lower part of the hair germ and remains expressed in the inner layer of the ORS of the hair (Gambardella et al.,2000). Additionally it is expressed in keratinocytes of the hair matrix (Gambardella et al.,2000). This expression is observed on both sides of the dermal papilla (Gambardella et al.,2000; Schlake,2006). Due to a colocalization and putative binding sides with Igfbp5 (Insulin-like growth factor binding protein 5) a role of Krox20 in hair shaft differentiation and zigzag hair development was suggested (Schlake,2006) .

The expression pattern of Krox20-Cre recombinase in the skin was studied and overall matches with the *Krox20* expression (Young et al.,2003). It starts at P1 as sparse and small patterns in the back skin of the mice (Young et al.,2003). Then it can be found in the epidermis around the hair follicle and the upper parts of the hair follicle (P10 to P18) (Young et al.,2003). In adult mice Krox20-Cre expression can be seen in the complete back skin but is absent in the tail and footpad skin (Young et al.,2003).

1.4 Project

Skin is the outer protection for our body and is exposed to various damaging agents all the time. Therefore a functioning damage repair is essential to maintain the barrier function of the skin. That malfunction of DNA damage signaling and repair has a broad impact on the skin can be seen as NBS patients show miscellaneous pathologies of the skin. Still little is known about the DNA damage response and repair pathways and functions in the skin.

To examine the role of Nbn in skin and hair follicles mice with a knockout of *Nbn* in *Krox20* specific tissue were generated. With this model the influence of Nbn in the

homeostasis of the skin and hair was researched as the onset of deletion occurs after birth of the mice. This was the first study to evaluate the function of Nbn in skin.

The interesting question on whether Nbn and Atm function together in DNA damage signaling and repair in the skin was looked into. As p53 is known to play a role in cell cycling and apoptosis the influence of p53 on the *Nbn* deleted mice was worth investigating. Furthermore a rescue of a neurological phenotype with the combination of *Nbn* deletion and *p53* was observed (Frappart et al.,2005). On the other hand the phenotype was aggravated by a deletion together with *Atm* (Dar et al.,2011). Those studies were performed in the neuronal system of the mice and the question was if those observations are similar in skin. Therefore mice with an additional *Atm* or *p53* deletion were created.

2. Materials and Methods

2.1 Materials

2.1.1 Buffers and Solutions

	Chemicals	Concentration
Antigen Retrieval Solution	Citric Acid	1,8 mM
	Sodium Citrate	8,2 mM
	Tween 20	0,05 %
	ddH_2O	
Blocking Solution	BSA	1 %
	Triton X100	0,4 %
	Normal goat serum	5 %
	PBS 1x	
Eosin solution	Eosin Y	14 mM
	Ethanol 70 %	
Hematoxylin solution	Hematoxylin	3 mM
	ddH_2O	1 l
	Sodium iodate	1 mM
	Potassium aluminum sulfate dodecahydrate	105 mM
	Chloral hydrate	303 mM
	Citric acid monohydrate	4 mM
PCR Buffer with $MgCl_2$	KCl	0,5 M
	Tris-HCl pH=8.3	0,1 M
	$MgCl_2$	0,015 M
	ddH_2O	
PBS 10X	Sodium Chloride	137 mM
	Potassium Chloride	27 mM
	Di-Sodium hydrogen phosphate dihydrate	10 mM
	Potassium dihydrogen phosphate	2 mM
	ddH_2O	

Tail Buffer	Tris-HCl (pH=8)	50 mM
	EDTA	100 mN
	SDS	1 %
	NaCl	100 mM
	ddH_2O	
TE 10/1	Tris-HCl (pH=7,5)	1 M
	EDTA	0,5 M
	ddH_2O	

2.1.2 Antibodies

2.1.2.1 Primary Antibodies

Name	**Acronym**	**Host**	**Company**
anti Neutrophils	Neutrophils	Rat	Acris antibodies
Anti-Cytokeratin 15	K15	Mouse	Abcam
Anti-gamma H2A.X (phospho S139)	γH2A.X	Rabbit	Abcam
Anti-IL17	IL-17	Rabbit	Abcam
Caspase-3 activ	Caspase 3	Rabbit	BD Biosciences
Keratin 10	K10	Rabbit	Covance
Keratin 14	K14	Rabbit	Covance
Ki67 (SP6)	Ki67	Rabbit	Thermo Scientific
p53 (CM5)	p53	Rabbit	Vector Laboratories
p63 (H-137)	p63	Mouse	Santa Cruz
PCNA (PC10)	PCNA	Mouse	Santa Cruz
Phospho-Akt (Ser473)	pAkt	Rabbit	Cell signaling
Phospho-Histone H3 (Ser10)	H3P	Mouse	Cell signaling
Phospho-S6 (Ser235/236)	S6	Rabbit	Cell signaling
Phospho-specific p44/42 MAPK (Erk1/2)	Erk1/2	Rabbit	Cell signaling

Phospho-Stat3 (Try705) (D3A7)	pStat3	Rabbit	Cell signaling
Anti-CD3	CD3	Rabbit	Rockland Immunochemicals
53BP1	53BP1	Rabbit	Bethyl Laboratories

2.1.2.2 Secondary Antibodies

Name	Host	Company
Anti-Mouse IgG (H+L)-Cy3	donkey	Dianova
Anti-Rabbit IgG (H+L)-Cy3	donkey	Dianova
Anti-Mouse IgG (H+L)-FITC	donkey	Dianova
Anti-Rabbit IgG (H+L)-FITC	donkey	Dianova
Anti-Mouse IgG (H+L)-Biotin	goat	Jackson
Anti-Rabbit IgG (H+L)-Biotin	goat	Dianova
Anti-Rat IgG (H+L)-Biotin	goat	Jackson
Anti-Mouse IgG (H+L)-HRPO	goat	Dianova
Anti-Rabbit Immunoglobulins/HRP	goat	Dako

2.1.3 Primers

Primer	Sequence (5'-3')
ATMc P1	CCCAGTGTATATGCCACCGACTGAG
ATMc P2	ACCACTCGAAGAACACCGCTTCGC
ATMc P3	GCCTGGTCTACATCCTGAGCTCCAGGACAGCC
HPRT F	GCTGGTGAAAAGGACCTCT
HPRT R	CACAGGACTAGAACACCTGC
Krox20-3F	GTGTCGCGCGTCAGCATGCGTG
Krox20-4R	GGGAGCGAAGCTACTCGGATACGG
Nbn 102F	ATGTGGAAGCTGCTCCCGGC
Nbn 648R	CTGTTTCTTAGATTCAACTGC
Nbs Intron 5 F	ATAAGACAGTCACCACTGCG

Nbs LoxPtestR	AATACAGTGACTCCTGGAGG
NeoSeq#5	TGGGCTCTATGGCTTCTGA
P53neo18.5	TCCTCGTGCTTTACGGTATC
P53x6.5	TATACTCAGAGCCGGCCT
P53x7	ACAGCGTGGTGGTACCTTAT

2.1.4 Chemicals and Kits

Chemical	**Company**
2-mercaptoethanol	Gibco
Acetic acid	Roth
Agarose	Axygen
Biotin-16-dUTP	Roche
Bovine Serum Albumin Fraction V (BSA)	Sigma
Chloral hydrate	Roth
Citric acid monohydrate	Roth
Di-Sodium hydrogen phosphate dihydrate	Merck
Dispase II	Roche
DMEM	Gibco
DPX	Sigma-Aldrich
Eosin Y	Roth
Ethanol	Roth
Ethylendiamin tetraacetic acid (EDTA) disodiumsalt dihydrate	Roth
Formaldehyde	Sigma
Giemsa solution	Sigma-Aldrich
Glycine	Roth
Hematoxylin	Merck
Hepes	Gibco
Hydrogen peroxide	Roth
Magnesium chloride	Sigma
Methanol	Sigma-Aldrich

Methyl green chloride salt	Sigma-Aldrich
Normal goat serum	Vector Laboratories
Paraformaldehyde	Sigma-Aldrich
Potassium aluminum sulfate dodecahydrate	Roth
Potassium chloride	Sigma
Potassium dihydrogen phosphate	Merck
Proteinase K	Roth
Roti-Phenol	Roth
Sodium chloride	Roth
Sodium citrate	Roth
Sodium dodecylsulfate (SDS)	Serva
Sodium iodate	Roth
Sodium pyruvate	Gibco
Streptavidin-Cy3	Sigma
Sucrose	Roth
SuperScript® II Reverse Transcriptase	Invitrogen
Terminal Deoxynucleotidyl Transferase (TdT)	Thermo Scientific
Tris-base	Sigma
Triton X100	Sigma
TRIzol	Invitrogen
Trypsine	Gibco
Tween 20	Roth
Vectashield mounting medium with DAPI	Vector Laboratories
Vectastain ABC Kit	Vector Laboratories
VIP peroxidase substrate kit	Vector Laboratories
Xylene	AppliChem

2.1.5 Instruments

Instrument	Company
TPersonal Thermocycler	Biometra
DNA Engine Thermal Cycler PTC-200	Bio-Rad
PowerPac Basic	Bio-Rad
UV Transilluminator UST-20M-8K	Biostep
EF 28mm f/1.8 USM	Canon
EOS 500D	Canon
Centrifuge 5415R	Eppendorf
Centrifuge 5418	Eppendorf
Centrifuge 5804R	Eppendorf
Thermomixer compact	Eppendorf
MR Hei-Standard	Heidolph Instruments
Unimax 1010	Heidolph Instruments
Manual Rotary Microtome RM2235	Leica Biosystems
Water bath HI1210	Leica Biosystems
NanoDrop 1000	PEQLAB
Basic pH Meter PB-11	Sartorius
pH-Einstabmesskette PY-P10	Sartorius
Vortex Genie 2	Scientific Industries
Cyber-shot DSC-W230	Sony
Bioblock Scientific 92675	Thermolyne Corp.
Excelsior ES Tissue Processor	Thermo Fisher Scientific
AxioCam MRc	Zeiss
AxioImager.A2	Zeiss
HAL 100 halogen illuminator	Zeiss
HBO 100 Microscope Illuminating System	Zeiss

2.1.6 Software

Software	Company
Adobe Illustrator	Adobe Systems
AxioVision	Zeiss
Microsoft PowerPoint	Microsoft Corporation
Microsoft Word	Microsoft Corporation
Sigma Plot	Systat Software, Inc

2.2 Methods

2.2.1 Animals

Animals were kept in the DKFZ (Deutsches Krebsforschungszentrum, Heidelberg, Germany) animal facility with a 12 hours day and 12 hours night rhythm. Cages were individually ventilated. Animals were feed ad libitum.

Killing of the animals was done with CO_2 and cervical dislocation.

2.2.1.1 Tissue preparation

After animals were killed the back skin was collected. The tissue was fixated in 4 % Paraformaldehyde overnight at 4 °C and partially kept in PFA for storage.

To embed tissue samples in paraffin they were placed in plastic holders and embedded using the tissue processor Excelsior ES. This was performed in the routine laboratory of the neuropathology (DKFZ, Heidelberg, Germany). Sections were done using a microtome. Skin was cut into 5 µm thigh sections. They were collected on glass slides, dried at 37 °C overnight and stored in boxes at room temperature.

2.2.2 Gene targeting

Deletion of *Nbn* in the mice was accomplished through excision of Exon 6 using LoxP sites and Cre recombinase. The gene targeting strategy is described by Frappart et al. (Frappart et al.,2005) and is shown in Figure 10. For the studie of Nbn function in

the skin *Nbn* deleted mice were crossed with Krox20-Cre mice (Young et al.,2003) to obtain mice with Nbn depletion in the epidermis.

The Krox20-Cre mice were described by Voiculescu et al. (Voiculescu et al.,2000) and were kindly provided by Patrick Charnay (Institut National de la Sante´ et de la Recherche Medicale, Ecole Normale Superieure, Paris, France). Furthermore mice were crossed with Atm and p53 deficient mice. Mice deficient for p53 (B6.129S2-*Trp53*^{tm1Tyj}/J) were as described by Jacks et al. (Jacks et al.,1994) and were obtained from Jackson Laboratory (Bar Harbor, Maine). Atm deficient mice were described by Herzog et al. (Herzog et al.,1998) and were kindly provided by Peter J. McKinnon (St. Jude Children's Research Hospital, Memphis, USA).

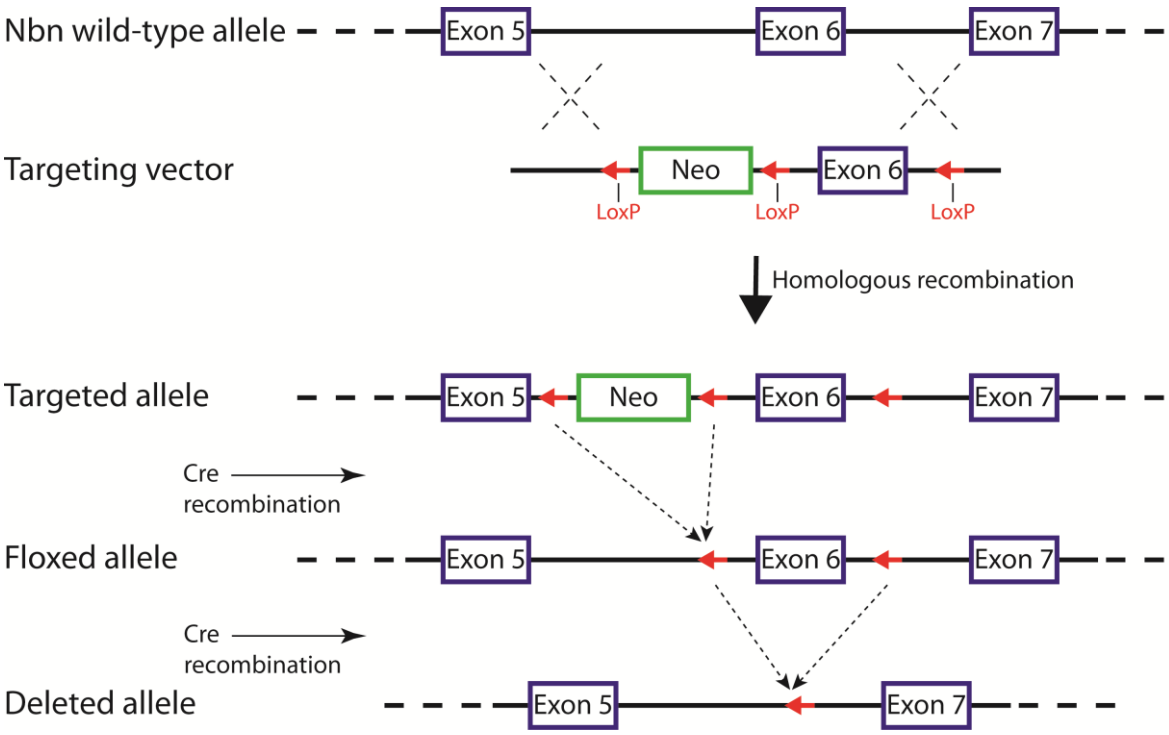

Figure 10: Gene targeting strategy

The gene targeting strategy for generation of Nbn deficient mice is shown in Figure 10. Exons 5, 6 and 7 are depicted. The localization of inserted Neomycin (Neo) cassette and LoxP sites are indicated. The consequences of Homologous and Cre recombination are visualized.

2.2.2.1 Study group for deletion in the skin

The control group (*Nbn*^{Ctrl}) contained two genotypes *Nbn*$^{F/F}$*Krox20-Cre*$^{-}$ and *Nbn*$^{F/\Delta}$*Krox20-Cre*$^{-}$. *Nbn*$^{Krox20\text{-}Cre}$ group consisted of *Nbn*$^{F/F}$*Krox20-Cre*$^{+}$ and

Nbn$^{F/\Delta}$*Krox20-Cre*$^{+}$ mice. The group of p53 deleted mice (*Nbs1*$^{Krox20\text{-}Cre}$*p53*$^{-/-}$) contained mice with the genotypes *Nbn*$^{F/F}$*p53*$^{-/-}$*Krox20-Cre*$^{+}$ and *Nbn*$^{F/\Delta}$*p53*$^{-/-}$*Krox20-Cre*$^{+}$. Mice with the genotypes *Nbn*$^{F/F}$*Atm*$^{F/F}$*Krox20-Cre*$^{+}$ and *Nbn*$^{F/\Delta}$*Atm*$^{F/F}$*Krox20-Cre*$^{+}$ formed the group of *Nbn/Atm*$^{Krox20\text{-}Cre}$ mice.

2.2.3 Confirmation of genotypes

To verify the correct genetic background of mice their DNA was isolated, amplified and analyzed.

2.2.3.1 DNA isolation

To isolate the DNA from tissues for mice the tip of the tails were collected in a 1,5 ml Eppendorf tube. 500 µl Tail Buffer and 25 µl Proteinase K (10 mg/ml) were added to the sample. It was incubated overnight at 55 °C or 2 h at 55 °C (shaking with 1000 rpm). Afterwards the sample was completely dissolved by vortexing. 300 µl NaCl (5 M) were added, it was vortexed and centrifuged 7 min at 14.000 g. The supernatant was transferred into a new Eppendorf tube, 500 µl Isopropanol (100 %) were added, vortexed and centrifuged 7 min at 14.000 g. Supernatant was discarded. 500 µl Ethanol (70 %) were added and the sample was centrifuged 7 min at 14.000 g. All Ethanol was discarded and the pellet was air-dried at room temperature. Then 100 µl $TE_{10/1}$ were added and the sample was vortexed to dissolve the DNA.

2.2.3.2 Polymerase chain reaction for DNA

For each genotype a different polymerase chain reaction (PCR) was performed to amplify the corresponding DNA fragments from the isolated samples.

Atm

	Concentration	**Volume [µl]**
PCR Buffer with $MgCl_2$	10 x	2
dNTP	10 mM	0,5
ATMc P1	10 µM	1

ATMc P2	10 µM	1
ATMc P3	10 µM	1
Taq	5 U/µl	0,4
H_2O		14,1
Total		19

Step	**Temperature [°C]**	**Time**	
Denaturation	94	3 min	
Denaturation	94	30 sec	45x
Annealing	61	30 sec	
Elongation	68	30 sec	
Elongation	68	7 min	
Keeping in machine	18	∞	

The expected DNA fragments were Floxed (897 bp), wild-type (797 bp) and Delta (374 bp).

Krox20-Cre

	Concentration	**Volume [µl]**
PCR Buffer with $MgCl_2$	10 x	2
DMSO	100%	1
dNTP	10 mM	0,5
Krox20-3F	10 µM	0,75
Krox20-4R	10 µM	0,75
NeoSeq#5	10 µM	0,75
Taq	5 U/µl	0,2
H_2O		13,05
Total		19

Step	Temperature[°C]	Time	
Denaturation	94	5 min	
Denaturation	94	30 sec	45x
Annealing	60	45 sec	
Elongation	68	1 min	
Elongation	68	7 min	
Keeping in machine	18	∞	

The expected DNA fragments were wild-type (165 bp) and Krox20-Cre (900 bp).

Nbn

	Concentration	Volume [µl]
PCR Buffer with $MgCl_2$	10 x	2,5
dNTP	10 mM	0,5
Nbs Intron 5 F	10 µM	1
Nbs LoxPtestR	10 µM	1
Taq	5 U/µl	0,4
H_2O		17,6
Total		23

Step	Temperature [°C]	Time	
Denaturation	94	4 min	
Denaturation	94	30 sec	45x
Annealing	60	1 min	
Elongation	65	2 min 30 sec	
Elongation	65	7 min	
Keeping in machine	18	∞	

The expected DNA fragments were wild-type (1432 bp), Floxed (1160 bp) and Delta (576 bp).

p53

	Concentration	Volume [µl]
PCR Buffer with $MgCl_2$	10 x	2,5
dNTP	10 mM	0,5
P53x7	10 µM	0,75
P53x6.5	10 µM	0,75
P63neo18.5	10 µM	0,75
Taq	5 U/µl	0,4
H_2O		17,35
Total		23

Step	Temperature [°C]	Time	
Denaturation	95	4 min	
Denaturation	95	30 sec	45x
Annealing	60	2 min	
Elongation	68	2 min	
Elongation	68	5 min	
Keeping in machine	18	∞	

The expected DNA fragments were wild-type (450 bp) and knockout (650 bp).

2.2.3.3 DNA gel

DNA fragment size and availability were measured using gel electrophoresis to separate the fragments according to their sizes. Therefore an agarose gel was used, samples were loaded together with loading buffer and the gel was run with 120 V. Gel concentration was dependent on the fragment sizes expected. 2 % gels were used for small and 1,5 % gels for middle to big sized DNA fragment separation.

2.2.4 Visualization in the skin

Morphology, cell distribution and the existence of proteins and their modifications within tissue samples were visualized. Visualization of protein expression, modifications and potential colocalization in the mouse tissue was done via Immunohistochemistry and Immunofluorescent staining. Hematoxylin and eosin staining was performed for morphological analysis. Mast cells distribution in the skin was detected by Giemsa staining. TUNEL (TdT-mediated dUTP-biotin nick end labeling) reaction was performed to show apoptotic cells.

For all staining procedures paraffin had to be removed from the sections. Threfore paraffin slides were deparaffinized by putting them in Xylene three times and into Ethanol with declining concentration (100 %, 95 %, 70 %, 50 %) for 5 min each. Afterwards slides were washed in water. Washing steps were always performed with PBS 1x if not mentioned otherwise.

2.2.4.1 Immunohistochemistry

Slides were boiled (2 times 5 min at 700 W in microwave) in unmasking and antigen retrieval solution. After cooling down paraffin slides were treated for 20 min with 3 % Hydrogen peroxide. The sections were washed with PBS 1x and blocked with blocking solution for 1 hour. The primary antibody was diluted in blocking solution and applied to the slides overnight. The next day slides were washed and the secondary antibody was diluted in blocking solution. It was incubated on the slides for 1-2 hours. After washing ABC complex was applied for 30 min at 37 °C. Slides were washed and developed with VIP peroxidase substrate kit to reach a sufficient staining. Afterwards sections were counterstained with Methyl green chloride salt solution and dehydrated by putting them in Ethanol (70 %, 95 %, 100 %) and three times into Xylene. Slides were mounted with DPX, left to air-dry and stored at room temperature.

2.2.4.2 Immunofluorescent staining

Fluorescent staining with one antibody is similar to immunohistochemistry staining. The beginning procedure was the same. The secondary antibody (FITC for green, Cy3 for red) was incubated on the sections for 1 hour at 37 °C. Then mounted with Vector

shield mounting medium containing 4',6-diamidino-2-phenylindole (DAPI) and stored at 4 °C in the dark.

Two proteins in the same tissue were visualized with a fluorescent double staining. For a double staining the same procedure as for immunohistochemistry was used to begin with. When both primary antibodies were known to have a specific binding they were applied at the same time. Both secondary antibodies were also applied together. If the binding of one antibody was weak this antibody was applied first and also bound with its secondary antibody. Afterwards the second primary antibody was incubated overnight and its secondary antibody was administered the next day. Mounting with Vector shield mounting medium containing DAPI was done after both antibodies and their respective secondary antibodies were bound to the sections.

2.2.4.3 Hematoxylin and eosin staining

First the slides were deparaffinized and then stained with Hematoxylin solution (after Mayer). Afterwards they were washed in water for the desired staining. Slides were stained with Eosin solution and residual staining was removed by washing in water. Dehydration was performed and the slides were mounted with DPX, dried and stored at room temperature.

The Hematoxylin and eosin staining was performed in the routine laboratory of the neuropathology (DKFZ, Heidelberg, Germany).

2.2.4.4 Giemsa staining

Giemsa staining was done to visualize Mast cells in the skin samples. The slides were deparaffinized and afterwards stained in preheated Giemsa solution. A washing step in water was done and slides were treated with Acetic acid 1 %. Slides were washed with water and three changes each of Methanol and Xylene prior to mounting with DPX.

2.2.4.5 TUNEL

TUNEL reaction was performed to visualize the DNA fragmentation in apoptotic cells. The slides were deparaffinized and washed with PBS 1x. Then slides were incubated with the TUNEL reaction mix (for 50 µl: Buffer TdT 5x 10 µl + dUTP-biotin 0,33 µl + TdT 20 U/µl 0,75 µl + H_2O 38,92 µl) for 1,5 hours at 37 °C. After washing ABC complex was applied for 30 min at 37 °C. Slides were washed and developed with VIP peroxidase substrate kit to reach a sufficient staining. Afterwards sections were counterstained with Methyl green chloride salt solution and dehydrated by putting them in Ethanol (70 %, 95 %, 100 %) and three times into Xylene. Slides were mounted with DPX, left to air-dry and stored at room temperature.

When a double staining with an antibody was conducted the TUNEL reaction mix was used but no ABC complex was applied. The sections were washed with PBS 1x and blocked with blocking solution for 1 hour. The primary antibody was diluted in blocking solution and applied to the slides overnight. The next day slides were washed, a secondary antibody (FITC) was diluted in blocking solution together with Streptavidin-Cy3. The slides were incubated for 45 min at 37 °C. Afterwards they were mounted with Vector shield mounting medium containing DAPI and stored at 4 °C in the dark.

2.2.5 Keratinocyte isolation

In 50 ml Medium 0,25 g Dispase II were dissolved. Animals were killed. The back was shaven and back skin was isolated. The skin was put dermal side down in Dispase II solution overnight at 4 °C. The next day epidermis and dermis were separated. The epidermis was shaken in Trypsine 5x for 30 min at room temperature. Medium was added to stop Trypsine and cells were singularized. Afterwards the medium was filtered through a cell strainer to remove the debris of hair. The medium containing single cells was centrifuged for 10 min at 405 g. The liquid was removed and cells were suspended in PBS 1x.

2.2.6 Protein expression analysis via mRNA

The deletion of *Nbn* in the epidermis was confirmed by an analysis of mRNA of the keratinocytes. RNA was isolated from the epidermal cells and via revers transcription

translated into cDNA (complementary DNA). The amount of cDNA was amplified with a PCR and existence or absence of the *Nbn* fragment was visualized. To confirm the result Hypoxanthin-Phosphoribosyl-Transferase (HPRT) expression analysis was used as control.

2.2.6.1 RNA isolation

PBS 1x was removed from the cells and Trizol was added. Samples were homogenized and incubated at room temperature. Rotiphenol was added and incubated at room temperature. Afterwards samples were centrifuged and the aqueous phase, containing the RNA, was transferred into a new tube. Isopropanol was added. The sample was mixed and incubated at room temperature. RNA was pelleted and washed with Ethanol 70 % to remove salts. Ethanol was discarded and the RNA pellet was air-dried at room temperature. It was dissolved in DNase/RNase free water. The concentration was measured using NanoDrop 1000.

2.2.6.2 cDNA synthesis

cDNA was synthesized using SuperScript® II Reverse Transcriptase. It was done according to the product manual using 2 µg of RNA.

2.2.6.3 PCR for RNA analysis

PCR was performed with 2 µl of reverse transcription product.

	Concentration	**Volume [µl]**
PCR Buffer with $MgCl_2$	10 x	2
dNTP	10 mM	2
HPRT F	10 µM	1
HPRT R	10 µM	1
Nbn 102F	10 µM	1
Nbn 648R	10 µM	1
Taq	5 U/µl	0,2

H_2O	9,8
Total	18

Step	**Temperature [°C]**	**Time**	
Denaturation	95	4 min	
Denaturation	95	30 sec	45x
Annealing	61	1 min	
Elongation	68	1 min	
Elongation	68	7 min	
Keeping in machine	18	∞	

The expected fragments were Nbn (567 bp) and HPRT (249 bp).

2.2.6.4 RNA gel

RNA fragment size and availability were measured using gel electrophoresis to separate the fragments according to their sizes. Therefore an agarose gel was used, samples were loaded together with loading buffer and the gel was run with 120 V. Gel concentration was 1,5 %.

2.2.7 GEO data analyses

Data on *NBN* expression in human psoriasis was obtained from GEO Profiles database (Edgar et al.,2002; Barrett et al.,2013). The GEO accessions were analyzed using the GEO2R analysis tool provided on the accession display for each GEO data set and values for NBN were extracted. Additionally the GEO Profiles of each data set were searched for NBN. Values from the GEO2R analyses and GEO Profiles were compared. The data was used for statistical analyses and visualization of individual patient values for *NBN* mRNA.

2.2.8 Statistical analyses

Statistical analyses were performed using Sigma Plot. Pictures of skin were taken and cells were counted. For the analyses in the skin cells were counted in the epidermis and hair follicles or in the dermis (Neutrophils and Mast cells) that were visible in pictures (referred to as sections) with a size of 444 µm * 333 µm (for Neutrophils 902 µm * 676 µm). For each analysis five representative sections were counted. No calculation of cells per mm^2 was performed as epidermis size increased in the animals and therefore such a calculation would falsify the results. The mean and standard deviation were calculated. A Normality Test (Shapiro-Wilk) was performed. If Normality was confirmed a t-test was done. Mann-Whitney Rank Sum Test was conducted when the Normality Test failed. Differences were considered significant when $P < 0,05$. In graphs of the statistical analyses the standard deviation is shown as error bars and the P value as stars.

3. Results

The results of the study of deletion of *Nbn*, *Nbn* and *p53* and *Nbn* and *Atm* in the epidermis are presented.

For each experiment a short explanation is given why it was conducted. The results of the experiments are shown and described. The pictures shown are representative images for the corresponding genotype and age of the animals. Interpretations and further explanations are given in the chapter "Conclusions and Discussion".

3.1 Analyses of genomic deletions and integrations

The gene construct for *Nbn* as shown in (Figure 10) was integrated into the mice. The proper integration and the individual genotype from each mouse were determined through DNA analysis.

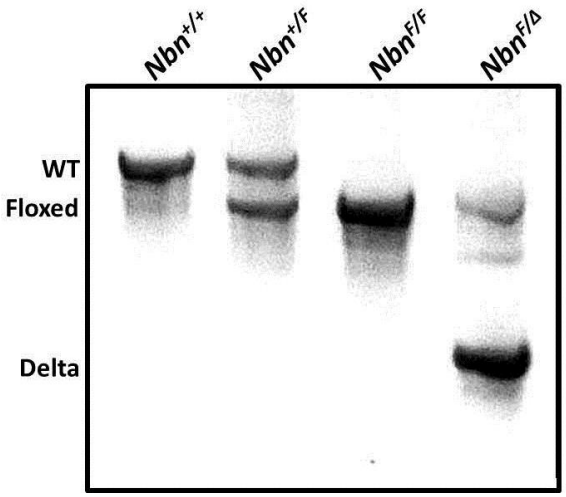

Figure 11: Analysis of *Nbn* DNA expression

The integration of flox-sides for *Nbn* was determined via DNA extraction. The genotypes shown are $Nbn^{+/+}$, $Nbn^{+/F}$, $Nbn^{F/F}$ and $Nbn^{F/\Delta}$. The fragments for wild-type (WT), Floxed and Delta *Nbn* are visible.

DNA extraction from the tails and analysis thereof showed the status of *Nbn* gene expression in the mice (Figure 11). The bands for wild-type (WT), Floxed and Delta are visible. $Nbn^{+/+}$ animals had two wild-type alleles. Animals with one wild-type and one Floxed allele were $Nbn^{+/F}$. Animals with two Floxed ($Nbn^{F/F}$) or Floxed/Delta ($Nbn^{F/\Delta}$) alleles had the *Nbn* deletion genotype. Mice with one or two wild-type alleles were not used for further experiments.

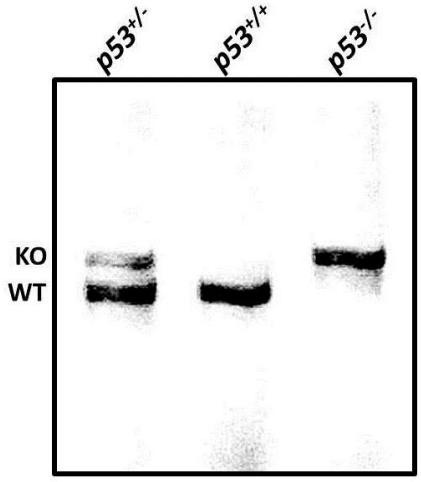

Figure 12: DNA expression of *p53*

The expression and deletion of *p53* was determined via DNA extraction. The fragments for knockout (KO) and wild-type (WT) *p53* are visible. The genotypes $p53^{+/-}$, $p53^{+/+}$ and $p53^{-/-}$ are shown.

Tail DNA analysis for *p53* expression in the mice showed knockout and wild-type *p53* (Figure 12). $p53^{+/-}$ mice had one wild-type and one KO allele. Mice with two wild-type alleles were $p53^{+/+}$. Mice were only used for $Nbn^{Krox20\text{-}Cre}p53^{-/-}$ studies when both alleles were KO ($p53^{-/-}$).

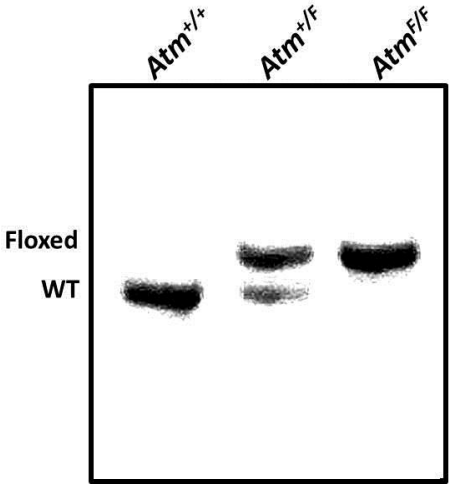

Figure 13: *Atm* DNA expression

The integration of flox-sides for *Atm* was confirmed via DNA extraction. The genotypes shown are $Atm^{+/+}$, $Atm^{+/F}$ and $Atm^{F/F}$. The fragments for Floxed and wild-type (WT) are visible.

Atm status of the mice was also evaluated by tail DNA analysis (Figure 13). Mice with two wild-type alleles were $Atm^{+/+}$. $Atm^{+/F}$ animals had one wild-type and one Floxed allele. The animals that were used for $Nbn/Atm^{Krox20\text{-}Cre}$ had two Floxed alleles and were $Atm^{F/F}$.

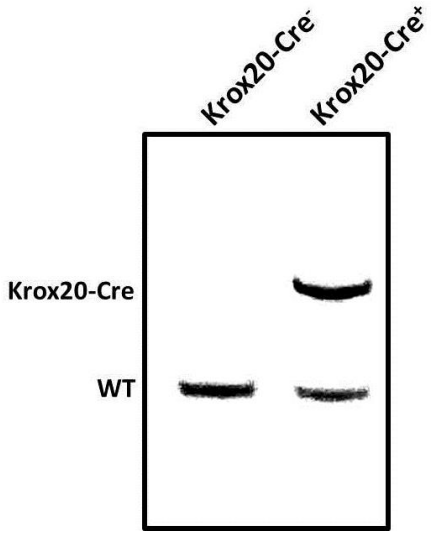

Figure 14: Krox20-Cre expression

The integration of Krox20-Cre was confirmed via DNA extraction. The fragments for Krox20-Cre and wild-type (WT) are visible. The genotypes *Krox20-Cre*$^{+}$ and *Krox20-Cre*$^{-}$ are shown.

The integration of Krox20-Cre recombinase was tested via DNA analysis (Figure 14). It was shown by the appearance of the specific DNA band for Krox20-Cre recombinase (Krox20-Cre^{+}) in addition to the wild-type band. Animals positive for DNA of Krox20-Cre were used for the deletion animals while mice without Cre recombinase (Krox20-Cre^{-}) were used in the control group.

The complete analyses of all different genes identified the genotype of each animal. The mice were grouped according to the combination of gene expressions.

3.2 Consequences of *Nbn* deletion in the epidermis

3.2.1 Analysis of expression and deletion of *Nbn* in the epidermis

The deletion of *Nbn* in the epidermis was confirmed with an isolation of keratinocytes from the skin. RNA was extracted from the keratinocytes and transcribed via reverse transcription into cDNA. It was amplified and visualized.

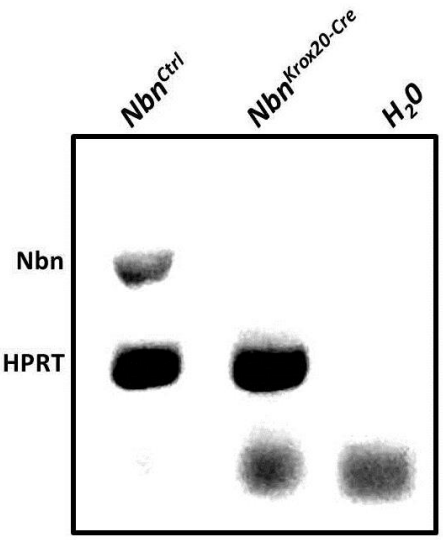

Figure 15: RNA expression analysis of Nbn in keratinocytes

The expression and deletion of *Nbn* and *HPRT* was determined via RNA extraction. The fragments for Nbn is visible in Nbn^{Ctrl}, HPRT is expressed in Nbn^{Ctrl} and $Nbn^{Krox20\text{-}Cre}$.

The *Nbn* band in the control RNA (Nbn^{Ctrl}) verified the expression of *Nbn* in the epidermis in mice (Figure 15). Loss of the *Nbn* band confirmed the deletion of *Nbn* in the genetically modified animals ($Nbn^{Krox20\text{-}Cre}$). The fragment for HPRT was used as an internal control to evaluate the isolation of RNA and the amount of analyzed RNA in relation between samples. HPRT was present in the same concentration in both RNAs. In the samples from $Nbn^{Krox20\text{-}Cre}$ and H_2O control debris from primers were visible.

3.2.2 Examination of mice morphology

Nbn^{Ctrl}, $Nbn^{Krox20\text{-}Cre}$, $Nbn^{Krox20\text{-}Cre}p53^{-/-}$ and $Nbn/Atm^{Krox20\text{-}Cre}$ mice were monitored for morphological changes. Animals were collected at 18 (P18) and 35 days (P35) and 3 months (3m) after birth (Figure 16). The fur color did not have any impact on the genotype of the animals.

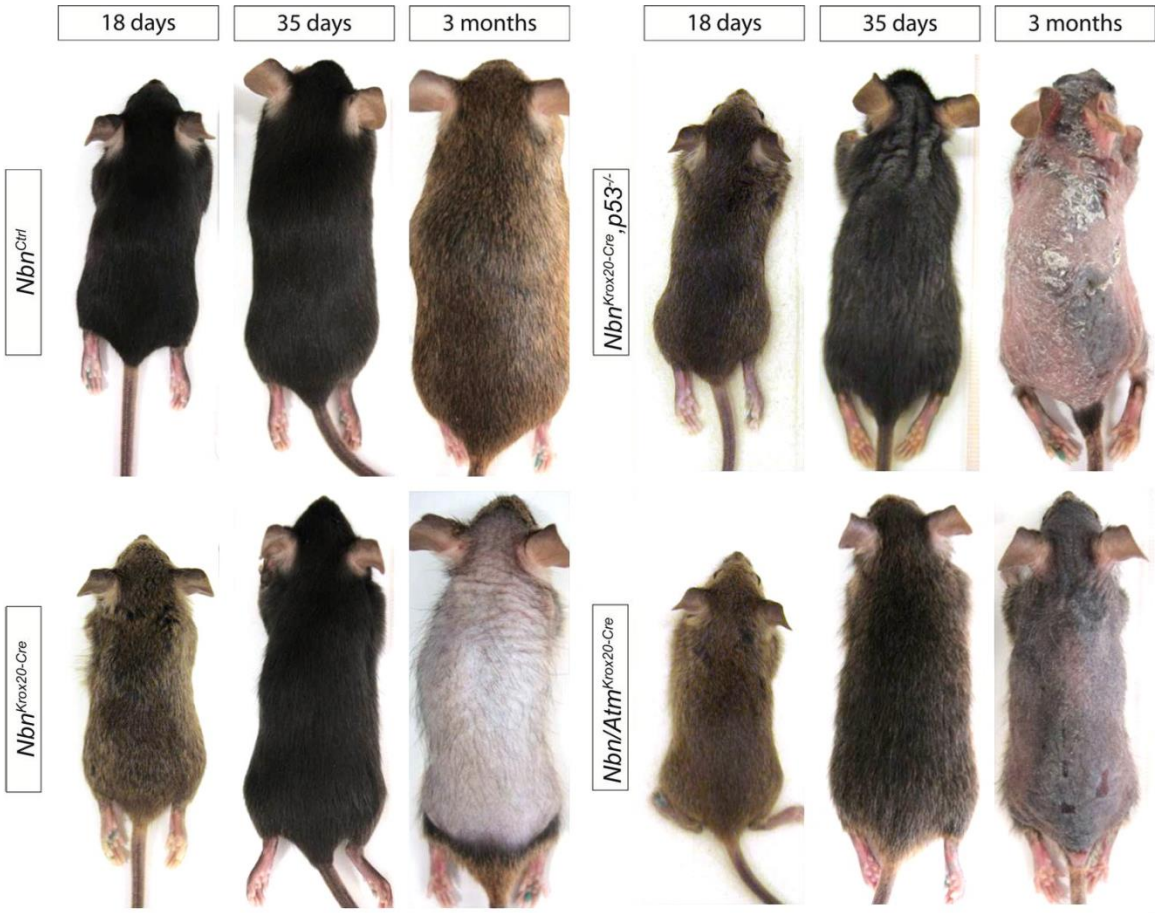

Figure 16: Morphology of mice from different genotypes and ages

In Figure 16 pictures of *Nbn*^{Ctrl}, *Nbn*$^{Krox20\text{-}Cre}$, *Nbn*$^{Krox20\text{-}Cre}$*p53*$^{-/-}$ and *Nbn/Atm*$^{Krox20\text{-}Cre}$ mice at different points in time are shown. Those are 18, 35 days and 3 months after birth.

For *Nbn*^{Ctrl} animals a thick fur coat could be seen at all ages (Figure 16). At the age of P18 no differences between *Nbn*^{Ctrl} and mutated mice were visible. 35 days after birth first small changes in the skin structure were obvious while handling the animals and could be seen in the neck area of the *Nbn*$^{Krox20\text{-}Cre}$*p53*$^{-/-}$ mice. The skin was more elastic than in *Nbn*^{Ctrl} mice. Nearly complete loss of fur on the animals back skin was observed in *Nbn*$^{Krox20\text{-}Cre}$, *Nbn*$^{Krox20\text{-}Cre}$*p53*$^{-/-}$ and *Nbn/Atm*$^{Krox20\text{-}Cre}$ mice at 3 months of age. The changes of the skin texture were more pronounced. Scaly hardened skin areas were detected on all 3 months old deletion animals. They were most prominent on the skin of *Nbn*$^{Krox20\text{-}Cre}$*p53*$^{-/-}$ mice.

To evaluate the morphological changes further skin was collected, fixed and embedded in paraffin. Skin samples were stained with H&E to show the morphological structure (Figure 17).

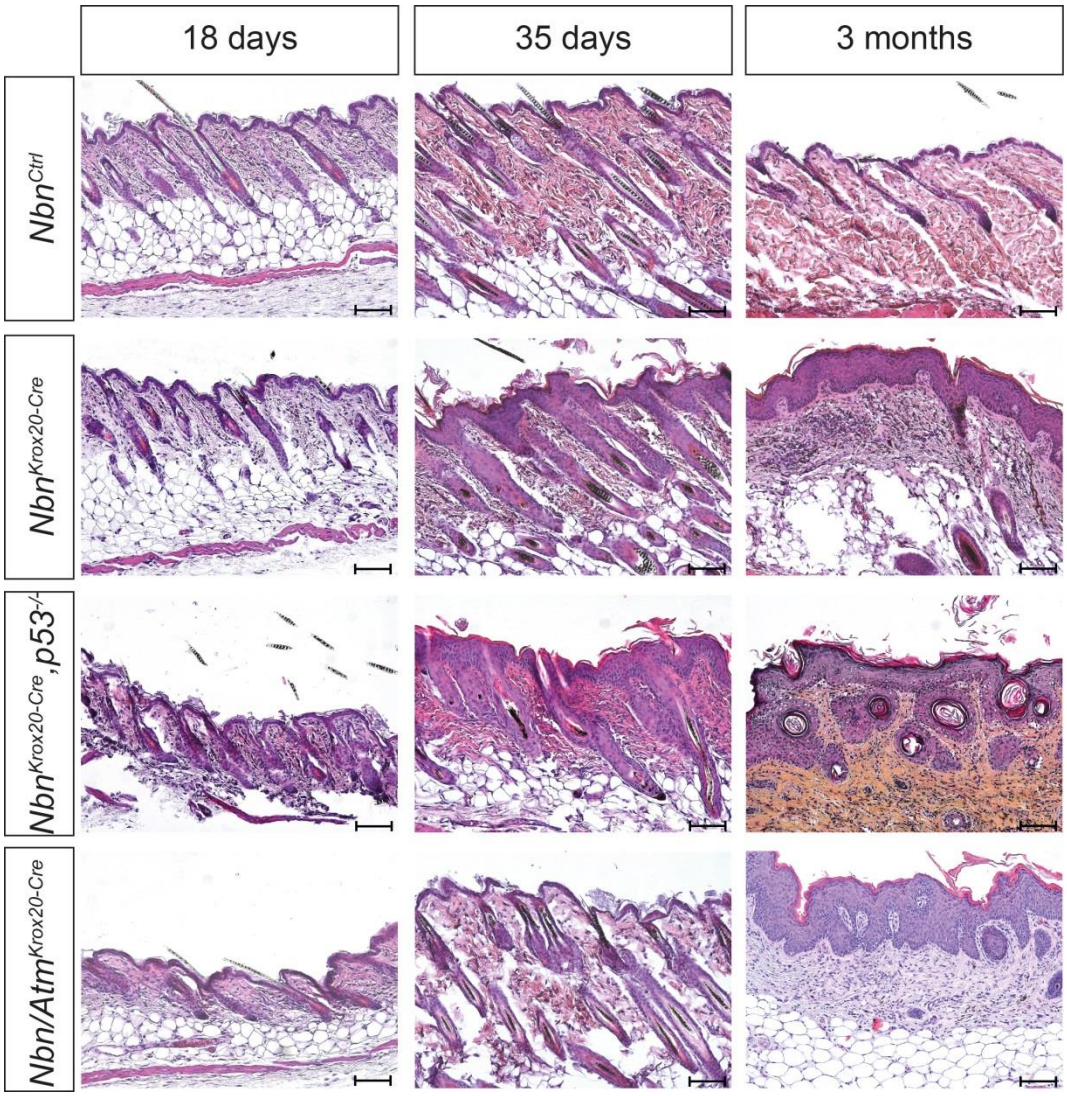

Figure 17: Histological analysis of skin morphology

Sections from skin of *Nbn*^{Ctrl}, *Nbn*$^{Krox20\text{-}Cre}$, *Nbn*$^{Krox20\text{-}Cre}$*p53*$^{-/-}$ and *Nbn/Atm*$^{Krox20\text{-}Cre}$ mice at different ages (18, 35 days and 3 months after birth) are shown. Skin was stained with H&E. Scale bar: 100 µm

Analysis of H&E staining confirmed the changes seen on visual examination. While control animals showed a high number of hair follicles and a thin layer of epidermis at all stages, in *Nbn*$^{Krox20\text{-}Cre}$, *Nbn*$^{Krox20\text{-}Cre}$*p53*$^{-/-}$ and *Nbn/Atm*$^{Krox20\text{-}Cre}$ mice stark changes were visible at 3 months. Only single hair follicles were left and those had an altered structure. The epidermis was highly enlarged. Changes in the morphology were already observed to a certain degree in deletion mice 35 days after birth. For *Nbn*$^{Krox20\text{-}Cre}$, *Nbn*$^{Krox20\text{-}Cre}$*p53*$^{-/-}$ and *Nbn/Atm*$^{Krox20\text{-}Cre}$ animals at 35 days the epidermis started to enlarge and hair follicles looked altered but were still present. In addition to the changes visible in 3 months old *Nbn*$^{Krox20\text{-}Cre}$ and *Nbn/Atm*$^{Krox20\text{-}Cre}$ mice, *Nbn*$^{Krox20\text{-}Cre}$*p53*$^{-/-}$ mice

showed invaginations of the epidermis. Those formed cyst-like structures that contained dead keratinocytes and were surrounded by keratinocytes even when they were localized in dermal areas.

3.2.3 Analysis of DNA damage distribution and apoptosis in the epidermis

Possible causes of the hair loss can be an elevated rate of apoptosis in the hair follicle. In addition a lack of apoptosis within the epidermis could cause the increase in epidermis size.

To investigate both possibilities stainings with different apoptosis marker were done. p53 staining was conducted to show a possible increase in apoptosis. It was stained for p53 independent apoptosis with activated Caspase 3. DNA damages, especially DSBs, were visualized with γH2A.X. In addition TUNEL reaction was performed to show apoptotic cells.

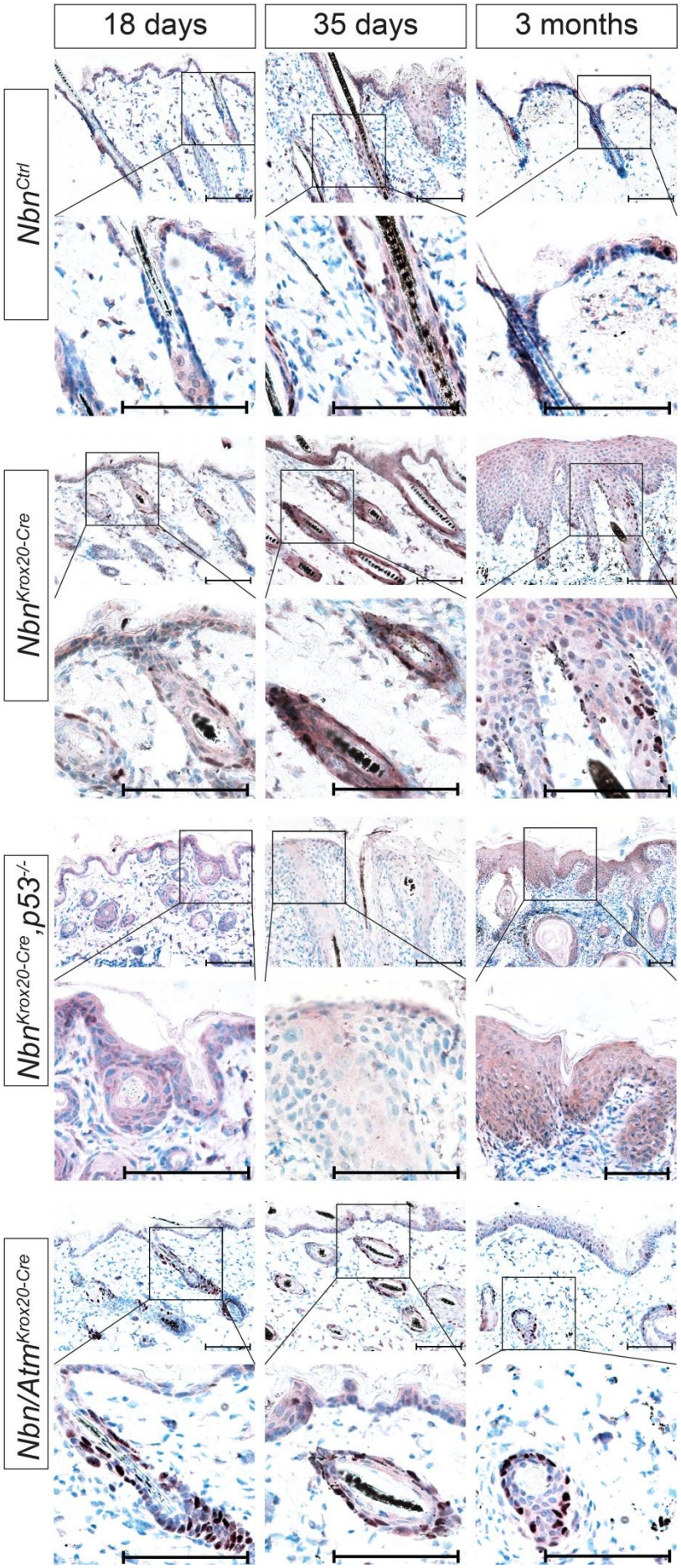

Figure 18: p53 expression in mouse skin

p53 expression was visualized with an antibody. The skin of $Nbn^{Krox20\text{-}Cre}$, $Nbn^{Krox20\text{-}Cre}p53^{-/-}$, $Nbn/Atm^{Krox20\text{-}Cre}$ and Nbn^{Ctrl} is shown. Mice were collected at 18, 35 days and 3 months after birth.

Scale bar: 100 µm

p53 expression in the skin is shown in Figure 18. In the epidermis and around the hair follicle in control mice few p53 positiv cells can be seen. Most were locolazied around the hair follicle at the age of 35 days. In $Nbn^{Krox20\text{-}Cre}$ and $Nbn/Atm^{Krox20\text{-}Cre}$ mice some positive cells were visible. Those increased in number in the few remaining hair follicle structures that could be seen at 3 months after birth. In the *p53* deleted skin only background staining and no positive cells were observed, as was expected due to the deletion of *p53* in the mice.

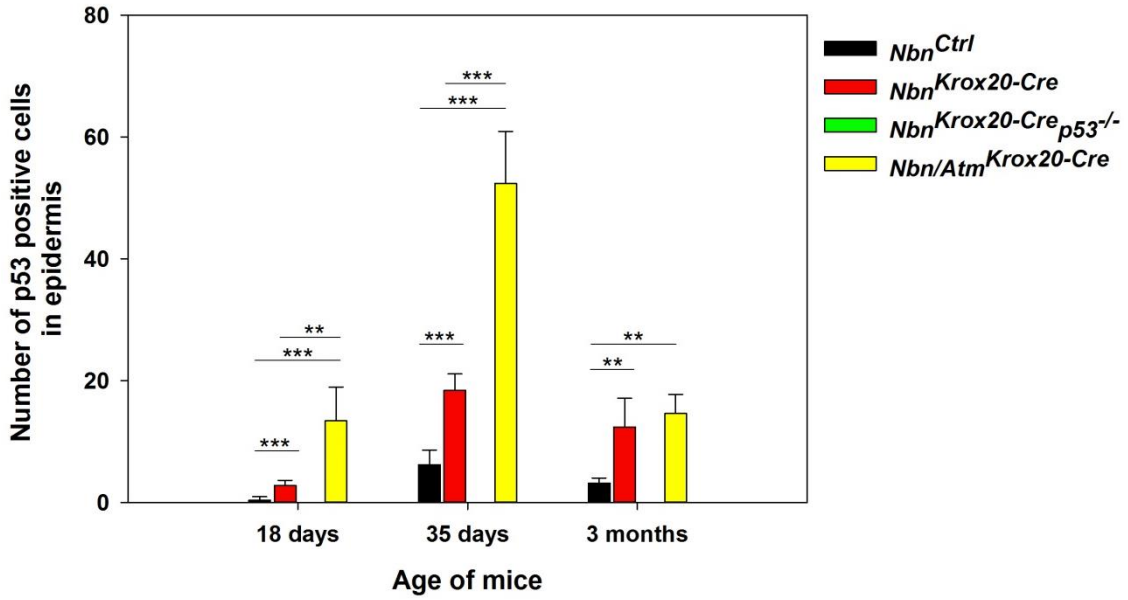

Figure 19: Analysis of p53 expression in the epidermis

The number of p53 expressing cells was counted. Statistical analysis was performed. The data was sorted by age. Nbn^{Ctrl}, $Nbn^{Krox20\text{-}Cre}$, $Nbn^{Krox20\text{-}Cre}p53^{-/-}$ and $Nbn/Atm^{Krox20\text{-}Cre}$ were compared. (n = 5; **P < 0,01; ***P < 0,001)

Counting of p53 positive cells and statistical comparison between Nbn^{Ctrl}, $Nbn^{Krox20\text{-}Cre}$, $Nbn^{Krox20\text{-}Cre}p53^{-/-}$ and $Nbn/Atm^{Krox20\text{-}Cre}$ mice was conducted (Figure 19). In mice 18 days after birth Nbn^{Ctrl} had 0,4 (± 0,55), $Nbn^{Krox20\text{-}Cre}$ had 2,8 (± 0,84) and $Nbn/Atm^{Krox20\text{-}Cre}$ had 13,4 (± 5,55) p53 positive cells. At 35 days after birth Nbn^{Ctrl} showed 6,2 (± 2,39), $Nbn^{Krox20\text{-}Cre}$ 18,4 (± 2,7) and $Nbn/Atm^{Krox20\text{-}Cre}$ showed 52,4 (± 8,53) cells per section that were p53 positive. The number of cells with p53 expression changed to Nbn^{Ctrl} 3,2 (± 0,84), $Nbn^{Krox20\text{-}Cre}$ 12,4 (± 4,72) and $Nbn/Atm^{Krox20\text{-}Cre}$ 14,6 (± 3,13) in the mice. All animals with p53 deletion showed no p53 positive cells. A statistical difference was detected between Nbn^{Ctrl} and $Nbn^{Krox20\text{-}Cre}$ at all ages. The same was true for Nbn^{Ctrl} and $Nbn/Atm^{Krox20\text{-}Cre}$. At day 18 and day 35

after birth the number of p53 positive cells in *Nbn/Atm*$^{Krox20\text{-}Cre}$ mice was significantly higher than in *Nbn*$^{Krox20\text{-}Cre}$ mice.

The number of p53 positive cell was increased in *Nbn*$^{Krox20\text{-}Cre}$ and *Nbn/Atm*$^{Krox20\text{-}Cre}$ mice. The elevation was more prominent in *Nbn/Atm*$^{Krox20\text{-}Cre}$ animals.

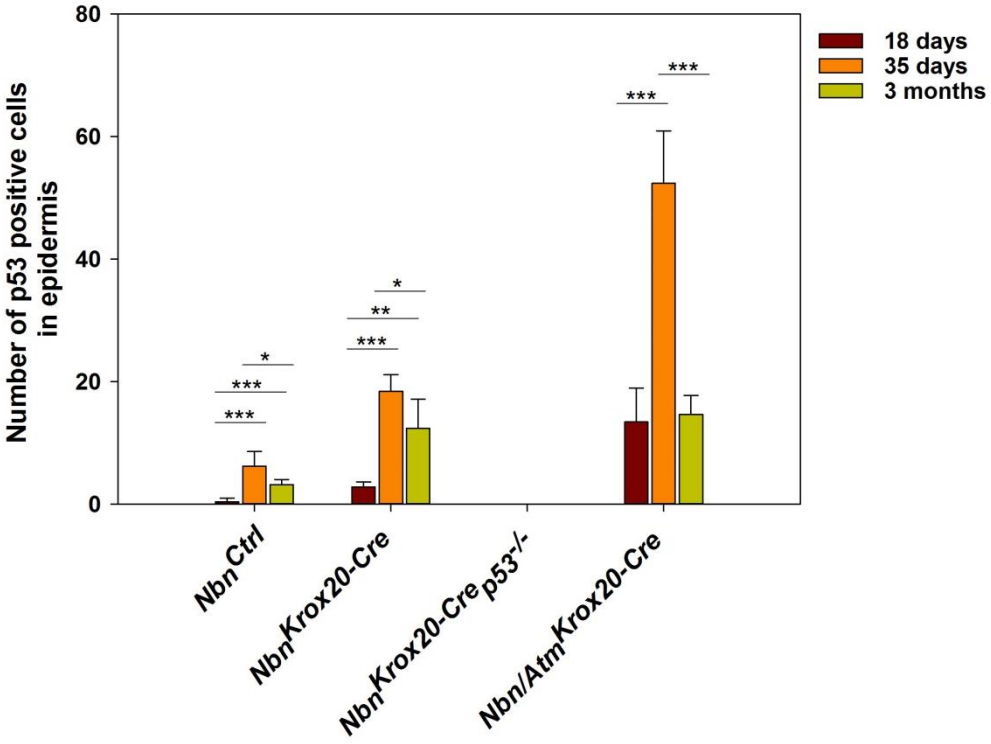

Figure 20: Age dependent p53 expression in epidermis

The number of p53 expressing cells was sorted by genotypes and analyzed statistically. (n = 5; *P < 0,05; **P < 0,01; ***P < 0,001)

The differences in number of p53 positive cells were studied in regard to variations within the individual groups dependent on the age of animals (Figure 20). In *Nbn*^{Ctrl}, *Nbn*$^{Krox20\text{-}Cre}$ and *Nbn/Atm*$^{Krox20\text{-}Cre}$ mice a significant increase from day 18 to day 35 and from day 18 and 3 months was seen. The comparison of P35 to 3 months old animals showed a significant decrease in cell number in those genotypes.

The number of p53 expressing cells had reached its peak at the age of 35 days in all animals.

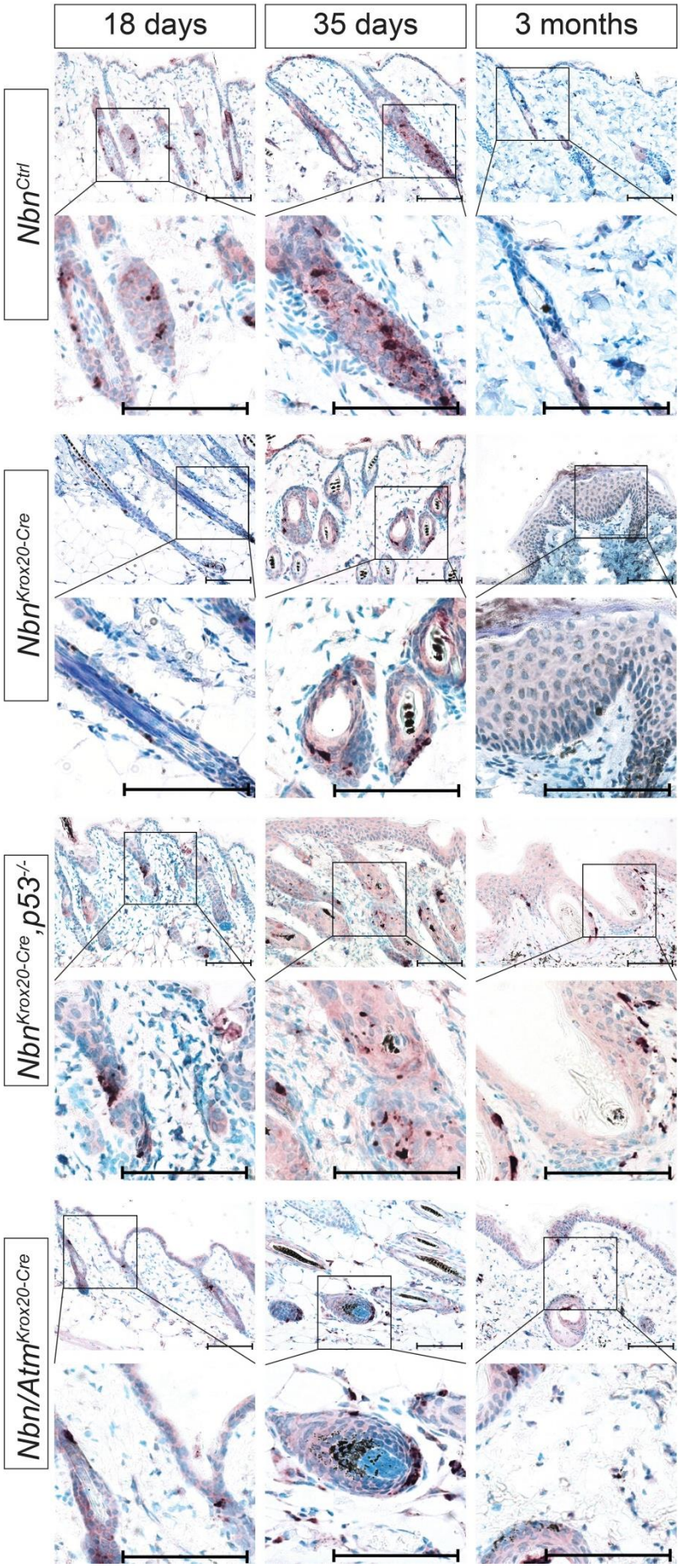

Figure 21: Activated Caspase 3 distribution in the skin

Skin of different ages (P18, P35 and 3 months) of mice was stained for the activated form of Caspase 3. Sections from *Nbn*^{Ctrl}, *Nbn*$^{Krox20\text{-}Cre}$, *Nbn*$^{Krox20\text{-}Cre}$*p53*$^{-/-}$ and *Nbn/Atm*$^{Krox20\text{-}Cre}$ are shown.

Scale bar: 100 µm

The antibody staining against active Caspase 3 is depicted in Figure 21. The Nbn^{Ctrl} mice showed positive cells in der epidermal structures at all points in time. An amount of Caspase 3 cells was also found in $Nbn^{Krox20\text{-}Cre}$, $Nbn^{Krox20\text{-}Cre}p53^{-/-}$ and $Nbn/Atm^{Krox20\text{-}Cre}$ mice at 18 and 35 days after birth. Most of those positive cells were detected around the hair follicle. In 3 months old animals $Nbn^{Krox20\text{-}Cre}$ and $Nbn/Atm^{Krox20\text{-}Cre}$ only few cells with activated Caspase 3 were present while in $Nbn^{Krox20\text{-}Cre}p53^{-/-}$ mice more cells were visible.

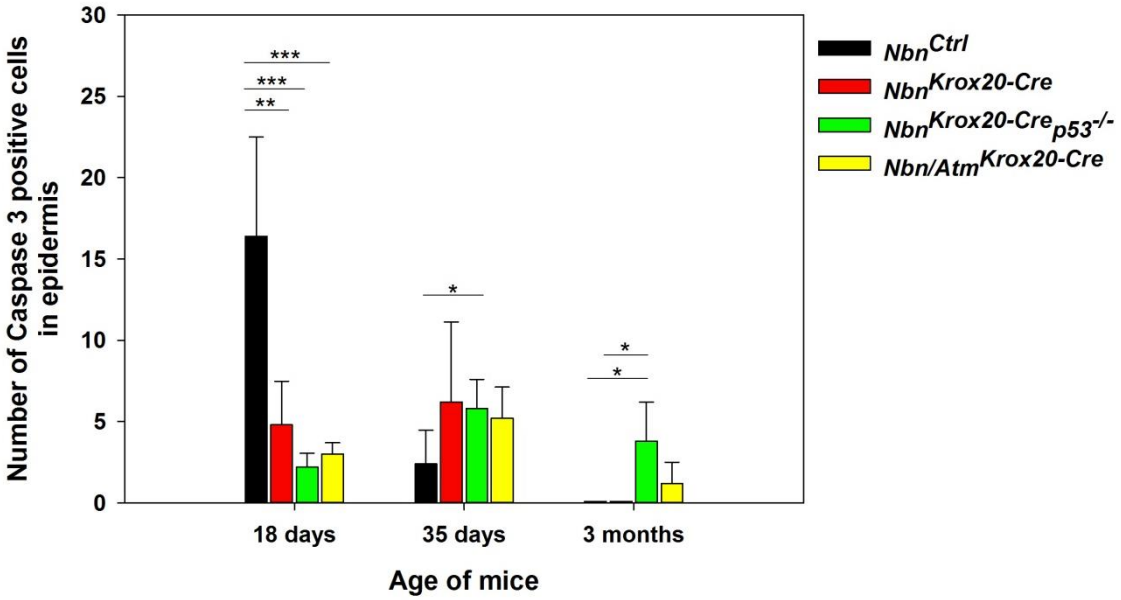

Figure 22: Evaluation of active Caspase 3 in epidermis

The staining for active Caspase 3 was analyzed statistically. The number of cells in the epidermis and hair follicle was counted. It was sorted according to age. (n = 5; *P < 0,05; **P < 0,01; ***P < 0,001)

The amount of Caspase 3 positive cells in the epidermis of the mice was evaluated (Figure 22). It showed a significant higher number of Caspase 3 cells in control animals at P18 (Nbn^{Ctrl} 16,4 ± 6,1) than in animals with deletions ($Nbn^{Krox20\text{-}Cre}$ 4,8 ± 2,68; $Nbn^{Krox20\text{-}Cre}p53^{-/-}$ 2,2 ± 0,84 and $Nbn/Atm^{Krox20\text{-}Cre}$ 3 ± 0,7). This was reversed at day 35 (Nbn^{Ctrl} 2,4 ± 2,07; $Nbn^{Krox20\text{-}Cre}$ 6,2 ± 4,92; $Nbn^{Krox20\text{-}Cre}p53^{-/-}$ 5,8 ± 1,79 and $Nbn/Atm^{Krox20\text{-}Cre}$ 5,2 ± 1,92). In 3 months old Nbn^{Ctrl} and $Nbn^{Krox20\text{-}Cre}$ mice no Caspase 3 activated cells were observed. In $Nbn^{Krox20\text{-}Cre}p53^{-/-}$ mice (3,8 ± 2,39) and in $Nbn/Atm^{Krox20\text{-}Cre}$ mice (1,2 ± 1,3) a significant higher amount of Caspase 3 active cells were detected. At P35 a significant increase in $Nbn^{Krox20\text{-}Cre}p53^{-/-}$ compared to Nbn^{Ctrl} was visible. This was also observed 3 months after birth. Here an increase of $Nbn^{Krox20\text{-}Cre}p53^{-/-}$ in comparison to $Nbn^{Krox20\text{-}Cre}$ was detected too.

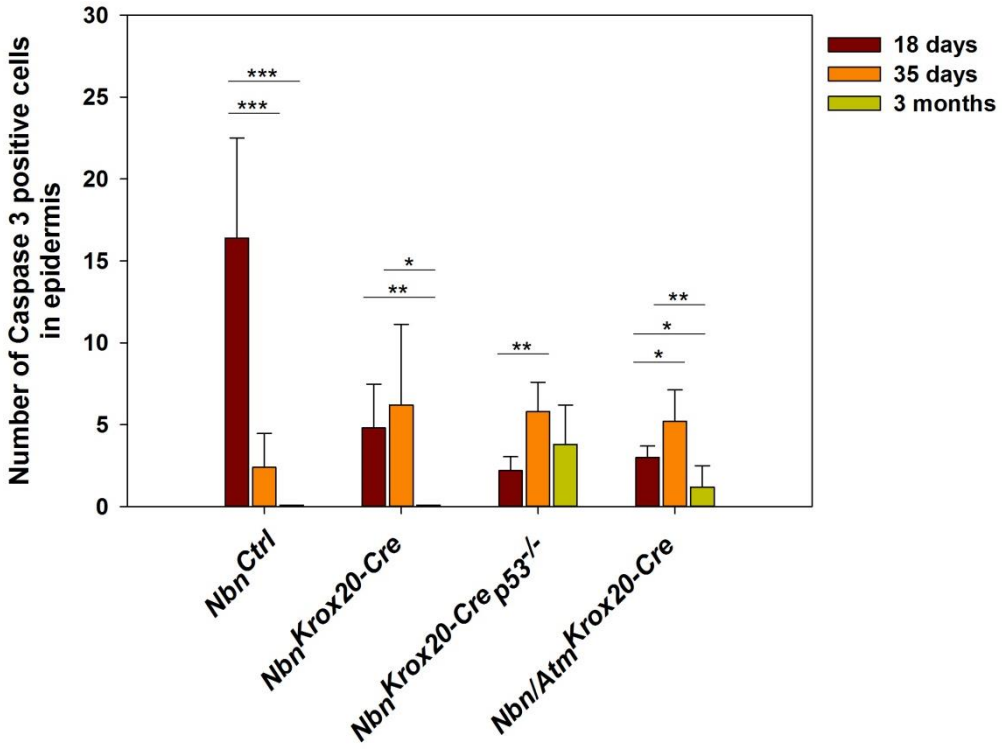

Figure 23: Changes in activated Caspase 3 dependent on age

In *Nbn*^{Ctrl}, *Nbn*$^{Krox20\text{-}Cre}$, *Nbn*$^{Krox20\text{-}Cre}$*p53*$^{-/-}$ and *Nbn/Atm*$^{Krox20\text{-}Cre}$ mouse epidermis the cells with active Caspase 3 were counted. The number of Caspase 3 positive cells was sorted by genotype and analyzed. (n = 5; *P < 0,05; **P < 0,01; ***P < 0,001)

Sorting of cells with activated Caspase 3 by age revealed a high amount of cells in 18 days old *Nbn*^{Ctrl} mice (Figure 23). Both at 35 days and 3 months it was significantly decreased. In *Nbn*$^{Krox20\text{-}Cre}$, *Nbn*$^{Krox20\text{-}Cre}$*p53*$^{-/-}$ and *Nbn/Atm*$^{Krox20\text{-}Cre}$ a significant increase was detected from P18 to P35. After day 35 the number decreased again in those animals.

The number of cells with active Caspase 3 in the epidermis was elevated at 35 days after birth in *Nbn*$^{Krox20\text{-}Cre}$, *Nbn*$^{Krox20\text{-}Cre}$*p53*$^{-/-}$ and *Nbn/Atm*$^{Krox20\text{-}Cre}$ mice.

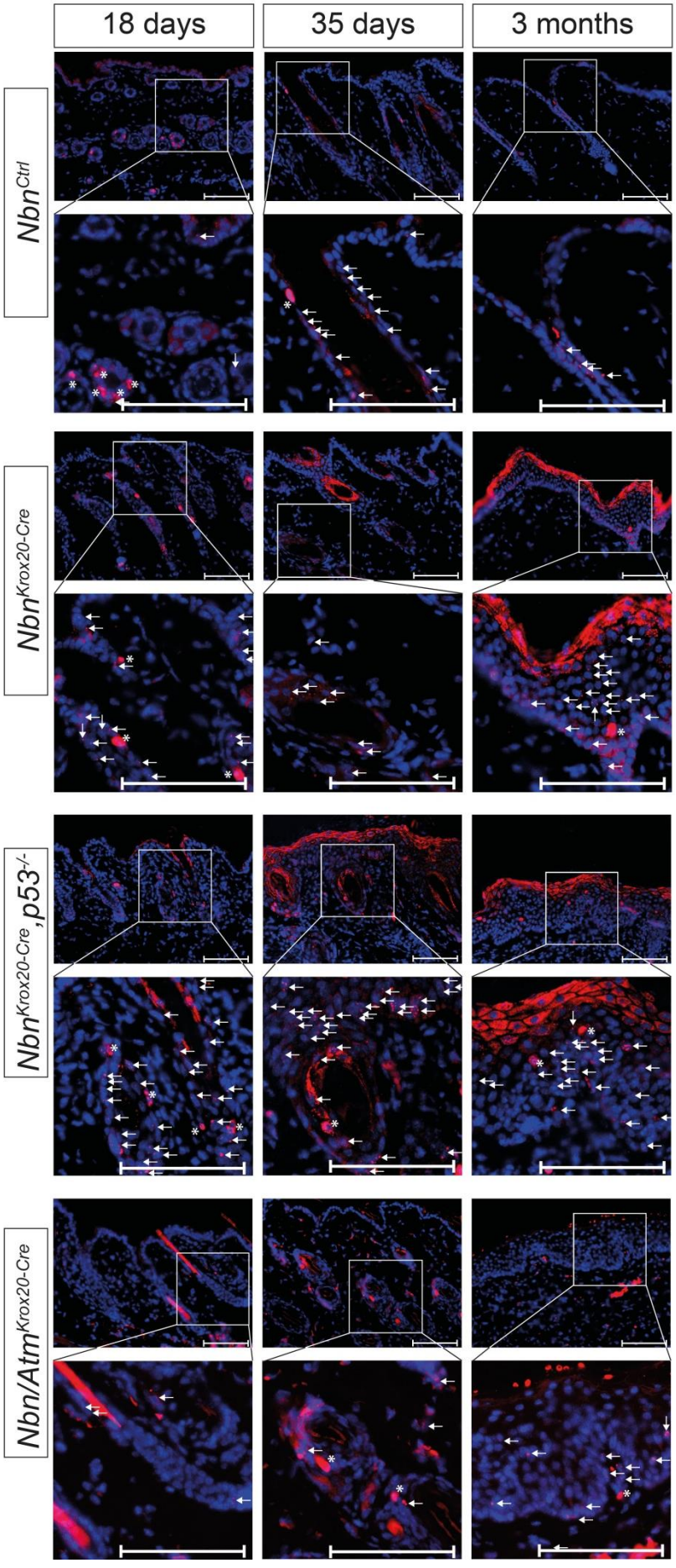

Figure 24: yH2A.X foci distribution in the skin

Skin of 3 months, 18 and 35 days old mice was stained for phosphorylated Histone H2A.X. The mice were *Nbn*^{Ctrl}, *Nbn*$^{Krox20\text{-}Cre}$, *Nbn*$^{Krox20\text{-}Cre}$*p53*$^{-/-}$ and *Nbn/Atm*$^{Krox20\text{-}Cre}$ mice. The arrows indicate cells with γH2A.X foci and stars show γH2A.X positive apoptotic cells. The red staining shows γH2A.X and DAPI is stained in blue.

Scale bar: 100 µm

Staining of the skin showed an increase in γH2A.X foci (Figure 24). Some of these foci were found at all ages in *Nbn*^{Ctrl} mice. Cells with γH2A.X foci were located along the hair follicles in those animals. In *Nbn*$^{Krox20\text{-}Cre}$ and *Nbn*$^{Krox20\text{-}Cre}$*p53*$^{-/-}$ animals a higher amount of positive cells was detected at all points in time. They were localized mostly in cells of the hair follicle and few foci were found in keratinocytes of the epidermal layers. In *Nbn/Atm*$^{Krox20\text{-}Cre}$ less γH2A.X foci were present.

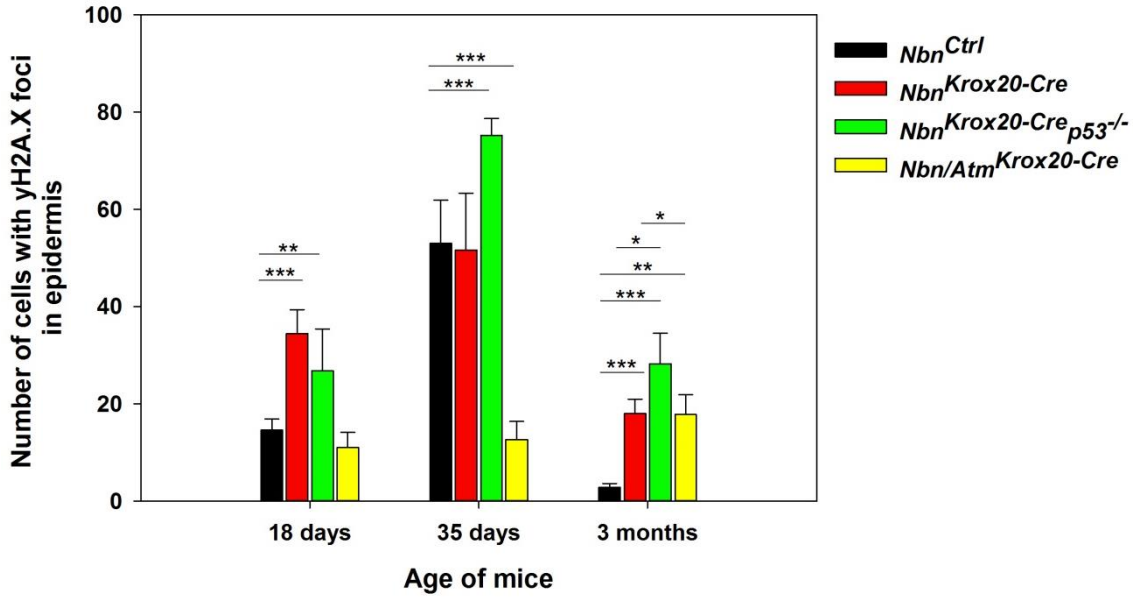

Figure 25: Analysis of γH2A.X foci positive cells in the epidermis

Numbers of cells with γH2A.X foci were enumerated. A statistical analysis was executed. The number of cells was shown for *Nbn*^{Ctrl}, *Nbn*$^{Krox20\text{-}Cre}$, *Nbn*$^{Krox20\text{-}Cre}$*p53*$^{-/-}$ and *Nbn/Atm*$^{Krox20\text{-}Cre}$ mice and put in order according to age of the mice. (n = 5; *P < 0,05; **P < 0,01; ***P < 0,001)

The cells with γH2A.X foci were counted in the mice (Figure 25). 18 days after birth *Nbn*^{Ctrl} showed 14,6 (± 2,3), *Nbn*$^{Krox20\text{-}Cre}$ had 34,4 (± 4,93), *Nbn*$^{Krox20\text{-}Cre}$*p53*$^{-/-}$ 26,8 (± 8,61) and *Nbn/Atm*$^{Krox20\text{-}Cre}$ showed 11 (± 3,16) cells with γH2A.X foci per section. The numbers changed to *Nbn*^{Ctrl} 53 (± 8,92), *Nbn*$^{Krox20\text{-}Cre}$ 51,6 (± 11,72), *Nbn*$^{Krox20\text{-}Cre}$*p53*$^{-/-}$ 75,2 (± 3,49) and *Nbn/Atm*$^{Krox20\text{-}Cre}$ 12,6 (± 3,78) at 35 days after birth. Sections from mice 3 months after birth showed 2,8 (± 0,84) for *Nbn*^{Ctrl}, 18 (± 2,92) for *Nbn*$^{Krox20\text{-}Cre}$, 28,2 (± 6,3) for *Nbn*$^{Krox20\text{-}Cre}$*p53*$^{-/-}$ and 17,8 (± 4,03) for *Nbn/Atm*$^{Krox20\text{-}Cre}$ animals. Statistical analysis of the number of γH2A.X foci revealed significant increases in *Nbn*$^{Krox20\text{-}Cre}$ and *Nbn*$^{Krox20\text{-}Cre}$*p53*$^{-/-}$ mice. Those existed at 18 days and 3 months after birth. At 3 months the increase was also seen in *Nbn/Atm*$^{Krox20\text{-}Cre}$ animals while at 35 days the number of cells was significantly

decreased. There was no increase in *Nbn*$^{Krox20\text{-}Cre}$ but in *Nbn*$^{Krox20\text{-}Cre}$*p53*$^{-/-}$ mice compared to *Nbn*^{Ctrl}. γH2A.X foci positive cells were increased in *Nbn*$^{Krox20\text{-}Cre}$*p53*$^{-/-}$ in comparison to *Nbn*$^{Krox20\text{-}Cre}$ mice.

An increase of cells with γH2A.X foci was detected in deletion mice.

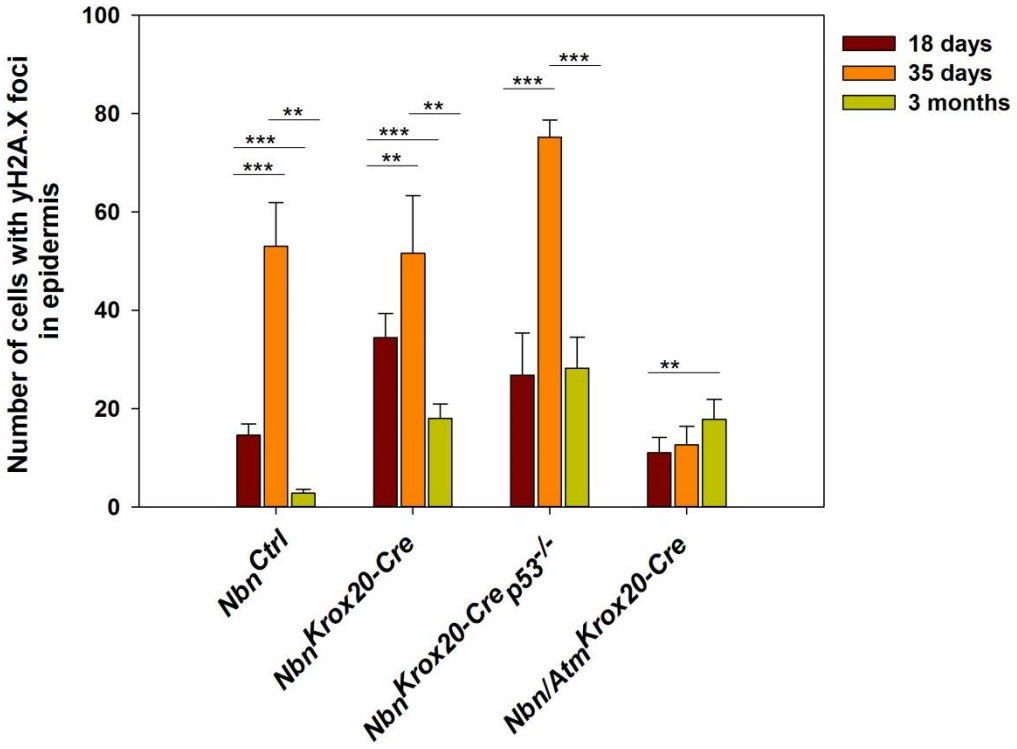

Figure 26: Age dependents of the number of γH2A.X foci containing cells

The numbers of cells were sorted by *Nbn*^{Ctrl}, *Nbn*$^{Krox20\text{-}Cre}$, *Nbn*$^{Krox20\text{-}Cre}$*p53*$^{-/-}$ and *Nbn/Atm*$^{Krox20\text{-}Cre}$. For each genotype numbers from 18, 35 days and 3 months old animals were shown. (n = 5; **P < 0,01; ***P < 0,001)

Cells with γH2A.X foci were analyzed regarding the age of the animals within the different groups (Figure 26). *Nbn*^{Ctrl} mice showed a significant increase of foci from 18 to 35 days. 3 months after birth the cell number with foci was decreased and was lower than at 18 days of age. An increase was detected in *Nbn*$^{Krox20\text{-}Cre}$ mice between P18 and P35. Afterwards the γH2A.X foci decreased and reached a lower level than at P18. The increase for 35 day old animals was also observed in *Nbn*$^{Krox20\text{-}Cre}$*p53*$^{-/-}$ mice. In *Nbn/Atm*$^{Krox20\text{-}Cre}$ animals no increase was detected at 35 days but at 3 months compared to 18 day old mice.

The increase of foci peaked at 35 days in *Nbn*^{Ctrl}, *Nbn*$^{Krox20\text{-}Cre}$ and *Nbn*$^{Krox20\text{-}Cre}$*p53*$^{-/-}$ mice.

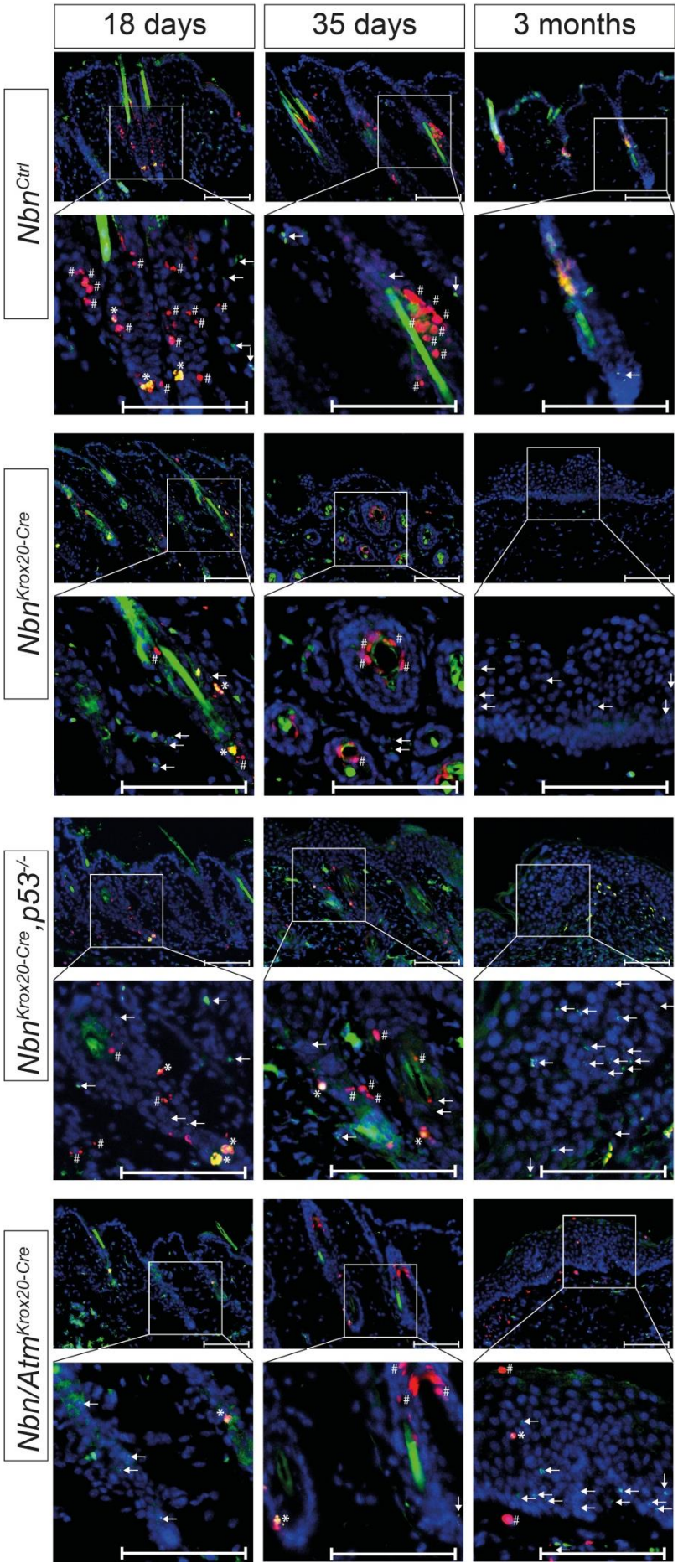

Figure 27: Colocalization study of γH2A.X foci and TUNEL positive cells

Skin of mice from *Nbn*^{Ctrl}, *Nbn*$^{Krox20\text{-}Cre}$, *Nbn*$^{Krox20\text{-}Cre}$*p53*$^{-/-}$ and *Nbn/Atm*$^{Krox20\text{-}Cre}$ are depicted. The skin was collected at 18, 35 days and 3 months after birth. It was stained against phosphorylated Histone H2A.X and TUNEL reaction was performed. The arrows indicate cells with γH2A.X foci. Stars show γH2A.X positive apoptotic cells and hash marks TUNEL positive cells. The green staining shows γH2A.X, red is TUNEL and DAPI is stained in blue. Yellow staining shows an overlap of TUNEL and γH2A.X.

Scale bar: 100 µm

A colocalization study from cells containing γH2A.X foci and positive TUNEL cells was done (Figure 27). TUNEL positive cells were located along the hair follicles in Nbn^{Ctrl} (P18, P35, 3 months), $Nbn^{Krox20\text{-}Cre}$ (P18, P35), $Nbn^{Krox20\text{-}Cre}p53^{-/-}$ (P18, P35) and $Nbn/Atm^{Krox20\text{-}Cre}$ (P18, P35) animals. A comparable distribution of γH2A.X foci in the hair follicles was observed. In the epidermis no TUNEL positive cells were detected in Nbn^{Ctrl}, $Nbn^{Krox20\text{-}Cre}$ and $Nbn^{Krox20\text{-}Cre}p53^{-/-}$ animals. In $Nbn/Atm^{Krox20\text{-}Cre}$ few positive cells were found at 3 months of age. In the epidermis of 3 months old animals (except Nbn^{Ctrl}) few γH2A.X foci positive cells were visible in the epidermis. All cells that were considered apoptotic cells due to complete staining with γH2A.X were also positive for TUNEL. No colocalistaion of TUNEL and γH2A.X foci in cells was detected.

TUNEL staining confirmed the apoptotic character of cells stained completely with γH2A.X antibody. The existence of γH2A.X foci within a cell did not indicate completed apoptosis in the cell as cells with γH2A.X foci were not stained for TUNEL. TUNEL positive cells did not contain γH2A.X foci.

3.2.4 Analysis of differentiation of keratinocytes

The different stages of keratinocyte differentiation are characterized with changes in keratin expression. Keratin 15 is a marker for stem cells within the hair follicle and in stem cells in the basal layer of the epidermis (Liu et al.,2003; Morris et al.,2004). The basal layer with its proliferating cells is distinguished with the expression of Keratin 14 (Fuchs and Green,1980). With the start of differentiation of the keratinocytes they leave the basal layer and Keratin 14 expression is lost. Keratin 10 is started to be expressed (Fuchs and Green,1980). It is maintained during the complete differentiation of the keratinocytes.

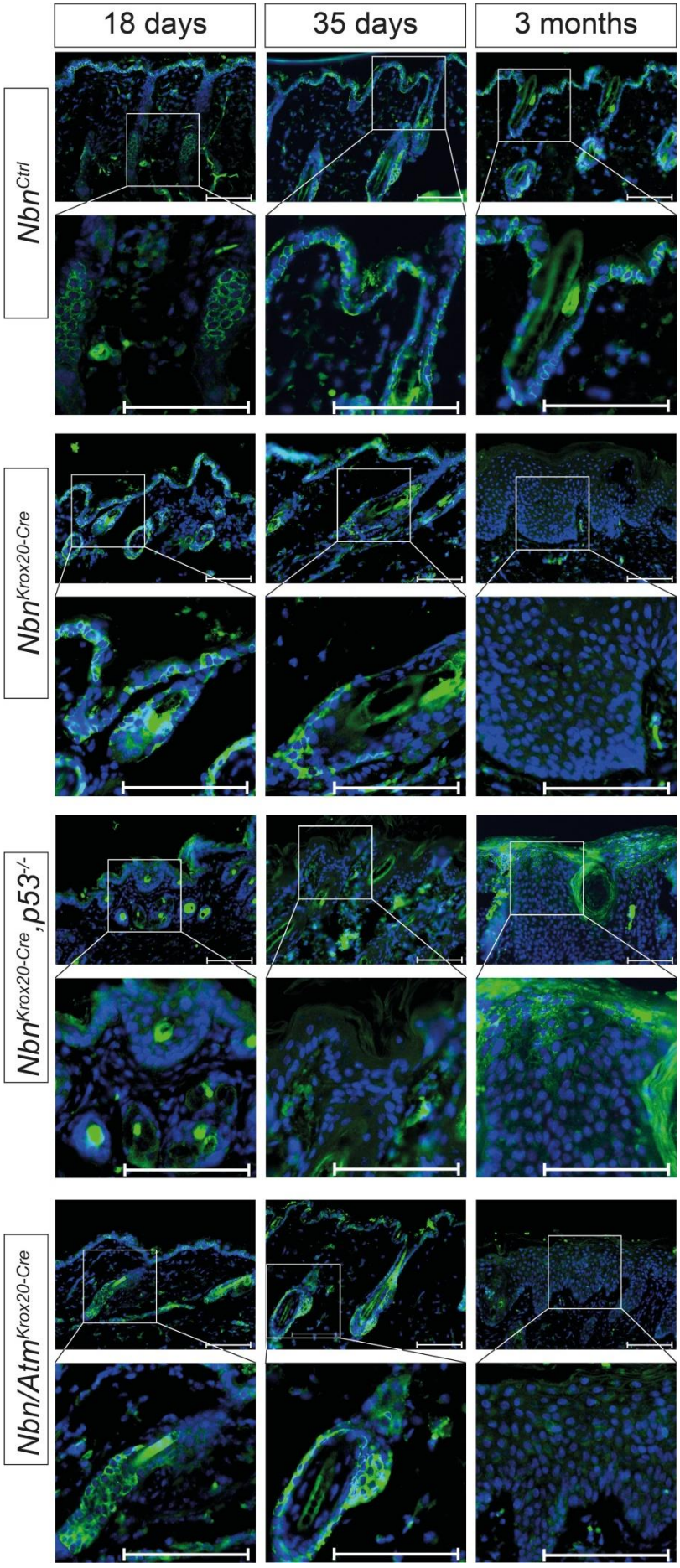

Figure 28: Staining for Keratin 15 positive cells

Analysis of Keratin 15 positive cell distribution is shown in Figure 28. Skin of *Nbn*^{Ctrl}, *Nbn*$^{Krox20\text{-}Cre}$, *Nbn*$^{Krox20\text{-}Cre}$*p53*$^{-/-}$ and *Nbn/Atm*$^{Krox20\text{-}Cre}$ mice was stained in green for Keratin 15. DAPI was stained in blue. The skin was from 18, 35 days and 3 months old animals.

Scale bar: 100 µm

The normal distribution of Keratin 15 positive cells in the epidermis and along the hair follicle is visible in the control animals of all ages (Figure 28). Keratin 15 positive cells localize in the basal layer of the epidermis and in the bulge area of the hair follicles. This pattern can also be seen in *Nbn*$^{Krox20\text{-}Cre}$, *Nbn*$^{Krox20\text{-}Cre}$*p53*$^{-/-}$ and *Nbn/Atm*$^{Krox20\text{-}Cre}$ mice at 18 and 35 days after birth. With 3 months no Keratin 15 positive cells were detected in *Nbn*$^{Krox20\text{-}Cre}$, *Nbn*$^{Krox20\text{-}Cre}$*p53*$^{-/-}$ and *Nbn/Atm*$^{Krox20\text{-}Cre}$ animals.

Disappearance of Keratin 15 expressing cells revealed the loss of hair follicle stem cells in *Nbn*$^{Krox20\text{-}Cre}$, *Nbn*$^{Krox20\text{-}Cre}$*p53*$^{-/-}$ and *Nbn/Atm*$^{Krox20\text{-}Cre}$ mice.

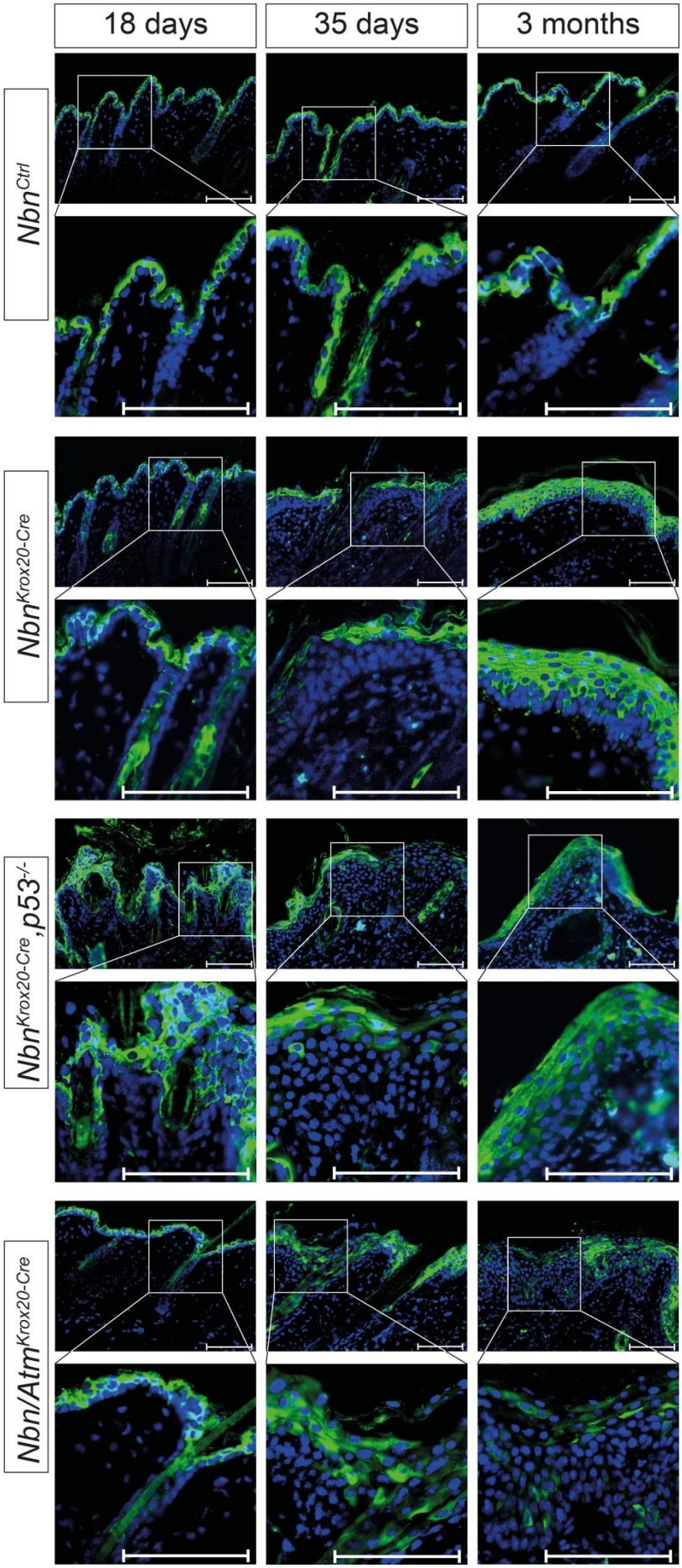

Figure 29: Keratin 10 staining of mouse skin

Skin of mice, at the age of 18, 35 days and 3 months after birth, from *Nbn*^{Ctrl}, *Nbn*$^{Krox20\text{-}Cre}$, *Nbn*$^{Krox20\text{-}Cre}$*p53*$^{-/-}$ and *Nbn/Atm*$^{Krox20\text{-}Cre}$ mice was stained with anti-Keratin 10. Keratin 10 staining is green and DAPI is blue.

Scale bar: 100 µm

Keratin 10 is a marker for differentiating epidermal layers. It was observed in the upperpart of the epidermis (one layer) and partially within hair follicles from *Nbn*^{Ctrl} mice at all stages (Figure 29). The same observation was made in *Nbn*$^{Krox20\text{-}Cre}$, *Nbn*$^{Krox20\text{-}Cre}$*p53*$^{-/-}$ and *Nbn/Atm*$^{Krox20\text{-}Cre}$ mice at day 18 and day 35 after birth. *Nbn*$^{Krox20\text{-}Cre}$, *Nbn*$^{Krox20\text{-}Cre}$*p53*$^{-/-}$ and *Nbn/Atm*$^{Krox20\text{-}Cre}$ mice with 3 months showed 3-4 layers of Keratin 10 positive differentiated cells. It was seen that the layers did not have a clear boundary and that some Keratin 10 negative cells were spread between positive cells. In addition the DAPI staining visualized few epidermal layers beneath the Keratin 10 layers that were not positive.

The distribution of Keratin 10 in the epidermis of *Nbn*$^{Krox20\text{-}Cre}$, *Nbn*$^{Krox20\text{-}Cre}$*p53*$^{-/-}$ and *Nbn/Atm*$^{Krox20\text{-}Cre}$ mice showed an accumulation of differentiated keratinocytes.

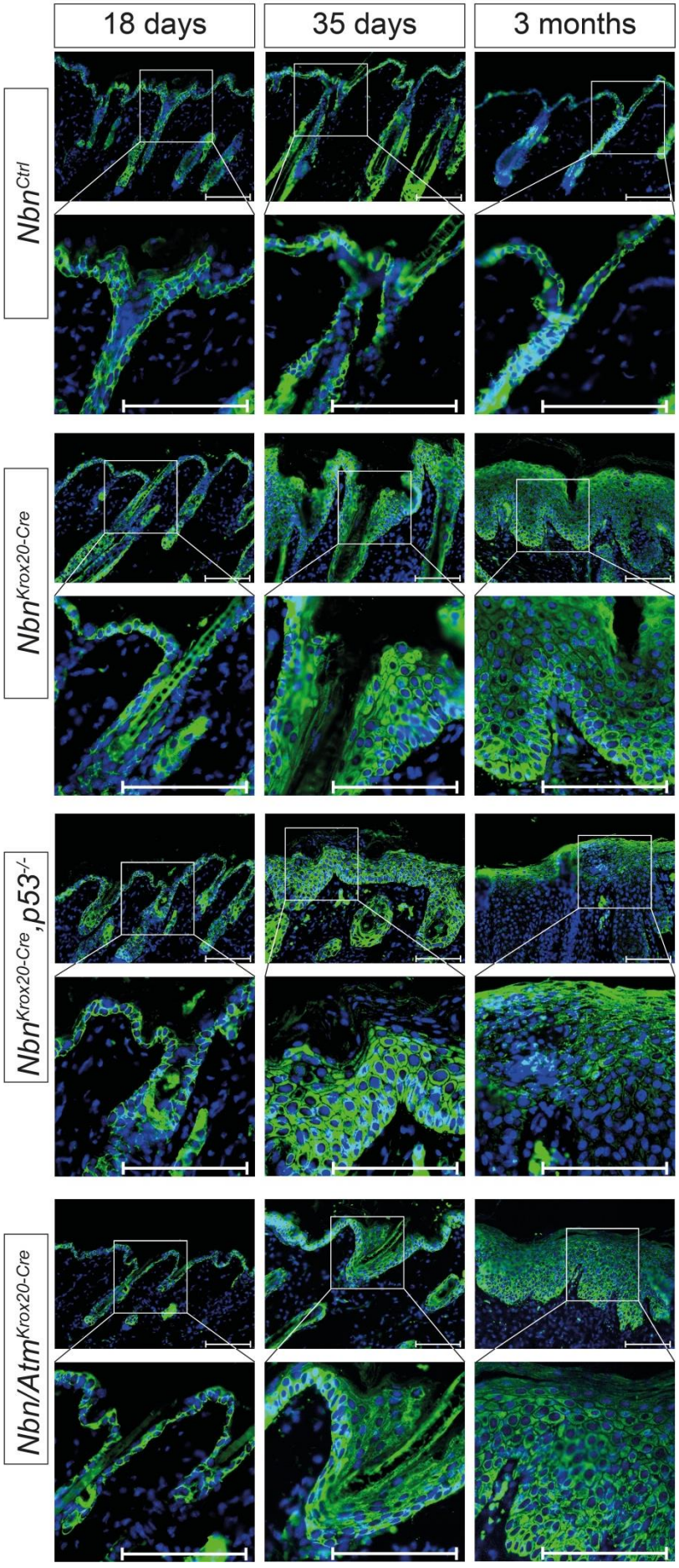

Figure 30: Analysis of Keratin 14 expression in mouse skin

Epidermis of control, *Nbn*$^{Krox20\text{-}Cre}$, *Nbn*$^{Krox20\text{-}Cre}$*p53*$^{-/-}$ and *Nbn/Atm*$^{Krox20\text{-}Cre}$ mice was stained with an antibody against Keratin 14 (Figure 30). Keratin 14 staining is green and DAPI is blue.

Scale bar: 100 µm

Keratin 14 is expressed in proliferating basal keratinocytes. The expression pattern was seen in control animals (Figure 30). *Nbn*^{Ctrl} mice of all ages showed the Keratin 14 in one layer of epidermal cells and along the hair follicle. The same pattern was visible in skin of 18 day old *Nbn*$^{Krox20\text{-}Cre}$, *Nbn*$^{Krox20\text{-}Cre}$*p53*$^{-/-}$ and *Nbn/Atm*$^{Krox20\text{-}Cre}$ mice. When the mice reached 35 days the expression pattern changed. In all deletion lines few layers of Keratin 14 positive keratinocytes existed. The number of cells increased even more in *Nbn*$^{Krox20\text{-}Cre}$ and *Nbn/Atm*$^{Krox20\text{-}Cre}$ epidermis. Keratin 14 expression in those animals reached up to the outer border of the epidermis to the environment in animals collected 3 months after birth. In 3 months old *Nbn*$^{Krox20\text{-}Cre}$*p53*$^{-/-}$ mice keratinocytes showed Keratin 14 in the upper layers of the epidermis but not in the basal layer anymore.

The expression of Keratin 14 in *Nbn*$^{Krox20\text{-}Cre}$, *Nbn*$^{Krox20\text{-}Cre}$*p53*$^{-/-}$ and *Nbn/Atm*$^{Krox20\text{-}Cre}$ mice demonstrated an accumulation of proliferating non-differentiated keratinocytes and a disturbed differentiation.

3.2.5 Evaluation of apoptosis in hair follicle stem cells

With the staining of Keratin 15 the disappearance of hair follicle stem cells was illustrated. The extinction of Keratin 15 cells might be due to a loss of stem cell properties of the cells or apoptosis in the stem cells after DNA damages. Investigation of DNA damages was done with a double staining of Keratin 15 and 53BP1 (Figure 31). Apoptosis in the stem cells was analyzed through double staining with Keratin 15 and TUNEL (Figure 32).

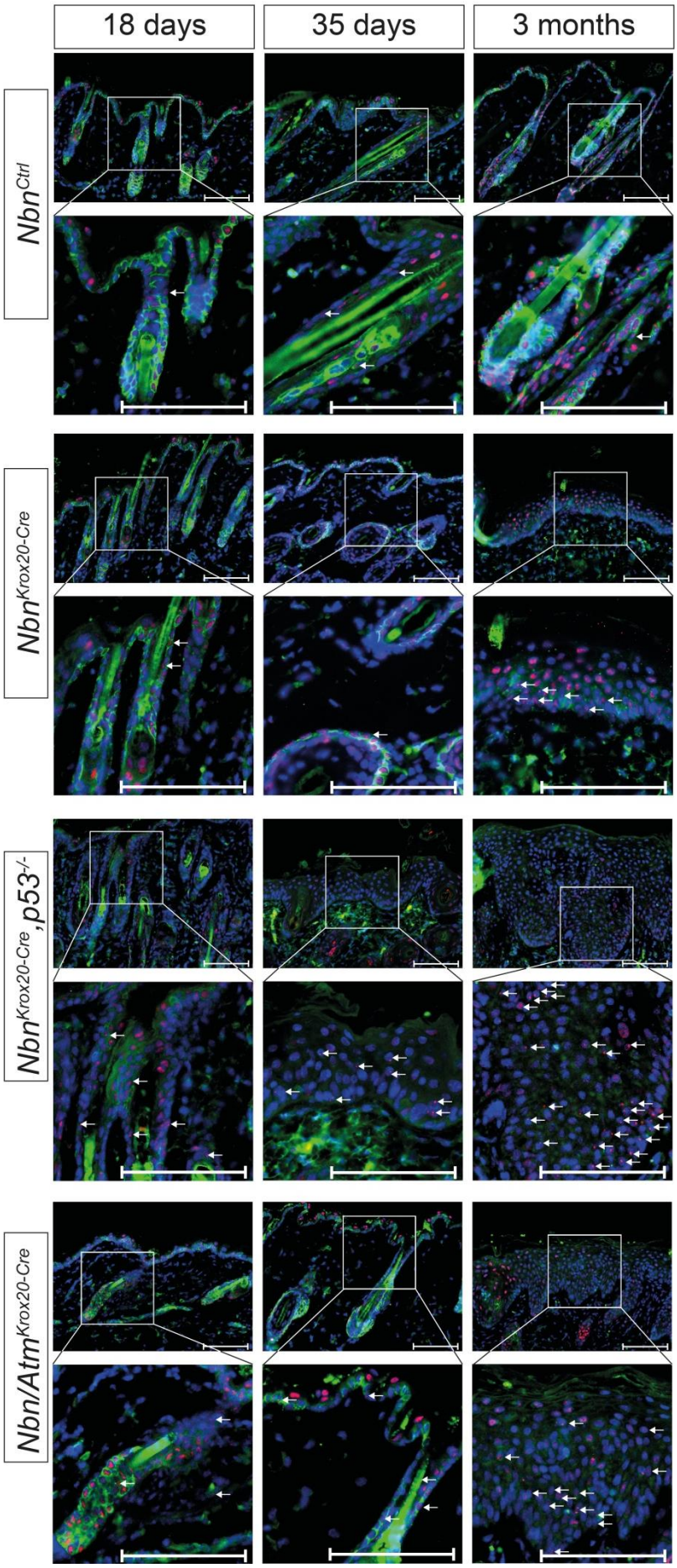

Figure 31: Staining of Keratin 15 and 53BP1

Skin of *Nbn*^{Ctrl}, *Nbn*$^{Krox20\text{-}Cre}$, *Nbn*$^{Krox20\text{-}Cre}$*p53*$^{-/-}$ and *Nbn/Atm*$^{Krox20\text{-}Cre}$ mice was stained against Keratin 15 and 53BP1. The animals were collected at P18, P35 and 3 months. The staining for 53BP1 is in red. Keratin 15 positive cells were stained in green and DAPI is blue. The arrows indicate cells positive for 53BP1 foci.

Scale bar: 100 µm

The staining of 53BP1 (Figure 31) showed a general staining of the nucleus in some cells but also foci formation in other cells. This foci formation indicates the response to DNA damages (Anderson et al.,2001; Panier and Boulton,2014). A few cells with foci were present in all animals collected. In Nbn^{Ctrl} mice they partially colocalized with the Keratin 15 positive cells at all ages. This was the case in $Nbn^{Krox20\text{-}Cre}$, $Nbn^{Krox20\text{-}Cre}p53^{-/-}$ and $Nbn/Atm^{Krox20\text{-}Cre}$ mice with 18 and 35 days of age too. But the number of Keratin 15 positive cells was already decreased in 35 days old deleted mice. In 3 months $Nbn^{Krox20\text{-}Cre}$, $Nbn^{Krox20\text{-}Cre}p53^{-/-}$ and $Nbn/Atm^{Krox20\text{-}Cre}$ old mice most foci were visible in the lower parts of the epidermis while Keratin 15 was not detected at that age anymore (see Figure 28).

The staining showed few stem cells with signs for DNA damages.

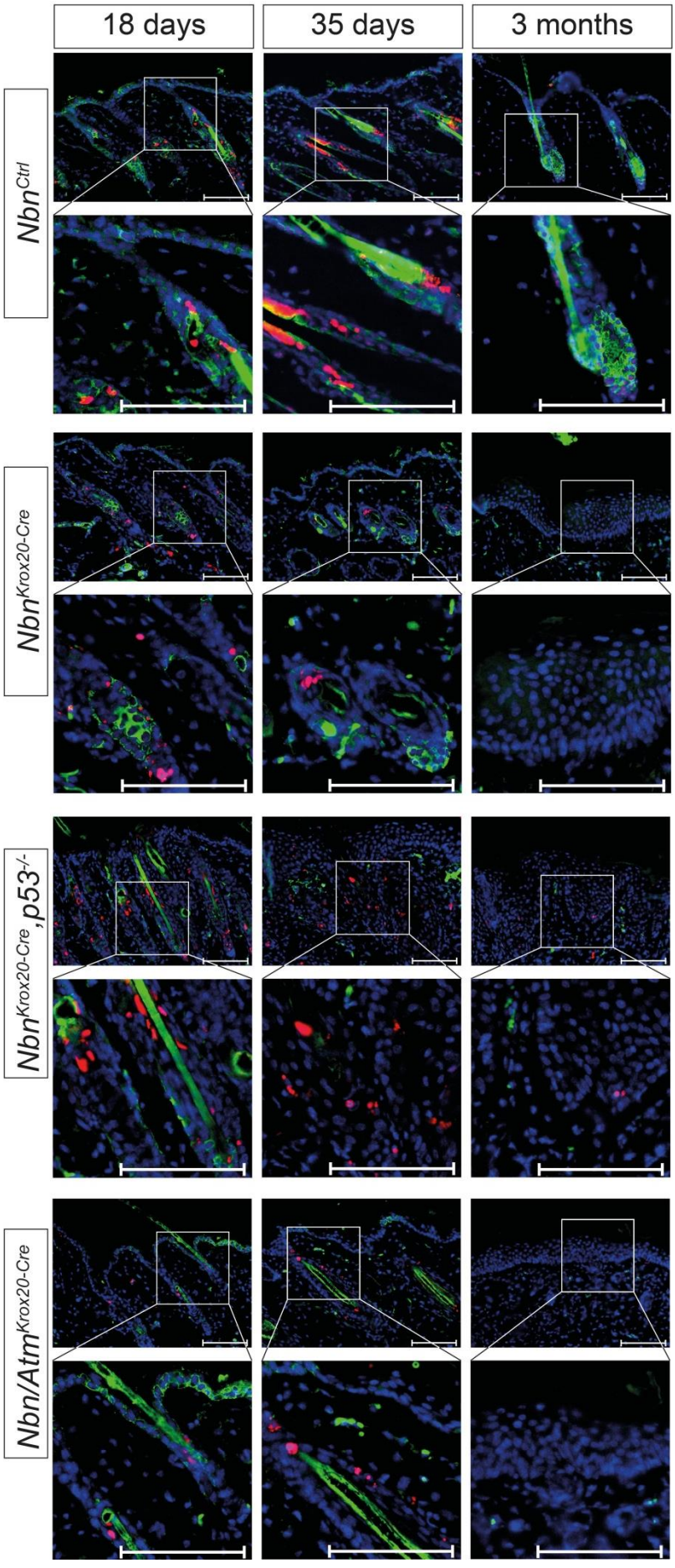

Figure 32: Colocalisation of Keratin 15 and TUNEL

Figure 32 shows stainings of *Nbn*^{Ctrl}, *Nbn*$^{Krox20\text{-}Cre}$, *Nbn*$^{Krox20\text{-}Cre}$*p53*$^{-/-}$ and *Nbn/Atm*$^{Krox20\text{-}Cre}$ mouse skin. The skin was collected at 18 and 35 days and 3 months after birth. It was stained against Keratin 15 and TUNEL reaction was performed. The staining for TUNEL is in red, Keratin 15 in green and DAPI is stained in blue.

Scale bar: 100 µm

In *Nbn*^{Ctrl} mice no overlap of TUNEL and Keratin 15 in cells was detected in all animals collected (Figure 32). The same was seen in the other mice. No cells with Keratin 15 expression and positive for TUNEL staining were detected in *Nbn*$^{Krox20\text{-}Cre}$, *Nbn*$^{Krox20\text{-}Cre}$*p53*$^{-/-}$ and *Nbn/Atm*$^{Krox20\text{-}Cre}$ animals at any point in time.

Lack of TUNEL staining in Keratin 15 stem cells demonstrated that disappearance of hair follicle stem cells was not due to apoptosis. It seems to be a consequence of the loss of stem cell integrity.

3.2.6 Characterization of proliferation of keratinocytes

The enlargement of the epidermis can have various reasons. It can be due to an increased number of proliferating cells, difficulties in differentiation of the keratinocytes or invasion of non-epidermal cells into the epidermis. The later reason should be visible in an altered appearance of epidermal structure and appearance of other cells normally not localized in the epidermis. This was not observed (Figure 17). The problems in differentiation were already demonstrated (Figure 28 to Figure 30). To visualize higher proliferation different markers had to be considered as protein expression changes according to the different steps in cell cycle progression. PCNA is expressed during DNA replication (S phase) (Tan et al.,1986; Baserga,1991). A typical marker for mitosis is Histone 3 phosphorylation at Serine 10 (Gurley et al.,1974; Li et al.,2013). Ki67 is a marker for S, G2 and M phase and is not present in G0 and early G1 phase (Gerdes et al.,1984). p63 is generally expressed in the proliferating keratinocytes of the basal layer (Yang et al.,1998; Koster et al.,2007; Xin et al.,2011).

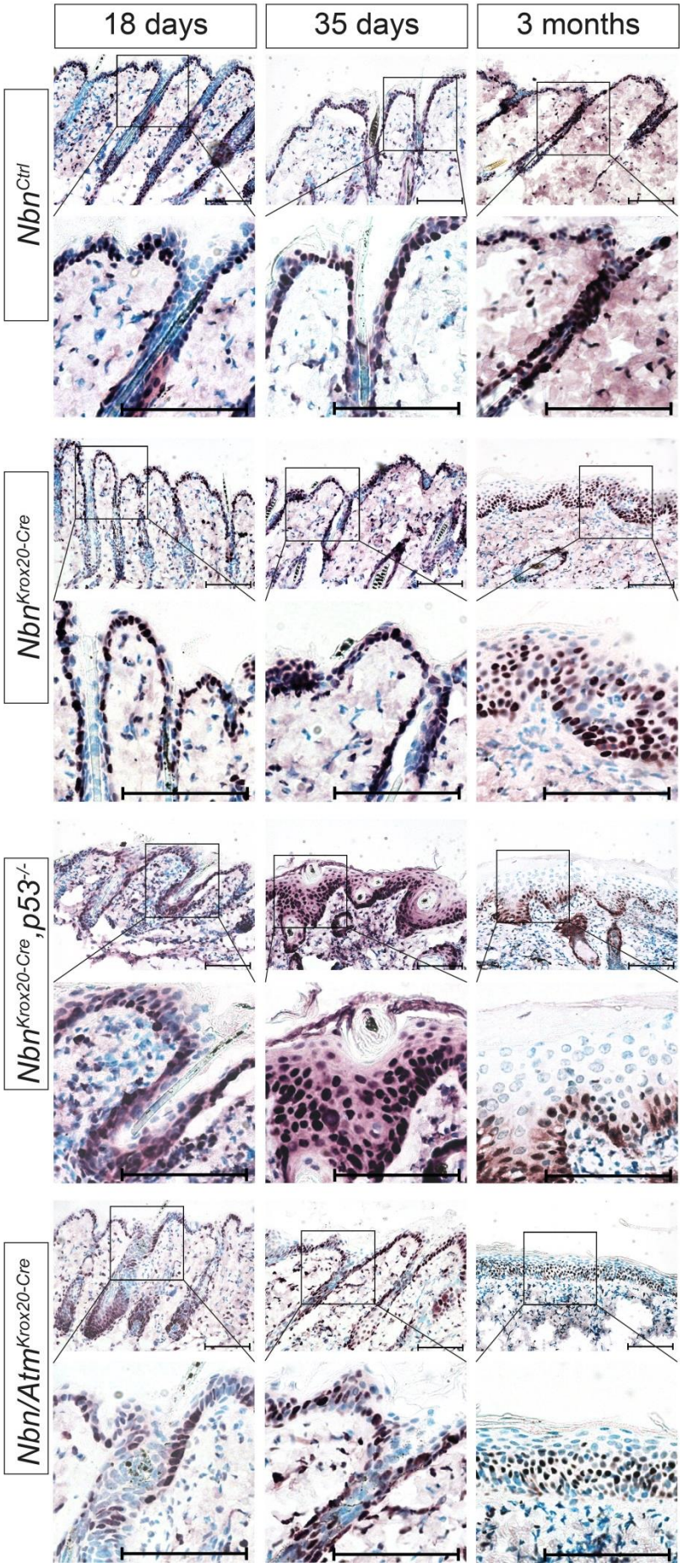

Figure 33: Distribution of PCNA positive cells in the epidermis

Cells positive for PCNA were visualized with antibody staining in Figure 33. The skin was taken from mice at the age of 18, 35 days and 3 months after birth. The mice were *Nbn*^{Ctrl}, *Nbn*$^{Krox20\text{-Cre}}$, *Nbn*$^{Krox20\text{-}Cre}$*p53*$^{-/-}$ and *Nbn/Atm*$^{Krox20\text{-}Cre}$.

Scale bar: 100 μm

The analysis of distribution of PCNA positive cells in the epidermis showed one layer of proliferating cells with one layer of non-proliferating cells on top for all mice with the age of 18 and 35 days (Figure 33). In Nbn^{Ctrl} this was also observed for 3 months old mice. In $Nbn^{Krox20\text{-}Cre}$, $Nbn^{Krox20\text{-}Cre}p53^{-/-}$ and $Nbn/Atm^{Krox20\text{-}Cre}$ mice with 3 months PCNA staining was not seen in one single layer. It comprised more than half of the enlarged epidermis. The cells were not organized in distinguishable layers but were distributed more or less randomly. Some PCNA positive cells were observed between cells not stained and an area of non-proliferating cells was placed in between PCNA positive cells.

PCNA staining demonstrated the elevation in proliferating cell number. A possible localization of proliferating cells outside the basal layer was hinted at.

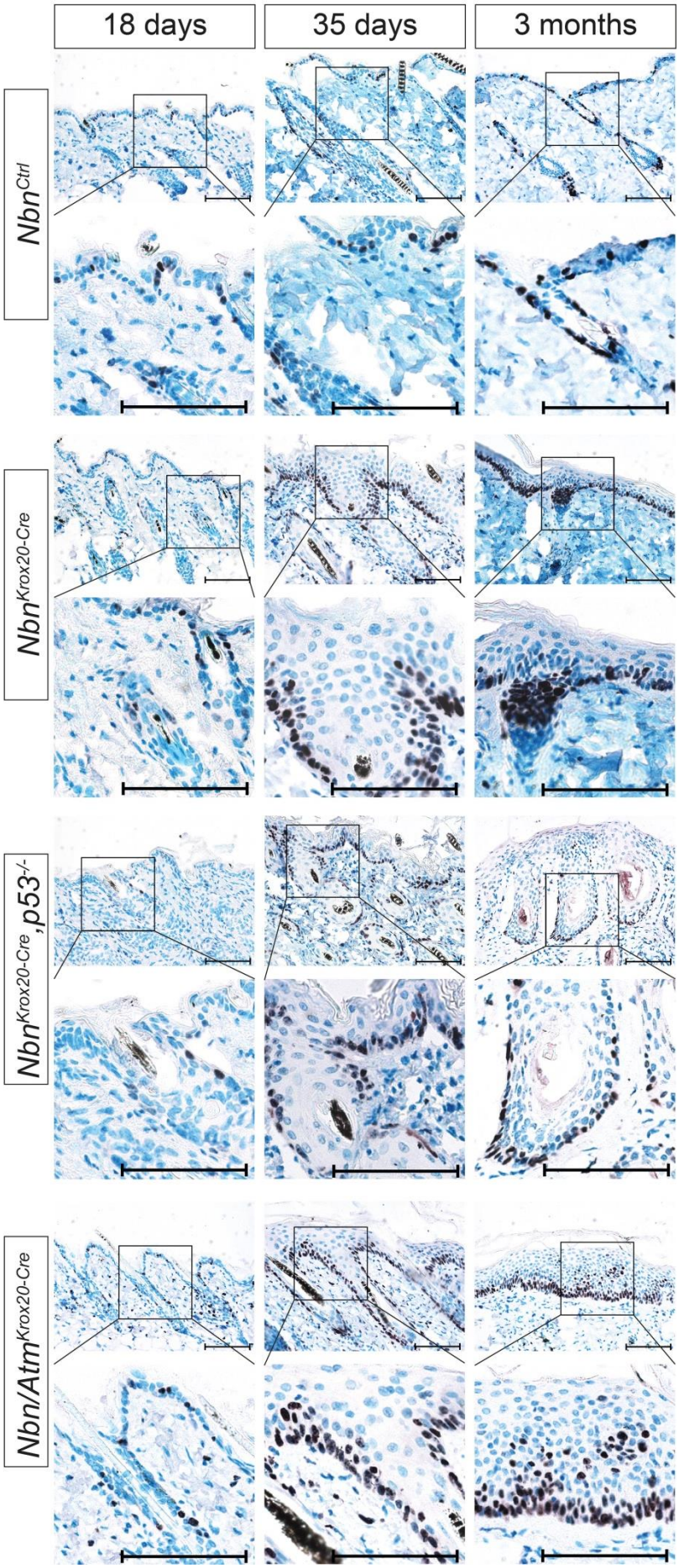

Figure 34: Visualization of Ki67 expression in skin cells

Skin from *Nbn*^{Ctrl}, *Nbn*$^{Krox20\text{-Cre}}$, *Nbn*$^{Krox20\text{-Cre}}$*p53*$^{-/-}$ and *Nbn/Atm*$^{Krox20\text{-Cre}}$ mice was stained. The mice were collected at 18 and 35 days and 3 months after birth. The staining was done with an antibody against Ki67.

Scale bar: 100 µm

In control animals some Ki67 positive cells were seen in der basal layer of the epidermis and around the hair follicle at 18, 35 days and 3 months after birth (Figure 34). The number of Ki67 positive cells in P18 *Nbn*$^{Krox20\text{-}Cre}$, *Nbn*$^{Krox20\text{-}Cre}$*p53*$^{-/-}$ and *Nbn/Atm*$^{Krox20\text{-}Cre}$ animals appeared to be at the same level as for P18 *Nbn*^{Ctrl} mice. Starting with 35 days after birth the number of Ki67 positive cells increased in *Nbn*$^{Krox20\text{-}Cre}$, *Nbn*$^{Krox20\text{-}Cre}$*p53*$^{-/-}$ and *Nbn/Atm*$^{Krox20\text{-}Cre}$ animals. At this age all positive cells were detected in the basal layer of the epidermis and in the hair follicle. At the age of 3 months some cells were also observed above the basal layer.

A proliferation increase was confirmed with Ki67 staining and a localization of proliferating cells outside the basal layer was indicated.

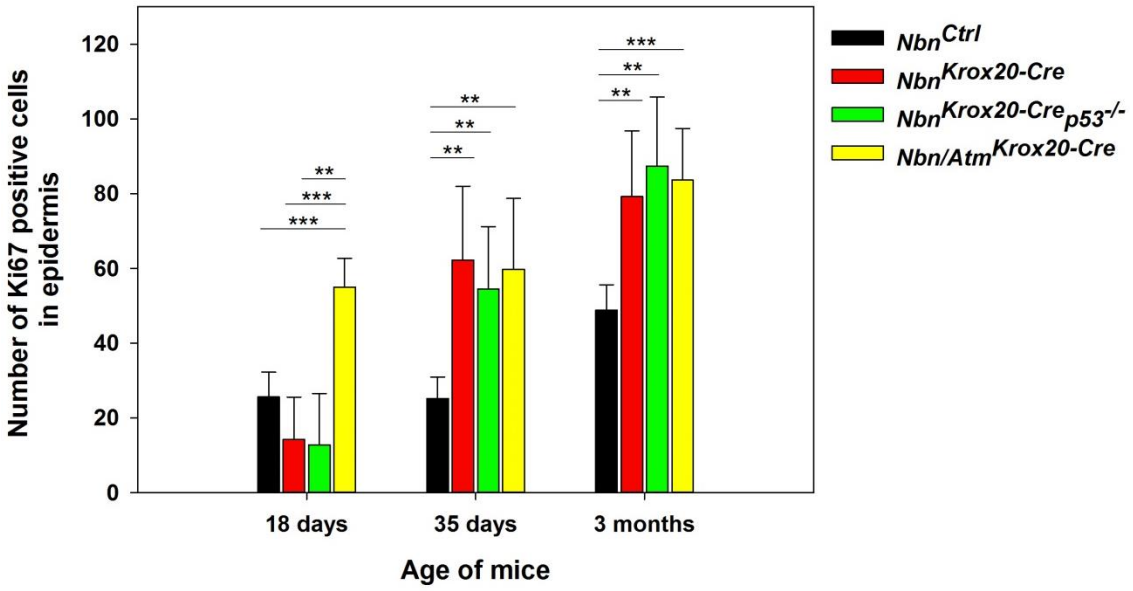

Figure 35: Analysis of number of Ki67 positive cells in the epidermis

Ki67 positive cells in the epidermis and the hair follicle were counted. Numbers from *Nbn*^{Ctrl}, *Nbn*$^{Krox20\text{-}Cre}$, *Nbn*$^{Krox20\text{-}Cre}$*p53*$^{-/-}$ and *Nbn/Atm*$^{Krox20\text{-}Cre}$ were arranged by age. (n = 5; **P < 0,01; ***P < 0,001)

The amount of Ki67 positive cells in the epidermis of the mice was evaluated (Figure 35). In mice 18 days after birth *Nbn*^{Ctrl} had 25,6 (± 6,58), *Nbn*$^{Krox20\text{-}Cre}$ had 14,2 (± 11,37), *Nbn*$^{Krox20\text{-}Cre}$*p53*$^{-/-}$ had 12,8 (± 13,68) and *Nbn/Atm*$^{Krox20\text{-}Cre}$ had 55 (± 7,71) Ki67 positive cells. At 35 days after birth *Nbn*^{Ctrl} showed 25,2 (± 5,72), *Nbn*$^{Krox20\text{-}Cre}$ 62,2 (± 19,79), *Nbn*$^{Krox20\text{-}Cre}$*p53*$^{-/-}$ 54,4 (± 16,77) and *Nbn/Atm*$^{Krox20\text{-}Cre}$ showed 59,8 (± 18,87) cells per section that were Ki67 positive. The number of cells with Ki67 expression changed to *Nbn*^{Ctrl} 48,8 (± 6,76), *Nbn*$^{Krox20\text{-}Cre}$ 79,2 (± 17,54),

Nbn$^{Krox20\text{-}Cre}$*p53*$^{-/-}$ 87,4 (± 18,49) and *Nbn/Atm*$^{Krox20\text{-}Cre}$ 83,6 (± 13,81) in the mice 3 months after birth. Statistical analysis of Ki67 expression in the epidermis was conducted. At the age of 18 days the number of positive cells was statistically increased in *Nbn/Atm*$^{Krox20\text{-}Cre}$ mice. When 35 days and 3 months old the *Nbn*$^{Krox20\text{-}Cre}$, *Nbn*$^{Krox20\text{-}Cre}$*p53*$^{-/-}$ and *Nbn/Atm*$^{Krox20\text{-}Cre}$ mice had a significant gain of Ki67 cells compared to *Nbn*^{Ctrl}.

Ki67 cell number increased in all deletion animals starting with 35 days.

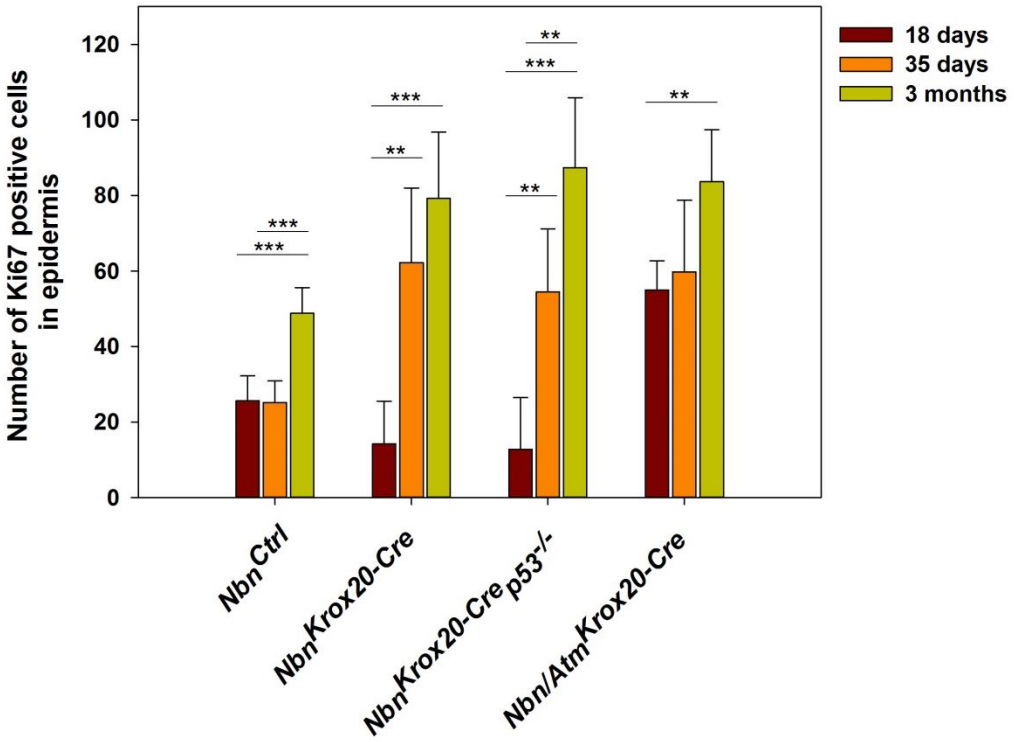

Figure 36: Assessment of changes of Ki67 expression with age

Statistical data from Ki67 epidermal cells were compared. The comparison of age specific differences was done within genotypes. . (n = 5; **P < 0,01; ***P < 0,001)

An age dependent evaluation of Ki67 cells was performed and is depicted in Figure 36. In *Nbn*^{Ctrl} mice a significant increase was detected at 3 months compared to 18 and 35 days. *Nbn*$^{Krox20\text{-}Cre}$ and *Nbn*$^{Krox20\text{-}Cre}$*p53*$^{-/-}$ presented a rise in cells with Ki67 at the age of 35 days and 3 months. The number of cells was also elevated in *Nbn/Atm*$^{Krox20\text{-}Cre}$ mice at 3 months.

The amount of Ki67 positive cells increased with the aging of the animals. This was most prominent in *Nbn*$^{Krox20\text{-}Cre}$ and *Nbn*$^{Krox20\text{-}Cre}$*p53*$^{-/-}$ mice.

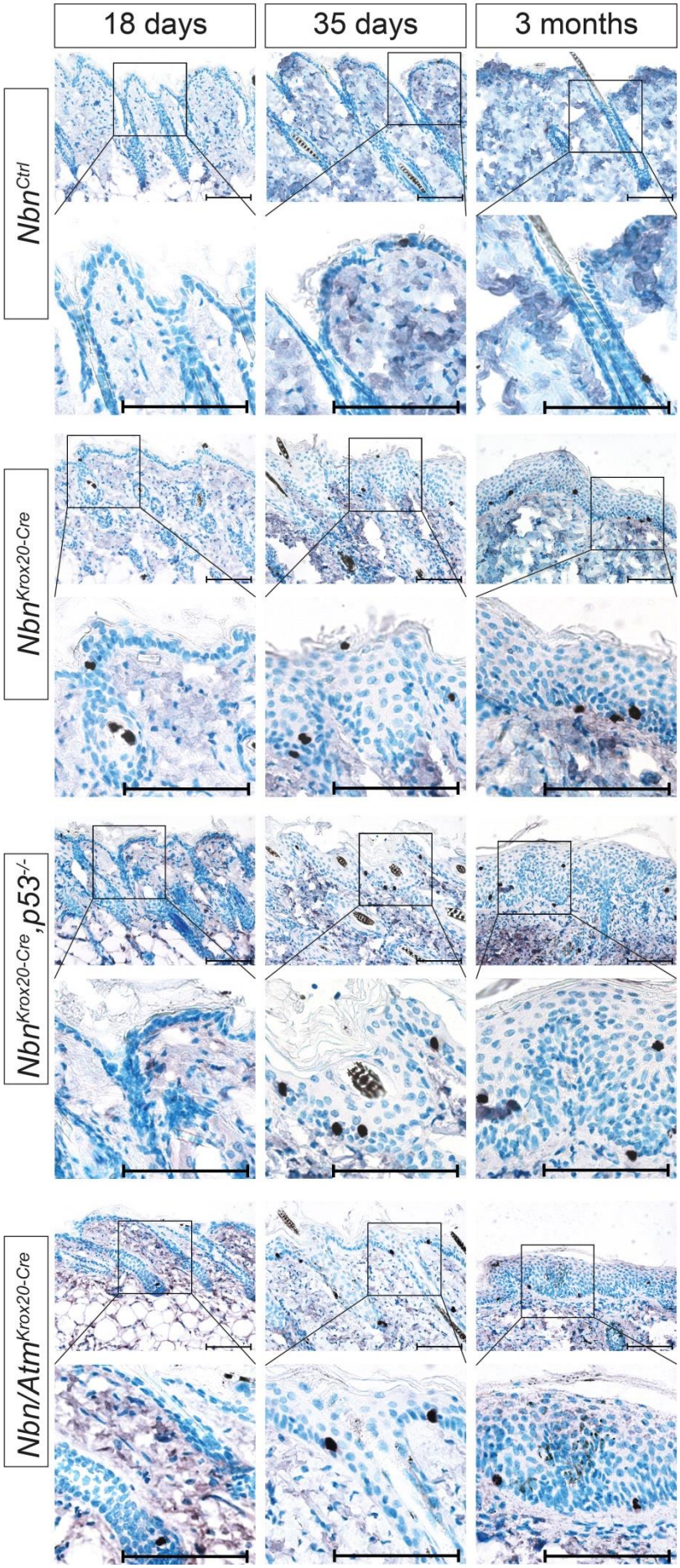

Figure 37: Staining for phosphorylated Histone 3

Skin from mice at different points in time (18, 35 days and 3 months) was collected. Mice were *Nbn*^{Ctrl}, *Nbn*$^{Krox20\text{-Cre}}$, *Nbn*$^{Krox20\text{-}Cre}$*p53*$^{-/-}$ and *Nbn/Atm*$^{Krox20\text{-}Cre}$. A staining against H3P was performed.

Scale bar: 100 µm

The staining for phosphorylation of Histone 3 (H3P) in Figure 37 showed only scattered H3P positive cells in *Nbn*^{Ctrl} mice at 18, 35 days and 3 months after birth. Those cells were placed within the basal layer of the epidermis or around the hair follicle. In *Nbn*$^{Krox20\text{-}Cre}$, *Nbn*$^{Krox20\text{-}Cre}$*p53*$^{-/-}$ and *Nbn/Atm*$^{Krox20\text{-}Cre}$ mice the number was increased at all points in time in comparison to *Nbn*^{Ctrl}. The cells were distributed throughout the complete epidermis.

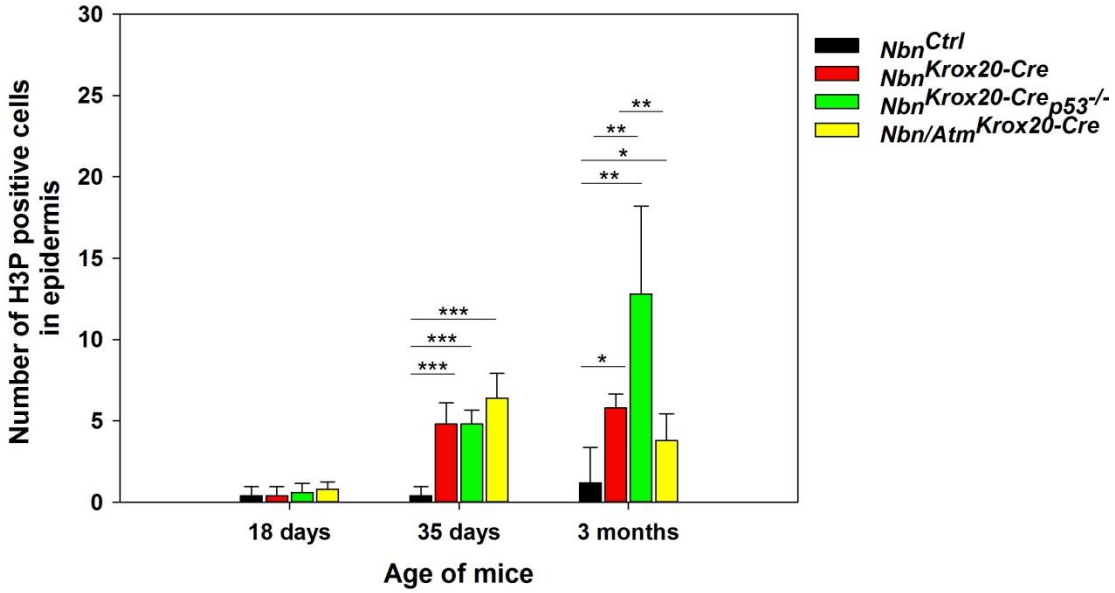

Figure 38: Analysis of H3P in the epidermis

In *Nbn*^{Ctrl}, *Nbn*$^{Krox20\text{-}Cre}$, *Nbn*$^{Krox20\text{-}Cre}$*p53*$^{-/-}$ and *Nbn/Atm*$^{Krox20\text{-}Cre}$ mice phosphorylated Histone 3 positive cells were enumerated. An age depended analysis was performed. (n = 5; *P < 0,05; **P < 0,01; ***P < 0,001)

Mice with an age of 18 days showed nearly no H3P positive cells no matter which genotype (*Nbn*^{Ctrl} 0,4 (± 0,55); *Nbn*$^{Krox20\text{-}Cre}$ 0,4 (± 0,55); *Nbn*$^{Krox20\text{-}Cre}$*p53*$^{-/-}$ 0,6 (± 0,55); *Nbn/Atm*$^{Krox20\text{-}Cre}$ 0,8 (± 0,45)) (Figure 38). With 35 days a significant increase can be seen for *Nbn*$^{Krox20\text{-}Cre}$ (4,8 ± 1,3), *Nbn*$^{Krox20\text{-}Cre}$*p53*$^{-/-}$ (4,8 ± 0,84) and *Nbn/Atm*$^{Krox20\text{-}Cre}$ (6,4 ± 1,52) compared with *Nbn*^{Ctrl} (0,4 ± 0,55). At 3 months the number of H3P cells remained significantly higher in deletion mice (*Nbn*$^{Krox20\text{-}Cre}$ 5,8 (±0,84); *Nbn*$^{Krox20\text{-}Cre}$*p53*$^{-/-}$ 12,8 (± 5,4); *Nbn/Atm*$^{Krox20\text{-}Cre}$ 3,8 (± 1,64)) than in the control group (*Nbn*^{Ctrl} 1,2 (± 2,17)). Both in *Nbn*$^{Krox20\text{-}Cre}$ and *Nbn*$^{Krox20\text{-}Cre}$*p53*$^{-/-}$ mice the amount of cells was higher than in *Nbn/Atm*$^{Krox20\text{-}Cre}$.

The number of cells with a phosphorylation of Histone 3 increased in genetically modified mice.

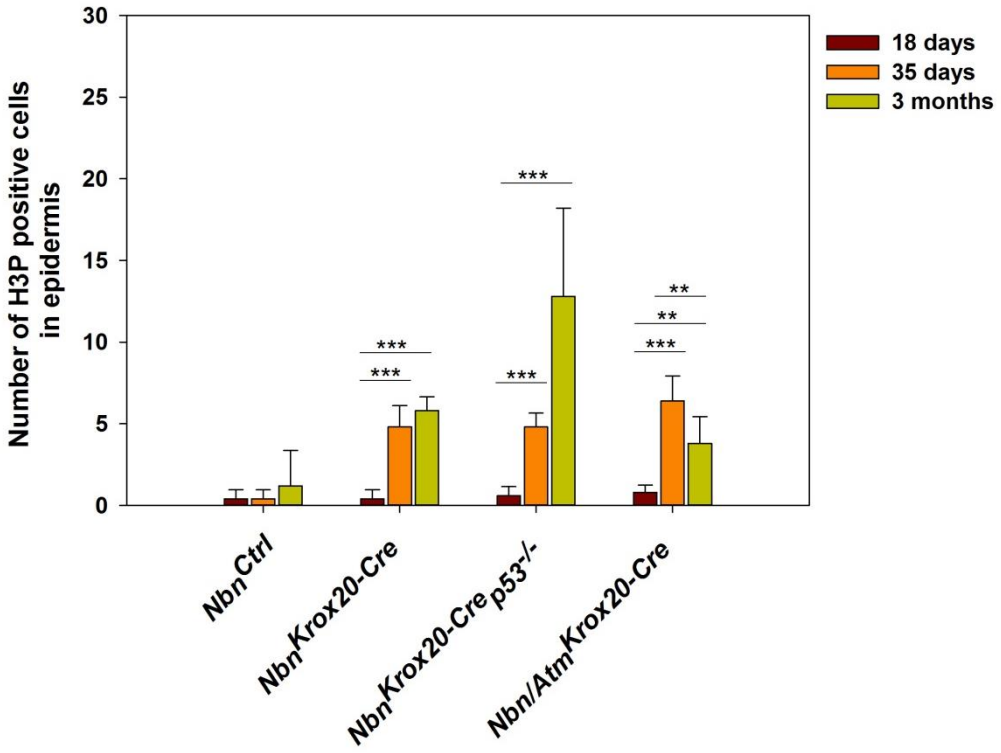

Figure 39: Evaluation of changes in H3P expression with aging of the animals

H3P positive cells were sorted according to genotype and statistically evaluated. The *Nbn*^{Ctrl}, *Nbn*$^{Krox20\text{-}Cre}$, *Nbn*$^{Krox20\text{-}Cre}$*p53*$^{-/-}$ and *Nbn/Atm*$^{Krox20\text{-}Cre}$ mice were collected at P18, P35 and 3 months. (n = 5; **P < 0,01; ***P < 0,001)

The quantity of H3P positive cells remained at a low level in *Nbn*^{Ctrl} mice at all points in time (Figure 39). In *Nbn*$^{Krox20\text{-}Cre}$, *Nbn*$^{Krox20\text{-}Cre}$*p53*$^{-/-}$ and *Nbn/Atm*$^{Krox20\text{-}Cre}$ animals number of positive cells increased from day 18 to day 35 after birth. In *Nbn*$^{Krox20\text{-}Cre}$ and *Nbn*$^{Krox20\text{-}Cre}$*p53*$^{-/-}$ mice the number remained at the same level in 3 months old mice. Animals with the genotype *Nbn/Atm*$^{Krox20\text{-}Cre}$ exhibited a decrease of H3P cells at 3 months after birth.

Histone 3 phosphorylation increased in *Nbn*$^{Krox20\text{-}Cre}$ and *Nbn*$^{Krox20\text{-}Cre}$*p53*$^{-/-}$ mice with aging of the animals. In *Nbn/Atm*$^{Krox20\text{-}Cre}$ animals an increase was observed first (P18 to P35) followed by a decrease at 3 months that left the number of H3P cells still significantly above the amount at 18 days.

All markers for cells in different steps of the cell cycle in which proliferation takes place showed an increase in cells within proliferation phase. The enlargement is therefore partially due to an elevation of proliferation.

All proliferation stainings showed few proliferating cells that were spread into areas of non-proliferating cells. To investigate if those cells retained all characteristics of proliferating cells or if they started to express differentiation markers double stainings were conducted.

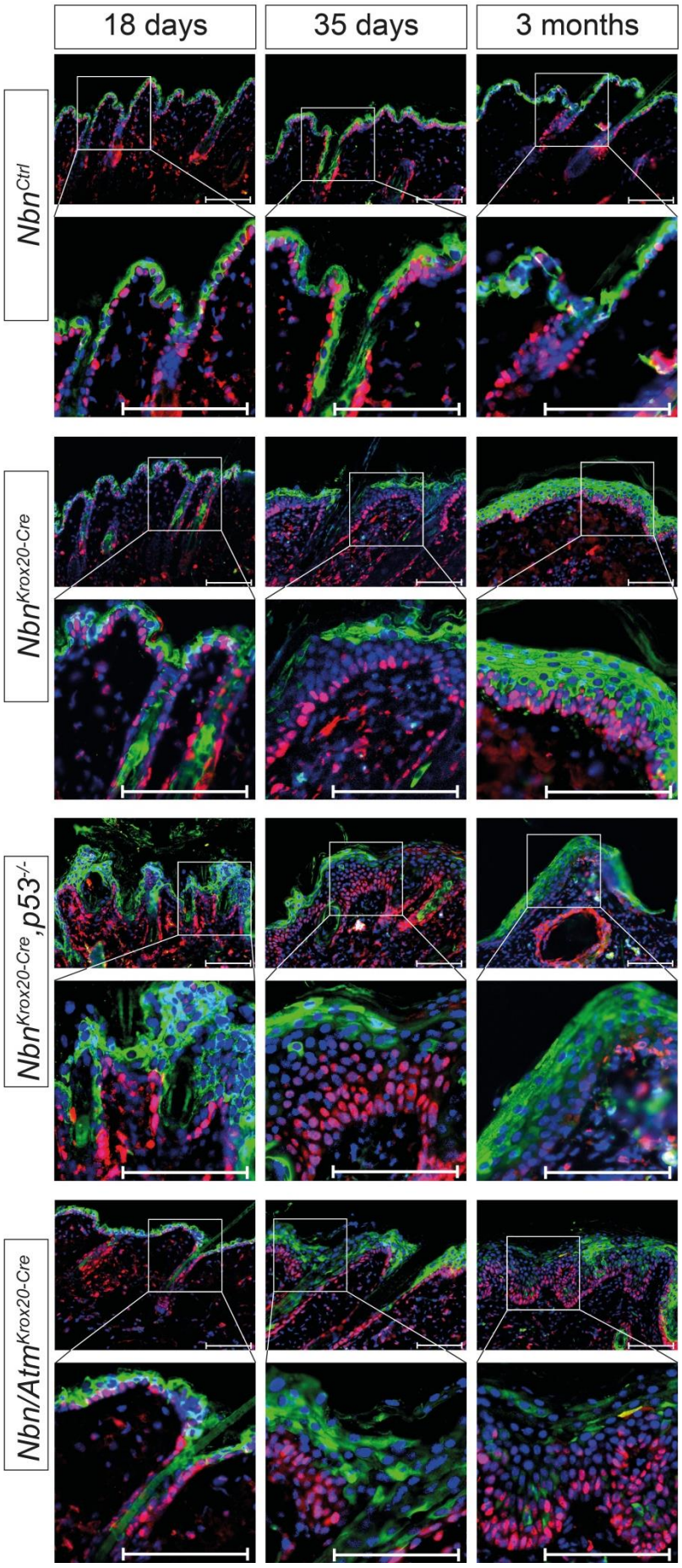

Figure 40: Analysis of colocalization from Keratin 10 and PCNA

Nbn^{Ctrl}, *Nbn*$^{Krox20\text{-}Cre}$, *Nbn*$^{Krox20\text{-}Cre}$*p53*$^{-/-}$ and *Nbn/Atm*$^{Krox20\text{-}Cre}$ were collected at 18, 35 days and 3 months after birth. Stainings against Keratin 10 and PCNA were done. Keratin 10 is stained in green, PCNA is colored in red and DAPI is blue.

Scale bar: 100 µm

Figure 40 shows the localization of proliferating cells with PCNA expression in comparison the differentiation marker Keratin 10. There was no overlapping of the stainings in any cells from *Nbn*^{Ctrl}, *Nbn*$^{Krox20\text{-Cre}}$, *Nbn*$^{Krox20\text{-}Cre}$*p53*$^{-/-}$ and *Nbn/Atm*$^{Krox20\text{-Cre}}$ mice. The PCNA cells in *Nbn*$^{Krox20\text{-}Cre}$, *Nbn*$^{Krox20\text{-}Cre}$*p53*$^{-/-}$ and *Nbn/Atm*$^{Krox20\text{-}Cre}$ 3 months old mice that were distributed through the epidermis localized between already differentiating cells with Keratin10 expression. On the other hand there were clearly distinguishable layers present in *Nbn*^{Ctrl} mice.

The double staining of PCNA and Keratin 10 showed a loss of the organized structure of the epidermis in mice with *Nbn, Nbn* and *p53* and *Nbn* and *Atm* deletion. Proliferating cells were not organized in one layer. More than one layer was always visible and the boundaries of the layers were lost. Differentiating cells were spread in between proliferating cells.

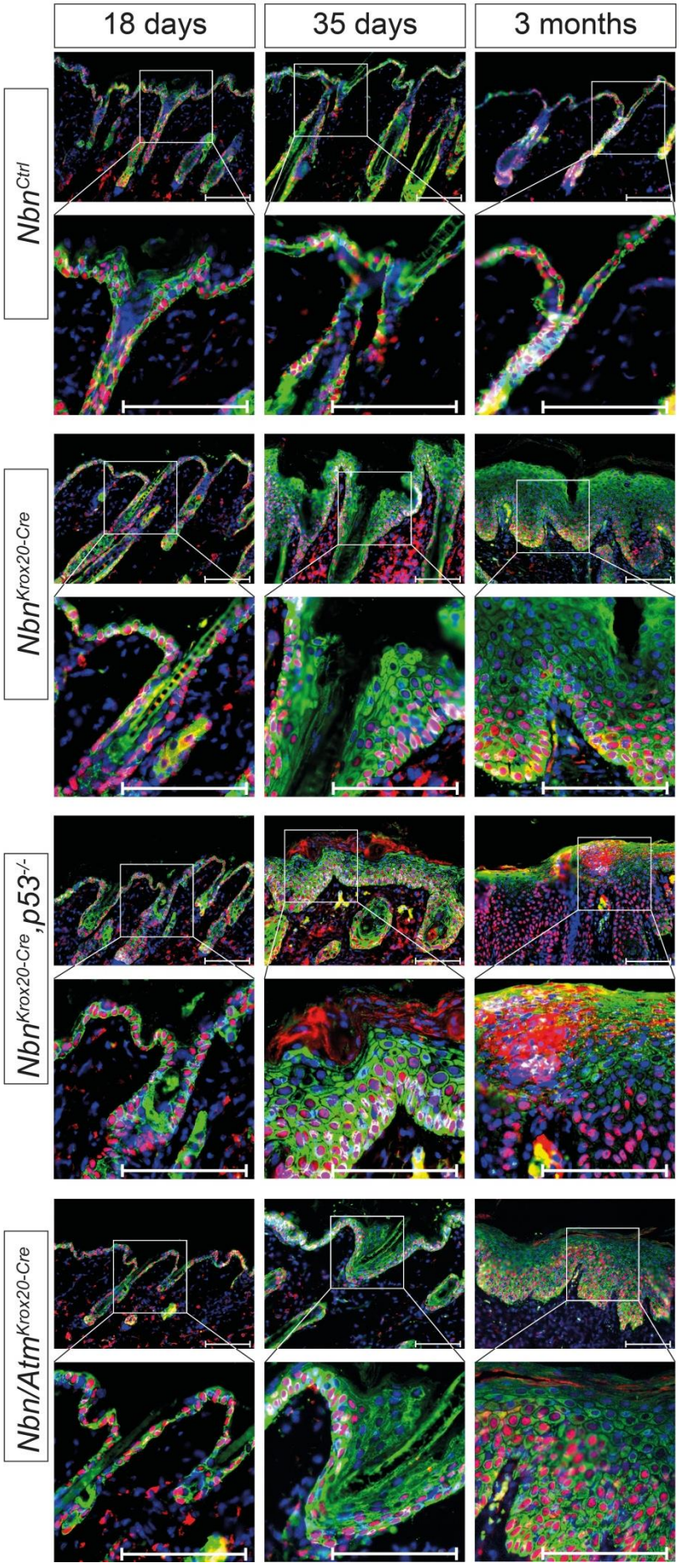

Figure 41: Staining of Keratin 14 and p63 positive cells in the epidermis

Skin from *Nbn*^{Ctrl}, *Nbn*$^{Krox20\text{-}Cre}$, *Nbn*$^{Krox20\text{-}Cre}$*p53*$^{-/-}$ and *Nbn/Atm*$^{Krox20\text{-}Cre}$ mice were stained. Antibody staining was performed against Keratin 14 and p63. The green staining visualizes Keratin 14, the red cells are p63 positive and DAPI is stained in blue.

Scale bar: 100 µm

In Nbn^{Ctrl} mice p63 positive cells showed an expression of Keratin 14 for all animals (Figure 41). At 18 days after birth this was the same in $Nbn^{Krox20\text{-}Cre}$, $Nbn^{Krox20\text{-}Cre}p53^{-/-}$ and $Nbn/Atm^{Krox20\text{-}Cre}$ mice. Both in P35 and 3 months old animals of $Nbn^{Krox20\text{-}Cre}$, $Nbn^{Krox20\text{-}Cre}p53^{-/-}$ and $Nbn/Atm^{Krox20\text{-}Cre}$ genotype all p63 positive cells were positive for Keratin 14. But not all Keratin 14 cells showed a positive staining for p63. The cells positive for both markers were oriented at the epidermal side towards the dermis. The upper layers showed no p63 but Keratin 14 expression.

Double staining of the proliferation marker of the basal keratinocytes p63 and Keratin 14 showed a partial colocalization. This colocalization was observed in the lower part of the epidermis.

Both double stainings of proliferation and differentiation markers showed that the proliferating cells retained the characteristics of non-differentiated cell. Those cells spread through the epidermis still belonged to a non-differentiated cell population. This also demonstrated that the epidermis lost its normal organizational structure with clearly distinguishable layers.

3.2.7 Psoriasis

The morphological evaluation of the mice showed, besides hair loss, a high increase of the number of layers of the epidermis and plaques on the surface of the mice. In addition the histological stainings revealed a rise of proliferation (acanthosis) and disturbed differentiation (parakeratosis). All those observations are typical for psoriasis (Griffiths and Barker,2007; Gudjonsson et al.,2007; Hertl,2011).

To clarify if the mice with a lack of *Nbn*, *Nbn* and *p53* and *Nbn* and *Atm* showed a psoriasis-like phenotype further experiments were conducted.

3.2.7.1 Analysis of invasion of leucocytes

The invasion of leucocytes is a typical sign for inflammation. Mast cell and Neutrophil invasion from the underlining tissue and blood system into the dermis towards the epidermal border is a typical sign for psoriasis (Griffiths and Barker,2007; Gudjonsson et al.,2007; Hertl,2011).

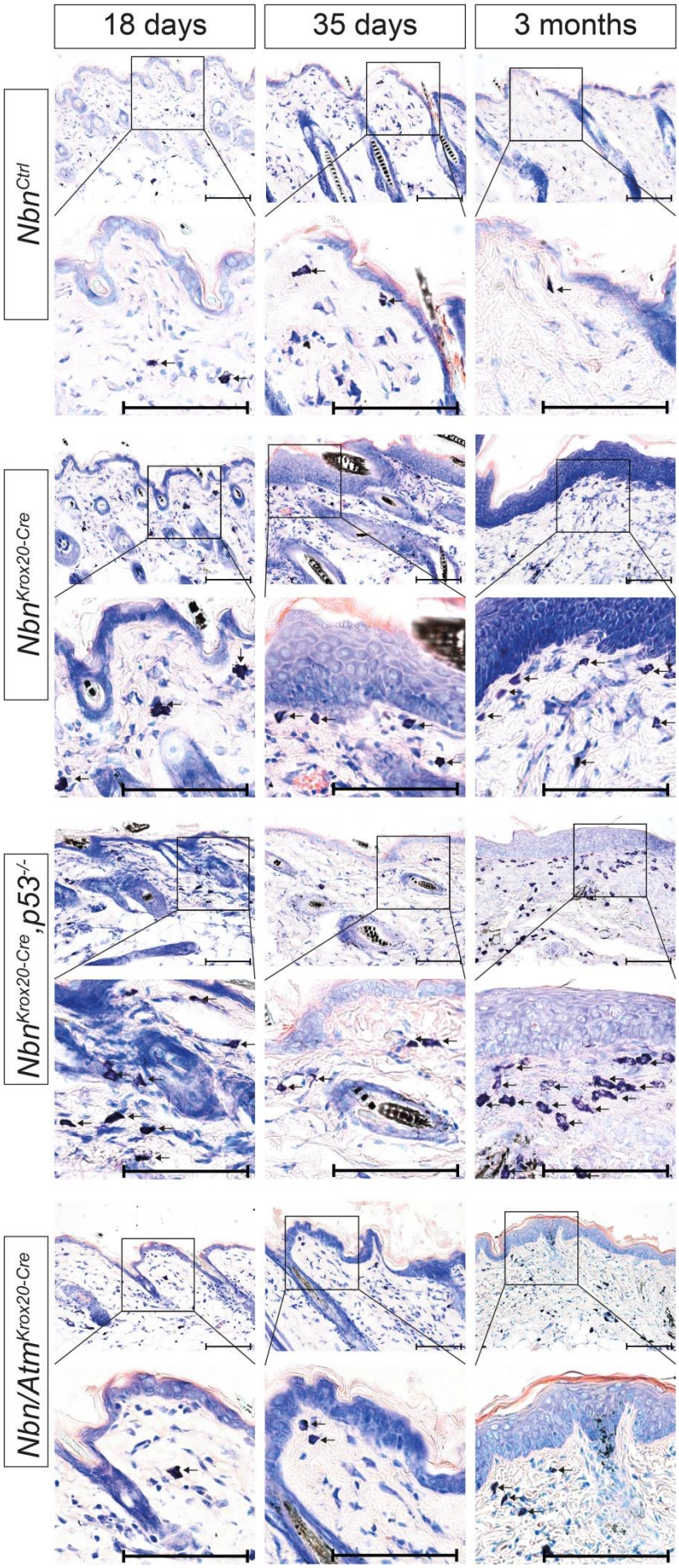

Figure 42: Analysis of localization of Mast cells

Giemsa staining was done on mouse skin from different ages (18, 35 days and 3 months). Skin was collected from *Nbn*^{Ctrl}, *Nbn*$^{Krox20\text{-}Cre}$, *Nbn*$^{Krox20\text{-}Cre}$*p53*$^{-/-}$ and *Nbn/Atm*$^{Krox20\text{-}Cre}$ mice. The epidermis and hair follicles are stained in a dark blue. Purple cells in the dermis are Mast cells. Mast cells are marked with arrows.

Scale bar: 100 µm

In skin from *Nbn*^{Ctrl} animals very few Mast cells were detected in animals of 18 days, 35 days and 3 months of age (Figure 42). In the dermis of *Nbn*$^{Krox20\text{-}Cre}$, *Nbn*$^{Krox20\text{-}Cre}$*p53*$^{-/-}$ and *Nbn/Atm*$^{Krox20\text{-}Cre}$ mice a higher number of Mast cells was observed at all points in time. They started to be present in the dermal part towards the underlying tissue (P18) und traveled upward towards the epidermis with the aging of the animals (P35, 3 months).

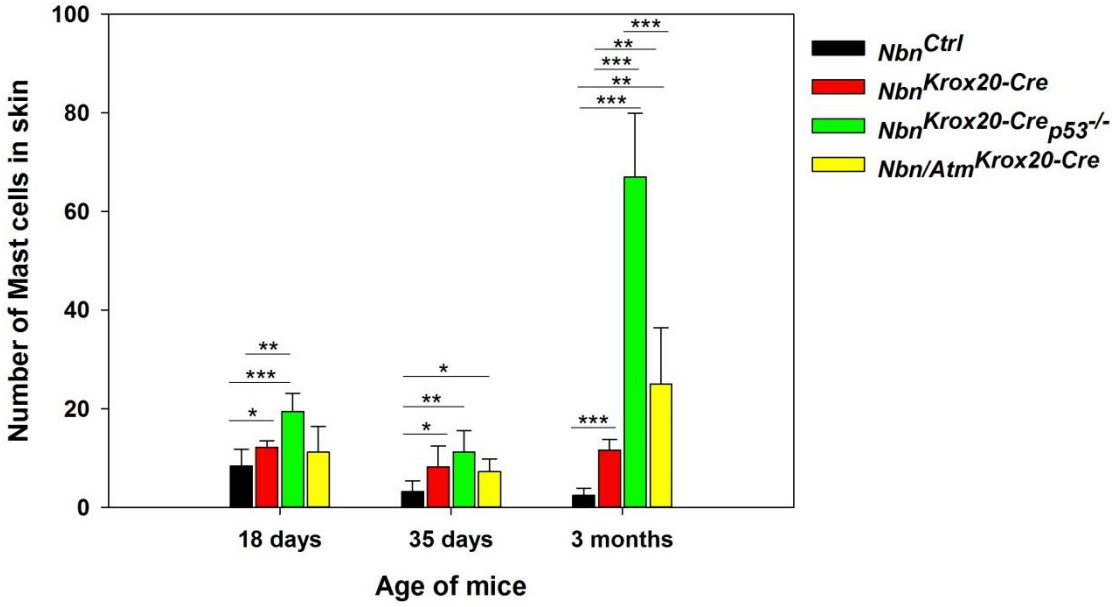

Figure 43: Statistical analysis of Mast cell occurrence in skin of mice

Mast cells in the dermis of the mice were counted. Statistical analysis was performed and results from *Nbn*^{Ctrl}, *Nbn*$^{Krox20\text{-}Cre}$, *Nbn*$^{Krox20\text{-}Cre}$*p53*$^{-/-}$ and *Nbn/Atm*$^{Krox20\text{-}Cre}$ mice were sorted according to age of the animals. (n = 5; *P < 0,05; **P < 0,01; ***P < 0,001)

The Mast cells were counted in the skin of the mice and the analysis is shown in Figure 43. 18 days after birth *Nbn*^{Ctrl} showed 8,4 (± 3,4), *Nbn*$^{Krox20\text{-}Cre}$ had 12,2 (± 1,3), *Nbn*$^{Krox20\text{-}Cre}$*p53*$^{-/-}$ 19,4 (± 3,7) and *Nbn/Atm*$^{Krox20\text{-}Cre}$ showed 11,2 (± 5,2) Mast cells per section. The numbers changed to *Nbn*^{Ctrl} 3,2 (± 2,2), *Nbn*$^{Krox20\text{-}Cre}$ 8,2 (± 4,3), *Nbn*$^{Krox20\text{-}Cre}$*p53*$^{-/-}$ 11,2 (± 4,4) and *Nbn/Atm*$^{Krox20\text{-}Cre}$ 7,2 (± 2,6) at 35 days after birth. Sections from mice 3 months after birth showed 2,4 (± 1,5) for *Nbn*^{Ctrl}, 11,6 (± 2,2) for *Nbn*$^{Krox20\text{-}Cre}$, 67 (± 12,9) for *Nbn*$^{Krox20\text{-}Cre}$*p53*$^{-/-}$ and 25 (± 11,4) Mast cells for *Nbn/Atm*$^{Krox20\text{-}Cre}$ animals. Analysis of Mast cell number in the skin of mice revealed a significant increase in *Nbn*$^{Krox20\text{-}Cre}$ and *Nbn*$^{Krox20\text{-}Cre}$*p53*$^{-/-}$ animals at 18 days after birth. At 35 days the amount of Mast cells was also elevated in *Nbn/Atm*$^{Krox20\text{-}Cre}$ mice. *Nbn*$^{Krox20\text{-}Cre}$*p53*$^{-/-}$ animals with 3 months showed the highest increase. The Mast cell

number was not only significantly higher than in the control group but also compared to *Nbn*$^{Krox20\text{-}Cre}$ and *Nbn/Atm*$^{Krox20\text{-}Cre}$ mice. The level of cells in *Nbn/Atm*$^{Krox20\text{-}Cre}$ animals was significantly higher than in *Nbn*^{Ctrl} and *Nbn*$^{Krox20\text{-}Cre}$ mice.

Mast cell number increased most prominently in *Nbn*$^{Krox20\text{-}Cre}$*p53*$^{-/-}$ animals.

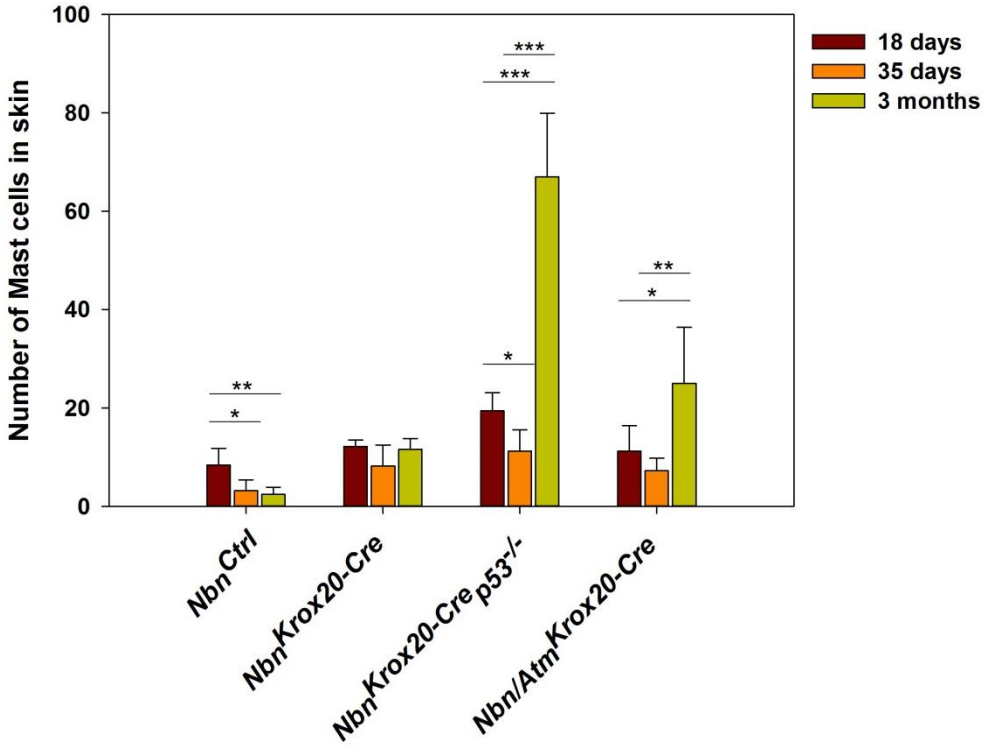

Figure 44: Study on shift in Mast cells number with age

In *Nbn*^{Ctrl}, *Nbn*$^{Krox20\text{-}Cre}$, *Nbn*$^{Krox20\text{-}Cre}$*p53*$^{-/-}$ and *Nbn/Atm*$^{Krox20\text{-}Cre}$ mice Mast cells in the dermis were counted. The number of Mast cells was sorted by genotype and analyzed. (n = 5; *P < 0,05; **P < 0,01; ***P < 0,001)

In *Nbn*^{Ctrl} mice the number of Mast cells was highest at 18 days (Figure 44). It significantly decreased at 35 days and 3 months. Mast cell number in *Nbn*$^{Krox20\text{-}Cre}$ mice remained at the same level at all points in time. In *Nbn*$^{Krox20\text{-}Cre}$*p53*$^{-/-}$ animals the number of Mast cells decreased from P18 to P35. From day 35 to 3 months after birth it increased significantly. A significant increase of Mast cells in *Nbn/Atm*$^{Krox20\text{-}Cre}$ mice was detected at 3 months.

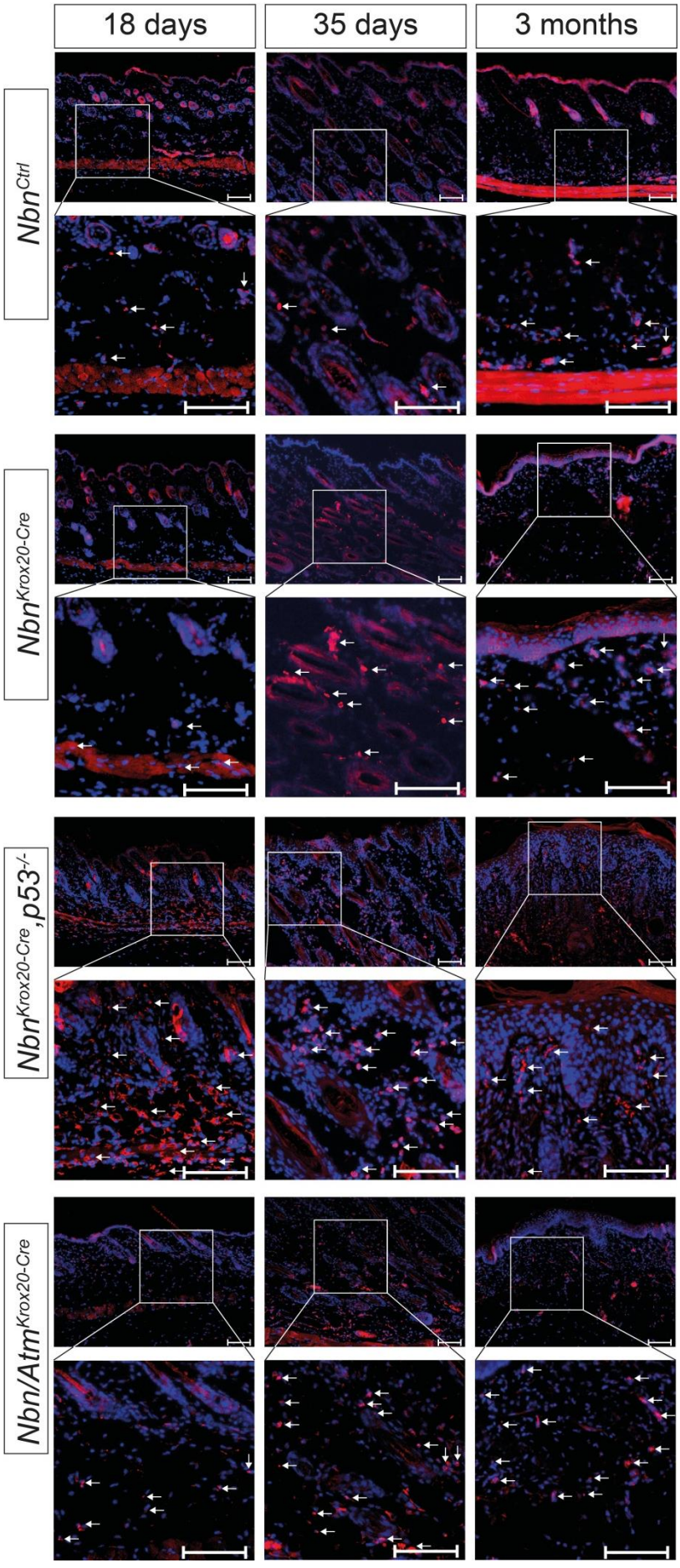

Figure 45: Staining against Neutrophils

Skin of mice from different ages (P18, P35 and 3 months) of *Nbn*^{Ctrl}, *Nbn*$^{Krox20\text{-}Cre}$, *Nbn*$^{Krox20\text{-}Cre}$*p53*$^{-/-}$ and *Nbn/Atm*$^{Krox20\text{-}Cre}$ mice are depicted. It was stained against Neutrophils. Neutrophils are red and blue is the staining of DAPI. Arrows mark single or clusters of Neutrophils.

Scale bar: 50 µm

Neutrophils in the skin of *Nbn*^{Ctrl} animals were visible only in the part of the dermis towards the underlying tissue (Figure 45). This distribution of Neutrophils in the skin was the same at 18, 35 days and 3 months after birth. The number of Neutrophils increased in *Nbn*$^{Krox20\text{-}Cre}$, *Nbn*$^{Krox20\text{-}Cre}$*p53*$^{-/-}$ and *Nbn/Atm*$^{Krox20\text{-}Cre}$ mice compared to control animals at all ages animals were collected. The localization of Neutrophils in those animals changed from the dermal border to the underlying tissue (P18) to the border between dermis and epidermis (P35 and 3 months).

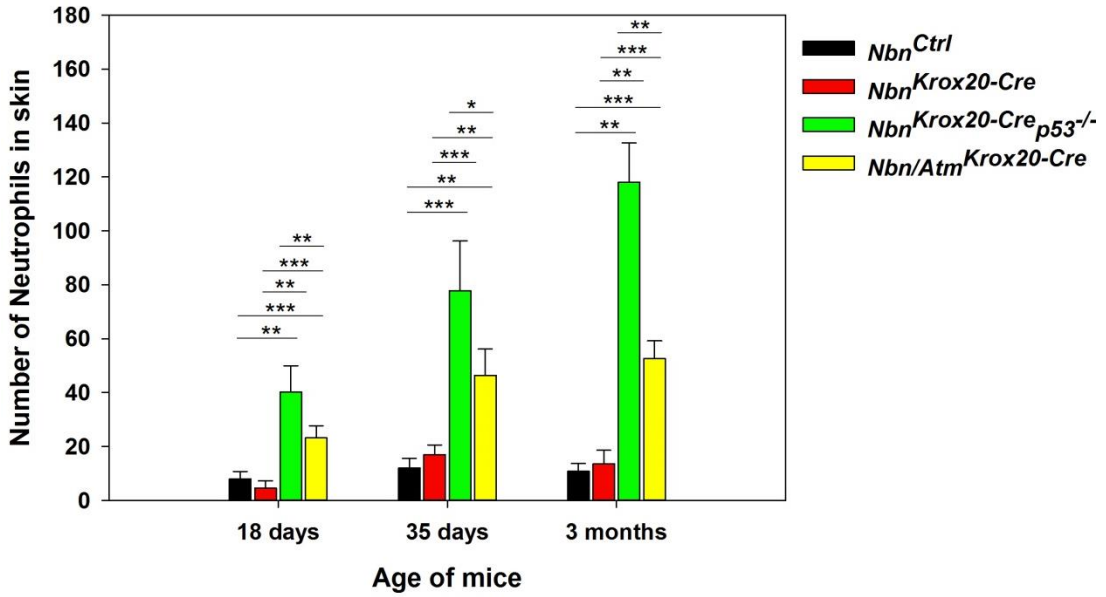

Figure 46: Analysis of Neutrophils in the skin of mice

Number of Neutrophils was counted in the dermis of *Nbn*^{Ctrl}, *Nbn*$^{Krox20\text{-}Cre}$, *Nbn*$^{Krox20\text{-}Cre}$*p53*$^{-/-}$ and *Nbn/Atm*$^{Krox20\text{-}Cre}$ mice. Numbers were analyzed and are shown grouped by age (P18, P35 and 3 months). (n = 5; *P < 0,05; **P < 0,01; ***P < 0,001)

At 18 days after birth *Nbn*$^{Krox20\text{-}Cre}$*p53*$^{-/-}$ (40,2 ± 9,73) and *Nbn/Atm*$^{Krox20\text{-}Cre}$ (23,2 ± 4,44) mouse skin showed an increase in number of Neutrophils compared to *Nbn*^{Ctrl} (8 ± 2,74) and *Nbn*$^{Krox20\text{-}Cre}$ (4,6 ± 2,7) (Figure 46). The amount of Neutrophils in *Nbn/Atm*$^{Krox20\text{-}Cre}$ was significantly lower than in *Nbn*$^{Krox20\text{-}Cre}$*p53*$^{-/-}$. *Nbn*^{Ctrl} and *Nbn*$^{Krox20\text{-}Cre}$ mice had a similar number of Neutrophils in the dermis. All those observations were the same in 35 days and 3 months old mice. 35 days after birth *Nbn*^{Ctrl} showed 12 (± 3,6), *Nbn*$^{Krox20\text{-}Cre}$ showed 17 (± 3,6), *Nbn*$^{Krox20\text{-}Cre}$*p53*$^{-/-}$ presented 77,8 (± 18,46) and *Nbn/Atm*$^{Krox20\text{-}Cre}$ had 46,4 (± 9,74) Neutrophils per section. The count of cells changed to 10,8 (± 2,87) for *Nbn*^{Ctrl}, 13,6 (± 5,08) in *Nbn*$^{Krox20\text{-}Cre}$,

118 (± 14,61) for *Nbn*$^{Krox20\text{-}Cre}$*p53*$^{-/-}$ and 52,6 (± 6,54) in *Nbn/Atm*$^{Krox20\text{-}Cre}$ mice 3 months after birth.

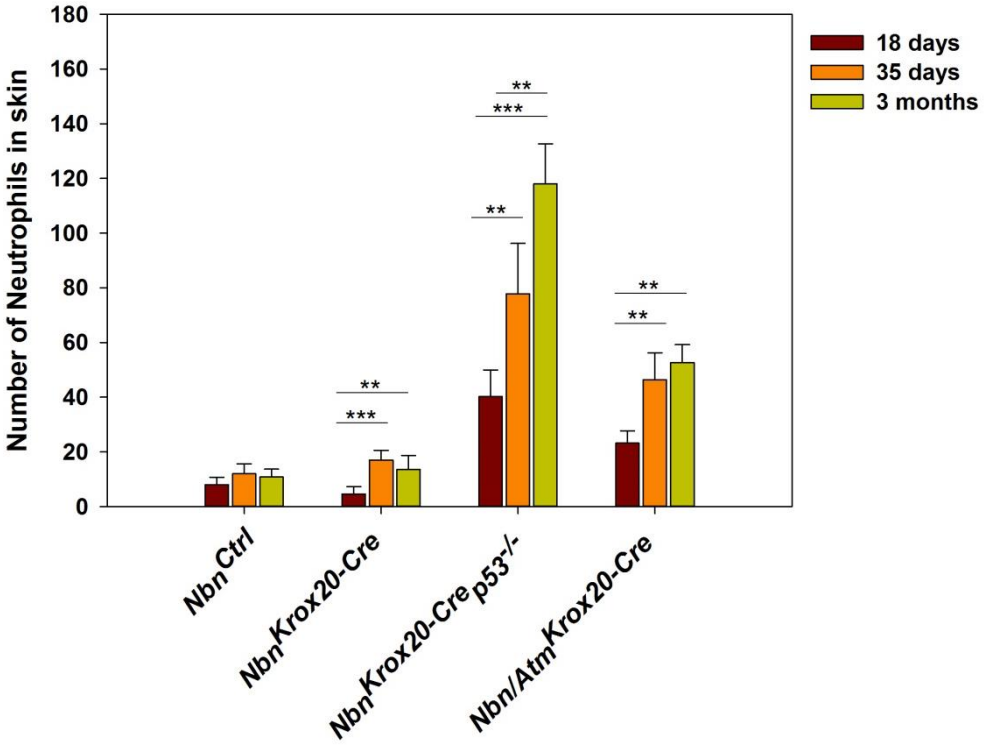

Figure 47: Evaluation of age dependent Neutrophil accumulation in skin

Neutrophils from *Nbn*^{Ctrl}, *Nbn*$^{Krox20\text{-}Cre}$, *Nbn*$^{Krox20\text{-}Cre}$*p53*$^{-/-}$ and *Nbn/Atm*$^{Krox20\text{-}Cre}$ mice were analyzed to shown the age dependent variations within genotypes. Animals were collected at 18, 35 days and 3 months after birth. (n = 5; **P < 0,01; ***P < 0,001)

The amount of Neutrophils in *Nbn*^{Ctrl} mice remained the same in animals collected 18, 35 days and 3 months after birth (Figure 47). *Nbn*$^{Krox20\text{-}Cre}$ mice showed a significant increase of Neutrophils from 18 to 35 days and from 18 days to 3 months of age. In *Nbn*$^{Krox20\text{-}Cre}$*p53*$^{-/-}$ animals this was also the case. In addition an increase from 35 days to 3 months was detected. *Nbn/Atm*$^{Krox20\text{-}Cre}$ animals exhibited an elevation from Neutrophil numbers in 35 days to 3 months old animals compared to 18 days.

The number of Neutrophils and Mast cells rose with the aging of the *Nbn*$^{Krox20\text{-}Cre}$, *Nbn*$^{Krox20\text{-}Cre}$*p53*$^{-/-}$ and *Nbn/Atm*$^{Krox20\text{-}Cre}$ animals. Both Mast cells and Neutrophils invaded the dermis and spread till they reached the border between dermis and epidermis.

3.2.7.2 Study of CD3 T-cells in the epidermis

The existence of T-cells is a sign of inflammation. T-cells with an expression of CD3 (cluster of differentiation 3) are commonly observed in skin with psoriatic lesions (Weinshenker et al.,1989; Bos and De Rie,1999).

A study of CD3 positive T-cell was conducted in the skin of the mice.

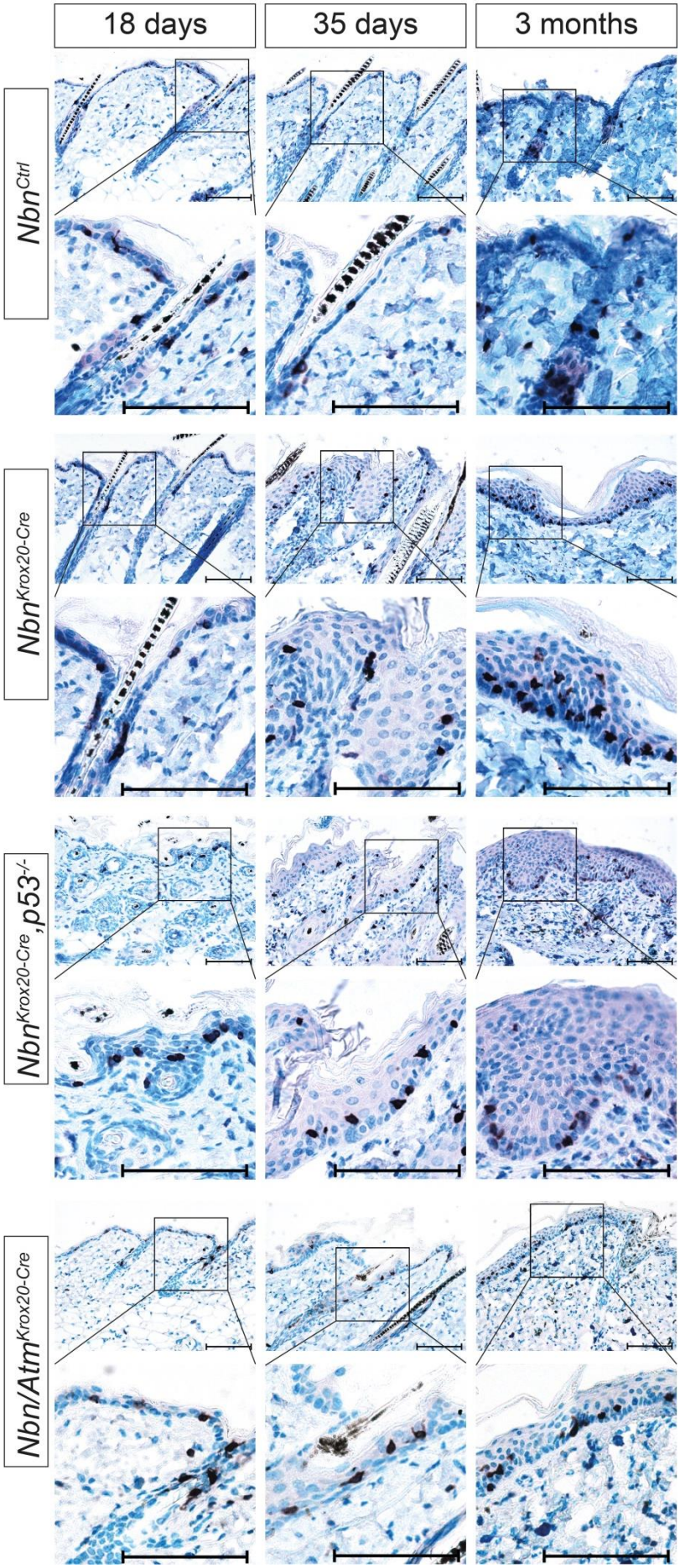

Figure 48: Study of CD3 positive cells

CD3 positive T-cells in the skin of *Nbn*^{Ctrl}, *Nbn*$^{Krox20\text{-}Cre}$, *Nbn*$^{Krox20\text{-}Cre}$*p53*$^{-/-}$ and *Nbn/Atm*$^{Krox20\text{-}Cre}$ mice were stained with an anti CD3 antibody. The staining was performed in 3 months, 18 and 35 days old mice.

Scale bar: 100 µm

In *Nbn*^{Ctrl} mice few CD3 positive T-cells were present in the epidermis and along the hair follicles in all collected animals (Figure 48). A comparable amount of cells was observed in the *Nbn*$^{Krox20\text{-}Cre}$, *Nbn*$^{Krox20\text{-}Cre}$*p53*$^{-/-}$ and *Nbn/Atm*$^{Krox20\text{-}Cre}$ mice at day 18. Starting at 35 days a higher the amount of CD3 positive cells was seen in *Nbn*$^{Krox20\text{-}Cre}$, *Nbn*$^{Krox20\text{-}Cre}$*p53*$^{-/-}$ and *Nbn/Atm*$^{Krox20\text{-}Cre}$ mice.

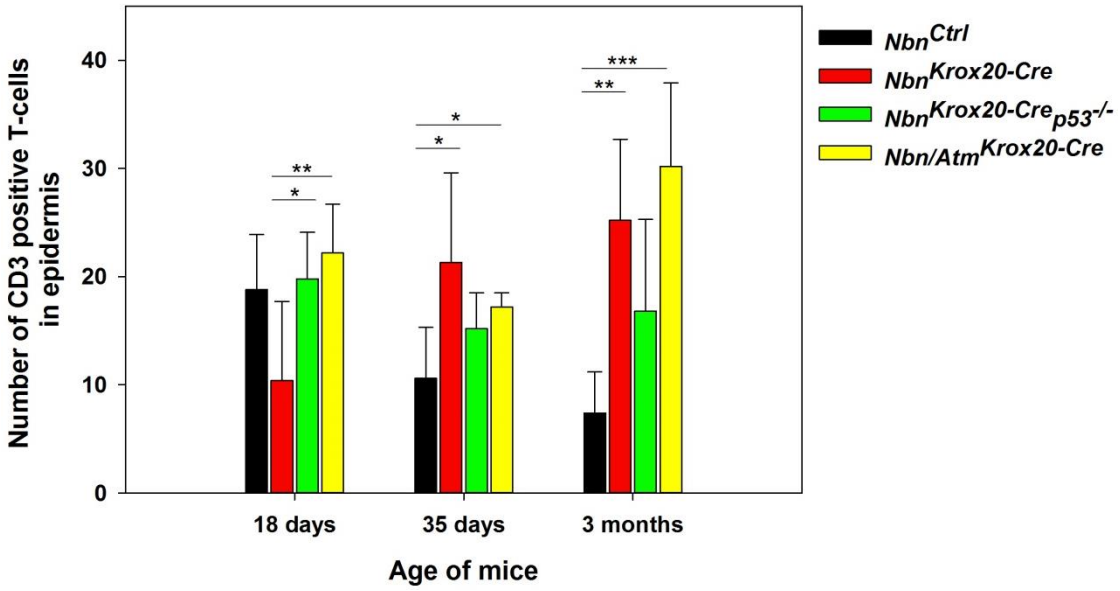

Figure 49: Assessment of CD3 positive cells in the epidermis

In the epidermis of *Nbn*^{Ctrl}, *Nbn*$^{Krox20\text{-}Cre}$, *Nbn*$^{Krox20\text{-}Cre}$*p53*$^{-/-}$ and *Nbn/Atm*$^{Krox20\text{-}Cre}$ mice the number of CD3 positive cells was counted. They were studied in regard to ages of the animals. Skin was collected at 18, 35 days and 3 months after birth. (n = 5; *P < 0,05; **P < 0,01; ***P < 0,001)

At 18 days no increase in CD3 positive T-cells was detected between *Nbn*^{Ctrl} (18,8 ± 5,1) and *Nbn*$^{Krox20\text{-}Cre}$ (10,4 ± 7,3), *Nbn*$^{Krox20\text{-}Cre}$*p53*$^{-/-}$ (19,8 ± 4,3) and *Nbn/Atm*$^{Krox20\text{-}Cre}$ mice (22,2 ± 4,5) (Figure 49). Only the number of *Nbn*$^{Krox20\text{-}Cre}$ CD3 cells was significantly less than in *Nbn*$^{Krox20\text{-}Cre}$*p53*$^{-/-}$ and *Nbn/Atm*$^{Krox20\text{-}Cre}$. The numbers of CD3 positive cells per section in 35 days old animals were 10,6 (± 4,7) for *Nbn*^{Ctrl}, 21,3 (± 8,3) for *Nbn*$^{Krox20\text{-}Cre}$, 15,2 (± 3,3) in *Nbn*$^{Krox20\text{-}Cre}$*p53*$^{-/-}$ and 17,2 (± 1,3) in *Nbn/Atm*$^{Krox20\text{-}Cre}$ mice. With 3 months *Nbn*^{Ctrl} presented 7,4 (± 3,8), *Nbn*$^{Krox20\text{-}Cre}$ had 25,2 (± 7,5), *Nbn*$^{Krox20\text{-}Cre}$*p53*$^{-/-}$ showed 16,8 (± 8,5) and *Nbn/Atm*$^{Krox20\text{-}Cre}$ showed 30,2 (± 7,7) CD3 positive cells per section. In 35 days and 3 months old animals a statistically significant increase was seen between *Nbn*^{Ctrl} and *Nbn*$^{Krox20\text{-}Cre}$ and *Nbn/Atm*$^{Krox20\text{-}Cre}$ mice. The number of T-cells in *Nbn*$^{Krox20\text{-}Cre}$*p53*$^{-/-}$ was not changed significantly in 35 days and 3 months old animals.

An increase in CD3 T-cells was observed in *Nbn*$^{Krox20\text{-}Cre}$ and *Nbn/Atm*$^{Krox20\text{-}Cre}$ mice.

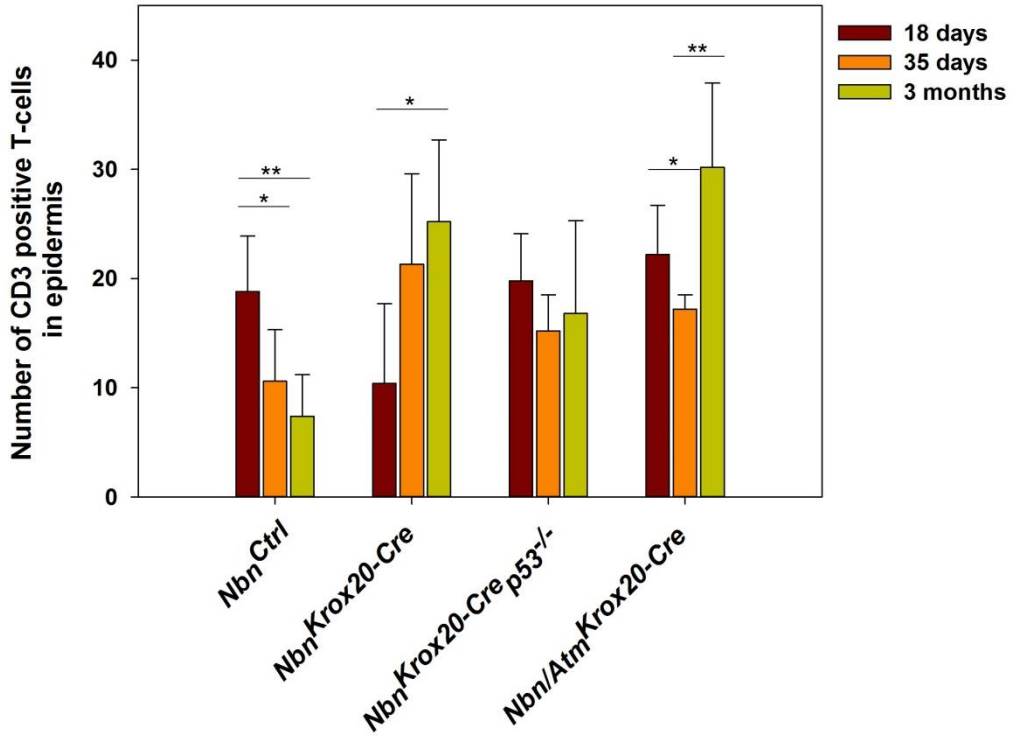

Figure 50: Analysis of age related changes of CD3 in the epidermis

CD3 cells were analyzed by genotype (*Nbn*^{Ctrl}, *Nbn*$^{Krox20\text{-}Cre}$, *Nbn*$^{Krox20\text{-}Cre}$*p53*$^{-/-}$ and *Nbn/Atm*$^{Krox20\text{-}Cre}$). The different collection times are shown (18, 35 days and 3 months). (n = 5; *P < 0,05; **P < 0,01)

Nbn^{Ctrl} mice expressed a significant decrease of CD3 positive T-cells from P18 to P35 and 3 months (Figure 50). An increase in CD3 positive T-cells was detected from 18 day old *Nbn*$^{Krox20\text{-}Cre}$ mice to 3 months old animals. The level of CD3 cells remained constant in *Nbn*$^{Krox20\text{-}Cre}$*p53*$^{-/-}$ mice. *Nbn/Atm*$^{Krox20\text{-}Cre}$ mice showed a decrease from 18 to 35 days. At the age of 3 months the cell number was significantly increased.

In control animals the number of CD3 cells decreases with the aging of the animals. In *Nbn*$^{Krox20\text{-}Cre}$ and *Nbn/Atm*$^{Krox20\text{-}Cre}$ mice this was reversed while in *Nbn*$^{Krox20\text{-}Cre}$*p53*$^{-/-}$ animals the level of T-cells remained the same at all collected ages.

3.2.7.3 Characterization of Stat3 phosphorylation at Tyrosine 705

An activation of Stat3 is commonly observed in psoriasis (Sano et al.,2005). The activation occurs through a phosphorylation at Tyrosine (Tyr) 705. This phosphorylation triggers a relocalization of Stat3 in the nucleus of the cells.

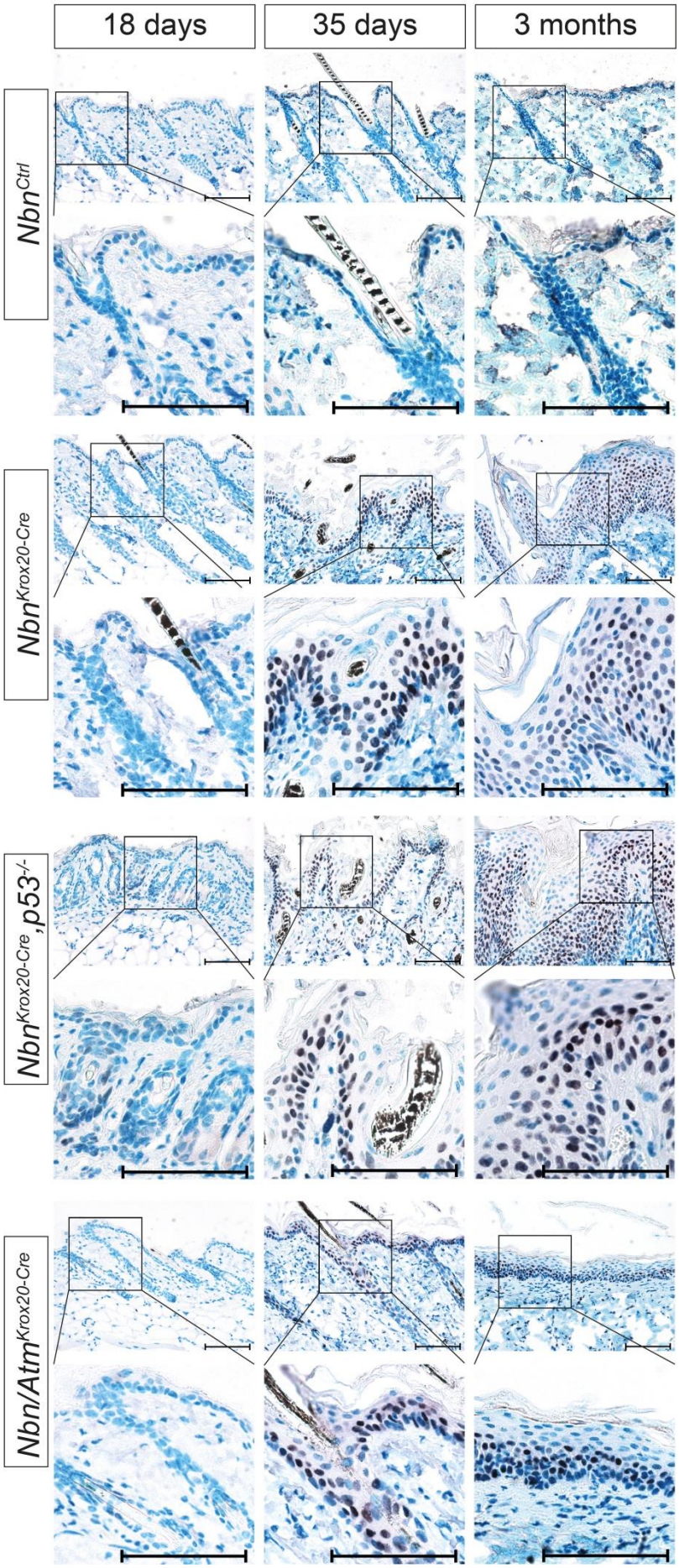

Figure 51: Visualization of Stat3 phosphorylation at Tyr 705

Nbn^{Ctrl}, *Nbn*$^{Krox20\text{-}Cre}$, *Nbn*$^{Krox20\text{-}Cre}$*p53*$^{-/-}$ and *Nbn/Atm*$^{Krox20\text{-}Cre}$ mice skin was stained. The staining was performed against Stat3 phosphorylated at Tyr 705. The animals were collected 18 and 35 days and 3 months after birth.

Scale bar: 100 µm

Stat3 activation by phosphorylation at Tyr 705 was not detected in the epidermis of Nbn^{Ctrl} mice at any point in time (Figure 51). At the age of 18 days no positive cells were visible in $Nbn^{Krox20\text{-}Cre}$, $Nbn^{Krox20\text{-}Cre}p53^{-/-}$ and $Nbn/Atm^{Krox20\text{-}Cre}$ mice. Starting with 35 days after birth those animals showed Stat3 Tyr 705 positive cells. In $Nbn^{Krox20\text{-}Cre}$ and $Nbn^{Krox20\text{-}Cre}p53^{-/-}$ mice the number of cells increased further with 3 months. The positive cells were spread within the whole epidermis. The epidermis of $Nbn/Atm^{Krox20\text{-}Cre}$ mice was not completely positive for Stat3 phosphorylation. In these animals few spots in the epidermis remained without Stat3 activation.

Analysis revealed an activation of Stat3 with phosphorylation at Tyr 705 in $Nbn^{Krox20\text{-}Cre}$, $Nbn^{Krox20\text{-}Cre}p53^{-/-}$ and $Nbn/Atm^{Krox20\text{-}Cre}$ mice at 35 days and 3 months after birth.

3.2.7.4 Analysis of Akt phosphorylation

Interleukin-22 expression is elevated in psoriasis (Wolk et al.,2006; Lowes et al.,2008). Cell proliferation resulting from IL-22 was found to be regulated by the PI3K (Phosphoinositide 3-kinase)/Akt/mTOR signaling cascade (Mitra et al.,2012). Additionally the phosphorylation of Akt was described in human psoriasis (Madonna et al.,2012). Those facts led to an analysis of Akt phosphorylation in the skin of our mice.

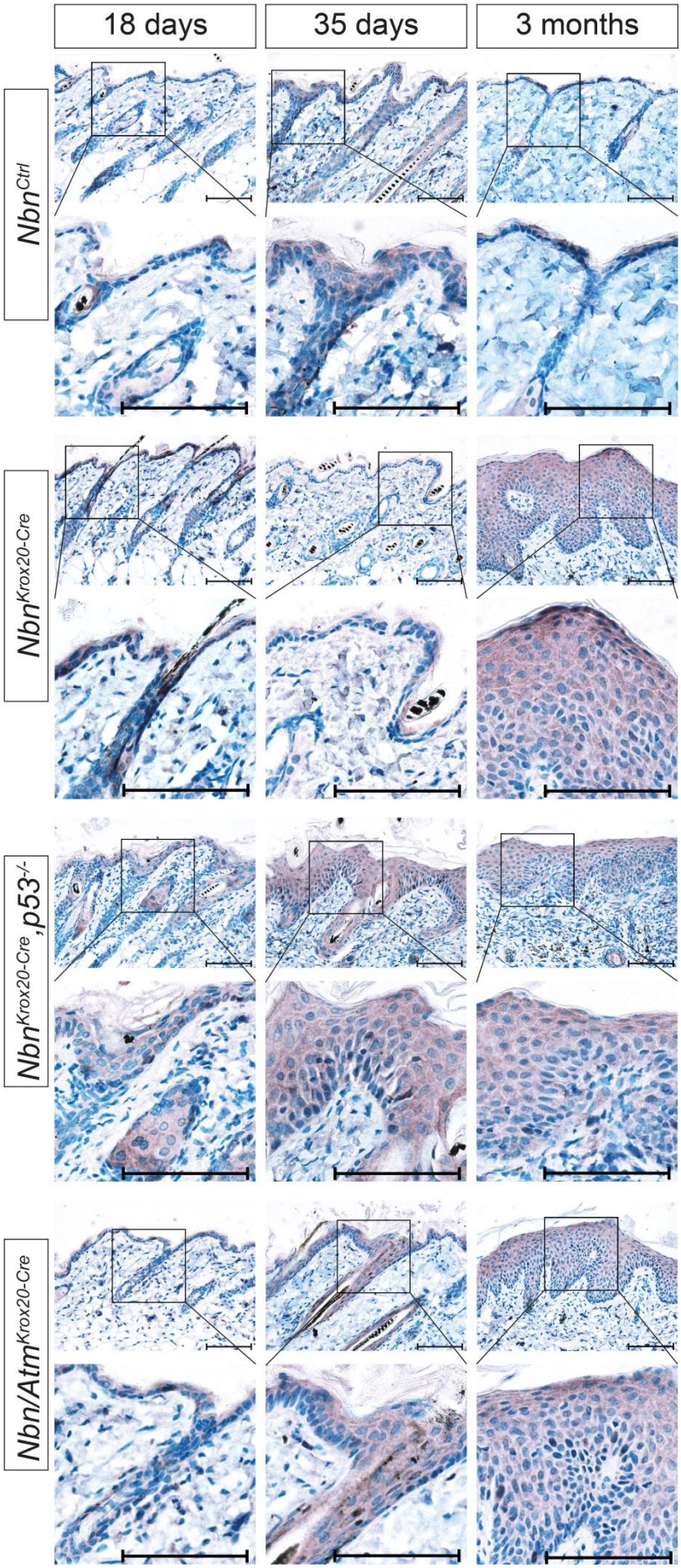

Figure 52: Study of Akt phosphorylation

Phosphorylation of Akt is visualized with an antibody staining. The staining was done on mice skin from *Nbn*^{Ctrl}, *Nbn*$^{Krox20\text{-}Cre}$, *Nbn*$^{Krox20\text{-}Cre}$*p53*$^{-/-}$ and *Nbn/Atm*$^{Krox20\text{-}Cre}$ mice. Mice were collected with the age of 18, 35 days and 3 months.

Scale bar: 100 µm

Phosphorylated Akt was only visible in very few epidermal cells of *Nbn*^{Ctrl} animals of all ages (Figure 52). It was only detected in suprabasal layers. The basal layer of *Nbn*^{Ctrl} animals remained without Akt phosphorylation. A similar pattern was seen in P18 animals of *Nbn*$^{Krox20\text{-Cre}}$, *Nbn*$^{Krox20\text{-}Cre}$*p53*$^{-/-}$ and *Nbn/Atm*$^{Krox20\text{-}Cre}$ mice. In *Nbn*$^{Krox20\text{-}Cre}$ mice at 35 days it was the same but with 3 months a distribution in most of the epidermis, including the basal layer, was detected. *Nbn*$^{Krox20\text{-}Cre}$*p53*$^{-/-}$ and *Nbn/Atm*$^{Krox20\text{-}Cre}$ animals exhibited phosphorylated Akt in most of the epidermal cells at 35 days. At 3 months epidermal cells were positive for Akt phosphorylation only a few non-positive cells remained in the basal layer.

A slight increase in phosphorylation of Akt was detected in mice skin of 3 months old *Nbn*$^{Krox20\text{-Cre}}$, *Nbn*$^{Krox20\text{-}Cre}$*p53*$^{-/-}$ and *Nbn/Atm*$^{Krox20\text{-}Cre}$ mice.

3.2.7.5 Visualization of S6 phosphorylation in the epidermis

In skin from psoriasis patients a phosphorylation of the regulator for mRNA translation S6 (ribosomal protein S6) was found (Buerger et al.,2013). Therefore the skin of the mice was examined for S6 phosphorylation.

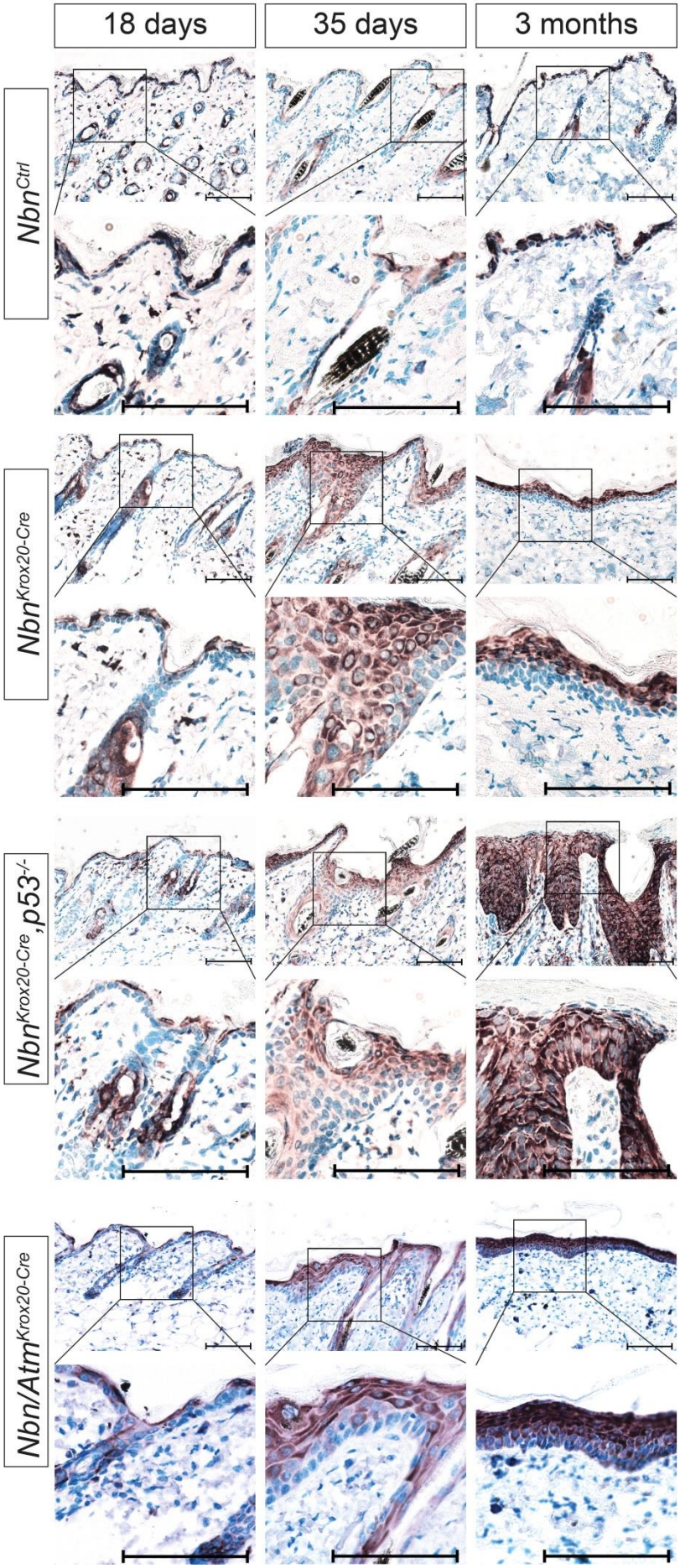

Figure 53: Characterization of S6 phosphorylation in the skin

Antibody against phosphorylated S6 was applied to mice skin. The skin of *Nbn*^{Ctrl}, *Nbn*$^{Krox20\text{-Cre}}$, *Nbn*$^{Krox20\text{-Cre}}$*p53*$^{-/-}$ and *Nbn/Atm*$^{Krox20\text{-Cre}}$ was collected at 18, 35 days and 3 months after births.

Scale bar: 100 µm

The phosphorylation of S6 was detected in the suprabasal layers of the epidermis and in the hair follicle bulge area in control animals from each collected point in time (Figure 53). In *Nbn*$^{Krox20\text{-}Cre}$ and *Nbn/Atm*$^{Krox20\text{-}Cre}$ mice the same distribution of phosphorylated S6 was observed in 18 days and 3 months old animals. At the age of 35 days a raised amount of positive cells in the hair follicle was apparent in *Nbn*$^{Krox20\text{-}Cre}$, *Nbn*$^{Krox20\text{-}Cre}$*p53*$^{-/-}$ and *Nbn/Atm*$^{Krox20\text{-}Cre}$ mice. In *Nbn*$^{Krox20\text{-}Cre}$*p53*$^{-/-}$ mice the expression was still elevated at 3 months of age and epidermal cells of the basal layer were positive. The outmost suprabasal layers showed no phosphorylation of S6.

The pattern of S6 phosphorylation was changed in the *Nbn*$^{Krox20\text{-}Cre}$*p53*$^{-/-}$ mice. In *Nbn*$^{Krox20\text{-}Cre}$*p53*$^{-/-}$ and *Nbn/Atm*$^{Krox20\text{-}Cre}$ animals the amount of cells with phosphorylation of S6 increased but the expression pattern was the same as in *Nbn*^{Ctrl} mice.

To evaluate a correlation of S6 phosphorylation and proliferation a staining with PCNA was conducted.

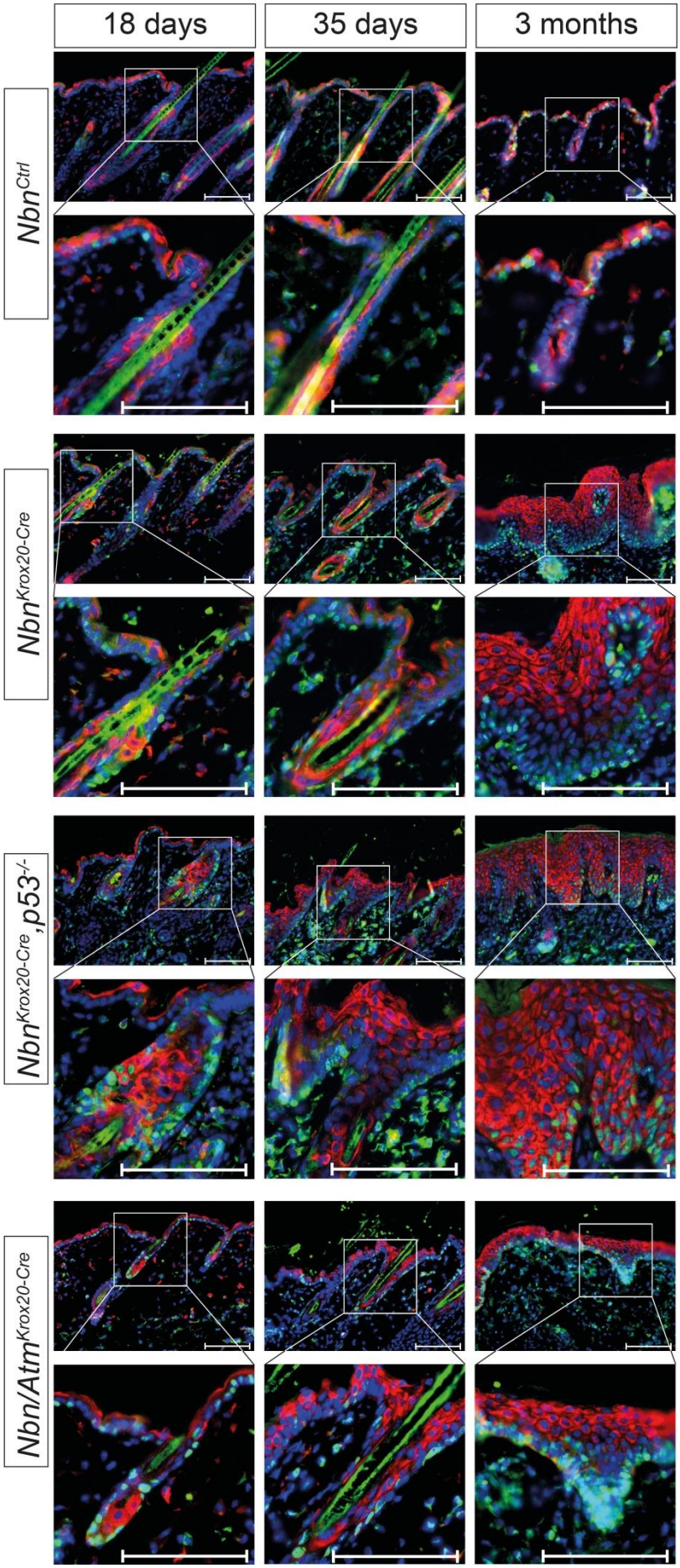

Figure 54: S6 phosphorylation in relation to PCNA

Staining for PCNA (green) and S6 (red) positive cells was performed on Nbn^{Ctrl}, $Nbn^{Krox20\text{-}Cre}$, $Nbn^{Krox20\text{-}Cre}p53^{-/-}$ and $Nbn/Atm^{Krox20\text{-}Cre}$ mice. Skin was obtained from mice at the age of 3 months, 18 and 35 days. Cells were also stained with DAPI (blue).

Scale bar: 100 µm

Epidermis of Nbn^{Ctrl}, $Nbn^{Krox20\text{-}Cre}$ and $Nbn/Atm^{Krox20\text{-}Cre}$ mice showed no colocalization of PCNA and S6 in cells (Figure 54). This was the same in 18, 35 days and 3 months old mice. For $Nbn^{Krox20\text{-}Cre}p53^{-/-}$ mice at 18 and 35 days after births the observation was similar. In 3 months old $Nbn^{Krox20\text{-}Cre}p53^{-/-}$ mice an expression of PCNA and S6 phosphorylation was detected in some cells.

A colocalization of phosphorylated S6 and PCNA was only detected in $Nbn^{Krox20\text{-}Cre}p53^{-/-}$ with an age of 3 months.

3.2.7.6 Study of Erk1/2 phosphorylation in the epidermis

In psoriasis Interleukine-17 level is elevated (Lowes et al.,2008) and IL 17 was found to activate extracellular signal-regulated kinase (Erk1/2) (Guo et al.,2014). Additionally a connection between Nbn and the Erk1/2 pathway was found (Hematulin et al.,2008) and a positive regulation of ATM and HRR was described (Golding et al.,2007). Therefore the status of Erk1/2 phosphorylation in the mice was checked.

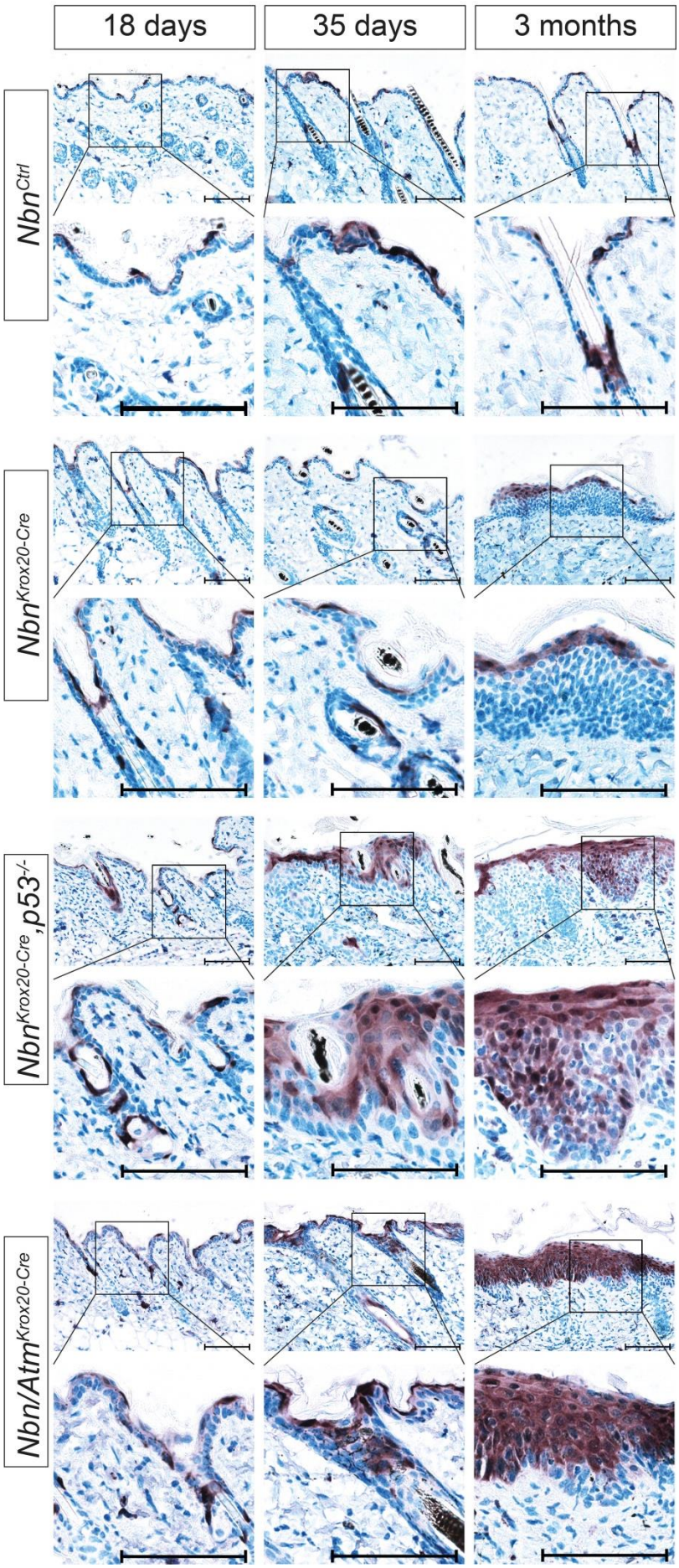

Figure 55: Analysis of Erk1/2 phosphorylation

Nbn^{Ctrl}, *Nbn*$^{Krox20\text{-}Cre}$, *Nbn*$^{Krox20\text{-}Cre}$*p53*$^{-/-}$ and *Nbn/Atm*$^{Krox20\text{-}Cre}$ mouse skins were stained against pErk1/2. Skin was collected at 3 months, 18 and 35 days after birth.

Scale bar: 100 µm

Nbn^{Ctrl} animals showed few cells with Erk1/2 phosphorylation in the suprabasal layer and at the hair follicle (Figure 55). This was the same for animals at the age of 18, 35 days and 3 months. In *Nbn*$^{Krox20\text{-}Cre}$ mice phosphorylated Erk1/2 is also only detected in suprabasal layers in all animals. Animals with the genotype *Nbn*$^{Krox20\text{-}Cre}$*p53*$^{-/-}$ and *Nbn/Atm*$^{Krox20\text{-}Cre}$ started to show Erk1/2 phosphorylation in most epidermal cells with 35 days and 3 months. First it was detected in the suprabasal layers and then reached down in the lower layers. Few cells in the basal layer remained without Erk1/2 phosphorylation.

A change in Erk1/2 phosphorylation pattern was detected in *Nbn*$^{Krox20\text{-}Cre}$*p53*$^{-/-}$ and *Nbn/Atm*$^{Krox20\text{-}Cre}$ animals.

3.2.8 Expression of NBN in human psoriasis

So far no analysis of NBN expression in the skin of human psoriasis patients was published. Therefore GEO Profiles database (Edgar et al.,2002; Barrett et al.,2013) was screened for data from skin of psoriasis patients. Three studies were found and data was analyzed (GEO accession GSE13355 (Nair et al.,2009), GEO accession GSE6710 (Reischl et al.,2007) and GEO accession GSE14905 (Yao et al.,2008)).

The data from GEO accession GSE13355 (Nair et al.,2009) contained both positive and negative values. A statistical analysis could not be performed. The data contained information from a control group (n = 64) and from psoriasis patients (n = 58). From psoriasis patients sample from psoriatic plaques and uninvolved skin were taken.

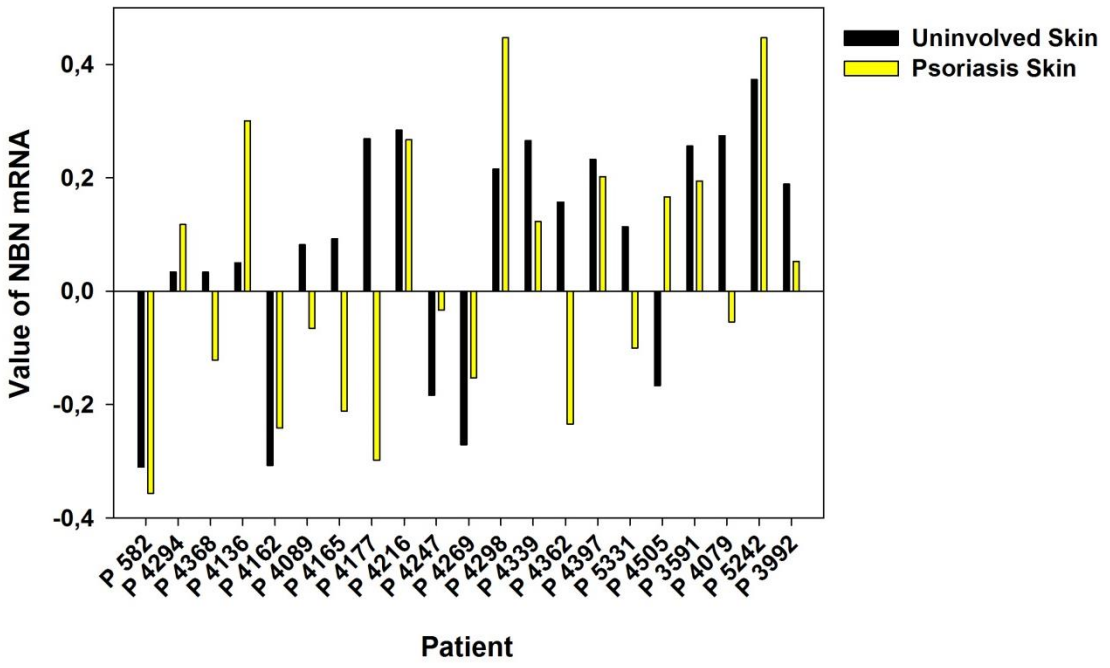

Figure 56: NBN mRNA from GSE13355 individual patients

The values for NBN mRNA of 21 patients are depicted. The levels of NBN mRNA from uninvolved skin and from psoriatic plaques are shown.

Individual patients showed a decrease of NBN while others showed an increase from uninvolved skin to psoriasis. The data from 21 representative patient samples are shown in Figure 56. An increase in NBN mRNA level was detected in patients 4294, 4136, 4162, 4247, 4269, 4298, 4505 and 5242. In patients 582, 4368, 4089, 4665, 4177, 4216, 4339, 4362, 4397, 5331, 3591, 4079 and 3992 a decrease in NBN mRNA was observed.

The samples from the study of GEO accession GSE6710 (Reischl et al.,2007) were collected from 13 patients. Skin from psoriasis and uninvolved areas were analyzed.

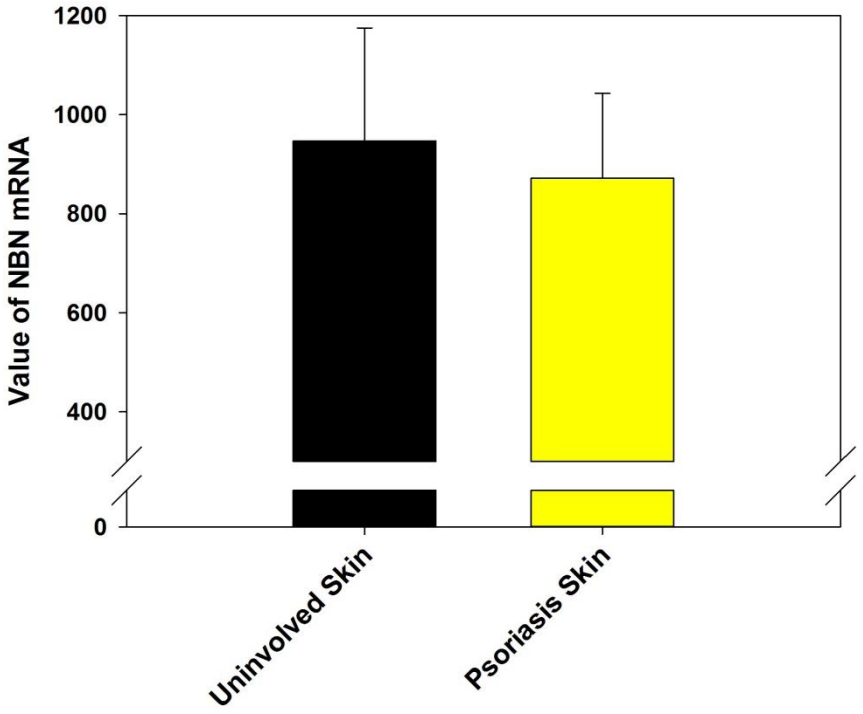

Figure 57: Statistical analysis of NBN mRNA in GSE6710

The value of NBN mRNA in the dataset of GSE6710 was analyzed. The level of uninvolved skin and psoriasis are shown. n = 13

The statistical analysis of the samples showed no differences in the level of NBN mRNA between skin from psoriatic plaques and uninvolved skin (Figure 57). The value was for uninvolved skin 947 ± 228 and for psoriasis 871 ± 171. A tendency towards a reduction of NBN level was seen and led to look analysis of data from individual patients.

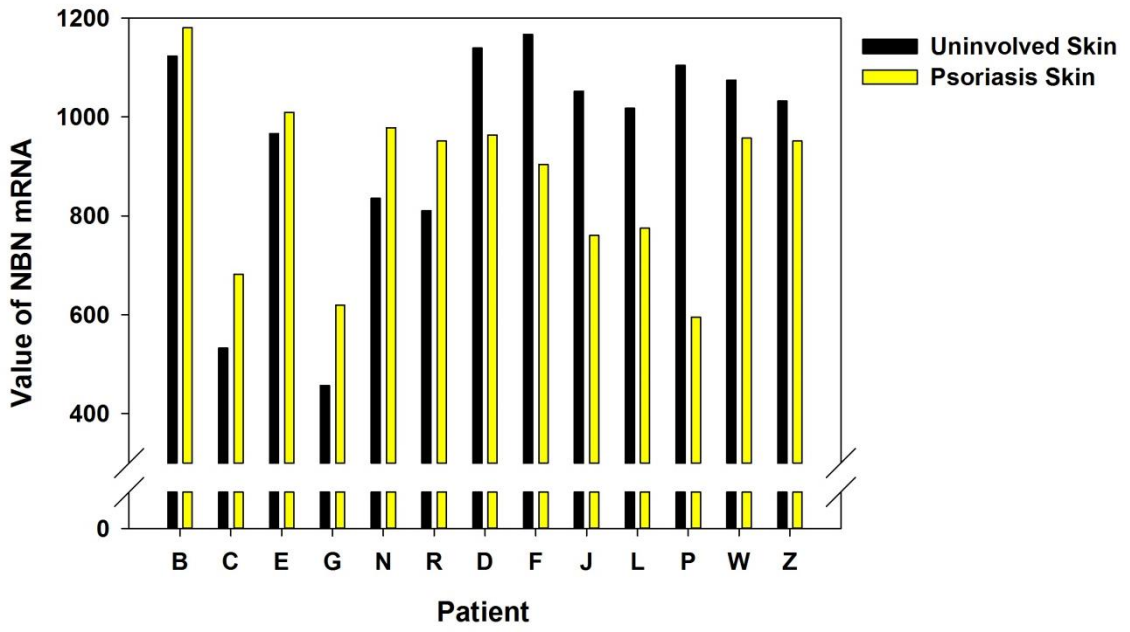

Figure 58: Values of NBN mRNA from individual patients of GSE6710

The values of NBN mRNA of 13 patients from the GSE6710 data are shown. The patients were labeled with letters. The levels of uninvolved skin and psoriasis of each patient are depicted.

The examination of the individual patient data (Figure 58) revealed an increase of NBN mRNA in six patients (patient B, C, E, G, N and R). For patients D, F, J, L, P, W and Z the level of NBN decreased from uninvolved skin to psoriatic plaques.

The data from GEO accession GSE14905 (Yao et al.,2008) was analyzed in regard to NBN levels. In the study samples from 21 healthy controls were collected. From 28 psoriasis patients samples from psoriatic plaques and uninvolved skin were taken.

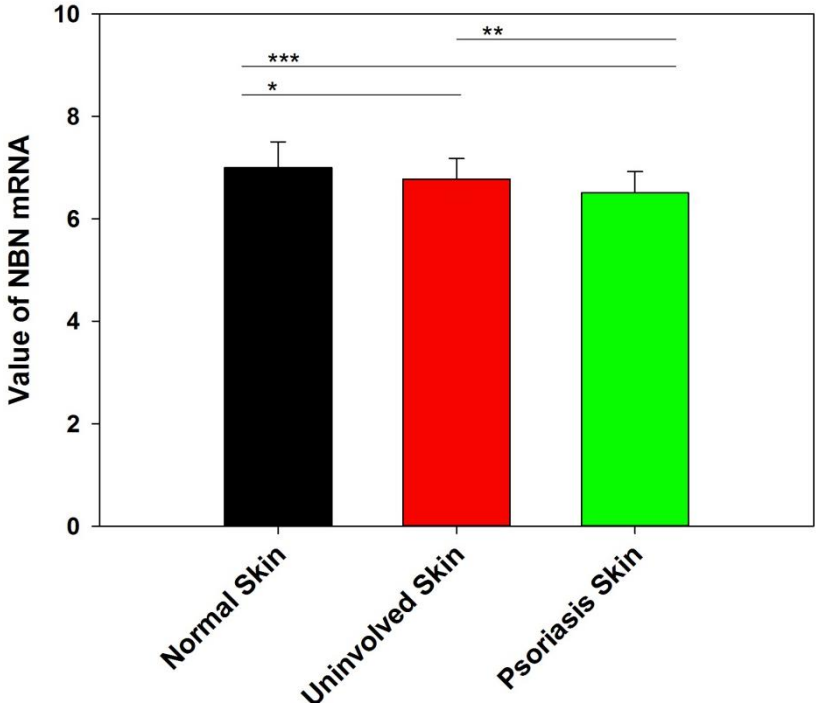

Figure 59: Statistical analysis of NBN values from GSE14905

NBN mRNA values were analyzed. The values of healthy controls (normal skin; n = 21) and from psoriasis patients (uninvolved and psoriasis skin; n = 28) are shown. (*P < 0,05; **P < 0,01; ***P < 0,001)

The statistical analysis of NBN mRNA values from GSE14905 showed a decrease of mRNA levels (Figure 59). Normal skin from the control group showed the highest level of NBN mRNA (7 ± 0,5). A statistical significant decrease was detected in uninvolved skin (6,7 ± 0,3) and in psoriasis skin (6,5 ± 0,4) compared to control skin. The level of NBN mRNA was also significantly decreased between samples from involved skin and psoriatic plaques in psoriasis patients.

4. Conclusions and Discussion

4.1 Nbn is essential for skin homeostasis

An important role of *NBN* in skin homeostasis was suggested due to the different skin diseases that were found in patients with NBS. Examples for those are Porokeratosis and the thin and sparse hair observed in the patients (Wolf and Shwayder,2009; Chrzanowska et al.,2012). Discovery of *NBN* mutations in malignant melanomas pointed additionally towards an important role of *NBN* in the maintenance of regular skin function (Debniak et al.,2003; Thirumaran et al.,2006; Meyer et al.,2007).

To obtain data on the expression of *NBN* in skin GEO Profiles database (Edgar et al.,2002; Barrett et al.,2013) was looked into and data sets were analyzed. So far no papers were published containing analysis of data in regard to general *NBN* expression in healthy human skin. All data obtained from GEO datasets was data from microarray analyses.

NBN expression was found in the skin of healthy humans (GEO accession GSE1719 (Strunnikova et al.,2005), GEO accession GSE5667 (Plager et al.,2007; Plager et al.,2010) and GEO accession GSE31652 (Krueger et al.,2012)). In hair follicles its expression was also detected (GEO accession GSE3058 (Kim et al.,2006) and GEO accession GSE3419 (Ohyama et al.,2006)). In studies of gene expression in psoriasis *NBN* was found to be expressed (GEO accession GSE13355 (Nair et al.,2009), GEO accession GSE6710 (Reischl et al.,2007) and GEO accession GSE14905 (Yao et al.,2008)). Analysis of the data revealed that GEO accession GSE13355 (Nair et al.,2009) contained both positive and negative values. Therefore statistical analysis was not performed. No statistical differences was found in data from GEO accession GSE6710 (Reischl et al.,2007). Samples of individual patients showed a decrease of NBN level from non-lesional skin to psoriatic plaques in some patients while others showed an increase (GEO accession GSE13355 (Nair et al.,2009), GEO accession GSE6710 (Reischl et al.,2007)). The data analysis of the third study identified a significant decrease in *NBN* expression from a non-patient group to lesion free patient skin (GEO accession GSE14905 (Yao et al.,2008)). The level of *NBN* was significantly lower in psoriatic plaques compared to both the control group and to non-lesional skin

of the same patients (GEO accession GSE14905 (Yao et al.,2008)). The status of NBN in psoriasis seems to vary from patient to patient. Therefore the overall expression of NBN in a complete study depends on the patients included. If NBN status needs to be determined each patient has to be evaluated individually.

In the conducted study *Nbn* was deleted in the epidermis using Krox20-Cre recombinase. The deletion of Exon 6 was shown to lead to a null mutation of Nbn (Dumon-Jones et al.,2003; Frappart et al.,2005). The deletion occurred after birth. It started at P1 in small patches, spread to the hair follicles and the surrounding epidermis between P10 to P18 and was deleted in the complete back skin in adult mice. As Krox20-Cre recombinase is not expressed in the tail no effects were expected in this area (Young et al.,2003).

The expression of *Nbn* in the skin of mice was not documented before. Therefore RNA was extracted and confirmed the expression of *Nbn* in the keratinocytes of mice from the control group. Deletion of *Nbn* was also confirmed with the absence of *Nbn* on RNA level.

Visual examination showed healthy mice at birth. The development of the mice continued in the same way for control and deletion mice. At the first point in time of animal collection (P18) no differences between Nbn^{Ctrl} and $Nbn^{Krox20\text{-}Cre}$ mice were apparent. Both analysis of histological morphology and visual examination of the mice showed no differences. At this point in time Krox20-Cre expression had already caused a deletion of *Nbn* in the hair follicles and the surrounding epidermis. The hair on the back reached the catagen phase at 18 days after birth and were in a regression phase (Muller-Rover et al.,2001; Alonso and Fuchs,2006). First differences were observed both in visual examination and in histology at 35 days after birth. The hair follicles and epidermis showed altered structures and the hair started to thin out. At the age of 35 days the hair follicles are in the first anagen phase after hair follicle morphogenesis (Muller-Rover et al.,2001). In this phase growth of new hair is initiated from the hair follicles stem cells to replace or add new hair to the dead club hair (Muller-Rover et al.,2001; Alonso and Fuchs,2006). At this age the next catagen phase is soon to follow. Three months after birth the hair cycle of the mice is in resting (telogen) phase (Muller-Rover et al.,2001). In adult mice of 3 months most of the fur was lost. The tail remained covered with fur, as expected due to the Krox20-Cre recombinase expression pattern.

Histology revealed the existence of single hair follicles with an altered structure in the skin of the mice. The epidermis was enlarged.

Those findings indicated an important role of *Nbn* in the perpetuation of skin homeostasis. Both hair follicle cycling and epidermal balance were highly affected by the deletion of *Nbn*.

4.2 Nbn is needed for repair of DNA damages in the hair follicle and maintenance of stem cells

The fur of mice started to thin out around 35 days after birth. Nearly the complete hair was gone at 3 months after birth. To examine the cause of the hair loss different stainings were conducted. The apoptosis rate and the amount of DNA damages in the hair follicles of the deletion mice was evaluated. In addition an analysis of the Keratin 15 expressing hair follicle stem cells was performed.

The role of p53 dependent apoptosis in the hair follicle cycling is not fully understood by now. A constant *p53* expression was shown during anagen and catagen phases, implicating an independence of the hair regression from p53 apoptosis (Seiberg et al.,1995). On the other hand *p53* deficient mice showed no hair loss and apoptosis after chemotherapy and the expression of *p53* in apoptotic catagen hair follicle cells was shown (Botchkarev et al.,2000; Botchkarev et al.,2001). In addition a difference in response to p53 increase was seen in different epidermal cells. While an increase of p53 in the keratinocytes in the epidermis causes growth arrest, it caused apoptosis in hair follicles (Song and Lambert,1999). Due to this unclear role of p53 in apoptosis of the different epidermal compartments the analysis of apoptosis in this study was done using various markers. It was stained against p53 for p53 dependent apoptosis. Active Caspase 3 staining was done to show p53 independent apoptosis and TUNEL reaction was performed to visualize apoptotic cells independent on the pathway involved.

Most cells positive for makers of apoptosis were localized in the hair follicles in all animals. This showed that apoptosis does not play a major role in the keratinocytes of the different epidermal layers. Sheading of those is only due to differentiation processes and not due to apoptosis. On the other hand in the cycling of hair follicles apoptosis

plays an important role in catagen phase for the regression of the hair follicle (Slominski et al.,1994; Lindner et al.,1997).

The role of apotosis in hair regression was visible in Nbn^{Ctrl} mice. They showed the highest amount of Caspase 3 active cells in the hair follicles at P18 (catagen phase). On day 35 after birth the amount was lower as the cells were in anagen phase but short before the next catagen phase started. Nearly no activity of Caspase 3 was detected in the hair follicles of 3 months old animals. At this point of time the hair follicle was in the resting phase and no apoptotic cells were expected to be found. In conclusion the Caspase 3 activity in Nbn^{Ctrl} mice was as expected from literature. In $Nbn^{Krox20\text{-}Cre}$, $Nbn^{Krox20\text{-}Cre}p53^{-/-}$ and $Nbn/Atm^{Krox20\text{-}Cre}$ mice few Caspase 3 active cells were detected at 18 days after birth. For those animals the peak of Caspase 3 activity was seen in 35 days old mice. The amount of p53 expressing cells in control animals was low during the observed time. It reached its peak in 35 days old control animals. Deletion mice showed a higher amount of p53 positive cells at all points in time but the peak also lays at 35 days.

Those observations of Caspase 3 activity and p53 expression in deletion animals could indicate a change in hair follicle cycle progression. In p53 deleted mice a change in hair cycling was described before (Botchkarev et al.,2001). On the other hand it could show an accumulation of apoptotic cells in the hair follicle due to an elevated rate of DNA damages independent of the hair cycle step. The lower activity of Caspase 3 and p53 expression in 3 months old mice with deletions was probably due to the lack of hair follicle structures. This also corresponds to the observations that apoptotic cells were mainly detected in the hair follicles. The discovery that the changes and absence of hair follicles in $Nbn^{Krox20\text{-}Cre}p53^{-/-}$ mice were comparable to those seen in $Nbn^{Krox20\text{-}Cre}$ and $Nbn/Atm^{Krox20\text{-}Cre}$ mice indicates an important role of p53 independent apoptosis in the hair loss in mice of this study. This would be in agreement with p53 independent apoptosis in hair regression observed by Seiberg et al. (Seiberg et al.,1995). On the other hand the amount of p53 positive cells in $Nbn/Atm^{Krox20\text{-}Cre}$ mice was significantly higher than in $Nbn^{Krox20\text{-}Cre}$. This could point to a more important role of p53 dependent apoptosis in animals with a combined deletion of *Atm* and *Nbn*. This is supported by the fact that functional Atm is known not to be required for p53 apoptosis in epidermis (Gurley and Kemp,2007).

DNA damage and especially DSB accumulation was screened via the number of γH2A.X foci. Those were highest in $Nbn^{Krox20\text{-}Cre}$ and$Nbn^{Krox20\text{-}Cre}p53^{-/-}$ mice at 35 days of age. In Nbn^{Ctrl} the amount at 35 days was comparable to $Nbn^{Krox20\text{-}Cre}$ mice but at 18 days was significantly lower. Even with the presences of hair follicles at 3 months the amount of γH2A.X foci decreased in the Nbn^{Ctrl} mice below the level of 18 days. This pointed out a general dependence of accumulation of DNA damages in the hair follicle on the hair cycle phase. During the dying of hair follicles in catagen DNA damages that arise are not repaired and therefore accumulate in the cells. The onset of new growth during the anagen (P35) phase explains a high amount of DNA damages. Those are due to the increase in DNA replication and proliferation in the cells. During those processes errors occur. In the hair follicles of control mice the errors are repaired, new hair are formed and show only a basal level of DNA damages in telogen (3 months) phase. In the deletion mice the errors cannot be repaired properly and the apoptosis rate increases, as seen through Caspase 3 activation, during the growth phase of the hair follicles. In stem cells of the epidermis the repair of DNA damages was described to be faster than in surrounding cells (Harfouche et al.,2010). Despite the lack of Nbn the repair is not possible anymore in the mice. In 3 months old animals nearly no hair follicles are observed anymore. Thus the low amount of γH2A.X foci at this stage can be explained. Only in $Nbn/Atm^{Krox20\text{-}Cre}$ mice the level of γH2A.X foci remained relatively low. A possible explanation would be that with the inactivation of both *Nbn* and *Atm* the amount of DNA damages that finally result in apoptosis is lower and that those cells die faster. On the other hand it can also suggest dependence of phosphorylation of Histone H2A.X on *Atm* in the epidermis. With the lack of Nbn and p53 Atm still causes phosphorylation of Histone H2A.X (Burma et al.,2001; Stiff et al.,2004). In the hair follicles no other member of the PIKK kinase family (e.g. DNA-PKcs, ATR) (Burma et al.,2001; Stiff et al.,2004; Friesner et al.,2005) seems to be able to substitute sufficiently for *Atm*. The peak of γH2A.X foci in 3 months old animals from $Nbn/Atm^{Krox20\text{-}Cre}$ showed the higher amount of DNA damages in the keratinocytes in those mice. This could point to different roles of *Atm* in hair follicle stem cells and basal keratinocytes. It could indicate that another PIKK kinase family member functions in basal keratinocytes. This would also support the activation of p53 apoptosis after loss of *Atm* postulated above and by others (Gurley and Kemp,2007).

Previously an important role of NHEJ in hair follicle stem cells was described (Sotiropoulou et al.,2010). The NHEJ was mediated through DNA-PK. Nbn is known to

be able to act in NHEJ. The importance of Atm for the formation of γH2A.X foci in the hair follicles in the mice here points additionally towards HRR. While NHEJ mostly happens during G0/G1 phase of the cell cycle HRR occurs during the rest of the cell cycle. With the proliferation markers it was shown that most cells of the hair follicle were not in G0 or G1 phase. Therefore HRR might have a more important role in the hair follicles at the collected points in time. It is possible that both the lack of Nbn leads to a defect not only in HRR but also in NHEJ in the hair follicle stem cells. The damages are not repaired at any step during cell cycling and this results in damage accumulation, partially in cell death and in loss of stem cell properties.

To analyze the apoptotic character of γH2A.X positive cells a staining in combination with TUNEL reaction was performed. This showed only few TUNEL positive cells in hair follicles of all animals. In the epidermis TUNEL staining was observed exclusively in *Nbn/Atm*$^{Krox20\text{-}Cre}$ mice at the age of 3 months. An overlap of TUNEL and γH2A.X was observed in cells completely positive for γH2A.X. In cells with γH2A.X foci no TUNEL was detected and inverted. This is probably due to the fact that γH2A.X foci show DSBs that arise at an early stage of a starting cell death while TUNEL staining showed fully apoptotic cells. The staining also gives rise to the idea that there might be another reason for the disappearance of the hair follicles besides cell death.

As Keratin 15 is a marker for stem cells in the hair follicles and in the basal layer of the epidermis, a staining was done to look at those cells. Keratin 15 was expressed in all mice from the control group in the expected compartments. In the deletion mice Keratin 15 staining could only be seen at 18 days and partially at the age of 35 days. 3 months old mice showed no Keratin 15 expression anymore. An analysis of the Keratin 15 cells with 53BP1 revealed DNA damages in stem cells in the hair follicles of the younger mice. This showed that hair follicle stem cells were either lost through apoptosis or changes occurred that abolished the stem cell properties of those cells. A limiting factor of DNA damages to stem cell self-renewal was recently demonstrated (Wang et al.,2012). It is possible that the hair follicle stem cells started to differentiate into basal keratinocytes (Cotsarelis et al.,1990; Taylor et al.,2000; Oshima et al.,2001; Ito et al.,2005; Levy et al.,2007). This could explain the raised proliferation at 35 days and the high population of basal keratinocytes at 3 months in deletion animals.

Several studies showed a higher resistance of epidermal and hair follicle stem cells against DNA damages due to a fast repair and apoptosis (El-Abaseri et al.,2006; Rachidi et al.,2007; Harfouche et al.,2010; Sotiropoulou et al.,2010). In one study a mouse model was used (Sotiropoulou et al.,2010) while the others worked with cell culture. The DNA damage induction was done with one-time application of UV or IR. DNA damage response in those experiments was not impaired. Due to these differences those studies do not contradict the results observed in this work. Here mouse models were used which were impaired in DNA damage response. Therefore a constant existence of non-repaired DNA damages occurred as compared to one-time DNA damages in the studies mentioned above. This can explain the different behaviors observed in hair follicle stem cell, e.g. no resistance against apoptosis, in our animals.

Two studies with defects in DNA damage response in skin of mouse models support the observations made here (Ruzankina et al.,2007; Sotiropoulou et al.,2013). The loss of hair follicle stem cells was also observed in mice lacking *ATR* (Ruzankina et al.,2007). In those mice the loss of stem cells was demonstrated after continuous depilation of the hair. In combination with *p53* deletion the results were similar or slightly more pronounced (Ruzankina et al.,2009). A study of *Brca1* deletion in the Keratin 14 expressing cells during the embryonic development revealed a decrease in hair follicles (Sotiropoulou et al.,2013). A combination with *p53* deletion resulted in a rescue of the phenotype (Sotiropoulou et al.,2013). Deletion of *Brca1* in adult Keratin 5 expressing keratinocytes led to delayed regeneration of hair after shaving and a progressive loss of hair follicle stem cells in those animals (Sotiropoulou et al.,2013). In our mice the effects seem to be more pronounced than in those studies. The effects can be detected without further manipulation of the animals and it occurs already after one completed hair cycle. In addition the pathways involved are probably corresponding to the ones involved in *ATR* deletion mice but differ from *Brca1* deletion mice. This conclusion can be drawn from the effect of additional *p53* deletion in the animals.

Due to all the different analyses it can be concluded, that the hair loss observed in mice with $Nbn^{Krox20\text{-}Cre}$, $Nbn^{Krox20\text{-}Cre}p53^{-/-}$ and $Nbn/Atm^{Krox20\text{-}Cre}$ is due to an increase of DNA damages and a failure in repair of those. It leads to a rise in apoptosis, disruption of epidermal stem cell properties and differentiation of those stem cells into basal keratinocytes. Those events result in the loss of hair follicle stem cells and thereby the

inability to regenerate hair follicles. Additionally it leads to an increase of the population of basal keratinocytes.

4.3 Nbn prevents development of a psoriasis-like phenotype

Nbn$^{Krox20\text{-}Cre}$, *Nbn*$^{Krox20\text{-}Cre}$*p53*$^{-/-}$ and *Nbn/Atm*$^{Krox20\text{-}Cre}$ mice with 3 months of age showed besides the hair loss, both acanthosis and parakeratosis. Those effects were demonstrated by the increase of proliferating cells and by the disturbed differentiation of keratinocytes observed in the mice. Invasion of the dermis with Mast cells and Neutrophils was observed. T-cells with CD3 expression were detected in the epidermis. An activation of Stat3 at Tyr 705 was observed in the mice. These are typical signs for psoriasis (Figure 60) (Weinshenker et al.,1989; Bos and De Rie,1999; Sano et al.,2005; Griffiths and Barker,2007; Gudjonsson et al.,2007; Hertl,2011).

Common sign for psoriasis in humans	Observed in this mouse model	Remarks
Scall development	Yes	
Elongation of rete ridges	No	Do not exist in mice
Increase of capillary number	No	
acanthosis	Yes	PCNA, Ki67, H3P, p63
parakeratosis	Partially; everywhere disturbed differentiation	Keratin 10, Keratin 14
Invasion of leucocytes	Yes	Mast cells, Neutrophils
Invasion of T-cells	Yes	CD3 T-cells
Activation of Stat3	Yes	Stat3 phosphorylation on Tyr 705

Figure 60: Signs of psoriasis

In Figure 60 a table of psoriasis signs is shown. It lists typical signs of psoriasis observed in human patients. The mouse model refers to *Nbn*^{Ctrl}, *Nbn*$^{Krox20\text{-}Cre}$, *Nbn*$^{Krox20\text{-}Cre}$*p53*$^{-/-}$ and *Nbn/Atm*$^{Krox20\text{-}Cre}$ mice with 3 months of age. The appearance of the psoriasis signs is stated. Under remarks the stainings that were done to show the psoriasis sign are named. Possible explanations for signs that were not detected are given.

The observed processes in our mice lead to the conclusion that in all genotypes the animals of 3 months show a psoriasis-like phenotype (Figure 60). In the double deleted mice with p53 a difference can be seen as those animals also show invaginations in the epidermis. To further evaluate the differences and to look into the pathways possibly involved in causing the psoriasis in Nbn deleted mice more analyses were performed.

Besides the activation of Stat3 being a general sign for psoriasis, Stat3 is known to activate *c-Myc* (Kiuchi et al.,1999). *c-Myc* is a cell cycle promotor and oncogene. The change of expression levels of *c-Myc* in human psoriasis patients is diversely discussed. An increase in *c-Myc* antibody staining was shown on frozen sections (Osterland et al.,1990) while analysis of RNA and *in situ* hybridization on tissue from human psoriasis patients no increase in *c-Myc* expression could be seen (Elder et al.,1990; Schmid et al.,1993). In mouse models an overexpression of *c-Myc* in suprabasal layers of the epidermis was shown to cause hyperplasia, hyperkeratosis and abnormal differentiation of keratinocytes (Pelengaris et al.,1999; Waikel et al.,1999). In addition the upregulation of *c-Myc* in mice skin caused a loss of stem cells (Waikel et al.,2001). From those studies it can be concluded, that, at least in mice, c-Myc has an influential role in epidermis homeostasis. The role in human psoriasis remains unclear. Targeted *c-Myc* overexpression in mice was described to cause changes in the skin as can be observed in our mice (Pelengaris et al.,1999; Waikel et al.,1999). An activating role of *c-Myc* in regulation of *NBN* expression was described (Chiang et al.,2003; Wan et al.,2013). The studies also showed a binding site for *c-Myc* on Intron1 of *NBN* (Chiang et al.,2003; Wan et al.,2013). Therefore it is possible that the activation of Stat3 seen in our mice might lead to *c-Myc* overexpression which results in increased proliferation and disturbance of differentiation.

In psoriasis, besides IL-17, Interleukin-22 (IL-22) expression is elevated (Wolk et al.,2006; Lowes et al.,2008). Both Interleukins are produced by Th17 cells (Liang et al.,2006). IL-22 was found to activate Stat3, MAPK and Erk1/2 (Lejeune et al.,2002). The cell proliferation in the epidermis induced via IL-22 was found to be regulated by the PI3K/Akt/mTOR signaling cascade (Mitra et al.,2012). IL-17 induced proliferation is regulated via mTOR (Saxena et al.,2011). In psoriasis PI3K was found to be overexpressed compared to normal tissue (Pike et al.,1989). The phosphorylation of Akt was described in human psoriasis (Madonna et al.,2012). mTOR is also activated in skin from psoriasis patients (Buerger et al.,2013). NBN was shown to interact with PI3K and

increases its activity (Chen et al.,2005; Chen et al.,2008). This leads to an activation of Akt and mTOR (Chen et al.,2005). mTOR is part of the mTORC2 complex and in this complex activates Akt additionally (Sarbassov et al.,2005). mTOR belongs to the family of PIKKs (Kunz et al.,1993; Keith and Schreiber,1995). *Nbn* was shown to interact with mTORC2 complex to activate Akt (Wang et al.,2013). The analysis of Akt phosphorylation via mTORC2 pathway detected only slight changes. Those were visible in skin of $Nbn^{Krox20\text{-Cre}}$, $Nbn^{Krox20\text{-}Cre}p53^{-/-}$ and $Nbn/Atm^{Krox20\text{-}Cre}$ mice at 3 months after birth. The activation of Akt through mTORC2 complex seems to be involved in development of the psoriasis-like phenotype in the mice.

MAPK and mTOR (via mTORC1) activate S6 kinase (S6K1) (Mukhopadhyay et al.,1992; Dufner and Thomas,1999; Hay and Sonenberg,2004). S6K1 then phosphorylates a regulator for mRNA translation S6 (Jeno et al.,1988; Dufner and Thomas,1999; Hay and Sonenberg,2004). In skin from psoriasis patients a phosphorylation of S6 was found (Buerger et al.,2013). Therefore the skin of the mice was examined for S6 phosphorylation. In Nbn^{Ctrl}, $Nbn^{Krox20\text{-Cre}}$ and $Nbn/Atm^{Krox20\text{-}Cre}$ mice the phosphorylation was only detected in the suprabasal layers of the epidermis. In 35 day old mice from $Nbn^{Krox20\text{-Cre}}$and $Nbn/Atm^{Krox20\text{-}Cre}$ S6 activation was also seen around the hair follicle. A double staining with the proliferation marker PCNA showed that cells with S6 phosphorylation all belonged to the differentiating keratinocytes. This is in line with the S6 phosphorylation pattern in suprabasal and differentiating keratinocytes described in human psoriasis (Buerger et al.,2013). The pattern of S6 activation in $Nbn^{Krox20\text{-Cre}}$and $Nbn/Atm^{Krox20\text{-}Cre}$ mice confirms a psoriasis-like phenotype. Also a higher activation of S6 after *Nbn* deletion can be seen.

S6 was also found to be phosphorylated by Erk1/2 using an mTOR independent pathway (Roux et al.,2007). IL-17 and IL-22 were found to activate Erk1/2 (Lejeune et al.,2002; Lee et al.,2008; Guo et al.,2014). An elevated level of MAPK and Erk1/2 was detected in biopsies from psoriasis patients (Johansen et al.,2005). MAPK dependent epidermal hyperplasia required Stat3 to develop (Tarutani et al.,2013). Besides those events a connection between *NBN* and the Erk1/2 pathway was found and a positive regulation of ATM and HRR was described (Golding et al.,2007; Hematulin et al.,2008). Due to this knowledge the phosphorylation status of Erk1/2 was checked in this study. An activation of Erk1/2 in Nbn^{Ctrl} and $Nbn^{Krox20\text{-Cre}}$ mice was detected in the Stratum corneum at all points of time. Both in $Nbn/Atm^{Krox20\text{-}Cre}$ and $Nbn^{Krox20\text{-}Cre}p53^{-/-}$

animals a higher level of Erk1/2 activation in all epidermal layers was observed starting at 35 days after birth.

The analyses of the mice revealed the role of Nbn in prevention of formation of a psoriasis-like phenotype in mice. Mice lacking Nbn show a vast number of changes that correspond to human psoriasis. Invasion of different immune cells can be observed. Epidermis enlarges due to higher proliferation and disturbed differentiation. Additionally many protein expressions and activations change similarly to human psoriasis. Furthermore the experiments confirm *Nbn* involvements seen in pathways that were described before. With the mouse model those interactions are now indicated *in vivo* and a possible link between the different networks is added.

4.4 Atm function differs between keratinocytes and hair follicle cells

Nbn and Atm are known to interact. The interaction is bidirectional. Together they function in cell cycle signaling, DNA damage signaling and repair (details in Introduction). Different mouse studies were conducted to show the consequences of combined deletion of *Nbn* and *Atm* and to shed light on the interdependence of the two proteins. In the CNS a joint function was detected due to the worsening of the single deletion phenotypes after combined elimination of *Nbn* and *Atm* (Dar et al.,2011). *Nbn* and *Atm* deletion was shown to have different cell type and time dependent consequences (Rodrigues et al.,2013). In epidermis autophosphorylated ATM was found to locate mostly in Golgi apparatus instead of the nuclear localization described in other cells (Ismail et al.,2011). Nuclear distribution in keratinocytes was detected after UV treatment or in precancerous lesions (Ismail et al.,2011). p53 apoptosis in epidermis was shown to be independent from Atm, while it was necessary in spleen, thymus and brain (Gurley and Kemp,2007). As the role of Atm in combination with Nbn seems to vary in different tissues and the role of Atm in the epidermis is still unclear a combined inactivation of *Nbn* and *Atm* was performed in this study. The mice of $Nbn^{Krox20\text{-Cre}}$ and $Nbn/Atm^{Krox20\text{-}Cre}$ groups showed largely the same results. Both show a psoriasis-like phenotype in aging animals and a hair loss due to increase in DNA damages, apoptosis and stem cell failure. Differences were only observed in the small details. The amount of p53 positive cells was higher after *Atm* was abolished in

addition. This showed that p53 apoptosis in the epidermal cells started to be more important when both Nbn and Atm fail. In *Nbn/Atm*$^{Krox20\text{-}Cre}$ mice the level of γH2A.X foci remained relatively low compared to *Nbn*^{Krox20}-Cre. No other PIKK kinase was able to completely replace Atm in its role in Histone H2A.X phosphorylation in the hair follicle. When no hair follicles were left at 3 months the level of γH2A.X foci was the same in *Nbn*^{Krox20}-Cre and *Nbn/Atm*$^{Krox20\text{-}Cre}$ mice. The observed Histone H2A.X phosphorylation at this point in time was in the keratinocytes of the epidermis. This demonstrated that another PIKK kinase family member functions in basal keratinocytes which also supports the observations made with p53. The psoriasis-like phenotype of *Nbn* deficient mice seems to worsen slightly with an additional *Atm* deficiency. This can be seen as the number of invading immune cells is increased while the presented phenotype of the mice remains similar. In the analyses of pathways a difference due to *Atm* deletion was detected in Erk1/2. Here the activation was increased. This indicates a role of Atm in the prevention of Erk1/2 phosphorylation.

The results from this study indicate a minor role of Atm in keratinocytes. In hair follicle cells Atm is needed for the phosphorylation of Histone H2A.X which makes DNA accessible for repair. The influence of Atm on Nbn in the skin is therefore dependent on the cell type. A possible role of Atm in circumvention of Erk1/2 phosphorylation in the skin was discovered.

4.5 p53 inhibits tumor formation in Nbn deficient epidermis

p53 is known to be involved in the regulation of cell cycle progression and apoptosis after DNA damages. Various mouse models were created to show the involvement of p53 in processes following DNA damages. The recovery of hematopoetic cells with *p53* depletion after treatment with cytotoxic agents showed the importance of p53 in apoptosis that normally takes place (Wlodarski et al.,1998). Often mice with a *p53* deletion rescued the phenotype of mice deficient in aspects of DNA damage signaling and repair. *p53* deletion in mice deficient for telomerase rescued the first generations (Chin et al.,1999). After four generations the combined defect of telomerase and p53 led to cancer development (Chin et al.,1999). Cells without Ku80 die (Lim et al.,2000). After additional *p53* deletion those cells were able to survive due to an impairment of G1/S checkpoint processing (Lim et al.,2000). Neuronal defects after *Nbn* deletion were

also rescued after *p53* depletion (Frappart et al.,2005). A decrease of hair follicles was detected after *Brca1* deletion in the Keratin 14 expressing cells (Sotiropoulou et al.,2013). An additional *p53* deletion resulted in development of hair in those mice (Sotiropoulou et al.,2013). In the absence of p53 the hair loss normally observed after chemotherapeutic treatment did not occur (Botchkarev et al.,2000). A rescue of epidermal stem cells was observed in mice with non-functional telomeres combined with *p53* deletion (Flores and Blasco,2009). On the other hand not all *p53* deletions resulted in a rescue. Inactivation of *ATR* led to the loss of hair follicle stem cells in mice (Ruzankina et al.,2007). After combined deletion of *ATR* and *p53* no rescue was observed (Ruzankina et al.,2009). The mice showed the same phenotype (Ruzankina et al.,2009). It was even slightly more pronounced (Ruzankina et al.,2009). Similar to this observation no rescue was observed in this study. $Nbn^{Krox20\text{-}Cre}p53^{-/-}$ mice showed the same rate in Caspase 3 activation as Nbn^{Krox20}-Cre mice. The hair loss occurred at roughly the same speed. The increase of γH2A.X foci at 35 days points more towards a worsening of the phenotype. Otherwise most of the observations seemed to match with the psoriasis-like phenotype in the other mice. On the other hand the lack of CD3 T-cells increase points toward another inflammatory process than psoriasis. The appearance of p53 in human psoriasis (Tadini et al.,1989; Yazici et al.,2007) also would not match with a psoriasis-like phenotype in our *p53* deletion mice. That the level of p53 in psoriasis patients increases after sun exposure of the lesion (Yazici et al.,2007) could point towards an activation of p53 apoptosis after DNA damages due to the sun light and UV treatment in psoriasis patients and not to a general expression of p53 in psoriasis lesions.

The phenotype of $Nbn^{Krox20\text{-}Cre}p53^{-/-}$ mice seemed more severe than of Nbn^{Krox20}-Cre mice on visual examination. Morphology of the skin revealed thickening of the epidermis like in Nbn^{Krox20}-Cre mice but additional invaginations of the epidermis and cyst-like structures. In our mice with *p53* deletion the p53 dependent apoptosis after DNA damages in psoriasis is not functioning. This leads to a higher inflammatory reaction that was visible in the raised number of Mast cells and Neutrophils that invaded the epidermis. Additionally the level of Erk1/2 activation was higher and S6 activation was observed in proliferating cells. This leads to an elevated rate of mitosis, seen in the higher rate of Histone 3 phosphorylation, in the epidermis. It results in a precancerous lesion in $Nbn^{Krox20\text{-}Cre}p53^{-/-}$ mice with the cyst-like structures. Development of squamous cell carcinoma after p53 deletion was detected before (Martinez-Cruz et al.,2008). This

process was mediated by inflammation and chromosomal instability (Martinez-Cruz et al.,2009). Both inflammation and non-repaired DNA damages that lead to chromosomal instability are present in the $Nbn^{Krox20\text{-}Cre}p53^{-/-}$ mice. This supports the classification of the cyst-like structures as precancerous lesions in the mice.

The results from this study show that p53 existence inhibits tumor formation and favors psoriasis in the skin of $Nbn^{Krox20\text{-}Cre}$ mice. Absence of both Nbn and p53 leads to a start of tumor formation in the epidermis.

4.6 Tests before PUVA treatment might protect psoriasis patients from skin cancer development

In patients with NBS thin and spares hair and Porokeratosis were described (Wolf and Shwayder,2009; Chrzanowska et al.,2012). *NBN* mutations were found in malignant melanoma and basal cell carcinoma (Debniak et al.,2003; Thirumaran et al.,2006; Meyer et al.,2007). Psoriasis patients exhibit a higher risk for non-melanoma skin cancer, such as squamous cell carcinoma and basal cell carcinoma (Pouplard et al.,2013). This is seen after the treatment with immune suppressing agents and PUVA (Pouplard et al.,2013). In psoriasis patients *NBN* decrease was detected in biopsies from skin lesions compared to non-affected areas (GEO accession GSE14905 (Yao et al.,2008). The non-patient control group showed higher *NBN* expression in the skin (GEO accession GSE14905 (Yao et al.,2008). But overall the status of NBN is highly dependent on the single patient as shown with the analysis of three studies (GEO accession GSE13355 (Nair et al.,2009), GEO accession GSE6710 (Reischl et al.,2007) and GEO accession GSE14905 (Yao et al.,2008)). It was already demonstrated that UVA application comparable to PUVA treatment causes DNA damages (Bredberg,1981; Pathak et al.,1986). The repair of those damages was suggested to function in DNA break dependent manner (Bredberg et al.,1982). In addition UV light was described to cause DNA damages that lead to mutations of p53 and probably skin cancer (Tornaletti et al.,1993). The decrease of NBN in some psoriasis patients indicates that DNA damage signaling and repair in those patients is partially inhibited or not functioning at all. The DNA damages caused by PUVA or other mutagenic treatment in patients with lower NBN level would not be repaired. This would lead to mutations of e.g. p53 and cause cancer development in the patients. This seems a likely process

considering the results in the mentioned studies. The study of DNA damage signaling and repair failure in mouse now confirms this. The study here demonstrates that the inactivation of the DNA damage signaling and repair protein Nbn leads to psoriasis development in prior healthy skin. In combination with p53 inactivation tumor development started.

Taking all these findings into account it should be considered to test the status of DNA damage signaling and repair in psoriasis patients prior to PUVA treatment. Such evaluation might protect patients from the development of non-melanoma skin cancers.

4.7 Summary statements

4.7.1 Function of Nbn and Atm in DNA damage repair is tissue dependent

Deletion of *Nbn* caused a failure to repair DNA damages in the hair follicle stem cells. It is possible that the lack of Nbn caused failure of both NHEJ and HRR. This resulted in increased p53 independent apoptosis and loss of cells. In the hair follicle stem cells it led to a possible differentiation into basal keratinocytes. In the differentiated cells of the epidermis *Nbn* deletion did not cause apoptosis but a disturbance of the differentiation and an increase in proliferation. The consequence of *Nbn* deactivation seems to depend on the whether the tissue is composed of stem/progenitor cells or differentiated cells.

The role of Atm in combination with Nbn is demonstrated to be tissue dependent. Even in proliferating cells differences are detected depending on the tissue. In hair follicle stem cell Atm was essential for formation of γH2A.X foci while Atm was shown not to be required for γH2A.X foci formation in the external germinal layer (EGL) of the cerebellum (Rodrigues et al.,2013). The Atm status influenced the occurrence of p53 dependent apoptosis in the hair follicles. In EGL apoptosis was always p53 independent (Rodrigues et al.,2013). A worsening of the *Nbn* deletion phenotype after *Atm* deficiency was detected in EGL (Rodrigues et al.,2013) while the impact in the epidermis was minimal.

While the loss of Nbn activity alone has various impacts on both proliferating and differentiated tissue the consequences of an additional deletion of *Atm* are detectable mostly in proliferating tissue. In differentiated cells it seems to have only fractional

impact. This was also seen in other studies and tissues (Zhou et al.,2012; Rodrigues et al.,2013).

4.7.2 Nbn is essential for skin homeostasis

The deletion of *Nbn* in the epidermis of mice showed the important role of *Nbn* in DNA damage repair in the skin and the maintenance of skin homeostasis.

The disrupted DNA damage response results in the inability of the hair follicles to regenerate. This is due to a rise in apoptosis and disruption of epidermal stem cell properties. Those cells then start to give rise to basal keratinocytes. The activation of Stat3 in the epidermis can also contribute to this process (Rao et al.,2013). Along with the hair follicle loss an enlargement of the epidermis was observed. Screening of different factors revealed a psoriasis-like phenotype in the *Nbn* deleted mice. The changes observed are indicated in Figure 61. The involvement of Nbn in the network of pathways that are altered in psoriasis is shown.

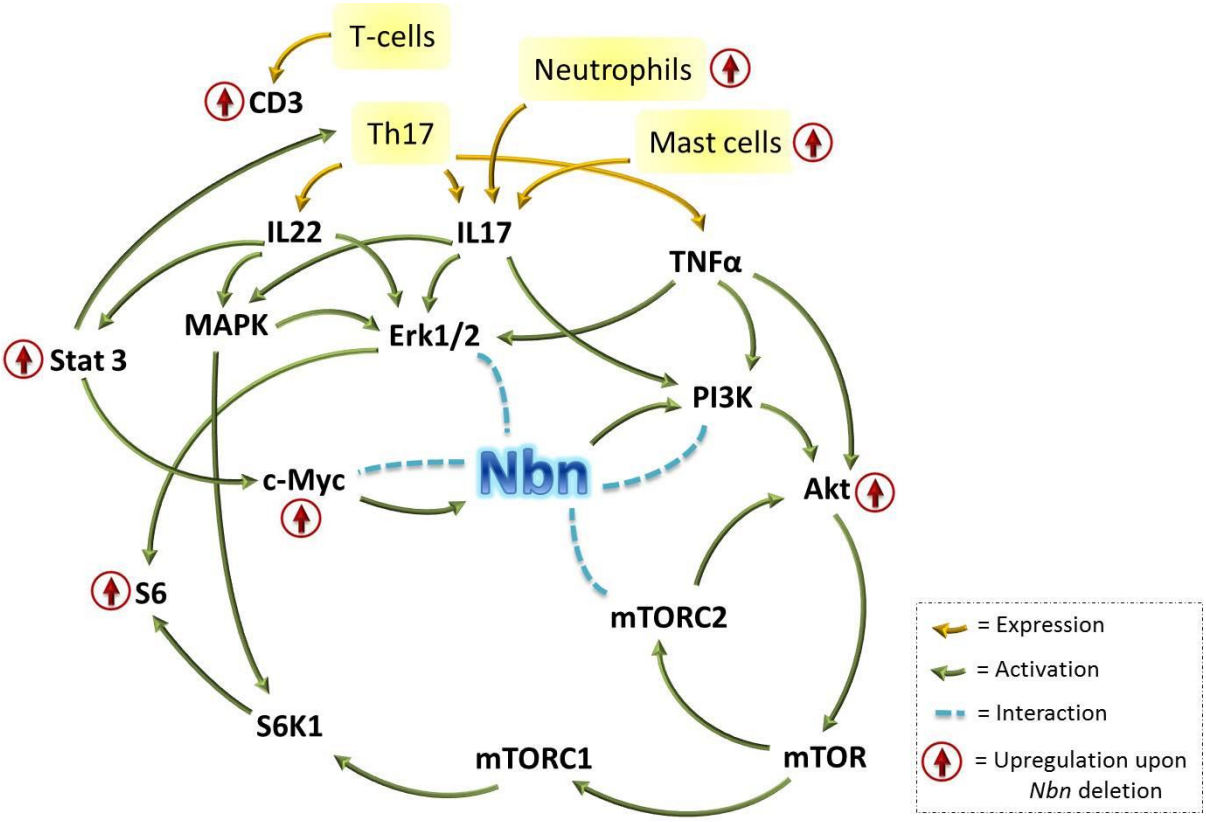

Figure 61: The Nbn/Psoriasis network

Immune cells typically involved in psoriasis and the factors they secret are visualized. Those factors activate different pathways known to be altered in psoriasis. These pathways are shown and a connection to Nbn is depicted. The relationships of the proteins are characterized. The links of the different proteins and pathways were found in literature (Jeno et al.,1988; Mukhopadhyay et al.,1992; Scott et al.,1998; Dufner and Thomas,1999; Kiuchi et al.,1999; Lejeune et al.,2002; Chiang et al.,2003; Hay and Sonenberg,2004; Chen et al.,2005; Hendarmin et al.,2005; Sarbassov et al.,2005; Liang et al.,2006; Golding et al.,2007; Huang et al.,2007; Roux et al.,2007; Yang et al.,2007; Chen et al.,2008; Hematulin et al.,2008; Lee et al.,2008; Lowes et al.,2008; Faurschou,2010; Kim et al.,2010; Lin et al.,2011; Mitra et al.,2012; Wan et al.,2013; Wang et al.,2013; Guo et al.,2014).

There are different interaction partners for Nbn in the pathways. As the animals showed no change in Erk1/2 activation after *Nbn* deletion, it can be excluded as a partner in the psoriasis-like phenotype. Both c-Myc and the PI3K/Akt/mTOR pathways are possible ways of *Nbn* deletion to induce the psoriasis-like phenotype in the mice. Deletion of *Nbn* caused an activation of Stat3 which might result in *c-Myc* over-activation that results in increased proliferation and disturbance of differentiation. The activation of S6 detected in the mice also is a known cause of increased proliferation. Here it is likely not a direct but an indirect effect of the *Nbn* deletion. *Nbn* deletion was before described to result in a decrease of Akt activation via mTORC2 (Wang et al.,2013). Therefore the slight activation of Akt seen in the mice is probably a consequence of an increase of Th17 cells and TNFα secretion. Such activation is also in

accordance with the activation role of Nbn for PI3K which is not taking place in the mice and also limits the activation of Akt (Chen et al.,2005; Chen et al.,2008).

The psoriasis-like phenotype could also have another possible source. The absence of hair follicles and the resulting increase of basal keratinocyte population could cause the phenotype of the mice. The high amount of apoptosis and the increase in cell proliferation might trigger a small inflammatory response. Due to the lack of Nbn and its regulatory role in the network of proteins the mice were not protected against further consequences, e.g. DNA damages in the highly proliferating cells, and the psoriasis-like phenotype was caused.

The findings from the inactivation of *Nbn* in the skin also point towards important consequences for the treatment of patients with psoriasis. The NBN level in some patients is decreased, as demonstrated by the analysis of GEO Profiles database, and a higher rate of non-melanoma skin cancers was detected after PUVA treatment (Pouplard et al.,2013). The combined inactivation of Nbn and p53 in the mice also resulted in precancerous lesions. In humans the correlation of NBN level and the development of skin cancers after PUVA should be evaluated. If DNA repair in psoriasis patients is indeed deficient, the role of UV irradiation and other mutagenic treatments should be reconsidered in this disease.

Overall the importance of functional DNA damage signaling and repair in the skin was demonstrated.

5. References

Ahmad, W., Faiyaz Ul Haque, M., Brancolini, V., Tsou, H. C., Ul Haque, S., Lam, H., Aita, V. M., Owen, J., Deblaquiere, M., Frank, J., Cserhalmi-Friedman, P. B., Leask, A., Mcgrath, J. A., Peacocke, M., Ahmad, M., Ott, J. and Christiano, A. M. (1998). "Alopecia universalis associated with a mutation in the human hairless gene." Science 279(5351): 720-724.

Alonso, L. and Fuchs, E. (2006). "The hair cycle." J Cell Sci 119(Pt 3): 391-393.

Anderson, L., Henderson, C. and Adachi, Y. (2001). "Phosphorylation and rapid relocalization of 53BP1 to nuclear foci upon DNA damage." Mol Cell Biol 21(5): 1719-1729.

Assaf, Y., Galron, R., Shapira, I., Nitzan, A., Blumenfeld-Katzir, T., Solomon, A. S., Holdengreber, V., Wang, Z. Q., Shiloh, Y. and Barzilai, A. (2008). "MRI evidence of white matter damage in a mouse model of Nijmegen breakage syndrome." Exp Neurol 209(1): 181-191.

Augustin, I., Gross, J., Baumann, D., Korn, C., Kerr, G., Grigoryan, T., Mauch, C., Birchmeier, W. and Boutros, M. (2013). "Loss of epidermal Evi/Wls results in a phenotype resembling psoriasiform dermatitis." J Exp Med 210(9): 1761-1777.

Bakkenist, C. J. and Kastan, M. B. (2003). "DNA damage activates ATM through intermolecular autophosphorylation and dimer dissociation." Nature 421(6922): 499-506.

Barrandon, Y. and Green, H. (1987). "Three clonal types of keratinocyte with different capacities for multiplication." Proc Natl Acad Sci U S A 84(8): 2302-2306.

Barrett, T., Wilhite, S. E., Ledoux, P., Evangelista, C., Kim, I. F., Tomashevsky, M., Marshall, K. A., Phillippy, K. H., Sherman, P. M., Holko, M., Yefanov, A., Lee, H., Zhang, N., Robertson, C. L., Serova, N., Davis, S. and Soboleva, A. (2013). "NCBI GEO: archive for functional genomics data sets--update." Nucleic Acids Res 41(Database issue): D991-995.

Bartkova, J., Horejsi, Z., Koed, K., Kramer, A., Tort, F., Zieger, K., Guldberg, P., Sehested, M., Nesland, J. M., Lukas, C., Orntoft, T., Lukas, J. and Bartek, J. (2005). "DNA damage response as a candidate anti-cancer barrier in early human tumorigenesis." Nature 434(7035): 864-870.

Baserga, R. (1991). "Growth regulation of the PCNA gene." J Cell Sci 98 (Pt 4): 433-436.

Basko-Plluska, Juliana L and Petronic-Rosic, V (2012). "Psoriasis: epidemiology, natural history, and differential diagnosis." Psoriasis: Targets and Therapy 2: 67-76.

Bhaskara, V., Dupre, A., Lengsfeld, B., Hopkins, B. B., Chan, A., Lee, J. H., Zhang, X., Gautier, J., Zakian, V. and Paull, T. T. (2007). "Rad50 adenylate kinase activity regulates DNA tethering by Mre11/Rad50 complexes." Mol Cell 25(5): 647-661.

Bogdanova, N., Feshchenko, S., Schurmann, P., Waltes, R., Wieland, B., Hillemanns, P., Rogov, Y. I., Dammann, O., Bremer, M., Karstens, J. H., Sohn, C., Varon, R. and Dork, T. (2008). "Nijmegen Breakage Syndrome mutations and risk of breast cancer." Int J Cancer 122(4): 802-806.

Bohr, V. A. (2002). "DNA damage and its processing. Relation to human disease." Journal of Inherited Metabolic Disease 25(3): 215-222.

Bork, P., Hofmann, K., Bucher, P., Neuwald, A. F., Altschul, S. F. and Koonin, E. V. (1997). "A superfamily of conserved domains in DNA damage-responsive cell cycle checkpoint proteins." FASEB J 11(1): 68-76.

Bos, J. D. and De Rie, M. A. (1999). "The pathogenesis of psoriasis: immunological facts and speculations." Immunol Today 20(1): 40-46.

Botchkarev, V. A., Komarova, E. A., Siebenhaar, F., Botchkareva, N. V., Komarov, P. G., Maurer, M., Gilchrest, B. A. and Gudkov, A. V. (2000). "p53 is essential for chemotherapy-induced hair loss." Cancer Res 60(18): 5002-5006.

Botchkarev, V. A., Komarova, E. A., Siebenhaar, F., Botchkareva, N. V., Sharov, A. A., Komarov, P. G., Maurer, M., Gudkov, A. V. and Gilchrest, B. A. (2001). "p53 Involvement in the control of murine hair follicle regression." Am J Pathol 158(6): 1913-1919.

Bredberg, A. (1981). "DNA damage in human skin fibroblasts exposed to UVA light used in clinical PUVA treatment." J Invest Dermatol 76(6): 449-451.

Bredberg, A., Lambert, B. and Soderhall, S. (1982). "Induction and repair of psoralen cross-links in DNA of normal human and xeroderma pigmentosum fibroblasts." Mutat Res 93(1): 221-234.

Bressan, D. A., Baxter, B. K. and Petrini, J. H. (1999). "The Mre11-Rad50-Xrs2 protein complex facilitates homologous recombination-based double-strand break repair in Saccharomyces cerevisiae." Mol Cell Biol 19(11): 7681-7687.

Buerger, C., Malisiewicz, B., Eiser, A., Hardt, K. and Boehncke, W. H. (2013). "Mammalian target of rapamycin and its downstream signalling components are activated in psoriatic skin." Br J Dermatol 169(1): 156-159.

Buis, J., Wu, Y., Deng, Y., Leddon, J., Westfield, G., Eckersdorff, M., Sekiguchi, J. M., Chang, S. and Ferguson, D. O. (2008). "Mre11 nuclease activity has essential roles in DNA repair and genomic stability distinct from ATM activation." Cell 135(1): 85-96.

Burden, A. D., Javed, S., Bailey, M., Hodgins, M., Connor, M. and Tillman, D. (1998). "Genetics of psoriasis: paternal inheritance and a locus on chromosome 6p." J Invest Dermatol 110(6): 958-960.

Burma, S., Chen, B. P., Murphy, M., Kurimasa, A. and Chen, D. J. (2001). "ATM phosphorylates histone H2AX in response to DNA double-strand breaks." J Biol Chem 276(45): 42462-42467.

Buscemi, G., Savio, C., Zannini, L., Micciche, F., Masnada, D., Nakanishi, M., Tauchi, H., Komatsu, K., Mizutani, S., Khanna, K., Chen, P., Concannon, P., Chessa, L. and Delia, D. (2001). "Chk2 activation dependence on Nbs1 after DNA damage." Mol Cell Biol 21(15): 5214-5222.

Carney, J. P., Maser, R. S., Olivares, H., Davis, E. M., Le Beau, M., Yates, J. R., 3rd, Hays, L., Morgan, W. F. and Petrini, J. H. (1998). "The hMre11/hRad50 protein complex and Nijmegen breakage syndrome: linkage of double-strand break repair to the cellular DNA damage response." Cell 93(3): 477-486.

Cerosaletti, K. M. and Concannon, P. (2003). "Nibrin forkhead-associated domain and breast cancer C-terminal domain are both required for nuclear focus formation and phosphorylation." J Biol Chem 278(24): 21944-21951.

Chavrier, P., Vesque, C., Galliot, B., Vigneron, M., Dolle, P., Duboule, D. and Charnay, P. (1990). "The segment-specific gene Krox-20 encodes a transcription factor with binding sites in the promoter region of the Hox-1.4 gene." EMBO J 9(4): 1209-1218.

Chavrier, P., Zerial, M., Lemaire, P., Almendral, J., Bravo, R. and Charnay, P. (1988). "A gene encoding a protein with zinc fingers is activated during G0/G1 transition in cultured cells." EMBO J 7(1): 29-35.

Chen, Y. C., Chiang, H. Y., Yang, M. H., Chen, P. M., Chang, S. Y., Teng, S. C., Vanhaesebroeck, B. and Wu, K. J. (2008). "Activation of phosphoinositide 3-

kinase by the NBS1 DNA repair protein through a novel activation motif." J Mol Med (Berl) 86(4): 401-412.

Chen, Y. C., Su, Y. N., Chou, P. C., Chiang, W. C., Chang, M. C., Wang, L. S., Teng, S. C. and Wu, K. J. (2005). "Overexpression of NBS1 contributes to transformation through the activation of phosphatidylinositol 3-kinase/Akt." J Biol Chem 280(37): 32505-32511.

Chiang, Y. C., Teng, S. C., Su, Y. N., Hsieh, F. J. and Wu, K. J. (2003). "c-Myc directly regulates the transcription of the NBS1 gene involved in DNA double-strand break repair." J Biol Chem 278(21): 19286-19291.

Chin, L., Artandi, S. E., Shen, Q., Tam, A., Lee, S. L., Gottlieb, G. J., Greider, C. W. and Depinho, R. A. (1999). "p53 deficiency rescues the adverse effects of telomere loss and cooperates with telomere dysfunction to accelerate carcinogenesis." Cell 97(4): 527-538.

Christophers, E. (2001). "Psoriasis--epidemiology and clinical spectrum." Clin Exp Dermatol 26(4): 314-320.

Chrzanowska, K. H., Gregorek, H., Dembowska-Baginska, B., Kalina, M. A. and Digweed, M. (2012). "Nijmegen breakage syndrome (NBS)." Orphanet J Rare Dis 7: 13.

Cotsarelis, G., Sun, T. T. and Lavker, R. M. (1990). "Label-retaining cells reside in the bulge area of pilosebaceous unit: implications for follicular stem cells, hair cycle, and skin carcinogenesis." Cell 61(7): 1329-1337.

Cybulski, C., Gorski, B., Debniak, T., Gliniewicz, B., Mierzejewski, M., Masojc, B., Jakubowska, A., Matyjasik, J., Zlowocka, E., Sikorski, A., Narod, S. A. and Lubinski, J. (2004). "NBS1 is a prostate cancer susceptibility gene." Cancer Res 64(4): 1215-1219.

Dar, I., Yosha, G., Elfassy, R., Galron, R., Wang, Z. Q., Shiloh, Y. and Barzilai, A. (2011). "Investigation of the functional link between ATM and NBS1 in the DNA damage response in the mouse cerebellum." J Biol Chem 286(17): 15361-15376.

Dasika, G. K., Lin, S. C., Zhao, S., Sung, P., Tomkinson, A. and Lee, E. Y. (1999). "DNA damage-induced cell cycle checkpoints and DNA strand break repair in development and tumorigenesis." Oncogene 18(55): 7883-7899.

Davidson, A. and Diamond, B. (2001). "Autoimmune diseases." N Engl J Med 345(5): 340-350.

De Bont, R. and Van Larebeke, N. (2004). "Endogenous DNA damage in humans: a review of quantitative data." Mutagenesis 19(3): 169-185.

De Jager, M., Trujillo, K. M., Sung, P., Hopfner, K. P., Carney, J. P., Tainer, J. A., Connelly, J. C., Leach, D. R., Kanaar, R. and Wyman, C. (2004). "Differential arrangements of conserved building blocks among homologs of the Rad50/Mre11 DNA repair protein complex." J Mol Biol 339(4): 937-949.

De Jager, M., Van Noort, J., Van Gent, D. C., Dekker, C., Kanaar, R. and Wyman, C. (2001). "Human Rad50/Mre11 is a flexible complex that can tether DNA ends." Mol Cell 8(5): 1129-1135.

Debniak, T., Gorski, B., Cybulski, C., Jakubowska, A., Kurzawski, G., Lener, M., Mierzejewski, M., Masojc, B., Medrek, K., Kladny, J., Zaluga, E., Maleszka, R., Chosia, M. and Lubinski, J. (2003). "Germline 657del5 mutation in the NBS1 gene in patients with malignant melanoma of the skin." Melanoma Res 13(4): 365-370.

Deng, Y., Guo, X., Ferguson, D. O. and Chang, S. (2009). "Multiple roles for MRE11 at uncapped telomeres." Nature 460(7257): 914-918.

Dephoure, N., Zhou, C., Villen, J., Beausoleil, S. A., Bakalarski, C. E., Elledge, S. J. and Gygi, S. P. (2008). "A quantitative atlas of mitotic phosphorylation." Proc Natl Acad Sci U S A 105(31): 10762-10767.

Desai-Mehta, A., Cerosaletti, K. M. and Concannon, P. (2001). "Distinct functional domains of nibrin mediate Mre11 binding, focus formation, and nuclear localization." Mol Cell Biol 21(6): 2184-2191.

Digweed, M. (1993). "Human genetic instability syndromes: single gene defects with increased risk of cancer." Toxicol Lett 67(1-3): 259-281.

Dolganov, G. M., Maser, R. S., Novikov, A., Tosto, L., Chong, S., Bressan, D. A. and Petrini, J. H. (1996). "Human Rad50 is physically associated with human Mre11: identification of a conserved multiprotein complex implicated in recombinational DNA repair." Mol Cell Biol 16(9): 4832-4841.

Dufner, A. and Thomas, G. (1999). "Ribosomal S6 kinase signaling and the control of translation." Exp Cell Res 253(1): 100-109.

Dumon-Jones, V., Frappart, P. O., Tong, W. M., Sajithlal, G., Hulla, W., Schmid, G., Herceg, Z., Digweed, M. and Wang, Z. Q. (2003). "Nbn heterozygosity renders mice susceptible to tumor formation and ionizing radiation-induced tumorigenesis." Cancer Res 63(21): 7263-7269.

Eckhart, L., Lippens, S., Tschachler, E. and Declercq, W. (2013). "Cell death by cornification." Biochim Biophys Acta 1833(12): 3471-3480.

Edgar, R., Domrachev, M. and Lash, A. E. (2002). "Gene Expression Omnibus: NCBI gene expression and hybridization array data repository." Nucleic Acids Res 30(1): 207-210.

Eedy, D. J., Burrows, D., Bridges, J. M. and Jones, F. G. (1990). "Clearance of severe psoriasis after allogenic bone marrow transplantation." BMJ 300(6729): 908.

El-Abaseri, T. B., Putta, S. and Hansen, L. A. (2006). "Ultraviolet irradiation induces keratinocyte proliferation and epidermal hyperplasia through the activation of the epidermal growth factor receptor." Carcinogenesis 27(2): 225-231.

Elder, L. T., Klein, S. B., Tavakkol, A., Fisher, G. J., Nickoloff, B. J. and Voorhees, J. J. (1990). "Growth factor and proto-oncogene expression in psoriasis." J Invest Dermatol 95(5 Suppl): 7S-9S.

Falck, J., Coates, J. and Jackson, S. P. (2005). "Conserved modes of recruitment of ATM, ATR and DNA-PKcs to sites of DNA damage." Nature 434(7033): 605-611.

Faurschou, A. (2010). "Role of tumor necrosis factor-alpha in the regulation of keratinocyte cell cycle and DNA repair after ultraviolet-B radiation." Dan Med Bull 57(10): B4179.

Finlan, L. E., Nenutil, R., Ibbotson, S. H., Vojtesek, B. and Hupp, T. R. (2006). "CK2-site phosphorylation of p53 is induced in DeltaNp63 expressing basal stem cells in UVB irradiated human skin." Cell Cycle 5(21): 2489-2494.

Flores, I. and Blasco, M. A. (2009). "A p53-dependent response limits epidermal stem cell functionality and organismal size in mice with short telomeres." PLoS One 4(3): e4934.

Frappart, P. O., Tong, W. M., Demuth, I., Radovanovic, I., Herceg, Z., Aguzzi, A., Digweed, M. and Wang, Z. Q. (2005). "An essential function for NBS1 in the prevention of ataxia and cerebellar defects." Nat Med 11(5): 538-544.

Friedberg, E. C. (2003). "DNA damage and repair." Nature 421(6921): 436-440.

Friedberg, E. C. (2008). "A brief history of the DNA repair field." Cell Res 18(1): 3-7.

Friedberg, E. C., Mcdaniel, L. D. and Schultz, R. A. (2004). "The role of endogenous and exogenous DNA damage and mutagenesis." Current Opinion in Genetics & Development 14(1): 5-10.

Friesner, J. D., Liu, B., Culligan, K. and Britt, A. B. (2005). "Ionizing radiation-dependent gamma-H2AX focus formation requires ataxia telangiectasia mutated and ataxia telangiectasia mutated and Rad3-related." Mol Biol Cell 16(5): 2566-2576.

Fuchs, E. (2007). "Scratching the surface of skin development." Nature 445(7130): 834-842.

Fuchs, E. and Green, H. (1980). "Changes in keratin gene expression during terminal differentiation of the keratinocyte." Cell 19(4): 1033-1042.

Gambardella, L., Schneider-Maunoury, S., Voiculescu, O., Charnay, P. and Barrandon, Y. (2000). "Pattern of expression of the transcription factor Krox-20 in mouse hair follicle." Mech Dev 96(2): 215-218.

Gatei, M., Young, D., Cerosaletti, K. M., Desai-Mehta, A., Spring, K., Kozlov, S., Lavin, M. F., Gatti, R. A., Concannon, P. and Khanna, K. (2000). "ATM-dependent phosphorylation of nibrin in response to radiation exposure." Nat Genet 25(1): 115-119.

Gauci, S., Helbig, A. O., Slijper, M., Krijgsveld, J., Heck, A. J. and Mohammed, S. (2009). "Lys-N and trypsin cover complementary parts of the phosphoproteome in a refined SCX-based approach." Anal Chem 81(11): 4493-4501.

Gerdes, J., Lemke, H., Baisch, H., Wacker, H. H., Schwab, U. and Stein, H. (1984). "Cell cycle analysis of a cell proliferation-associated human nuclear antigen defined by the monoclonal antibody Ki-67." J Immunol 133(4): 1710-1715.

Gilliam, A. C., Kremer, I. B., Yoshida, Y., Stevens, S. R., Tootell, E., Teunissen, M. B., Hammerberg, C. and Cooper, K. D. (1998). "The human hair follicle: a reservoir of CD40+ B7-deficient Langerhans cells that repopulate epidermis after UVB exposure." J Invest Dermatol 110(4): 422-427.

Golding, S. E., Rosenberg, E., Neill, S., Dent, P., Povirk, L. F. and Valerie, K. (2007). "Extracellular signal-related kinase positively regulates ataxia telangiectasia mutated, homologous recombination repair, and the DNA damage response." Cancer Res 67(3): 1046-1053.

Goldschmidt, H. and Sherwin, W. K. (1980). "Reactions to ionizing radiation." J Am Acad Dermatol 3(6): 551-579.

Gorgoulis, V. G., Vassiliou, L. V., Karakaidos, P., Zacharatos, P., Kotsinas, A., Liloglou, T., Venere, M., Ditullio, R. A., Jr., Kastrinakis, N. G., Levy, B., Kletsas, D., Yoneta, A., Herlyn, M., Kittas, C. and Halazonetis, T. D. (2005). "Activation of the DNA damage checkpoint and genomic instability in human precancerous lesions." Nature 434(7035): 907-913.

Gottlieb, T. M. and Jackson, S. P. (1993). "The DNA-dependent protein kinase: requirement for DNA ends and association with Ku antigen." Cell 72(1): 131-142.

Griffiths, C. E. and Barker, J. N. (2007). "Pathogenesis and clinical features of psoriasis." Lancet 370(9583): 263-271.

Group, The International Nijmegen Breakage Syndrome Study (2000). "Nijmegen breakage syndrome. The International Nijmegen Breakage Syndrome Study Group." Arch Dis Child 82(5): 400-406.

Gudjonsson, J. E., Johnston, A., Dyson, M., Valdimarsson, H. and Elder, J. T. (2007). "Mouse models of psoriasis." J Invest Dermatol 127(6): 1292-1308.

Guo, X., Jiang, X., Xiao, Y., Zhou, T., Guo, Y., Wang, R., Zhao, Z., Xiao, H., Hou, C., Ma, L., Lin, Y., Lang, X., Feng, J., Chen, G., Shen, B., Han, G. and Li, Y. (2014). "IL-17A signaling in colonic epithelial cells inhibits pro-inflammatory cytokine production by enhancing the activity of ERK and PI3K." PLoS One 9(2): e89714.

Gurley, K. E. and Kemp, C. J. (2007). "Ataxia-telangiectasia mutated is not required for p53 induction and apoptosis in irradiated epithelial tissues." Mol Cancer Res 5(12): 1312-1318.

Gurley, L. R., Walters, R. A. and Tobey, R. A. (1974). "Cell cycle-specific changes in histone phosphorylation associated with cell proliferation and chromosome condensation." J Cell Biol 60(2): 356-364.

Hardy, M. H. (1992). "The secret life of the hair follicle." Trends Genet 8(2): 55-61.

Harfouche, G., Vaigot, P., Rachidi, W., Rigaud, O., Moratille, S., Marie, M., Lemaitre, G., Fortunel, N. O. and Martin, M. T. (2010). "Fibroblast growth factor type 2 signaling is critical for DNA repair in human keratinocyte stem cells." Stem Cells 28(9): 1639-1648.

Hay, N. and Sonenberg, N. (2004). "Upstream and downstream of mTOR." Genes Dev 18(16): 1926-1945.

Hebert, J. M., Rosenquist, T., Gotz, J. and Martin, G. R. (1994). "FGF5 as a regulator of the hair growth cycle: evidence from targeted and spontaneous mutations." Cell 78(6): 1017-1025.

Hematulin, A., Sagan, D., Eckardt-Schupp, F. and Moertl, S. (2008). "NBS1 is required for IGF-1 induced cellular proliferation through the Ras/Raf/MEK/ERK cascade." Cell Signal 20(12): 2276-2285.

Hembree, J. R., Harmon, C. S., Nevins, T. D. and Eckert, R. L. (1996). "Regulation of human dermal papilla cell production of insulin-like growth factor binding protein-3 by retinoic acid, glucocorticoids, and insulin-like growth factor-1." J Cell Physiol 167(3): 556-561.

Hendarmin, L., Sandra, F., Nakao, Y., Ohishi, M. and Nakamura, N. (2005). "TNFalpha played a role in induction of Akt and MAPK signals in ameloblastoma." Oral Oncol 41(4): 375-382.

Henseler, T. and Christophers, E. (1985). "Psoriasis of early and late onset: characterization of two types of psoriasis vulgaris." J Am Acad Dermatol 13(3): 450-456.

Henseler, T. and Christophers, E. (1995). "Disease concomitance in psoriasis." J Am Acad Dermatol 32(6): 982-986.

Hertl, M. (2011). Autoimmune Diseases of the Skin: Pathogenesis, Diagnosis, Management, Springer.

Herzog, K. H., Chong, M. J., Kapsetaki, M., Morgan, J. I. and Mckinnon, P. J. (1998). "Requirement for Atm in ionizing radiation-induced cell death in the developing central nervous system." Science 280(5366): 1089-1091.

Hibberts, N. A., Howell, A. E. and Randall, V. A. (1998). "Balding hair follicle dermal papilla cells contain higher levels of androgen receptors than those from non-balding scalp." J Endocrinol 156(1): 59-65.

Hoeijmakers, J. H. J. (2009). "DNA Damage, Aging, and Cancer. (vol 361, pg 1475, 2009)." New England Journal of Medicine 361(19): 1914.

Hoeijmakers, Jan H. J. (2001). "Genome maintenance mechanisms for preventing cancer." Nature (London) 411(6835): 366-374.

Hofmann, K. and Bucher, P. (1995). "The FHA domain: a putative nuclear signalling domain found in protein kinases and transcription factors." Trends Biochem Sci 20(9): 347-349.

Hollaender, A. and Duggar, B. M. (1938). "The Effects of Sublethal Doses of Monochromatic Ultraviolet Radiation on the Growth Properties of Bacteria." J Bacteriol 36(1): 17-37.

Hopfner, K. P., Craig, L., Moncalian, G., Zinkel, R. A., Usui, T., Owen, B. A., Karcher, A., Henderson, B., Bodmer, J. L., Mcmurray, C. T., Carney, J. P., Petrini, J. H.

and Tainer, J. A. (2002). "The Rad50 zinc-hook is a structure joining Mre11 complexes in DNA recombination and repair." Nature 418(6897): 562-566.

Hopfner, K. P., Karcher, A., Craig, L., Woo, T. T., Carney, J. P. and Tainer, J. A. (2001). "Structural biochemistry and interaction architecture of the DNA double-strand break repair Mre11 nuclease and Rad50-ATPase." Cell 105(4): 473-485.

Hopfner, K. P., Karcher, A., Shin, D., Fairley, C., Tainer, J. A. and Carney, J. P. (2000). "Mre11 and Rad50 from Pyrococcus furiosus: cloning and biochemical characterization reveal an evolutionarily conserved multiprotein machine." J Bacteriol 182(21): 6036-6041.

Hopfner, K. P., Karcher, A., Shin, D. S., Craig, L., Arthur, L. M., Carney, J. P. and Tainer, J. A. (2000). "Structural biology of Rad50 ATPase: ATP-driven conformational control in DNA double-strand break repair and the ABC-ATPase superfamily." Cell 101(7): 789-800.

Huang, F., Kao, C. Y., Wachi, S., Thai, P., Ryu, J. and Wu, R. (2007). "Requirement for both JAK-mediated PI3K signaling and ACT1/TRAF6/TAK1-dependent NF-kappaB activation by IL-17A in enhancing cytokine expression in human airway epithelial cells." J Immunol 179(10): 6504-6513.

Huang, J., Grotzer, M. A., Watanabe, T., Hewer, E., Pietsch, T., Rutkowski, S. and Ohgaki, H. (2008). "Mutations in the Nijmegen breakage syndrome gene in medulloblastomas." Clin Cancer Res 14(13): 4053-4058.

Ismail, F., Ikram, M., Purdie, K., Harwood, C., Leigh, I. and Storey, A. (2011). "Cutaneous squamous cell carcinoma (SCC) and the DNA damage response: pATM expression patterns in pre-malignant and malignant keratinocyte skin lesions." PLoS One 6(7): e21271.

Ito, M., Liu, Y., Yang, Z., Nguyen, J., Liang, F., Morris, R. J. and Cotsarelis, G. (2005). "Stem cells in the hair follicle bulge contribute to wound repair but not to homeostasis of the epidermis." Nat Med 11(12): 1351-1354.

Jacks, T., Remington, L., Williams, B. O., Schmitt, E. M., Halachmi, S., Bronson, R. T. and Weinberg, R. A. (1994). "Tumor spectrum analysis in p53-mutant mice." Curr Biol 4(1): 1-7.

Jeno, P., Ballou, L. M., Novak-Hofer, I. and Thomas, G. (1988). "Identification and characterization of a mitogen-activated S6 kinase." Proc Natl Acad Sci U S A 85(2): 406-410.

Johansen, C., Kragballe, K., Westergaard, M., Henningsen, J., Kristiansen, K. and Iversen, L. (2005). "The mitogen-activated protein kinases p38 and ERK1/2 are increased in lesional psoriatic skin." Br J Dermatol 152(1): 37-42.

Johnson-Huang, L. M., Lowes, M. A. and Krueger, J. G. (2012). "Putting together the psoriasis puzzle: an update on developing targeted therapies." Dis Model Mech 5(4): 423-433.

Jones, P. H., Harper, S. and Watt, F. M. (1995). "Stem cell patterning and fate in human epidermis." Cell 80(1): 83-93.

Jones, P. H. and Watt, F. M. (1993). "Separation of human epidermal stem cells from transit amplifying cells on the basis of differences in integrin function and expression." Cell 73(4): 713-724.

Joseph, L. J., Le Beau, M. M., Jamieson, G. A., Jr., Acharya, S., Shows, T. B., Rowley, J. D. and Sukhatme, V. P. (1988). "Molecular cloning, sequencing, and mapping of EGR2, a human early growth response gene encoding a protein with "zinc-binding finger" structure." Proc Natl Acad Sci U S A 85(19): 7164-7168.

Jowitt, S. N. and Yin, J. A. (1990). "Psoriasis and bone marrow transplantation." BMJ 300(6736): 1398-1399.

Kang, J., Bronson, R. T. and Xu, Y. (2002). "Targeted disruption of NBS1 reveals its roles in mouse development and DNA repair." EMBO J 21(6): 1447-1455.

Kastan, M. B. and Lim, D. S. (2000). "The many substrates and functions of ATM." Nat Rev Mol Cell Biol 1(3): 179-186.

Kaufman, K. D. (1996). "Androgen metabolism as it affects hair growth in androgenetic alopecia." Dermatol Clin 14(4): 697-711.

Keith, C. T. and Schreiber, S. L. (1995). "PIK-related kinases: DNA repair, recombination, and cell cycle checkpoints." Science 270(5233): 50-51.

Kim, D. K. and Holbrook, K. A. (1995). "The appearance, density, and distribution of Merkel cells in human embryonic and fetal skin: their relation to sweat gland and hair follicle development." J Invest Dermatol 104(3): 411-416.

Kim, J. E., Son, J. E., Jung, S. K., Kang, N. J., Lee, C. Y., Lee, K. W. and Lee, H. J. (2010). "Cocoa polyphenols suppress TNF-alpha-induced vascular endothelial growth factor expression by inhibiting phosphoinositide 3-kinase (PI3K) and mitogen-activated protein kinase kinase-1 (MEK1) activities in mouse epidermal cells." Br J Nutr 104(7): 957-964.

Kim, S. J., Dix, D. J., Thompson, K. E., Murrell, R. N., Schmid, J. E., Gallagher, J. E. and Rockett, J. C. (2006). "Gene expression in head hair follicles plucked from men and women." Ann Clin Lab Sci 36(2): 115-126.

Kinner, A., Wu, W., Staudt, C. and Iliakis, G. (2008). "Gamma-H2AX in recognition and signaling of DNA double-strand breaks in the context of chromatin." Nucleic Acids Res 36(17): 5678-5694.

Kishimoto, J., Burgeson, R. E. and Morgan, B. A. (2000). "Wnt signaling maintains the hair-inducing activity of the dermal papilla." Genes Dev 14(10): 1181-1185.

Kitagawa, R., Bakkenist, C. J., Mckinnon, P. J. and Kastan, M. B. (2004). "Phosphorylation of SMC1 is a critical downstream event in the ATM-NBS1-BRCA1 pathway." Genes Dev 18(12): 1423-1438.

Kiuchi, N., Nakajima, K., Ichiba, M., Fukada, T., Narimatsu, M., Mizuno, K., Hibi, M. and Hirano, T. (1999). "STAT3 is required for the gp130-mediated full activation of the c-myc gene." J Exp Med 189(1): 63-73.

Koster, M. I., Dai, D., Marinari, B., Sano, Y., Costanzo, A., Karin, M. and Roop, D. R. (2007). "p63 induces key target genes required for epidermal morphogenesis." Proc Natl Acad Sci U S A 104(9): 3255-3260.

Kozlov, S. V., Graham, M. E., Peng, C., Chen, P., Robinson, P. J. and Lavin, M. F. (2006). "Involvement of novel autophosphorylation sites in ATM activation." EMBO J 25(15): 3504-3514.

Kracker, S., Bergmann, Y., Demuth, I., Frappart, P. O., Hildebrand, G., Christine, R., Wang, Z. Q., Sperling, K., Digweed, M. and Radbruch, A. (2005). "Nibrin functions in Ig class-switch recombination." Proc Natl Acad Sci U S A 102(5): 1584-1589.

Krueger, J. G., Fretzin, S., Suarez-Farinas, M., Haslett, P. A., Phipps, K. M., Cameron, G. S., Mccolm, J., Katcherian, A., Cueto, I., White, T., Banerjee, S. and Hoffman, R. W. (2012). "IL-17A is essential for cell activation and inflammatory gene circuits in subjects with psoriasis." J Allergy Clin Immunol 130(1): 145-154 e149.

Kruger, L., Demuth, I., Neitzel, H., Varon, R., Sperling, K., Chrzanowska, K. H., Seemanova, E. and Digweed, M. (2007). "Cancer incidence in Nijmegen breakage syndrome is modulated by the amount of a variant NBS protein." Carcinogenesis 28(1): 107-111.

Kruhlak, M., Crouch, E. E., Orlov, M., Montano, C., Gorski, S. A., Nussenzweig, A., Misteli, T., Phair, R. D. and Casellas, R. (2007). "The ATM repair pathway

inhibits RNA polymerase I transcription in response to chromosome breaks." Nature 447(7145): 730-734.

Kunz, J., Henriquez, R., Schneider, U., Deuter-Reinhard, M., Movva, N. R. and Hall, M. N. (1993). "Target of rapamycin in yeast, TOR2, is an essential phosphatidylinositol kinase homolog required for G1 progression." Cell 73(3): 585-596.

Lavin, Martin F. and Kozlov, Sergei (2007). "ATM activation and DNA damage response." Cell Cycle 6(8): 931-942.

Lee, J. H., Ghirlando, R., Bhaskara, V., Hoffmeyer, M. R., Gu, J. and Paull, T. T. (2003). "Regulation of Mre11/Rad50 by Nbs1: effects on nucleotide-dependent DNA binding and association with ataxia-telangiectasia-like disorder mutant complexes." J Biol Chem 278(46): 45171-45181.

Lee, J. H. and Paull, T. T. (2005). "ATM activation by DNA double-strand breaks through the Mre11-Rad50-Nbs1 complex." Science 308(5721): 551-554.

Lee, J. W., Wang, P., Kattah, M. G., Youssef, S., Steinman, L., Defea, K. and Straus, D. S. (2008). "Differential regulation of chemokines by IL-17 in colonic epithelial cells." J Immunol 181(9): 6536-6545.

Lejeune, D., Dumoutier, L., Constantinescu, S., Kruijer, W., Schuringa, J. J. and Renauld, J. C. (2002). "Interleukin-22 (IL-22) activates the JAK/STAT, ERK, JNK, and p38 MAP kinase pathways in a rat hepatoma cell line. Pathways that are shared with and distinct from IL-10." J Biol Chem 277(37): 33676-33682.

Levi, G., Topilko, P., Schneider-Maunoury, S., Lasagna, M., Mantero, S., Pesce, B., Ghersi, G., Cancedda, R. and Charnay, P. (1996). "Role of Krox-20 in endochondral bone formation." Ann N Y Acad Sci 785: 288-291.

Levy, V., Lindon, C., Zheng, Y., Harfe, B. D. and Morgan, B. A. (2007). "Epidermal stem cells arise from the hair follicle after wounding." FASEB J 21(7): 1358-1366.

Li, B., Huang, G., Zhang, X., Li, R., Wang, J., Dong, Z. and He, Z. (2013). "Increased phosphorylation of histone H3 at serine 10 is involved in Epstein-Barr virus latent membrane protein-1-induced carcinogenesis of nasopharyngeal carcinoma." BMC Cancer 13: 124.

Liang, S. C., Tan, X. Y., Luxenberg, D. P., Karim, R., Dunussi-Joannopoulos, K., Collins, M. and Fouser, L. A. (2006). "Interleukin (IL)-22 and IL-17 are coexpressed by Th17 cells and cooperatively enhance expression of antimicrobial peptides." J Exp Med 203(10): 2271-2279.

Lieber, M. R. and Wilson, T. E. (2010). "SnapShot: Nonhomologous DNA end joining (NHEJ)." Cell 142(3): 496-496 e491.

Lim, D. S., Kim, S. T., Xu, B., Maser, R. S., Lin, J., Petrini, J. H. and Kastan, M. B. (2000). "ATM phosphorylates p95/nbs1 in an S-phase checkpoint pathway." Nature 404(6778): 613-617.

Lim, D. S., Vogel, H., Willerford, D. M., Sands, A. T., Platt, K. A. and Hasty, P. (2000). "Analysis of ku80-mutant mice and cells with deficient levels of p53." Mol Cell Biol 20(11): 3772-3780.

Lin, A. M., Rubin, C. J., Khandpur, R., Wang, J. Y., Riblett, M., Yalavarthi, S., Villanueva, E. C., Shah, P., Kaplan, M. J. and Bruce, A. T. (2011). "Mast cells and neutrophils release IL-17 through extracellular trap formation in psoriasis." J Immunol 187(1): 490-500.

Lin, K. K., Chudova, D., Hatfield, G. W., Smyth, P. and Andersen, B. (2004). "Identification of hair cycle-associated genes from time-course gene expression profile data by using replicate variance." Proc Natl Acad Sci U S A 101(45): 15955-15960.

Lindner, G., Botchkarev, V. A., Botchkareva, N. V., Ling, G., Van Der Veen, C. and Paus, R. (1997). "Analysis of apoptosis during hair follicle regression (catagen)." Am J Pathol 151(6): 1601-1617.

Liu, B., Chen, X., Wang, Z. Q. and Tong, W. M. (2014). "DNA damage and oxidative injury are associated with hypomyelination in the corpus callosum of newborn Nbn(CNS-del) mice." J Neurosci Res 92(2): 254-266.

Liu, Y., Lyle, S., Yang, Z. and Cotsarelis, G. (2003). "Keratin 15 promoter targets putative epithelial stem cells in the hair follicle bulge." J Invest Dermatol 121(5): 963-968.

Longhese, M. P., Bonetti, D., Manfrini, N. and Clerici, M. (2010). "Mechanisms and regulation of DNA end resection." EMBO J 29(17): 2864-2874.

Lovejoy, Courtney A. and Cortez, David (2009). "Common mechanisms of PIKK regulation." DNA Repair 8(9): 1004-1008.

Lowe, N. J., Breeding, J., Kean, C. and Cohn, M. L. (1981). "Psoriasiform dermatosis in a rhesus monkey." J Invest Dermatol 76(2): 141-143.

Lowes, M. A., Kikuchi, T., Fuentes-Duculan, J., Cardinale, I., Zaba, L. C., Haider, A. S., Bowman, E. P. and Krueger, J. G. (2008). "Psoriasis vulgaris lesions contain discrete populations of Th1 and Th17 T cells." J Invest Dermatol 128(5): 1207-1211.

Madonna, S., Scarponi, C., Pallotta, S., Cavani, A. and Albanesi, C. (2012). "Anti-apoptotic effects of suppressor of cytokine signaling 3 and 1 in psoriasis." Cell Death Dis 3: e334.

Martinez-Cruz, A. B., Santos, M., Garcia-Escudero, R., Moral, M., Segrelles, C., Lorz, C., Saiz, C., Buitrago-Perez, A., Costa, C. and Paramio, J. M. (2009). "Spontaneous tumor formation in Trp53-deficient epidermis mediated by chromosomal instability and inflammation." Anticancer Res 29(8): 3035-3042.

Martinez-Cruz, A. B., Santos, M., Lara, M. F., Segrelles, C., Ruiz, S., Moral, M., Lorz, C., Garcia-Escudero, R. and Paramio, J. M. (2008). "Spontaneous squamous cell carcinoma induced by the somatic inactivation of retinoblastoma and Trp53 tumor suppressors." Cancer Res 68(3): 683-692.

Maser, R. S., Zinkel, R. and Petrini, J. H. (2001). "An alternative mode of translation permits production of a variant NBS1 protein from the common Nijmegen breakage syndrome allele." Nat Genet 27(4): 417-421.

Mazon, G., Mimitou, E. P. and Symington, L. S. (2010). "SnapShot: Homologous recombination in DNA double-strand break repair." Cell 142(4): 646, 646 e641.

Mckinnon, P. J. (2004). "ATM and ataxia telangiectasia - Second in Molecular Medicine Review Series." Embo Reports 5(8): 772-776.

Mcvey, M. and Lee, S. E. (2008). "MMEJ repair of double-strand breaks (director's cut): deleted sequences and alternative endings." Trends Genet 24(11): 529-538.

Meyer, P., Stapelmann, H., Frank, B., Varon, R., Burwinkel, B., Schmitt, C., Boettger, M. B., Klaes, R., Sperling, K., Hemminki, K. and Kammerer, S. (2007). "Molecular genetic analysis of NBS1 in German melanoma patients." Melanoma Res 17(2): 109-116.

Mitra, A., Raychaudhuri, S. K. and Raychaudhuri, S. P. (2012). "IL-22 induced cell proliferation is regulated by PI3K/Akt/mTOR signaling cascade." Cytokine 60(1): 38-42.

Miyoshi, K., Takaishi, M., Nakajima, K., Ikeda, M., Kanda, T., Tarutani, M., Iiyama, T., Asao, N., Digiovanni, J. and Sano, S. (2011). "Stat3 as a therapeutic target for the treatment of psoriasis: a clinical feasibility study with STA-21, a Stat3 inhibitor." J Invest Dermatol 131(1): 108-117.

Moldovan, G. L. and D'andrea, A. D. (2009). "How the fanconi anemia pathway guards the genome." Annu Rev Genet 43: 223-249.

Moll, J. M. and Wright, V. (1973). "Psoriatic arthritis." Semin Arthritis Rheum 3(1): 55-78.

Moreno-Herrero, F., De Jager, M., Dekker, N. H., Kanaar, R., Wyman, C. and Dekker, C. (2005). "Mesoscale conformational changes in the DNA-repair complex Rad50/Mre11/Nbs1 upon binding DNA." Nature 437(7057): 440-443.

Mori, J., Kakihana, K. and Ohashi, K. (2012). "Sustained remission of psoriasis vulgaris after allogeneic bone marrow transplantation." Br J Haematol 159(2): 121.

Morris, R. J., Liu, Y., Marles, L., Yang, Z., Trempus, C., Li, S., Lin, J. S., Sawicki, J. A. and Cotsarelis, G. (2004). "Capturing and profiling adult hair follicle stem cells." Nat Biotechnol 22(4): 411-417.

Mukhopadhyay, N. K., Price, D. J., Kyriakis, J. M., Pelech, S., Sanghera, J. and Avruch, J. (1992). "An array of insulin-activated, proline-directed serine/threonine protein kinases phosphorylate the p70 S6 kinase." J Biol Chem 267(5): 3325-3335.

Muller-Rover, S., Handjiski, B., Van Der Veen, C., Eichmuller, S., Foitzik, K., Mckay, I. A., Stenn, K. S. and Paus, R. (2001). "A comprehensive guide for the accurate classification of murine hair follicles in distinct hair cycle stages." J Invest Dermatol 117(1): 3-15.

Nair, R. P., Duffin, K. C., Helms, C., Ding, J., Stuart, P. E., Goldgar, D., Gudjonsson, J. E., Li, Y., Tejasvi, T., Feng, B. J., Ruether, A., Schreiber, S., Weichenthal, M., Gladman, D., Rahman, P., Schrodi, S. J., Prahalad, S., Guthery, S. L., Fischer, J., Liao, W., Kwok, P. Y., Menter, A., Lathrop, G. M., Wise, C. A., Begovich, A. B., Voorhees, J. J., Elder, J. T., Krueger, G. G., Bowcock, A. M. and Abecasis, G. R. (2009). "Genome-wide scan reveals association of psoriasis with IL-23 and NF-kappaB pathways." Nat Genet 41(2): 199-204.

Nakamura, M., Sundberg, J. P. and Paus, R. (2001). "Mutant laboratory mice with abnormalities in hair follicle morphogenesis, cycling, and/or structure: annotated tables." Exp Dermatol 10(6): 369-390.

Nijhof, J. G., Van Pelt, C., Mulder, A. A., Mitchell, D. L., Mullenders, L. H. and De Gruijl, F. R. (2007). "Epidermal stem and progenitor cells in murine epidermis accumulate UV damage despite NER proficiency." Carcinogenesis 28(4): 792-800.

Ohyama, M., Terunuma, A., Tock, C. L., Radonovich, M. F., Pise-Masison, C. A., Hopping, S. B., Brady, J. N., Udey, M. C. and Vogel, J. C. (2006). "Characterization and isolation of stem cell-enriched human hair follicle bulge cells." J Clin Invest 116(1): 249-260.

Oshima, H., Rochat, A., Kedzia, C., Kobayashi, K. and Barrandon, Y. (2001). "Morphogenesis and renewal of hair follicles from adult multipotent stem cells." Cell 104(2): 233-245.

Osterland, C. K., Wilkinson, R. D. and St Louis, E. A. (1990). "Expression of c-myc protein in skin and synovium in psoriasis and psoriatic arthritis." Clin Exp Rheumatol 8(2): 145-150.

Panier, S. and Boulton, S. J. (2014). "Double-strand break repair: 53BP1 comes into focus." Nat Rev Mol Cell Biol 15(1): 7-18.

Panteleyev, A. A., Van Der Veen, C., Rosenbach, T., Muller-Rover, S., Sokolov, V. E. and Paus, R. (1998). "Towards defining the pathogenesis of the hairless phenotype." J Invest Dermatol 110(6): 902-907.

Parisi, R., Symmons, D. P., Griffiths, C. E. and Ashcroft, D. M. (2013). "Global epidemiology of psoriasis: a systematic review of incidence and prevalence." J Invest Dermatol 133(2): 377-385.

Parkinson, D. B., Bhaskaran, A., Droggiti, A., Dickinson, S., D'antonio, M., Mirsky, R. and Jessen, K. R. (2004). "Krox-20 inhibits Jun-NH2-terminal kinase/c-Jun to control Schwann cell proliferation and death." J Cell Biol 164(3): 385-394.

Pathak, M. A., Zarebska, Z., Mihm, M. C., Jr., Jarzabek-Chorzelska, M., Chorzelski, T. and Jablonska, S. (1986). "Detection of DNA-psoralen photoadducts in mammalian skin." J Invest Dermatol 86(3): 308-315.

Paull, T. T. and Gellert, M. (1999). "Nbs1 potentiates ATP-driven DNA unwinding and endonuclease cleavage by the Mre11/Rad50 complex." Genes Dev 13(10): 1276-1288.

Paull, Tanya T. and Gellert, Martin (1998). "The 3' to 5' exonuclease activity of Mre11 facilitates repair of DNA double-strand breaks." Molecular Cell 1(7): 969-979.

Paus, R. and Cotsarelis, G. (1999). "The biology of hair follicles." N Engl J Med 341(7): 491-497.

Paus, R. and Foitzik, K. (2004). "In search of the "hair cycle clock": a guided tour." Differentiation 72(9-10): 489-511.

Pelengaris, S., Littlewood, T., Khan, M., Elia, G. and Evan, G. (1999). "Reversible activation of c-Myc in skin: induction of a complex neoplastic phenotype by a single oncogenic lesion." Mol Cell 3(5): 565-577.

Perera, G. K., Ainali, C., Semenova, E., Hundhausen, C., Barinaga, G., Kassen, D., Williams, A. E., Mirza, M. M., Balazs, M., Wang, X., Rodriguez, R. S., Alendar, A., Barker, J., Tsoka, S., Ouyang, W. and Nestle, F. O. (2014). "Integrative biology approach identifies cytokine targeting strategies for psoriasis." Sci Transl Med 6(223): 223ra222.

Pike, M. C., Lee, C. S., Elder, J. T., Voorhees, J. J. and Fisher, G. J. (1989). "Increased phosphatidylinositol kinase activity in psoriatic epidermis." J Invest Dermatol 92(6): 791-797.

Plager, D. A., Kahl, J. C., Asmann, Y. W., Nilson, A. E., Pallanch, J. F., Friedman, O. and Kita, H. (2010). "Gene transcription changes in asthmatic chronic rhinosinusitis with nasal polyps and comparison to those in atopic dermatitis." PLoS One 5(7): e11450.

Plager, D. A., Leontovich, A. A., Henke, S. A., Davis, M. D., Mcevoy, M. T., Sciallis, G. F., 2nd and Pittelkow, M. R. (2007). "Early cutaneous gene transcription changes in adult atopic dermatitis and potential clinical implications." Exp Dermatol 16(1): 28-36.

Plikus, M. V. and Chuong, C. M. (2008). "Complex hair cycle domain patterns and regenerative hair waves in living rodents." J Invest Dermatol 128(5): 1071-1080.

Polo, Sophie E. and Jackson, Stephen P. (2011). "Dynamics of DNA damage response proteins at DNA breaks: a focus on protein modifications." Genes & Development 25(5): 409-433.

Potter, G. B., Beaudoin, G. M., 3rd, Derenzo, C. L., Zarach, J. M., Chen, S. H. and Thompson, C. C. (2001). "The hairless gene mutated in congenital hair loss disorders encodes a novel nuclear receptor corepressor." Genes Dev 15(20): 2687-2701.

Pouplard, C., Brenaut, E., Horreau, C., Barnetche, T., Misery, L., Richard, M. A., Aractingi, S., Aubin, F., Cribier, B., Joly, P., Jullien, D., Le Maitre, M., Ortonne, J. P. and Paul, C. (2013). "Risk of cancer in psoriasis: a systematic review and meta-analysis of epidemiological studies." J Eur Acad Dermatol Venereol 27 Suppl 3: 36-46.

Rachidi, W., Harfourche, G., Lemaitre, G., Amiot, F., Vaigot, P. and Martin, M. T. (2007). "Sensing radiosensitivity of human epidermal stem cells." Radiother Oncol 83(3): 267-276.

Rahman, P., Gladman, D. D., Schentag, C. T. and Petronis, A. (1999). "Excessive paternal transmission in psoriatic arthritis." Arthritis Rheum 42(6): 1228-1231.

Ranganathan, V., Heine, W. F., Ciccone, D. N., Rudolph, K. L., Wu, X., Chang, S., Hai, H., Ahearn, I. M., Livingston, D. M., Resnick, I., Rosen, F., Seemanova, E., Jarolim, P., Depinho, R. A. and Weaver, D. T. (2001). "Rescue of a telomere length defect of Nijmegen breakage syndrome cells requires NBS and telomerase catalytic subunit." Curr Biol 11(12): 962-966.

Rao, D., Macias, E., Carbajal, S., Kiguchi, K. and Digiovanni, J. (2013). "Constitutive Stat3 activation alters behavior of hair follicle stem and progenitor cell populations." Mol Carcinog.

Reischl, J., Schwenke, S., Beekman, J. M., Mrowietz, U., Sturzebecher, S. and Heubach, J. F. (2007). "Increased expression of Wnt5a in psoriatic plaques." J Invest Dermatol 127(1): 163-169.

Rodrigues, P. M., Grigaravicius, P., Remus, M., Cavalheiro, G. R., Gomes, A. L., Martins, M. R., Frappart, L., Reuss, D., Mckinnon, P. J., Von Deimling, A., Martins, R. A. and Frappart, P. O. (2013). "Nbn and atm cooperate in a tissue and developmental stage-specific manner to prevent double strand breaks and apoptosis in developing brain and eye." PLoS One 8(7): e69209.

Rosenquist, T. A. and Martin, G. R. (1996). "Fibroblast growth factor signalling in the hair growth cycle: expression of the fibroblast growth factor receptor and ligand genes in the murine hair follicle." Dev Dyn 205(4): 379-386.

Roux, P. P., Shahbazian, D., Vu, H., Holz, M. K., Cohen, M. S., Taunton, J., Sonenberg, N. and Blenis, J. (2007). "RAS/ERK signaling promotes site-specific ribosomal protein S6 phosphorylation via RSK and stimulates cap-dependent translation." J Biol Chem 282(19): 14056-14064.

Ruzankina, Y., Pinzon-Guzman, C., Asare, A., Ong, T., Pontano, L., Cotsarelis, G., Zediak, V. P., Velez, M., Bhandoola, A. and Brown, E. J. (2007). "Deletion of the developmentally essential gene ATR in adult mice leads to age-related phenotypes and stem cell loss." Cell Stem Cell 1(1): 113-126.

Ruzankina, Y., Schoppy, D. W., Asare, A., Clark, C. E., Vonderheide, R. H. and Brown, E. J. (2009). "Tissue regenerative delays and synthetic lethality in adult mice after combined deletion of Atr and Trp53." Nat Genet 41(10): 1144-1149.

Saar, K., Chrzanowska, K. H., Stumm, M., Jung, M., Nurnberg, G., Wienker, T. F., Seemanova, E., Wegner, R. D., Reis, A. and Sperling, K. (1997). "The gene for the ataxia-telangiectasia variant, Nijmegen breakage syndrome, maps to a 1-cM interval on chromosome 8q21." Am J Hum Genet 60(3): 605-610.

Sabourin, M. and Zakian, V. A. (2008). "ATM-like kinases and regulation of telomerase: lessons from yeast and mammals." Trends Cell Biol 18(7): 337-346.

Saidi, A., Li, T., Weih, F., Concannon, P. and Wang, Z. Q. (2010). "Dual functions of Nbs1 in the repair of DNA breaks and proliferation ensure proper V(D)J recombination and T-cell development." Mol Cell Biol 30(23): 5572-5581.

Sano, S., Chan, K. S., Carbajal, S., Clifford, J., Peavey, M., Kiguchi, K., Itami, S., Nickoloff, B. J. and Digiovanni, J. (2005). "Stat3 links activated keratinocytes and immunocytes required for development of psoriasis in a novel transgenic mouse model." Nat Med 11(1): 43-49.

Sarbassov, D. D., Guertin, D. A., Ali, S. M. and Sabatini, D. M. (2005). "Phosphorylation and regulation of Akt/PKB by the rictor-mTOR complex." Science 307(5712): 1098-1101.

Sartori, Alessandro A., Lukas, Claudia, Coates, Julia, Mistrik, Martin, Fu, Shuang, Bartek, Jiri, Baer, Richard, Lukas, Jiri and Jackson, Stephen P. (2007). "Human CtIP promotes DNA end resection." Nature (London) 450(7169): 509.

Savitsky, K., Bar-Shira, A., Gilad, S., Rotman, G., Ziv, Y., Vanagaite, L., Tagle, D. A., Smith, S., Uziel, T., Sfez, S., Ashkenazi, M., Pecker, I., Frydman, M., Harnik, R., Patanjali, S. R., Simmons, A., Clines, G. A., Sartiel, A., Gatti, R. A., Chessa, L., Sanal, O., Lavin, M. F., Jaspers, N. G., Taylor, A. M., Arlett, C. F., Miki, T., Weissman, S. M., Lovett, M., Collins, F. S. and Shiloh, Y. (1995). "A single ataxia telangiectasia gene with a product similar to PI-3 kinase." Science 268(5218): 1749-1753.

Sawaya, M. E. (1994). "Biochemical mechanisms regulating human hair growth." Skin Pharmacol 7(1-2): 5-7.

Saxena, A., Raychaudhuri, S. K. and Raychaudhuri, S. P. (2011). "Interleukin-17-induced proliferation of fibroblast-like synovial cells is mTOR dependent." Arthritis Rheum 63(5): 1465-1466.

Schafer, M., Dutsch, S., Auf Dem Keller, U., Navid, F., Schwarz, A., Johnson, D. A., Johnson, J. A. and Werner, S. (2010). "Nrf2 establishes a glutathione-mediated gradient of UVB cytoprotection in the epidermis." Genes Dev 24(10): 1045-1058.

Schlake, T. (2006). "Krox20, a novel candidate for the regulatory hierarchy that controls hair shaft bending." Mech Dev 123(8): 641-648.

Schmid, P., Cox, D., Mcmaster, G. K. and Itin, P. (1993). "In situ hybridization analysis of cytokine, proto-oncogene and tumour suppressor gene expression in psoriasis." Arch Dermatol Res 285(6): 334-340.

Schmidt-Ullrich, R. and Paus, R. (2005). "Molecular principles of hair follicle induction and morphogenesis." Bioessays 27(3): 247-261.

Schneider-Maunoury, S., Topilko, P., Seitandou, T., Levi, G., Cohen-Tannoudji, M., Pournin, S., Babinet, C. and Charnay, P. (1993). "Disruption of Krox-20 results in alteration of rhombomeres 3 and 5 in the developing hindbrain." Cell 75(6): 1199-1214.

Schneider, M. R., Schmidt-Ullrich, R. and Paus, R. (2009). "The hair follicle as a dynamic miniorgan." Curr Biol 19(3): R132-142.

Scott, P. H., Brunn, G. J., Kohn, A. D., Roth, R. A. and Lawrence, J. C., Jr. (1998). "Evidence of insulin-stimulated phosphorylation and activation of the mammalian target of rapamycin mediated by a protein kinase B signaling pathway." Proc Natl Acad Sci U S A 95(13): 7772-7777.

Seiberg, M., Marthinuss, J. and Stenn, K. S. (1995). "Changes in expression of apoptosis-associated genes in skin mark early catagen." J Invest Dermatol 104(1): 78-82.

Shanbhag, N. M., Rafalska-Metcalf, I. U., Balane-Bolivar, C., Janicki, S. M. and Greenberg, R. A. (2010). "ATM-dependent chromatin changes silence transcription in cis to DNA double-strand breaks." Cell 141(6): 970-981.

Shiloh, Y. (2003). "ATM and related protein kinases: safeguarding genome integrity." Nat Rev Cancer 3(3): 155-168.

Shiloh, Y. (2006). "The ATM-mediated DNA-damage response: taking shape." Trends Biochem Sci 31(7): 402-410.

Sieber-Blum, M. and Grim, M. (2004). "The adult hair follicle: cradle for pluripotent neural crest stem cells." Birth Defects Res C Embryo Today 72(2): 162-172.

Sieber-Blum, M., Grim, M., Hu, Y. F. and Szeder, V. (2004). "Pluripotent neural crest stem cells in the adult hair follicle." Dev Dyn 231(2): 258-269.

Slominski, A., Paus, R., Plonka, P., Chakraborty, A., Maurer, M., Pruski, D. and Lukiewicz, S. (1994). "Melanogenesis during the anagen-catagen-telogen transformation of the murine hair cycle." J Invest Dermatol 102(6): 862-869.

Snowden, J. A. and Heaton, D. C. (1997). "Development of psoriasis after syngeneic bone marrow transplant from psoriatic donor: further evidence for adoptive autoimmunity." Br J Dermatol 137(1): 130-132.

Song, H., Wang, R., Wang, S. and Lin, J. (2005). "A low-molecular-weight compound discovered through virtual database screening inhibits Stat3 function in breast cancer cells." Proc Natl Acad Sci U S A 102(13): 4700-4705.

Song, S. and Lambert, P. F. (1999). "Different responses of epidermal and hair follicular cells to radiation correlate with distinct patterns of p53 and p21 induction." Am J Pathol 155(4): 1121-1127.

Sotiropoulou, P. A., Candi, A., Mascre, G., De Clercq, S., Youssef, K. K., Lapouge, G., Dahl, E., Semeraro, C., Denecker, G., Marine, J. C. and Blanpain, C. (2010). "Bcl-2 and accelerated DNA repair mediates resistance of hair follicle bulge stem cells to DNA-damage-induced cell death." Nat Cell Biol 12(6): 572-582.

Sotiropoulou, P. A., Karambelas, A. E., Debaugnies, M., Candi, A., Bouwman, P., Moers, V., Revenco, T., Rocha, A. S., Sekiguchi, K., Jonkers, J. and Blanpain, C. (2013). "BRCA1 deficiency in skin epidermis leads to selective loss of hair follicle stem cells and their progeny." Genes Dev 27(1): 39-51.

Staricco, R. G. (1963). "Amelanotic melanocytes in the outer sheath of the human hair follicle and their role in the repigmentation of regenerated epidermis." Ann N Y Acad Sci 100: 239-255.

Steffen, J., Varon, R., Mosor, M., Maneva, G., Maurer, M., Stumm, M., Nowakowska, D., Rubach, M., Kosakowska, E., Ruka, W., Nowecki, Z., Rutkowski, P., Demkow, T., Sadowska, M., Bidzinski, M., Gawrychowski, K. and Sperling, K. (2004). "Increased cancer risk of heterozygotes with NBS1 germline mutations in Poland." Int J Cancer 111(1): 67-71.

Stewart, G. S., Maser, R. S., Stankovic, T., Bressan, D. A., Kaplan, M. I., Jaspers, N. G., Raams, A., Byrd, P. J., Petrini, J. H. and Taylor, A. M. (1999). "The DNA double-strand break repair gene hMRE11 is mutated in individuals with an ataxia-telangiectasia-like disorder." Cell 99(6): 577-587.

Stiff, T., O'driscoll, M., Rief, N., Iwabuchi, K., Lobrich, M. and Jeggo, P. A. (2004). "ATM and DNA-PK function redundantly to phosphorylate H2AX after exposure to ionizing radiation." Cancer Res 64(7): 2390-2396.

Stracker, T. H. and Petrini, J. H. (2011). "The MRE11 complex: starting from the ends." Nat Rev Mol Cell Biol 12(2): 90-103.

Strunnikova, N., Hilmer, S., Flippin, J., Robinson, M., Hoffman, E. and Csaky, K. G. (2005). "Differences in gene expression profiles in dermal fibroblasts from control and patients with age-related macular degeneration elicited by oxidative injury." Free Radic Biol Med 39(6): 781-796.

Stuart, P., Malick, F., Nair, R. P., Henseler, T., Lim, H. W., Jenisch, S., Voorhees, J., Christophers, E. and Elder, J. T. (2002). "Analysis of phenotypic variation in psoriasis as a function of age at onset and family history." Arch Dermatol Res 294(5): 207-213.

Tadini, G., Cerri, A., Crosti, L., Cattoretti, G. and Berti, E. (1989). "P53 and oncogenes expression in psoriasis." Acta Derm Venereol Suppl (Stockh) 146: 33-35.

Takata, M., Sasaki, M. S., Sonoda, E., Morrison, C., Hashimoto, M., Utsumi, H., Yamaguchi-Iwai, Y., Shinohara, A. and Takeda, S. (1998). "Homologous recombination and non-homologous end-joining pathways of DNA double-

strand break repair have overlapping roles in the maintenance of chromosomal integrity in vertebrate cells." EMBO J 17(18): 5497-5508.

Tan, C. K., Castillo, C., So, A. G. and Downey, K. M. (1986). "An auxiliary protein for DNA polymerase-delta from fetal calf thymus." J Biol Chem 261(26): 12310-12316.

Tarutani, M., Nakajima, K., Takaishi, M., Ohko, K. and Sano, S. (2013). "Epidermal hyperplasia induced by Raf-MAPK signaling requires Stat3 activation." J Dermatol Sci 72(2): 110-115.

Tauchi, H., Matsuura, S., Kobayashi, J., Sakamoto, S. and Komatsu, K. (2002). "Nijmegen breakage syndrome gene, NBS1, and molecular links to factors for genome stability." Oncogene 21(58): 8967-8980.

Taylor, G., Lehrer, M. S., Jensen, P. J., Sun, T. T. and Lavker, R. M. (2000). "Involvement of follicular stem cells in forming not only the follicle but also the epidermis." Cell 102(4): 451-461.

Teunissen, M. B., Koomen, C. W., De Waal Malefyt, R., Wierenga, E. A. and Bos, J. D. (1998). "Interleukin-17 and interferon-gamma synergize in the enhancement of proinflammatory cytokine production by human keratinocytes." J Invest Dermatol 111(4): 645-649.

Thirumaran, R. K., Bermejo, J. L., Rudnai, P., Gurzau, E., Koppova, K., Goessler, W., Vahter, M., Leonardi, G. S., Clemens, F., Fletcher, T., Hemminki, K. and Kumar, R. (2006). "Single nucleotide polymorphisms in DNA repair genes and basal cell carcinoma of skin." Carcinogenesis 27(8): 1676-1681.

Topilko, P., Schneider-Maunoury, S., Levi, G., Baron-Van Evercooren, A., Chennoufi, A. B., Seitanidou, T., Babinet, C. and Charnay, P. (1994). "Krox-20 controls myelination in the peripheral nervous system." Nature 371(6500): 796-799.

Tornaletti, S., Rozek, D. and Pfeifer, G. P. (1993). "The distribution of UV photoproducts along the human p53 gene and its relation to mutations in skin cancer." Oncogene 8(8): 2051-2057.

Tupler, R., Marseglia, G. L., Stefanini, M., Prosperi, E., Chessa, L., Nardo, T., Marchi, A. and Maraschio, P. (1997). "A variant of the Nijmegen breakage syndrome with unusual cytogenetic features and intermediate cellular radiosensitivity." J Med Genet 34(3): 196-202.

Uyemura, K., Yamamura, M., Fivenson, D. F., Modlin, R. L. and Nickoloff, B. J. (1993). "The cytokine network in lesional and lesion-free psoriatic skin is characterized by a T-helper type 1 cell-mediated response." J Invest Dermatol 101(5): 701-705.

Van Der Burgt, I., Chrzanowska, K. H., Smeets, D. and Weemaes, C. (1996). "Nijmegen breakage syndrome." J Med Genet 33(2): 153-156.

Varon, R., Vissinga, C., Platzer, M., Cerosaletti, K. M., Chrzanowska, K. H., Saar, K., Beckmann, G., Seemanova, E., Cooper, P. R., Nowak, N. J., Stumm, M., Weemaes, C. M., Gatti, R. A., Wilson, R. K., Digweed, M., Rosenthal, A., Sperling, K., Concannon, P. and Reis, A. (1998). "Nibrin, a novel DNA double-strand break repair protein, is mutated in Nijmegen breakage syndrome." Cell 93(3): 467-476.

Verdun, R. E. and Karlseder, J. (2007). "Replication and protection of telomeres." Nature 447(7147): 924-931.

Vissinga, C. S., Yeo, T. C., Warren, S., Brawley, J. V., Phillips, J., Cerosaletti, K. and Concannon, P. (2009). "Nuclear export of NBN is required for normal cellular responses to radiation." Mol Cell Biol 29(4): 1000-1006.

Vogel, C. A., Stratman, E. J., Reck, S. J. and Lund, J. J. (2010). "Chronic noninfectious necrotizing granulomas in a child with Nijmegen breakage syndrome." Pediatr Dermatol 27(3): 285-289.

Voiculescu, O., Charnay, P. and Schneider-Maunoury, S. (2000). "Expression pattern of a Krox-20/Cre knock-in allele in the developing hindbrain, bones, and peripheral nervous system." Genesis 26(2): 123-126.

Wagner, E. F., Schonthaler, H. B., Guinea-Viniegra, J. and Tschachler, E. (2010). "Psoriasis: what we have learned from mouse models." Nat Rev Rheumatol 6(12): 704-714.

Waikel, R. L., Kawachi, Y., Waikel, P. A., Wang, X. J. and Roop, D. R. (2001). "Deregulated expression of c-Myc depletes epidermal stem cells." Nat Genet 28(2): 165-168.

Waikel, R. L., Wang, X. J. and Roop, D. R. (1999). "Targeted expression of c-Myc in the epidermis alters normal proliferation, differentiation and UV-B induced apoptosis." Oncogene 18(34): 4870-4878.

Wan, R. and Crowe, D. L. (2012). "Haploinsufficiency of the Nijmegen breakage syndrome 1 gene increases mammary tumor latency and metastasis." Int J Oncol 41(1): 345-352.

Wan, R., Wu, J., Baloue, K. K. and Crowe, D. L. (2013). "Regulation of the Nijmegen breakage syndrome 1 gene NBS1 by c-myc, p53 and coactivators mediates estrogen protection from DNA damage in breast cancer cells." Int J Oncol 42(2): 712-720.

Wang, J. Q., Chen, J. H., Chen, Y. C., Chen, M. Y., Hsieh, C. Y., Teng, S. C. and Wu, K. J. (2013). "Interaction between NBS1 and the mTOR/Rictor/SIN1 complex through specific domains." PLoS One 8(6): e65586.

Wang, J., Sun, Q., Morita, Y., Jiang, H., Gross, A., Lechel, A., Hildner, K., Guachalla, L. M., Gompf, A., Hartmann, D., Schambach, A., Wuestefeld, T., Dauch, D., Schrezenmeier, H., Hofmann, W. K., Nakauchi, H., Ju, Z., Kestler, H. A., Zender, L. and Rudolph, K. L. (2012). "A differentiation checkpoint limits hematopoietic stem cell self-renewal in response to DNA damage." Cell 148(5): 1001-1014.

Wang, X., Tredget, E. E. and Wu, Y. (2012). "Dynamic signals for hair follicle development and regeneration." Stem Cells Dev 21(1): 7-18.

Warmerdam, Daniel O. and Kanaar, Roland (2010). "Dealing with DNA damage: Relationships between checkpoint and repair pathways." Mutation Research-Reviews in Mutation Research 704(1-3): 2-11.

Watanabe, T., Nobusawa, S., Lu, S., Huang, J., Mittelbronn, M. and Ohgaki, H. (2009). "Mutational inactivation of the nijmegen breakage syndrome gene (NBS1) in glioblastomas is associated with multiple TP53 mutations." J Neuropathol Exp Neurol 68(2): 210-215.

Weinshenker, B. G., Bass, B. H., Ebers, G. C. and Rice, G. P. (1989). "Remission of psoriatic lesions with muromonab-CD3 (orthoclone OKT3) treatment." J Am Acad Dermatol 20(6): 1132-1133.

Wen, J., Cerosaletti, K., Schultz, K. J., Wright, J. A. and Concannon, P. (2012). "NBN Phosphorylation regulates the accumulation of MRN and ATM at sites of DNA double-strand breaks." Oncogene.

Wilkinson, D. G., Bhatt, S., Chavrier, P., Bravo, R. and Charnay, P. (1989). "Segment-specific expression of a zinc-finger gene in the developing nervous system of the mouse." Nature 337(6206): 461-464.

Willan, R. (1808). On Cutaneous Diseases, London.

Williams, Gareth J., Lees-Miller, Susan P. and Tainer, John A. (2010). "Mre11-Rad50-Nbs1 conformations and the control of sensing, signaling, and effector responses at DNA double-strand breaks." DNA Repair 9(12): 1299-1306.

Williams, R. S., Moncalian, G., Williams, J. S., Yamada, Y., Limbo, O., Shin, D. S., Groocock, L. M., Cahill, D., Hitomi, C., Guenther, G., Moiani, D., Carney, J. P., Russell, P. and Tainer, J. A. (2008). "Mre11 dimers coordinate DNA end bridging and nuclease processing in double-strand-break repair." Cell 135(1): 97-109.

Williams, R. S., Williams, J. S. and Tainer, J. A. (2007). "Mre11-Rad50-Nbs1 is a keystone complex connecting DNA repair machinery, double-strand break signaling, and the chromatin template." Biochem Cell Biol 85(4): 509-520.

Wlodarski, P., Wasik, M., Ratajczak, M. Z., Sevignani, C., Hoser, G., Kawiak, J., Gewirtz, A. M., Calabretta, B. and Skorski, T. (1998). "Role of p53 in hematopoietic recovery after cytotoxic treatment." Blood 91(8): 2998-3006.

Wolf, E. K. and Shwayder, T. A. (2009). "Nijmegen breakage syndrome associated with porokeratosis." Pediatr Dermatol 26(1): 106-108.

Wolk, K., Witte, E., Wallace, E., Docke, W. D., Kunz, S., Asadullah, K., Volk, H. D., Sterry, W. and Sabat, R. (2006). "IL-22 regulates the expression of genes responsible for antimicrobial defense, cellular differentiation, and mobility in keratinocytes: a potential role in psoriasis." Eur J Immunol 36(5): 1309-1323.

Wu, X., Ranganathan, V., Weisman, D. S., Heine, W. F., Ciccone, D. N., O'neill, T. B., Crick, K. E., Pierce, K. A., Lane, W. S., Rathbun, G., Livingston, D. M. and Weaver, D. T. (2000). "ATM phosphorylation of Nijmegen breakage syndrome protein is required in a DNA damage response." Nature 405(6785): 477-482.

Wyman, Claire and Kanaar, Roland (2006). DNA double-strand break repair: All's well that ends well. Annu Rev Genet. 40**:** 363-383.

Xin, Y., Lu, Q. and Li, Q. (2011). "IKK1 control of epidermal differentiation is modulated by notch signaling." Am J Pathol 178(4): 1568-1577.

Xu, C., Wu, L., Cui, G., Botuyan, M. V., Chen, J. and Mer, G. (2008). "Structure of a second BRCT domain identified in the nijmegen breakage syndrome protein Nbs1 and its function in an MDC1-dependent localization of Nbs1 to DNA damage sites." J Mol Biol 381(2): 361-372.

Yang, A., Kaghad, M., Wang, Y., Gillett, E., Fleming, M. D., Dotsch, V., Andrews, N. C., Caput, D. and Mckeon, F. (1998). "p63, a p53 homolog at 3q27-29, encodes multiple products with transactivating, death-inducing, and dominant-negative activities." Mol Cell 2(3): 305-316.

Yang, L., Li, Y., Cheng, M., Huang, D., Zheng, J., Liu, B., Ling, X., Li, Q., Zhang, X., Ji, W., Zhou, Y. and Lu, J. (2012). "A functional polymorphism at microRNA-629-binding site in the 3'-untranslated region of NBS1 gene confers an increased risk of lung cancer in Southern and Eastern Chinese population." Carcinogenesis 33(2): 338-347.

Yang, X. O., Panopoulos, A. D., Nurieva, R., Chang, S. H., Wang, D., Watowich, S. S. and Dong, C. (2007). "STAT3 regulates cytokine-mediated generation of inflammatory helper T cells." J Biol Chem 282(13): 9358-9363.

Yang, Y. G., Frappart, P. O., Frappart, L., Wang, Z. Q. and Tong, W. M. (2006). "A novel function of DNA repair molecule Nbs1 in terminal differentiation of the lens fibre cells and cataractogenesis." DNA Repair (Amst) 5(8): 885-893.

Yao, Y., Richman, L., Morehouse, C., De Los Reyes, M., Higgs, B. W., Boutrin, A., White, B., Coyle, A., Krueger, J., Kiener, P. A. and Jallal, B. (2008). "Type I interferon: potential therapeutic target for psoriasis?" PLoS One 3(7): e2737.

Yazici, A. C., Karabulut, A. A., Ozen, O., Eksioglu, M. and Ustun, H. (2007). "Expression of p53 in lesions and unaffected skin of patients with plaque-type and guttate psoriasis: a quantitative comparative study." J Dermatol 34(6): 367-374.

Yoo, J., Wolgamot, G., Torgerson, T. R. and Sidbury, R. (2008). "Cutaneous noncaseating granulomas associated with Nijmegen breakage syndrome." Arch Dermatol 144(3): 418-419.

You, Z., Chahwan, C., Bailis, J., Hunter, T. and Russell, P. (2005). "ATM activation and its recruitment to damaged DNA require binding to the C terminus of Nbs1." Mol Cell Biol 25(13): 5363-5379.

Young, P., Boussadia, O., Halfter, H., Grose, R., Berger, P., Leone, D. P., Robenek, H., Charnay, P., Kemler, R. and Suter, U. (2003). "E-cadherin controls adherens junctions in the epidermis and the renewal of hair follicles." EMBO J 22(21): 5723-5733.

Zanolli, M. D., Jayo, M. J., Jayo, J. M., Blaine, D., Hall, J. and Jorizzo, J. L. (1989). "Evaluation of psoriatic plaques that spontaneously developed in a cynomolgus monkey (Macaca fascicularis)." Acta Derm Venereol Suppl (Stockh) 146: 58.

Zhao, S., Weng, Y. C., Yuan, S. S., Lin, Y. T., Hsu, H. C., Lin, S. C., Gerbino, E., Song, M. H., Zdzienicka, M. Z., Gatti, R. A., Shay, J. W., Ziv, Y., Shiloh, Y. and Lee, E. Y. (2000). "Functional link between ataxia-telangiectasia and Nijmegen breakage syndrome gene products." Nature 405(6785): 473-477.

Zheng, J., Zhang, C., Jiang, L., You, Y., Liu, Y., Lu, J. and Zhou, Y. (2011). "Functional NBS1 polymorphism is associated with occurrence and advanced disease status of nasopharyngeal carcinoma." Mol Carcinog 50(9): 689-696.

Zhou, Z., Bruhn, C. and Wang, Z. Q. (2012). "Differential function of NBS1 and ATR in neurogenesis." DNA Repair (Amst) 11(2): 210-221.

Zhu, J., Petersen, S., Tessarollo, L. and Nussenzweig, A. (2001). "Targeted disruption of the Nijmegen breakage syndrome gene NBS1 leads to early embryonic lethality in mice." Curr Biol 11(2): 105-109.

Zhu, X. D., Kuster, B., Mann, M., Petrini, J. H. and De Lange, T. (2000). "Cell-cycle-regulated association of RAD50/MRE11/NBS1 with TRF2 and human telomeres." Nat Genet 25(3): 347-352.

Zorick, T. S. and Lemke, G. (1996). "Schwann cell differentiation." Curr Opin Cell Biol 8(6): 870-876.